FILLING STRATEGIES FOR AVOIDING WATER HAMMER IN STEAM FILLED PIPES

by

CARLOS ALEXANDRE O. C. LOBO

B.S. Mechanical Engineering (1980)
São Paulo University, São Paulo, Brazil

SUBMITTED TO THE DEPARTMENT OF
NUCLEAR ENGINEERING
IN PARTIAL FULFILLMENT OF THE REQUIREMENTS
FOR THE DEGREES OF

NUCLEAR ENGINEER

and

MASTER OF SCIENCE

at the

MASSACHUSETTS INSTITUTE OF TECHNOLOGY
December, 1988

Signature of Author _____
Department of Nuclear Engineering
December, 1988

Certified by _____
Peter Griffith
Professor of Mechanical Engineering
Thesis Supervisor

Certified by _____
Mujid S. Kazimi
Professor of Nuclear Engineering
Thesis Reader

Accepted by _____
Allan F. Henry
Chairman, Nuclear Engineering Department Committee

FILLING STRATEGIES FOR AVOIDING WATER HAMMER

IN STEAM FILLED PIPES

by

CARLOS ALEXANDRE O. C. LOBO

Submitted to the Department of Nuclear Engineering
on December 12, 1988 in partial fulfillment of the
requirements for the Degrees of Master of Science and
Nuclear Engineer

ABSTRACT

An experimental study was carried out to find ways of filling (with subcooled water) pipes of complex shape, initially filled with steam, without a steam bubble collapse related water hammer event.

The hypothesis underlying this work is that previously developed filling theories, for single pipes, could be used to determine the envelope of the safe (no water hammer) filling velocities for pipes of complex shape. Five different "L" shaped pipes were tested to verify if this was true.

Except for a degree of subcooling less than 20^{o}F, no lower slug water hammer boundary was found when testing a long, leveled, horizontal pipe. Moreover, the short horizontal legs of the "L" shaped pipes behaved like long, leveled, horizontal pipes. Therefore, an additional strategy, appropriate for a long, leveled, horizontal pipe, is still needed in order to permit us to fill pipes of complex shape.

In this work two approaches were used to deal with the long, leveled, horizontal pipe. In the first approach, a conservative analytical model was used to calculate the boundary of the allowable filling velocities. This approach results in such low filling velocities that it is of no practical use. In the second approach, we have experimentally shown that if modifications are introduced into existing piping systems, the so-called slug water hammer can be eliminated from the horizontal sections. These modifications consist of inclining the horizontal pipe and injecting the water laterally from the bottom or injecting the water, perpendicularly to the pipe axis, through nozzles distributed along the pipe length (The distance between two nozzles should be less than 48.D).

The final result of this work is that: If appropriate modifications are introduced into existing piping systems and the initial filling rate is limited by using an available theory for a vertical up single pipe, it is always possible to eliminate the loads induced by steam bubble collapse. There is, therefore, no damage caused to the pipes or its supports.

Several examples of nuclear piping systems are used to illustrate this work conclusions.

Thesis Supervisor: Peter Griffith
Title: Professor of Mechanical Engineering

ACKNOWLEDGEMENTS

I wish to express my gratitude to Professor Peter Griffith for his guidance and patience throughout this work. My sincere thanks to Professor Mujid S. Kazimi who so kindly accepted to be the thesis reader.

I am deeply grateful to the Brazilian Navy for having sponsored my studies at MIT. I would also like to mention that this research was possible because of the financial support of the Electric Power Research Institute (EPRI).

I would like to thank my friend Yuangching Chou for his patience to listen and encouragement. I am indebted to Mr. Norman Mac Askill and Mr. Joseph Caloggero (Tiny) for their help in the construction of the test apparatuses.

Finally, I would like to thank Elenice, Alice and Ricardo for all the joy they have brought to my life.

IN MEMORY OF MY PARENTS

JOAQUIM AMERICO AND GEYSA

TABLE OF CONTENTS

LIST OF FIGURES

NOMENCLATURE

A -> Pipe cross section area.

A_l -> Liquid cross section area = $(1 - \alpha).A$.

$A_g = A_s$ -> Steam cross section area.

A_{wa} -> Heat transfer area between the steam and the pipe wall.

c -> Water sound velocity

C_o -> Constant in equation (2 - 5).

C_l -> Constant in equation (2 - 5).

C_2 -> Coefficient in equation (3 - 23).

C_{pl} -> Water specific heat at constant pressure.

c_l -> Constant in equation (3 - 11).

D -> Pipe diameter or magnification factor.

E -> Steel Young's modulus of elasticity.

e -> Pipe wall thickness.

f -> Friction factor.

Fr -> Froude number.

g -> Gravity acceleration.

G -> Left over factor in equation (3 - 20).

g_c -> Gravity constant.

H -> Voided pipe length.

H_l -> Water pool height.

$H_g = H_s$ -> Steam height.

ΔH -> Water head difference.

h_{fg} -> Evaporation specific enthalpy.

h_s -> Steam enthalpy.

I -> Moment of inertia.

j_l^* -> Nondimensional liquid superficial velocity.

j_s^* -> Nondimensional steam superficial velocity.

K -> Constant in equation (4 - 2) or system stiffness.

K_T -> Constant in equation (A1 - 2).

K_1, K_2 & K_3 -> Constants in equation (A1 - 2) ($K_1 + K_2 + K_3 = K_T$).

k -> Joukowsky relation constant.

L or l -> Pipe length.

M -> System mass.

M_{air} -> A constant used to take into account the presence of air in the steam.

$\dot{m}_c$ -> Mass condensation rate of steam.

$\dot{m}_w$ -> Water mass filling rate.

n -> Constant in equation (4 - 2).

p -> Constant in equation (4 - 2) or applied load.

p_{max} -> Maximum value of a dynamic load.

ΔP -> Differential pressure.

$(\Delta P)_{friction}$ -> Pressure loss due to friction.

$(\Delta P)_{gravity}$ -> Pressure loss due to gravity.

$(\Delta P)_{inertia}$ -> Pressure loss due to liquid inertia.

$(\Delta P)_{fric.}$ -> Pressure loss due to wall friction.

$(\Delta P)_{loc.}$ -> Localized pressure loss.

$P_s - P_o$ -> Steam pressure.

$P_t = P_1$ -> Tank pressure.

q -> Constant in equation (4 - 2).

$\dot{q}_{int}$ -> Heat flux at the steam/water interface.

$\dot{q}_{wa}$ -> Heat flux from the steam to the pipe wall.

r -> Constant in equation (4 - 2).

R -> Bend radius.

Re -> Reynolds number.

Re^* -> Constant in equation (4 -2).

S_i -> Water/steam interface cross section length.

t -> Time.

t_1 -> Impulse duration.

$\bar{t}$ -> = $(t - t_1)$.

T -> Free vibration period.

T_{sub} -> Subcooling of the injected water.

Tw -> Temperature of the injected water.

U_b -> Bubble rise velocity.

Ugs -> Steam superficial velocity.

U_{ls} -> Liquid superficial velocity.

V -> Water (plug) velocity.

V_o -> Velocity inside the water pool in front of the water plug.

V_{av} -> Average filling velocity.

V_s -> Steam Velocity.

V' -> Water velocity.

v_s -> Steam volume.

x -> Length of the totally filled pipe, starting from the ball valve.

$\dot{x}$ -> Velocity of the water plug front.

y -> Length of the totally water filled pipe, starting from the tank.

y_o -> Initial length of the totally water filled pipe starting from the tank interface.

w -> Circular frequency.

z -> Single displacement (SDOF).

z_{max} -> Structure maximum displacement due to a dynamic load.

GREEK LETTERS

α -> Void fraction.

β -> Angle defined by equation (3 - 3).

κ_l -> Water bulk modulus of elasticity.

λ -> Constant in equation (4 -2).

μ -> Steel Poisson's ratio.

ν_l -> Water kinematic viscosity.

ν_s -> Steam kinematic viscosity.

$\rho = \rho_l$ -> Liquid density.

ρ_s -> Steam density.

θ -> Inclination angle.

CHAPTER - 1

INTRODUCTION

1.1 Water Hammer Events in the Nuclear Industry

The frequency of water hammers, in nuclear plants, had its peak in the early 1970's. The concern of NRC and the industry also grew during this period, especially after the severe accident in Indian Point 2. In this accident, which occurred in 1973, an 18 inch feedwater pipe fractured inside the containment during testing, because of a water hammer event. Researchers worries and efforts were then concentrated on the so-called steam generator water hammer, because of its damage potential. In 1978, NRC declared water hammer an Unresolved Safety Issue (USI).

Several studies, whose focus was on steam generator water hammer, were published. The recommendations derived from these studies (For instance, to use top discharge "J" tubes in the steam generator sparger ring or to make the feedwater line as short as possible) seem to have solved this problem.

Other modifications were also implemented for other different types of water hammer. These include the use of keep full pumps to avoid the formation of voids in BWR lines, even though the check valves there are supposed to isolate these lines. Because of these improvements and the increased operator awareness and knowledge, the frequency of the water hammer has decreased.

Most of the water hammer damage is limited to pipe supports. No radioactive release has resulted from any water hammer. According to Van

Duyne (1), up to now the damage distribution of water hammer events is: 1) Damage to components - 36%; 2) Damage to pipe supports or snubbers - 36%; 3) No physical damage - 19%; and 4) Pressure boundary failure - 9%. Considering that there is little risk to the general public, in 1984 NRC declared the water hammer USI resolved.

Although the water hammer frequency has decreased, the problem is far from being totally eliminated. Nowadays, utilities still experience large financial and credibility losses due to water hammer. For instance, damaged supports may require the operators to stop a plant for repairs. Recently, Stone & Webster (2) compiled for EPRI a data base containing a total of 281 reported water hammers. This document covers the last 20 years of operation of nuclear reactors, in the United States. Previously, NUREG/CR-2059 (3) collected a total of 195 water hammers between 1969 and 1981. Not even including the water hammers that were not reportable, in the last seven years more 86 events have occurred.

If not needed to insure the safety of the general public, economic considerations, operators safety and utility credibility reasons are sufficient justification for pursuing water hammer mitigation measures. In order to avoid water hammers, it is necessary to take into account the fact that many of them are caused by deteriorated equipment. This is difficult to detect. A typical example is when high pressure steam is separated from a low pressure water line by an isolation valve. This is common in BWR systems. If this isolation valve leaks, steam can migrate from the high pressure line into the water line. If the pressure increases in this water line because the pump is switched on, the steam bubble can collapse

violently, causing a water hammer. Some these equipment failures can eventually induce water hammers that result in very large financial losses.

The San Onofre Nuclear Generating Station - Unit 1, in November 1985, suffered a severe water hammer in its feedwater line (4). The failure of five check valves in its feedwater system was the underlying cause of the event. The leaky check valves permitted the horizontal feedwater pipe to void and to partially fill with steam. When the auxiliary feedwater (AFW) was injected into the pipe, the conditions for a condensation induced water hammer were then established. The resulting damage in the pipe can be appreciated by looking at figure - 1.1.

Kadak (5) gives another reason to find ways of avoiding water hammers. Some of the operating nuclear power plants have piping systems that have been weakened by intergranular stress corrosion cracking (IGSCC) or by the erosion and corrosion phenomena. Consequently, some of the pipes might fracture under smaller pressure surges than the ownwers anticipate

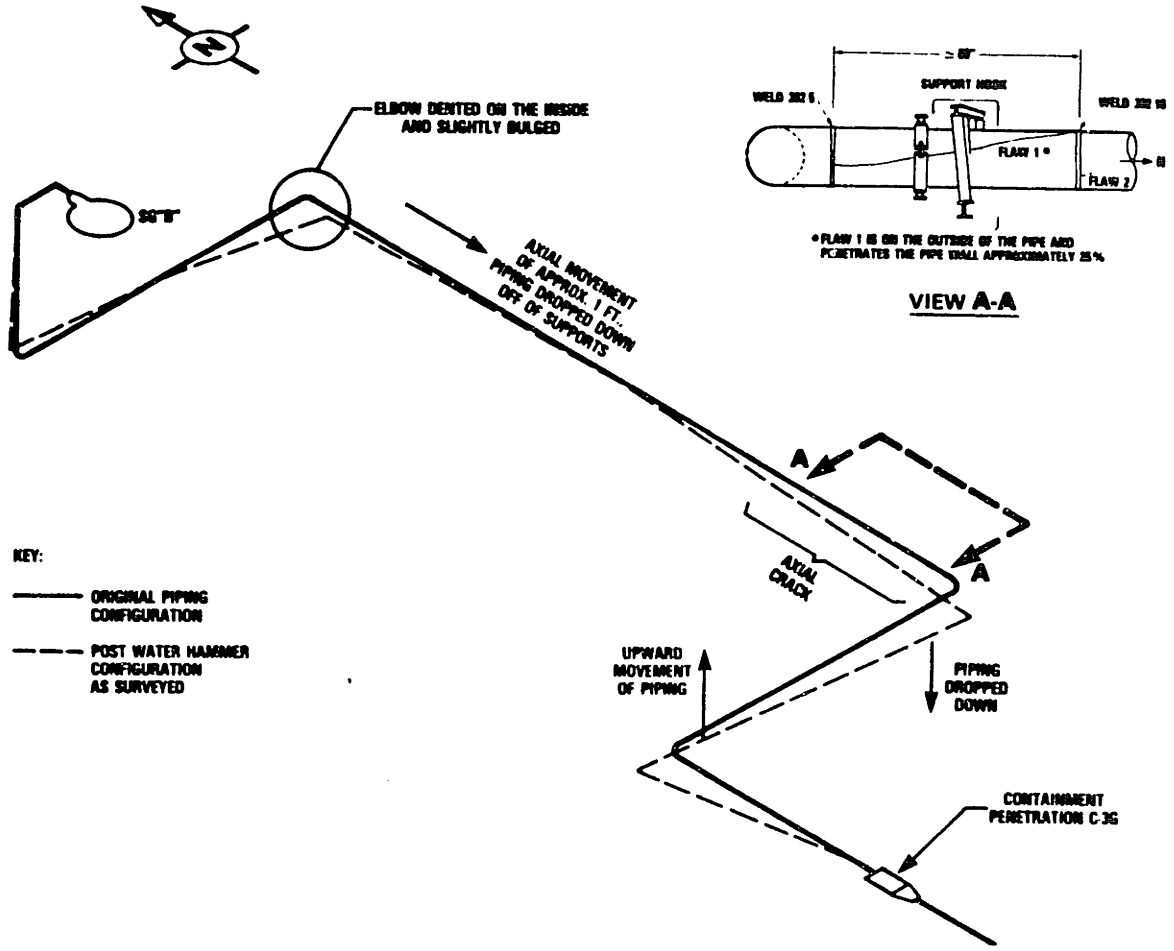

FIGURE - 1.1 San Onofre feedwater piping and support damage due to water hammer. Source -> (4)

1.2 Objective of the Present Study

Especially because of equipment deterioration (as a leaky valve), several scenarios can arise in nuclear piping systems that lead to condensation induced water hammer events. One solution for this problem is to always consider the possibility of steam inside the pipes and to use an initial filling procedure that can condense the trapped steam slowly, with no water hammer. When the pipes are finally full of water, the piping system can be switched into its normal operational condition.

Chou (6) tested three simple pipe geometries, which were: 1) A vertical pipe filled from below (vertical up); 2) A vertical pipe filled from the top (vertical down); and 3) A short leveled horizontal pipe (Length less than 48.D, where D is the pipe diameter). For these three pipe geometries, he was able to find theories that predict the filling velocity below which no water hammer will occur, when subcooled water is injected into a steam filled pipe.

The first objective of this work was to see if it is possible to determine the safe (no water hammer) filling rate of a piping system of complex shape, by simply determining the envelope of allowable filling velocities of its individual pipe sections. The idea was to use Chou's simple pipe theories to calculate this envelope.

Five different "L" shaped pipes were tested, to check whether or not the above idea was valid. As it will be described in chapter 4, the horizontal sections of these pipes would always limit the possible filling rate. Moreover, the single short horizontal pipe theory could not be used

because even short pipes, pipes less than 48.D, would behave like a long horizontal pipe.

A theory for a long horizontal pipe was needed. For reasons that will be explained in chapter 3, a conservative method was first used to calculate the allowable filling velocity for a long horizontal pipe. This approach resulted in such low water injection rates that the answer was of no practical use. However, it will be shown experimentally that by introducing modifications, as inclining and appropriately injecting the water, it is possible to avoid the intermediate water hammer (see Chapter - 2 for definition). When these modifications were introduced into the "L" shaped pipes, the vertical up single pipe theory always give a conservative boundary for the water hammer safe region.

A conservative bubble collapse model was also proposed, which can be applied to predict the pipe load in certain simple cases (see Chapter 3).

The final result of this work is that if some modifications are made in an existing complex piping system and the initial filling rate is appropriately limited, it is always possible to avoid water hammers due to the rapid collapse of steam. Thus, going to the water hammer mechanism classification given in Stone & Webster's report (2), this work will give one possible solution to deal with four of the seven proposed mechanisms. These are: 1) Mechanism 2 - Steam and subcooled water interactions in horizontal and near horizontal pipes; 2) Mechanism 3 - Subcooled water flow into a vertical initially steam filled pipe; 3) Mechanism 4 - Hot water entering a lower pressure line with subsequent flashed steam bubble collapse; and 4) Mechanism 4 - Water column separation and rejoining.

Finally, some examples of how improve existent nuclear piping systems, to avoid water hammers, are given in chapter 5.

CHAPTER - 2

BACKGROUND

2.1 Review of the Literature

It is possible to divide the published material, related to the nuclear plant water hammer issue, into two classes.

In the first class, the effort was concentrated on: 1) The review of reported hydraulic transients; 2) The identification of possible scenarios, in nuclear piping systems, that can provide the necessary conditions for the occurrence of a water hammer event; 3) The evaluation, according to the type of water hammer and the nuclear piping system, of the potential impact on plant safety; and 4) On suggesting mitigation measures.

NUREG - 0582 (7) is an effort of this type. It was published in 1978 and reflected the NRC staff's concern with the increasing number of water hammers in the preceding years. Water hammer was declared an USI (A-1) as a result of this study. NUREG/CR - 2059 (3) (1982) compiles all reported water hammer events between 1969 and 1981. NUREG/CR - 2781 (8) (1982) used the data from NUREG/CR - 2059 to produce a more detailed analysis of the water hammer issue. As result, several design and operational modifications were suggested in order to decrease the water hammer frequency. NRC declared the USI A-1 resolved in 1984. The technical findings and evaluations for this decision are given in NUREG - 0927 (9) (1984).

The last of the reports in this class is the one that will result from the contract that EPRI made with Stone & Webster. EPRI intends to obtain, as

final product from this contract, a comprehensive water hammer handbook for plant engineers and operators. The draft versions of tasks 1 (2), 2 (10) and 6 and 7 (11) are now available. These reports compile and analyze water hammers events up to 1988.

In the second class, the effort was concentrated in finding analytical models to describe water hammer events.

Block et al (12) (1976) studied extensively the so-called steam generator water hammer. Initiating mechanisms were analyzed. One-dimensional models for the dynamics of slugs with different boundary and initial conditions were proposed. In these models, the condensation rate was left as an independent parameter. Methods of calculating the impact pressure were developed based on the Joukowsky relation ($\Delta P = K.\rho.c.\Delta V$). However, the final conclusion was that, especially because of the unknown condensation rate, the models were not sufficiently mature to be used for predicting the steam generator water hammer. But, from the comprehension that was gained about the phenomena involved, the report was successful in suggesting ways of mitigating the problem (For instance, the use of sparger ring top discharge through "J" tubes).

Saha et al (13) (1980) studied condensation induced water hammer in preheat type steam generators. An one-dimensional analytical model was also proposed for the dynamics of a water slug. In this case the water slug would fill all the pipe cross section and advance against a steam bubble. The direct-contact condensation of steam in the water interface was left as an independent parameter. The model was considered not credible because of the present uncertainty of the condensation correlations.

Gruel (14) (1980) studied the collapse of a steam bubble. He used a simple apparatus where the steam bubble volume and the boundary conditions were very well defined. Adjusting the condensation rate, he was able to make his proposed bubble collapse one-dimensional model predict the measured pressure spikes. The same apparatus was used by Hurwitz (15) (1980) to study the pressure wave propagation and the interaction between the fluid and the structure.

Bjorge (16) (1982) proposed a model that used the Taitel-Dukler stratified-slug transition criterion (17) to study the initiation of a water hammer, in horizontal or nearly horizontal pipes, when subcooled water is injected into a steam filled pipe. The steam velocity and the water depth profile were calculated using an one-dimensional two-phase model. When a convenient multiplier was used in one of Bankoff and Kim's direct-contact condensation correlations (18), the critical inlet water flow rate for water hammer initiation was well predicted.

Jackobek (19) (1984) used a scale model of a two loop PWR to experimentally study the water hammer due to the injection of Emergency Core Cooling (ECC) water into the cold legs. His analytical model was a conservative version of Bjorge's approach. Instead of using a direct-contact condensation correlation, the steam mass flow rate was considered equal to the one necessary to bring the injected water to the saturation state. The Joukowsky relation was used to calculate the pressure spike magnitude. When the velocity of the water column coming from the downcomer was neglected, the agreement of the model and experiment was good. Notice that a factor (1/2) was omitted in the Joukowsky relation, as the water plug crashed against a water column rather than the blocked end of a pipe.

2.2 Chou's Simple Pipe Theories

As Chou's (6) (1988) simple pipe theories are frequently mentioned in this work, a brief review his results will be given in the next paragraphs. The objective is to only give an idea of what is involved in these models. The reader should go to the reference (6) for a complete description.

Vertical Up Single Pipe (Filled from the Bottom) Theory

Figure - 2.1 is a scheme of Chou's (6) vertical up pipe model. In this figure the pipe sections between the tank and the vertical section are not shown.

In Chou's one-dimensional model the steam was assumed to be stationary. Consequently, the only necessary conservation equations for the steam side were mass, volume and energy. Using also equations of state Chou reached to:

$$\frac{dv_s}{dt} = - U_{ls}.A - \frac{\dot{m}_c}{\rho_l} \qquad \text{eq(2 - 1)}$$

and,

$$\left[\frac{1}{\rho_s} - \left(\frac{\partial h_s}{\partial P_s}\right)_{\rho_s}\right].\frac{dP_s}{dt} = \frac{1}{v_s}.\left(\frac{\partial h_s}{\partial \rho_s}\right)_{P_s}.(\rho_s.U_{ls}.A - (1 - \frac{\rho_s}{\rho_l}).\dot{m}_c) \qquad \text{eq(2 - 2)}$$

The steam condensation rate was given by equation (2 - 3) and the heat

$$\dot{m}_c = \frac{q_{int}.A + q_{wa}.A_{wa}}{h_{fg}.M_{air}} \qquad \text{eq(2 - 3)}$$

transfer coefficients were obtained from previously published works. The uncertainty in the interface condensation rate ($\dot{q}_{int}$) was not important,

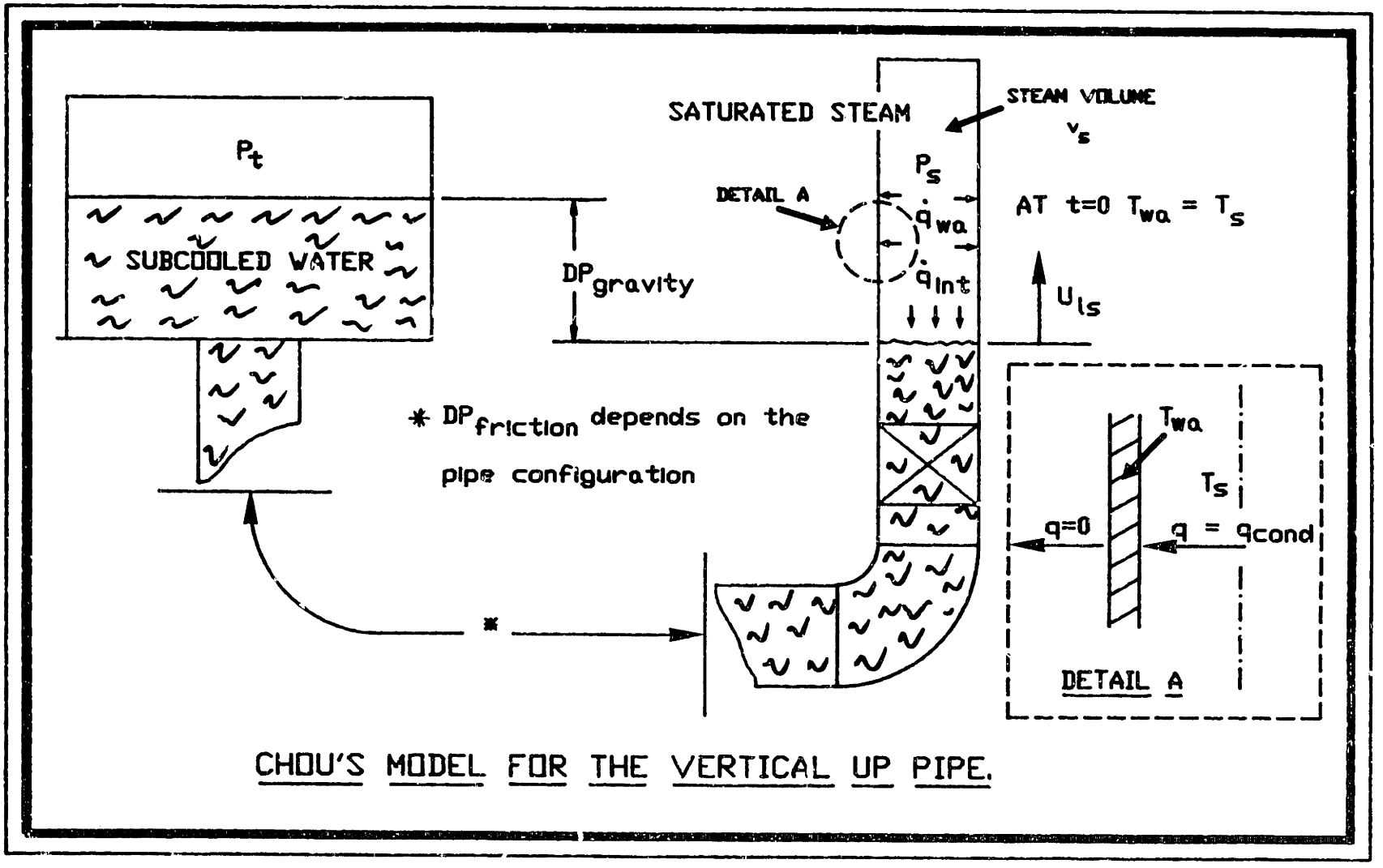

FIGURE - 2.1 Scheme for Chou's vertical up pipe theory.
Based on source -> (6)

because the wall condensation rate (q_{wa}) was one order of magnitude higher than the interface condensation rate. The constant M_{air} was used to take into account the air content in the steam.

As the water temperature was assumed constant, for the water side it was only necessary to solve the momentum equation. In Chou's thesis and in his computer program this equation was written for his pipe geometry. It is necessary to adapt the friction and the inertia terms of the momentum equation for different pipe arrangements. In general, the momentum equation can be written as:

$$(\Delta P)_{inertia} = (P_t - P_s) - (\Delta P)_{gravity} - (\Delta P)_{friction} \qquad eq(2 - 4)$$

The one-dimensional heat diffusion equation was used to calculate the wall temperature. The initial condition was $T_{wa} = T_s$. The boundary conditions were perfect insulation on the outer surface and film condensation on the inner surface.

Finally, the temperature and the steam pressure were correlated by using an equation derived from the Clapeyron equation.

Except at the moment of the collapse of the steam bubble, and when M_{air} was appropriately chosen, the model predicted the water velocities well (see figure - 2.2). The pressure spike magnitude was obtained by using the Joukowsky relation and the water velocity immediately before the bubble collapse was complete.

Because the interface condensation rate was one order of magnitude lower than the wall condensation rate, the calculated water hammer boundary

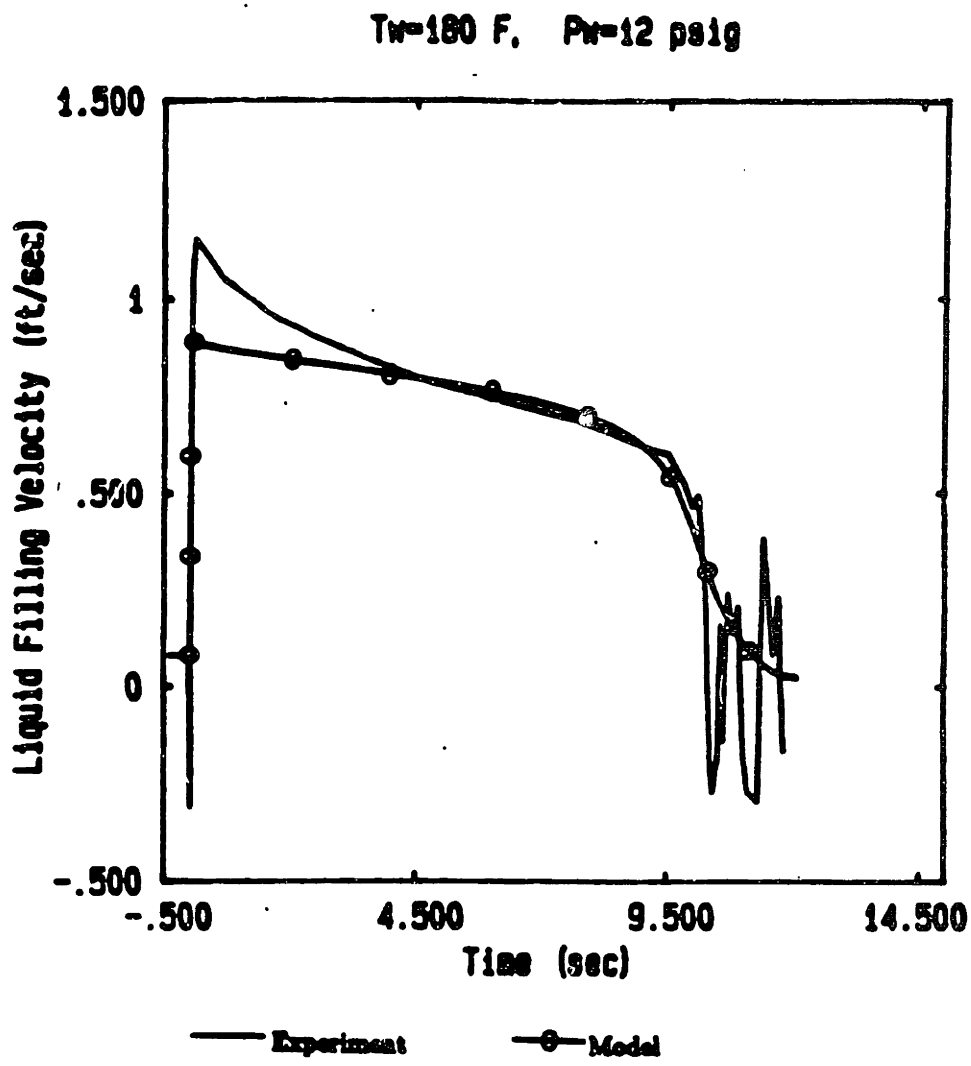

FIGURE - 2.2 Comparison between the calculated velocities and the experimental ones. Source -> (6)

did not depend on the water subcooling. This confirmed what Chou observed in his vertical up pipe tests.

Vertical Down Single Pipe (Filled from the Top) Theory

Chou's (6) flow visualization sketch for this geometry is reproduced in figure - 2.3. Chou hypothesized that a water hammer would occur when the liquid velocity was greater than the bubble rise velocity. In other words, the steam bubble could not escape (See the high filling rate flow visualization sketch - figure - 2.3). From the drift flux model (20), the bubble rise velocity can be expressed as:

$$U_b = C_o.(U_{ls} + U_{gs}) + C_1.\sqrt{\frac{\rho_l - \rho_s}{\rho_l}.g.D} \qquad \text{eq(2 - 5)}$$

Using Martin's results (21) (For a 2" pipe -> $C_o = 0.9$ and $C_1 = 0.6$) and the fact that at the transition U_{gs} and U_b are equal to zero, Chou found the following correlation to predict the water hammer boundary for this pipe geometry (D = 2").

$$U_{ls} = -0.67.\sqrt{\frac{\rho_l - \rho_s}{\rho_l}.g.D} \qquad \text{eq(2 - 6)}$$

Short Horizontal Pipe Theory

In an horizontal pipe two types of water hammers can occur. We called the first one the final water hammer. It is due to a steam bubble that is trapped at the end of the filling process. If the condensation is intense enough a water hammer can then result. We called the second type the intermediate water hammer. Its initiating mechanism is the transition from

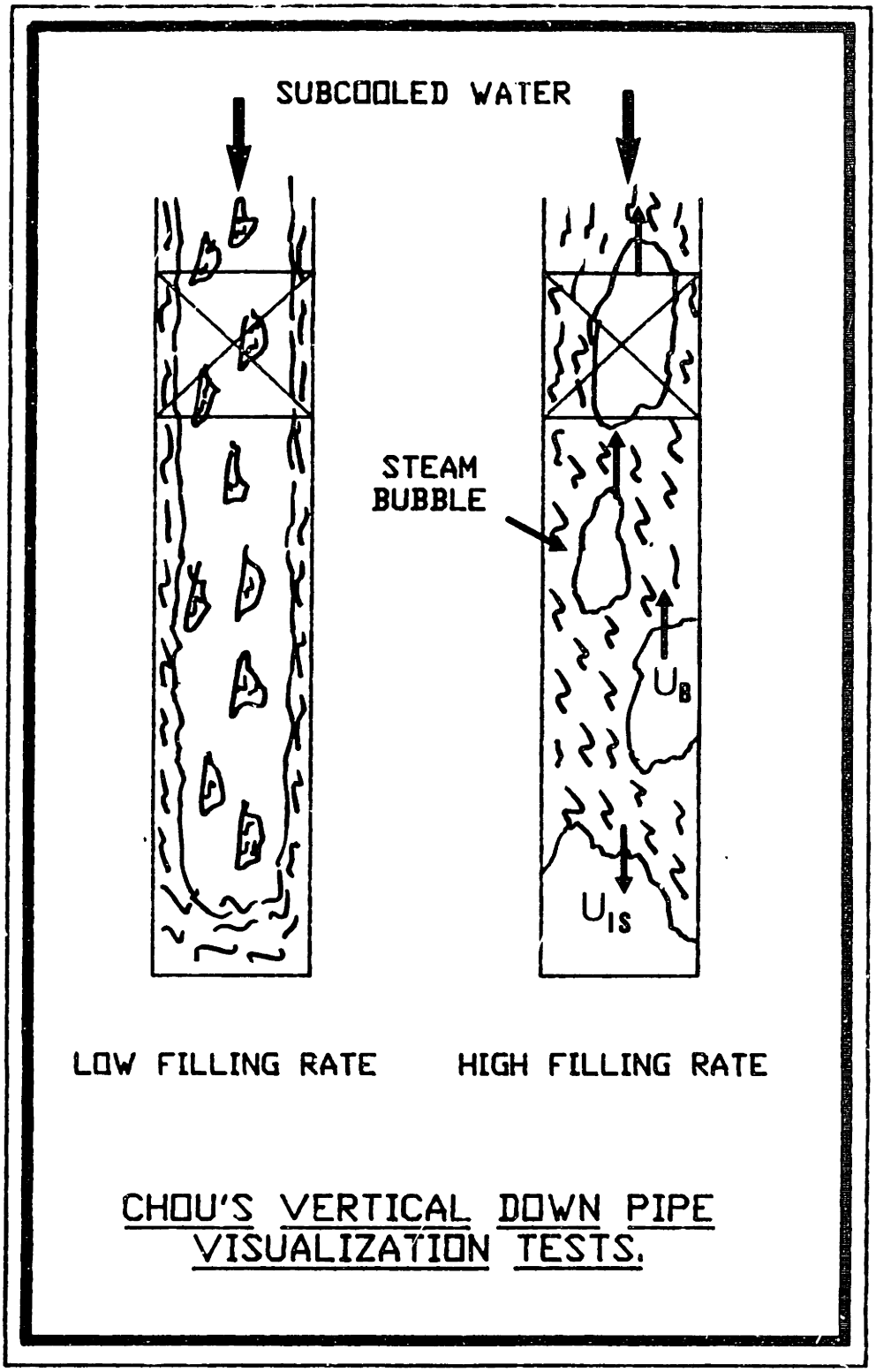

FIGURE - 2.3 Chou's flow visualization for the vertical down pipe tests. Based on source -> (6)

stratified to slug flow (see also Bjorge (16)). This transition is normally induced by the flow of steam above the water interface. After the slug is formed, condensation depressurizes more one side of the slug. The pressure differential created in this way accelerates the slug. An intermediate water hammer will often occur when the slug is forced to stop or pass through a bend.

Chou's (6) theory deals with the intermediate water hammer in a short (pipe length less than 48.D) leveled horizontal pipe.

When the pipe runs full no intermediate water hammer can occur. Wallis et al (22) proposed that the Froude number (Fr) value should be used to predict when an horizontal pipe will run full. Chou suggested that, for this condition, Froude should be equal to one. This correlation can be written as:

$$U_{ls} = \sqrt{g.D} \qquad \text{eq(2 - 7)}$$

Chou observed that the most limiting mechanism for the slug formation, in a short leveled horizontal pipe, was the water surge that would occur when the propagating water wave reached the pipe end. A sketch of his visualization tests is reproduced in figure - 2.4. Notice that, although a slug was also formed, the transition to slug flow was not induced by the steam flow.

The criterion used to establish the intermediate water hammer boundary was: The limiting water filling rate was the one that would cause a water surge to touch the top of the pipe wall (see figure - 2.4). Chou calculated this limit by using available methods of open-channel hydraulics (For instance, see Chow's book (23)). For a 2" pipe the calculated critical velocity was 0.46 ft/s.

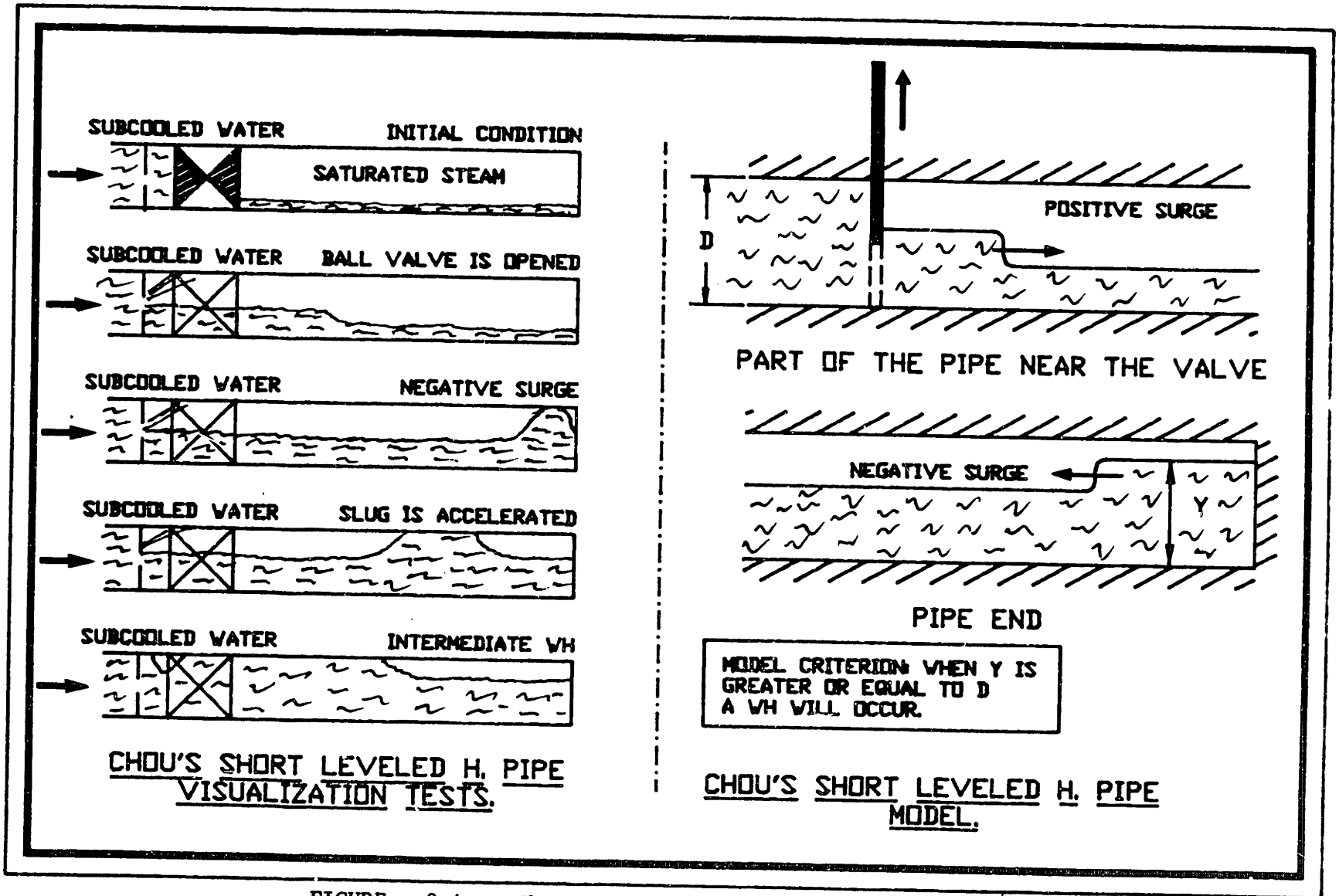

FIGURE - 2.4 Chou's short horizontal pipe - Visualization and model. Based on source (6)

This Work's Initial Idea

The initial hypothesis of this work was that Chou's (6) simple pipe theories could be used to determine the boundaries of the safe (no water hammer) filling rates of piping systems of complex shape. This would be done by determining the envelope of the more restricted theories of each pipe section of the complex arrangement. Figure - 2.5 illustrates this idea.

Consider a pipe arrangement made of two vertical pipe sections (with lengths L1 and L2) and a short leveled horizontal pipe, as the cartoon in the top right corner of figure - 2.5. The single pipe limiting theories are represented in this figure as lines 2, 3 and 4. According to Chou's theories: 1) Filling velocities above line 3 will cause water hammers in vertical pipes (2") which induce pressure spikes greater than P1; and 2) Filling velocities between lines 2 and 4 will cause a intermediate water hammer in the short leveled horizontal pipe.

Observing figure - 2.5 and assuming P1 to be the greater acceptable pressure in the system, it is clear that the safe region is under line 4. If the acceptable pressure were such that the vertical limit would lie above the running full limit (for a pressure P2), a second water hammer safe region would appear between lines 1 and 2.

The following chapters will show that a long leveled horizontal pipe theory is still needed in order to use this initial idea.

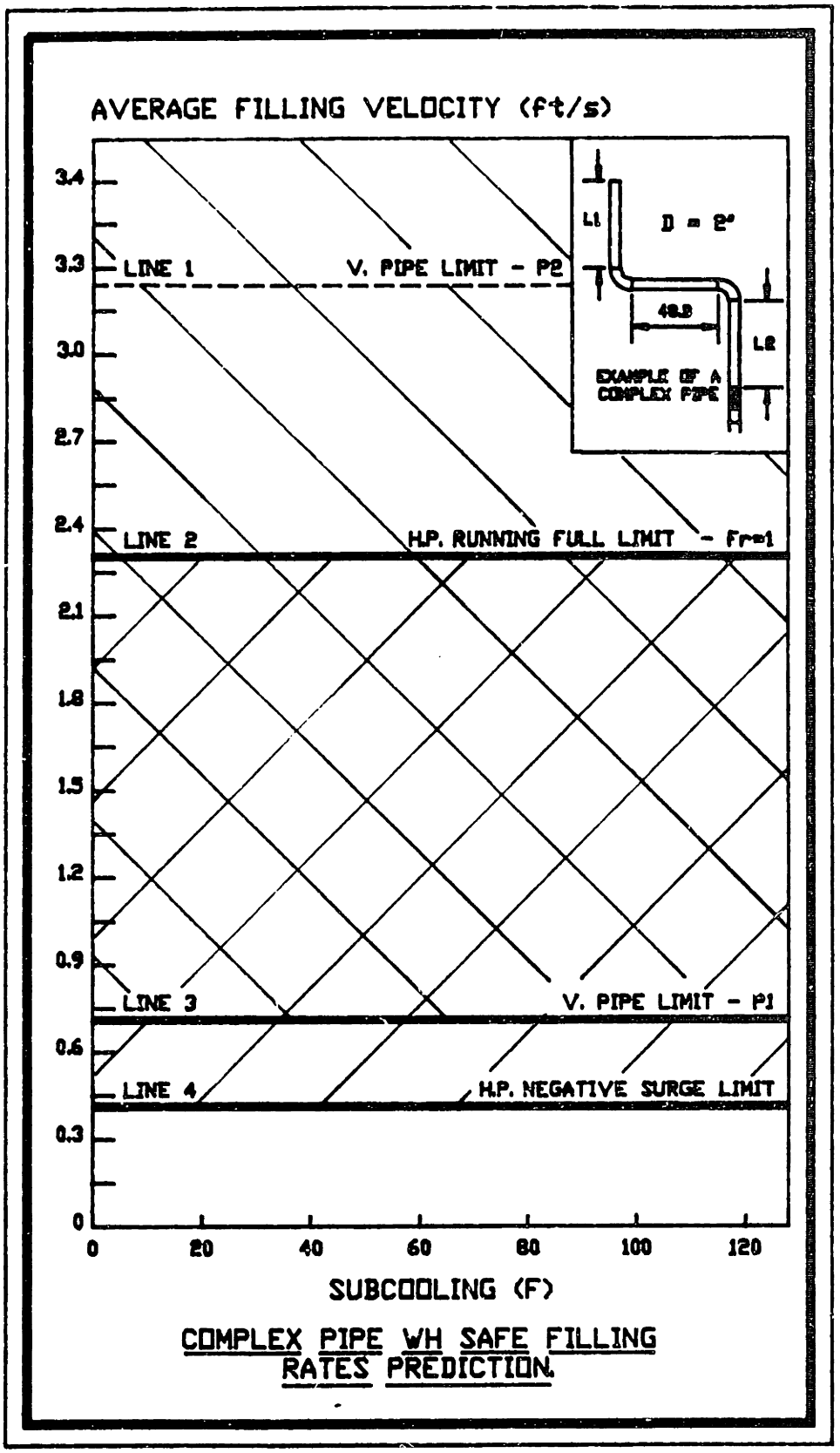

FIGURE - 2.5 Example of the initial idea of using the simple pipe theories to predict filling rates for pipes of complex shape.

CHAPTER - 3

LONG HORIZONTAL PIPES - SAFE FILLING LIMITS, FILLING STRATEGIES AND FORCE SIGNATURES

3.1 Motivation

As stated previously in section 1.2, one of the main objectives of this work was to check whether or not Chou's (6) simple pipe filling theories could be used to predict the safe filling limits for a complex piping system. In order to test this hypothesis, a series of "L" shaped pipes were tested and their stability maps were constructed, as it will be described in chapter 4.

It turned out that, except for the "L" in the vertical plane filled through the vertical leg, the leveled horizontal sections of these piping arrangements are what limit the possible water hammer safe filling rate. Moreover, for the "L" shaped pipes with short leveled horizontal sections, the filling velocities associated with the stability boundary are nonexistent or so small they cannot be used in any practical application. However, from physical reasoning, there might exist a filling rate that, although inducing a water hammer, will not cause any damage to the pipe or its supports. This idea will be elaborated in the following sections.

For single, short, and truly leveled horizontal pipes ($L \leq 48.D$) (see section 2.2 or Chou's thesis (6)), it was observed that the most limiting water hammer mechanism is due to the formation, at the dead end of the pipe, of a reflected wave which touches the top of the pipe wall. The calculation

derived from this observation gives 0.46 ft/s as the maximum filling rate for a 2" pipe. This value should not differ much when the dead end is replaced by a 90 degrees bend, as in a "L" shaped pipe. The explanation for the nonexistent or very small water hammer boundary for "L" shaped pipes is that short leveled horizontal sections, when connected to other pipe sections, behave like long horizontal pipes ($L > 48.D$), as will be shown in chapter 4.

From the above and the fact that Chou did not try to find ways of filling long horizontal pipes, it is clear that a filling theory for a long leveled horizontal pipe is still needed. This will be the first goal of our work.

The initiating water hammer mechanism, in this case, is a water slug that is formed when in stratified flow, due to the countercurrent flow of steam induced by condensation further up stream.

Bjorge (16) in order to study this phenomenon, constructed an apparatus that consisted of an horizontal pipe connected to a steam filled tank. Subcooled water could be introduced at the pipe end opposite to the tank, in a controlled manner. The water would fall into the tank after passing through a weir. Consequently, it was possible to find a relation between the water flow rate and the water depth inside the pipe, by using the critical flow theory (Fr=1 at the overfall). He could also increase the inlet water flow rate slowly, obtaining in this way a quasi steady state condition before the slug formation event. Not to mention the necessity that Bjorge had to use a multiplier (2,5) in one of Bankoff and Kim's (18) direct-contact condensation correlations (In order to make his model match

his experimental data), the transient characteristic of the injection of subcooled water into a steam filled pipe makes Bjorge's work not applicable for our present case. This will become more clear in the following sections.

Other important related studies are the ones from Block et al (12) and Saha et al (13). In these studies the authors have proposed models to describe the slug dynamics, leaving the steam condensation rate as a parameter to be defined by the user. But this direct-contact condensation rate is still itself a subject of research. Consequently, the prediction of water hammer safe filling rates for long leveled horizontal pipes is, up to now, an unresolved question.

It is clear, at this point, that the extrapolations of single pipe theories to complex piping systems is only possible if a way of dealing with long horizontal pipes is found. In the present study two approaches were employed to solve this problem. The first was to experimentally find ways to fill a long horizontal pipe avoiding the slug water hammer event. The second approach was through conservative calculations find filling rates that although causing water hammer, no real damage could be done to the pipes or its supports. As it will be explained in the following sections the first approach was successful, whereas the second gave filling rates values that were too small to be used.

3.2 Apparatus Description and Test Procedure

Apparatus Description

A sketch of the equipment for the long horizontal tests can be seen in figure - 3.1. It consisted basically of a 24 gal (≃ 92 l.) fiber glass insulated tank and two fiber glass insulated pipe sections made of 2", schedule 80 pipe (1.939" ID X 2.375" OD). Each pipe section had a length of ≃ 48.D (short horizontal pipe).

The pressure inside the tank could be varied and maintained constant throughout the test by the use of an air regulating valve (Watts Fluidair Inc - model M) and a 80 psi manometer (US Gauge/≃ 1 psi precision). As can be seen in figure - 3.1, steam could be admitted upstream the ball valve and purged through the tank vent valve. This had two purposes; 1) Bring the tank water to the desired temperature, and 2) Remove the air that comes with the fresh tap water.

In order to measure the flow rate, an orifice with a variable reluctance differential pressure transducer (P4) (Validyne model-DP 15 - 0.25% FS accuracy) installed across it was used. The orifice was positioned between two straight sections (30 in before and 27 in after) to guarantee fully developed flow before and after it (see (24)). When a slug was formed, it would travel against this orifice, producing a visible depression on its recorded trace. A second transducer (P3) (Validyne model-DP 15) was used to monitor the steam pressure inside the pipe and the water hammer due to the final trapped steam bubble. The signals of these transducers were

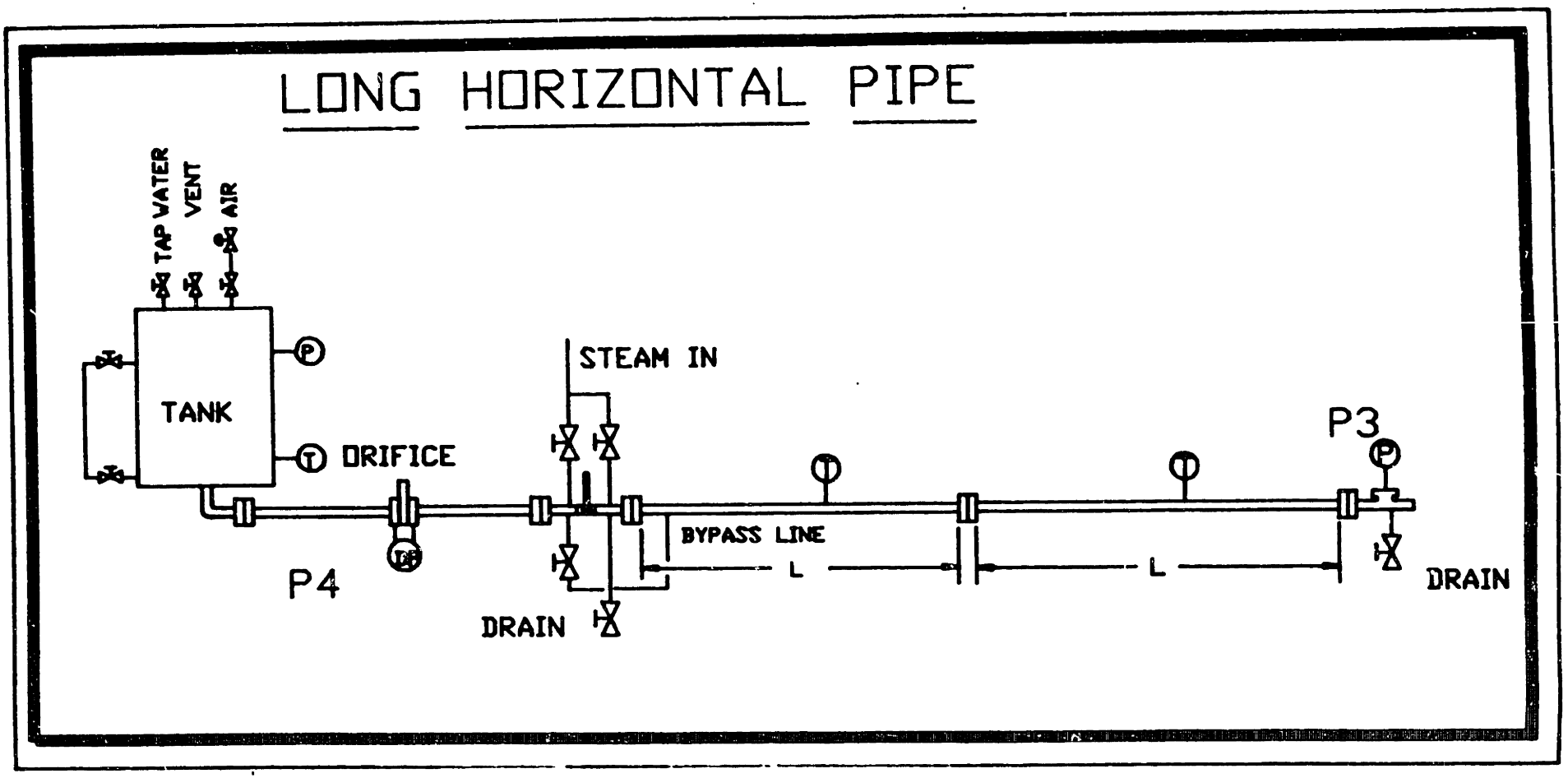

FIGURE - 3.1 Experimental apparatus used in the long horizontal pipe tests. The distance L is ≈ 48.D (short pipe limit), where D=2 in.

conditioned at Validyne CD 15 amplifiers and fed to an IBM PC AT with a Metrabyte AD board (Dash 16). This computer would then be run with the Unkelscope data acquisition software (25) (maximum number of sampled points = 4096 - minimum sampling interval for only one input = 2 ms). The transducers were calibrated against a dead weight instrument before every test series.

Water and steam temperatures were monitored at the locations indicated in figure - 3.1. The thermocouples were Omega K-type (Nickel-Chromium X Nickel-Aluminum) (precision $\pm$ 5%). The temperature values were read using an Omega 216 & A digital thermometer.

The possibility of injecting the subcooled water laterally was also provided. In order to do this a 0.5" bypass copper tubing was installed with a 0.5" ball valve. This way of injecting the water decreases its forward momentum.

Test Procedure

In general the tests were done according to the following sequence:

- The tank was partially filled with tap water;

- With the ball valve closed the tank water was brought to the desired temperature by passing steam through it;

- The tank was pressurized by opening the air valve and adjusting the regulating valve set point;

- The 2" pipe test section was drained by using MIT steam ($\simeq$ 60 psig and typically 10^{-4} air fraction);

- Before closing the steam valve, steam was allowed to flow through the pipe, in order to remove any remaining air;

- The drain valves were closed when the steam temperature was about 220°F. The test section remained with a small positive pressure;

- Subcooled water was injected into the 2" pipes by opening the ball valve;

- The pressure traces were recorded using the data acquisition system;

- The decision if a water hammer had occurred was based in a surge pressure/driving pressure ratio criterion.

3.3 Water Hammer Boundary Maps

3.3.1 Leveled Long Horizontal Pipe

Before starting the test description, it seems helpful to restate the intermediate and final water hammer classification (Chou (6) gives nice visualization drawings for these types of events).

- Intermediate water hammer is caused by a slug that travels towards the subcooled water injection point. What forces the slug motion is the pressure difference across the slug which is caused by steam condensing at the subcooled, injected water. A pressure spike is generated when the slug hits a dead end or junction (In this present case it would hit the orifice plate). The well-known Joukowsky relation, $\Delta P = k.\rho.c.\Delta V$, predicts the pressure spike magnitude. The initiating mechanisms can be either: 1) A negative surge that touches the upper pipe wall; 2) Or what is more likely, a slug that is formed because of the counterflow of steam induced by condensation upstream. This event is indicated as a pressure reduction on transducer P4 trace (see figures - 3.1, 3.4 and 3.5). It occurs before the orifice differential transducer voltage returns to its initial value, or the no flow condition. This is the reason for calling it an intermediate water hammer. No indication appears in transducer P3 trace because the pipe is not full at this occasion, and the steam space absorbs the reflected pressure wave.

- Final water hammer is caused by a steam bubble that is trapped when the pipe is almost totally full. The steam bubble then collapses violently

due to condensation on the surrounding liquid and pipe wall, as long as the filling velocity is above a certain threshold. This steam bubble can be located in any position along the pipe length. The indication of this event will appear better in the trace of transducer P3, as P4 is a differential transducer (The two sides of the transducer see the same pressure spike).

Figures - 3.2 and 3.3 are the stability maps for these two types of water hammer events. The points marked with crosses represent tests were a water hammer occurred (Of the type indicated at the top of the map). The points marked with a small black square represent tests with no water hammer event (Of the type indicated at the top of the map). This nomenclature will be used throughout this work.

Observing figure - 3.2, its is possible to conclude the following:

- In contrast to the short leveled horizontal pipe, the negative surge is not the limiting water hammer mechanism for the long leveled horizontal pipe. The line marked 1 represents the critical value of 0.46 ft/s, which is the filling velocity that the negative surge would touch the upper wall of a 2" pipe;

- Unless the subcooling is less than 20°F, no lower water hammer free boundary was found, although velocities as low as 0.1 ft/s were tried. Bjorge (16) previously established that the intermediate of water hammer should be characterized by three regions (two free of water hammer and one with water hammer). Above a certain filling rate, the one that makes the pipe run full, no water hammer is possible by obvious reason (first free region). For filling rates lower than a certain critical value, the condensation induced counterflow of steam cannot generate pressure

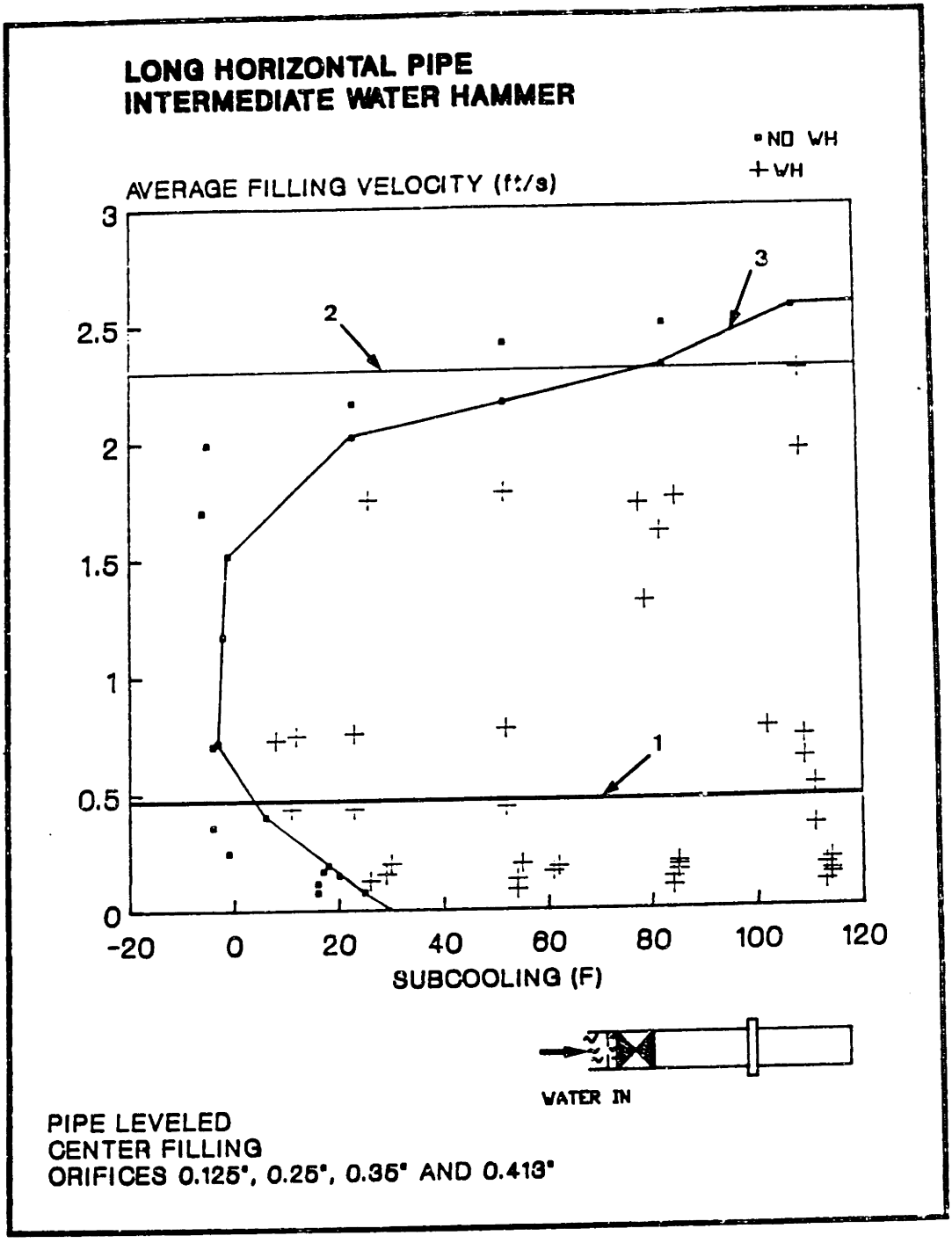

FIGURE - 3.2 Intermediate water hammer stability map for the long horizontal pipe (leveled).
Line-1 -> Short horizontal, single pipe theoretical stability boundary - 0.46 ft/s.
Line-2 -> Running full pipe limit - Fr=1 or average filling rate of 2.3 ft/s.
Line-3 -> Experimental stability boundary.

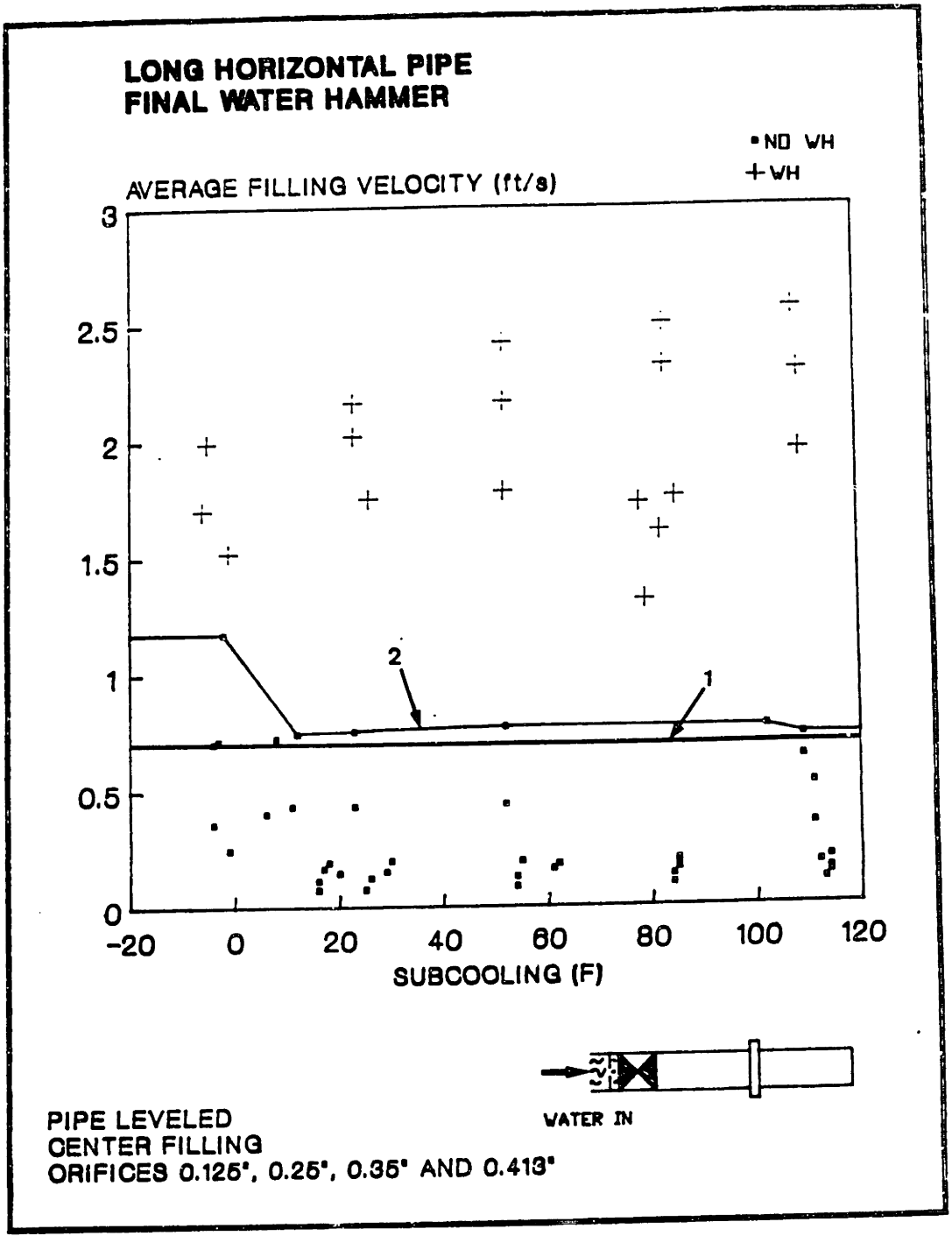

FIGURE - 3.3 Final water hammer stability map for the long horizontal pipe (leveled).
Line-1 -> Experimental vertical up, single pipe stability boundary - 0.7 ft/s.
Line-2 -> Experimental stability boundary.

instability waves (too small gas velocity) and, consequently, no water hammer will occur (second free region). Finally, the range of filling rates between the two previous critical values should be the intermediate water hammer region. It is important to remember that Bjorge only tested pipes that were approximately half full (his motivation was modelling the so-called steam generator water hammer). The difference, in this case, is that when the water distance to the upper pipe wall decreases, the necessary gas velocity to cause the slug transition also decreases. As these long pipes fill up through successive water layers, there is a point that, even for a very small filling rate, the counterflow of steam induced by condensation will be enough to cause the stratified-slug transition. This can be better understood by using Taitel-Dukler stratified-slug flow transition criterion (17), as it will be presented in section 3.4 - item 3

- Line 2 represents the running full pipe limit of Fr = 1 (for a 2" pipe V_{av} = 2.3 ft/s). The conclusion is that this criterion also works well for the long leveled horizontal pipe;

In figure - 3.3 Chou's (6) vertical up, single pipe, experimental water hammer boundary is drawn as line 1. The vertical up single pipe is used as a reference because it has the same physics of the long horizontal final water hammer. We also used Chou's experimental data, instead of his theoretical limit, because the transition from no water hammer to a water hammer event in our tests was not abrupt. It was necessary to use some personal judgement to decide how to classify a specific test. Using a surge/driving pressure ratio criterion, the most conservative boundary was always selected. It was not possible to establish a constant surge/driving pressure ratio (as in the

theory), and define in this manner the stability boundary. The conclusion reached, after observing figure - 3.3, is that the vertical up single pipe theory can be used as a limit for determining the long, leveled, horizontal pipe filling rate needed in order to avoid the final water hammer.

Comparing figures - 3.2 and 3.3, it is clear that the water hammer limiting mechanism for the long leveled horizontal pipe is the slug caused by the counterflow of steam induced by condensation. Except for introducing water at a higher temperature than the steam (negative subcooling), there is really no practical way of avoiding a water hammer in this configuration.

Figures - 3.4 and 3.5 are typical pressure traces of these tests. The depression in transducer P3 trace is caused by steam condensation. Figure - 3.5 illustrates well the fact that the intermediate water hammer is always present (The average filling velocity there was 0.185 ft/s). It is also apparent that, for very low velocities, the water hammer events should not cause any damage to the pipe or its supports (Observe that the depressions in P4 trace are small). In section 3.4 - item 3 we will try to establish a conservative damage safe boundary.

3.3.2 Long, Almost Horizontal, Inclined Up and Laterally Filled Pipe

The intermediate water hammer can be totally avoided if a long horizontal pipe is inclined by an angle of 0.5"/1' (Which is the standard slope used in power plant pipe construction, according to Swierzawki (26)), and the pipe is filled laterally from the bottom.

The apparatus of figure - 3.1 was used to prove experimentally the statement above. The only necessary modification was to incline up the

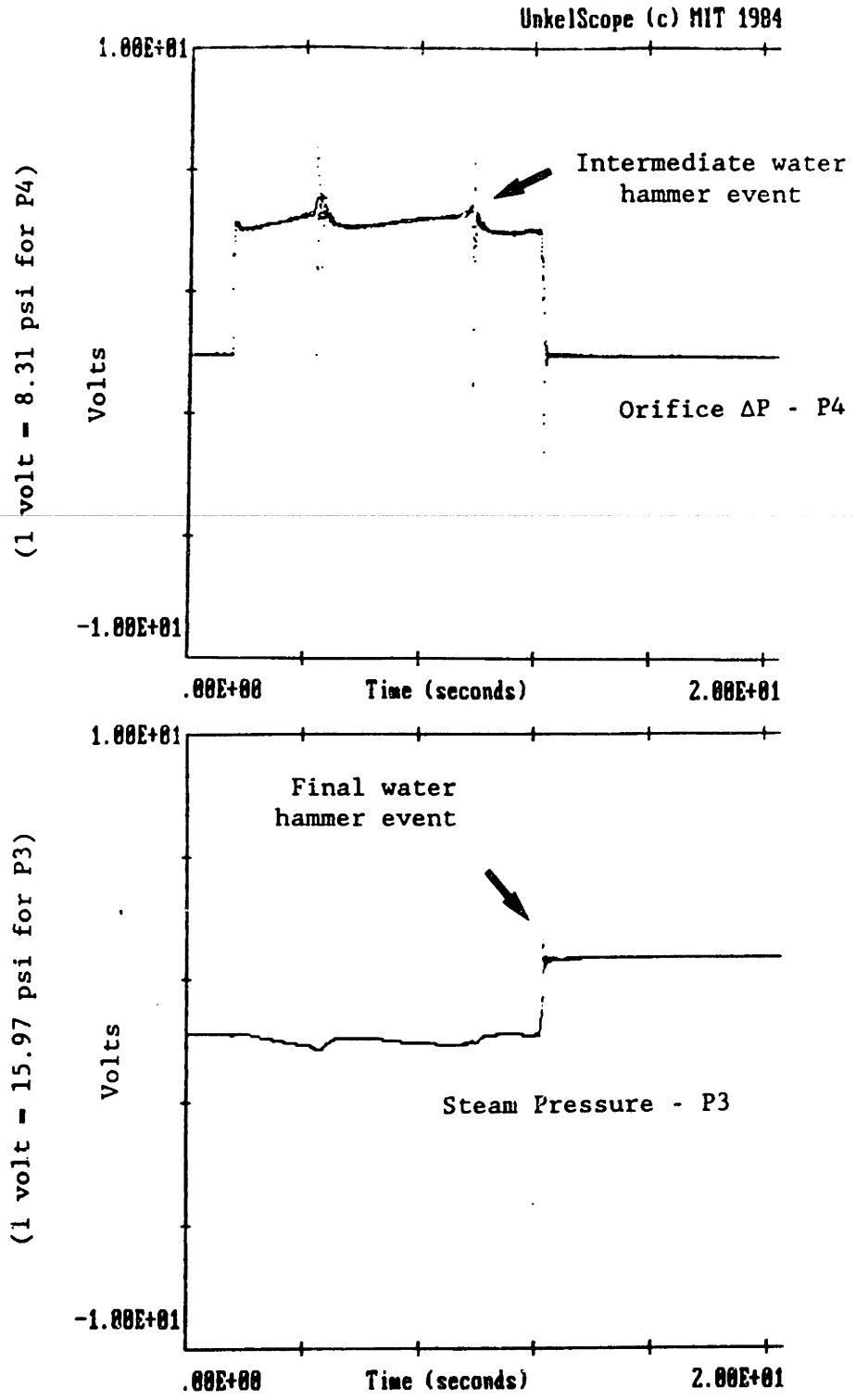

FIGURE - 3.4 Typical long horizontal pipe pressure response curves for a case with intermediate and final water hammer events.

Orifice 0.35 in - P_t=40 psia - T_w=146°F

T_{sub}=79°F - Av. Filling Veloc.= 1.31 ft/s .

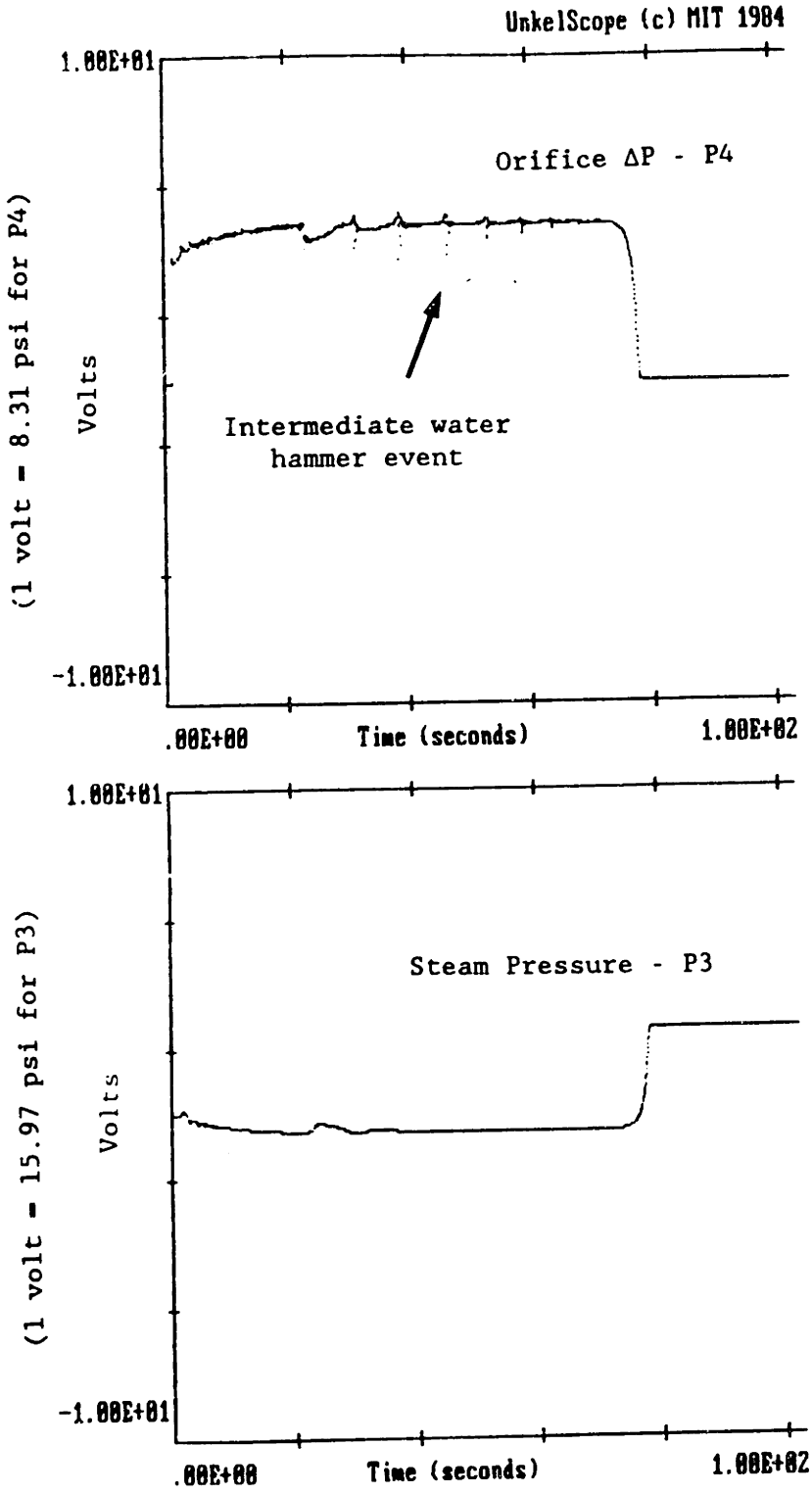

FIGURE - 3.5 Typical long horizontal pipe pressure response curves. This plot shows that even for very low filling rates the intermediate water hammer does not disappear.

Orifice 0.125 in - P_t=40 psia - T_w=142^{o}F

T_{sub}=85^{o}F - Av. Filling Veloc.= 0.185 ft/s ..

horizontal pipe test section.

The test procedure used was the same as for the long leveled horizontal pipe tests, which were already described in section 3.2. The only modification to this procedure was that the water was introduced by the copper tubing bypass line (see figure - 3.1).

The stability map resulting from such tests is shown in figure - 3.6. In figure - 3.8 typical pressure transducer traces are shown. No depression can be observed in transducer P4 trace. Indeed, these two figures demonstrate that no intermediate water hammer occurs in this configuration. What limits the water injection rate, in this case, is a filling velocity that can make the final trapped steam bubble collapse violently. Line 1, in figure - 3.6, is the vertical up single pipe experimental stability boundary (0.7 ft/s). The reasons to compare this type of water hammer with this experimental boundary were already explained in section 3.3 - item 1. Observing figure - 3.6, the conclusion is that the vertical up single pipe theory can be used to define a filling velocity so that no damage to the pipe or its supports will occur.

What is missing now is to explain why this occurs. It is important to point out that the presentation of the test results in this work does not follow the order they were done. We have chosen a sequence that will go from the simple pipe results to the complex piping systems ("L" shaped pipes). Previous to the tests just mentioned, we tried to fill five different "L" shaped pipes (see chapter 4), inclining their horizontal sections up and down and at the same time injecting the water axially and laterally. The explanation to be given is based on the experience gained with several

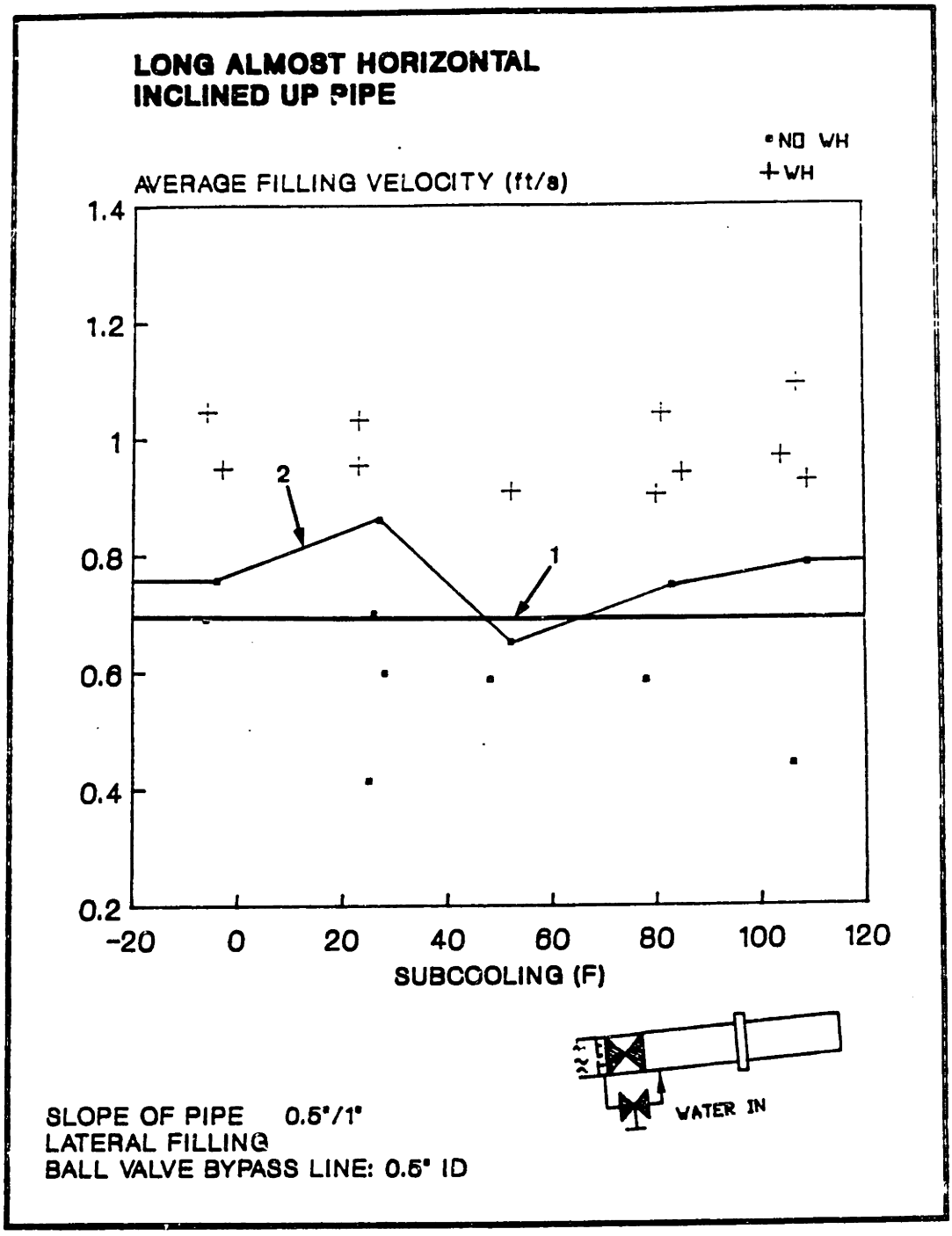

FIGURE - 3.6 Stability map for the long, almost horizontal , inclined up and laterally filled pipe.
Line-1 -> Experimental vertical up, single pipe stability boundary - 0.7 ft/s.
Line-2 -> Experimental stability boundary.

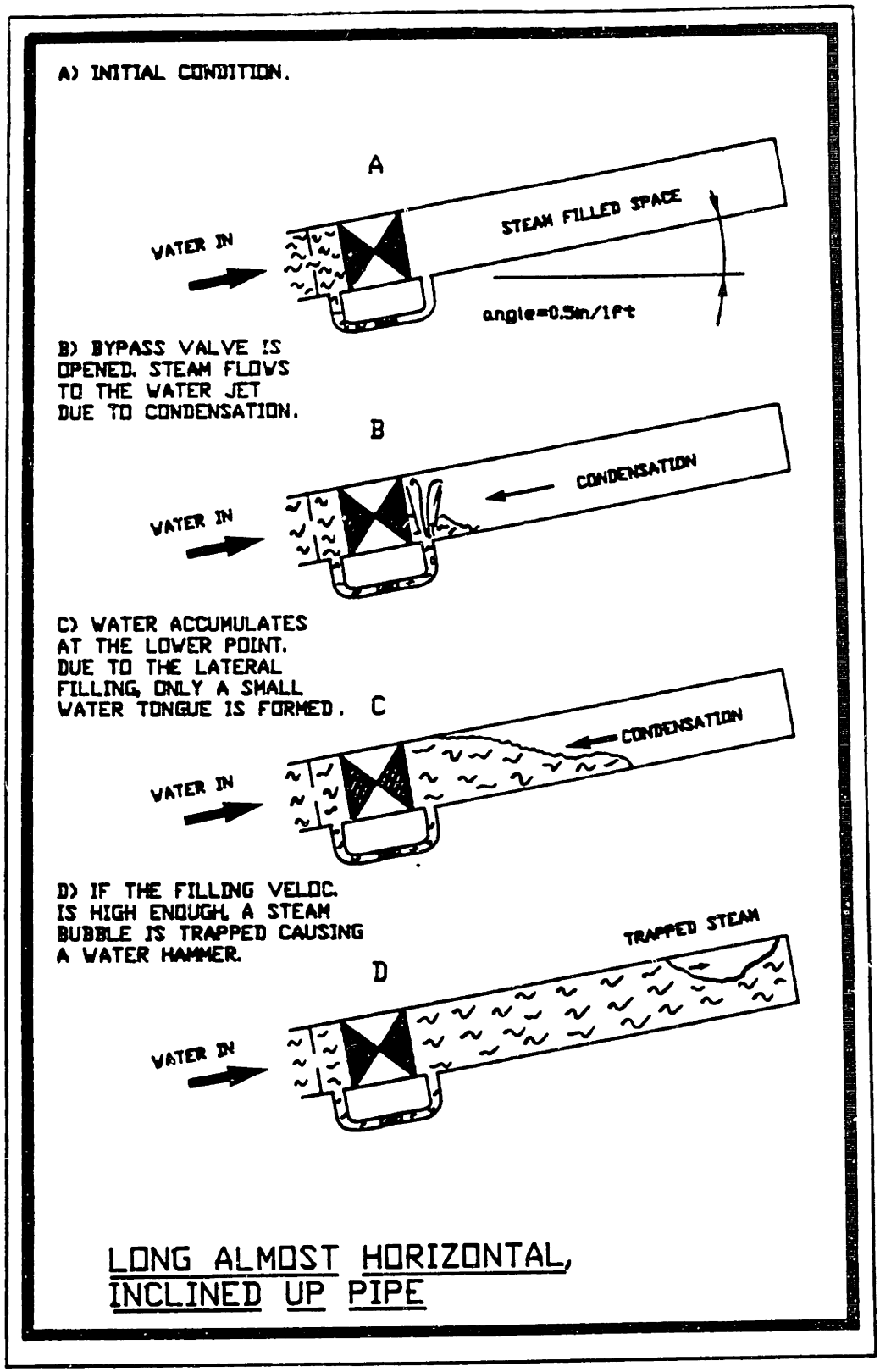

FIGURE - 3.7 Visualization tests for the long, almost horizontal, inclined up and laterally filled pipe.

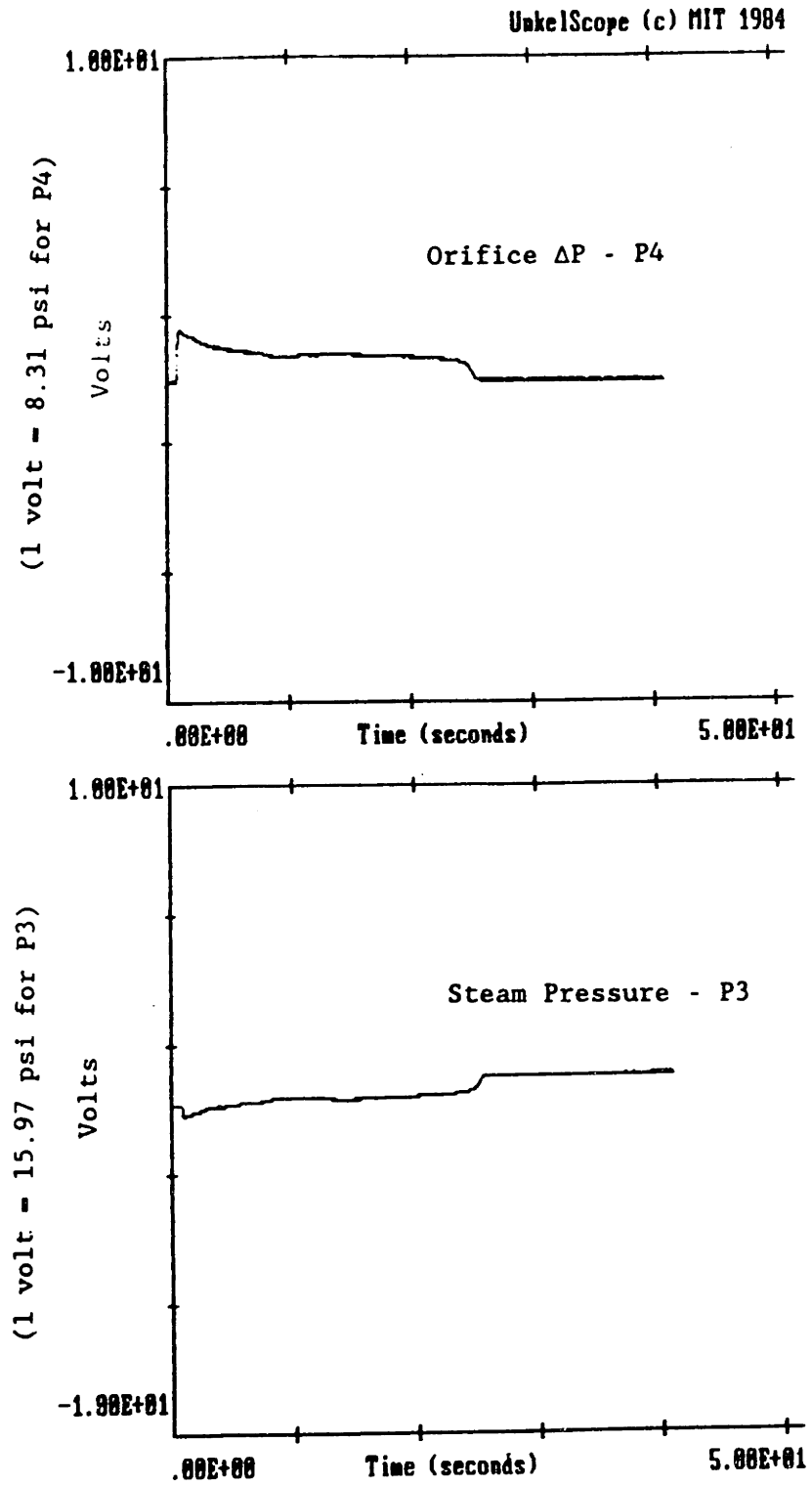

FIGURE - 3.8 Typical long, almost horizontal, inclined up and laterally filled pipe pressure response curves. The plot shows that with this configuration it is possible to avoid the intermediate water hammer.

Bypass line -> 0.5 in - P_t=13 psia - T_w=142^{o}F

T_{sub}=78^{o}F - Av. Filling Veloc.= 0.586 ft/s. .

filling and visualization tests.

As already said, the most critical intermediate water hammer for the long leveled horizontal pipe is caused by a slug generated by the counterflow of steam and water. The following influences this type of water hammer:

- When the distance between the water surface and the upper pipe wall is decreased, a smaller wave is needed to cause the stratified-slug flow transition. At the same time the gas area is smaller which, for a same condensation rate, gives a higher steam velocity. This increases the water steam interaction. The up inclination decreases this distance. Consequently, it will not be helpful to incline the pipe, unless the inclination is large enough to permit the water to accumulate at the bottom, maintaining the pipe full. The lateral injection has a similar effect in that it increases the inclination angle of the interface. This is because the wave front needs a larger height to compensate the loss of forward momentum, when the lateral filling is used instead of axial filling procedure.

- The steam that initially fills the pipe condenses rapidly, as soon as the valve is opened. A source of steam is needed to sustain the counterflow of steam necessary to cause the stratified-slug transition. A truly horizontal pipe cannot be totally drained, because of the surface tension. Tests with an electric probe (see section 4.2 - item 1) have shown that, after the pipe drainage ends, the depth of the remaining water inside a short leveled pipe can reach as much 0.5". When the pressure inside the pipe decreases due to condensation (see transducer P3 trace in figures 3.4 and 3.5), boiling immediately starts at the wall area that is wetted by the

remaining water pool.

If the pipe is totally drained the steam source is eliminated and the intermediate water hammer cannot occur. Inclining the pipe and injecting the water from the higher point (inclining down) totally drains the pipe. However, it is observed that in this case a thin water tongue wets the pipe as soon as the valve is opened. Because of this fact there is no advantage in inclining the pipe down. On the other hand, inclining the pipe and injecting the water from the lower point (inclining up) not only causes the wave height to be higher (which makes it more difficult to the steam to reach the surface), but also does not wet as much of the pipe as the downward inclination. This makes this last configuration less prone to the intermediate water hammer.

- Any procedure that causes a decrease in the condensation rate should be helpful. Steam is mainly condensed at the jet that is formed by the injected the subcooled water. Filling from the bottom an inclined pipe (inclined up) and introducing the water laterally decreases the condensation rate, because the water accumulates at the lower point insuring that the water jet will soon be entirely in contact with water and not steam. This decreases the condensation rate, as can be seen in figure - 3.8. Observe that after an initial dip, the transducer P3 trace continuously increases its value. Also, P4 trace shows that the filling velocity decreases along the test. This is because of the smaller condensation rate and increasing pressure in the steam bubble.

Consequently, the above explains why no intermediate water hammer occurs in a long, slightly inclined up pipe. Figure - 3.7 tries to represent

what was observed in the visualization tests carried out with this configuration. This figure just confirms what was already said. The visual experiments were preformed by changing the steel pipes to *LEXAN*, so that the filling process could be observed.

3.3.3 Long Horizontal Pipe Filled by Dividing it in Short Horizontal Sections

A second way that was imagined to fill a long leveled horizontal pipe was to inject the subcooled water through nozzles distributed along the pipe length, at distances $\leq$ 48.D. Figure - 3.9 is a scheme of the apparatus that was used. It is basically the same equipment used before with bypass lines that take the water to the marked points. The distance L was of $\simeq$ 48.D. The test procedure was the same as in section 3.3 - item 2.

The resultant stability map from these tests is drawn in figure - 3.10. Typical traces for transducers P4 and P3 are shown in figure - 3.11. No intermediate water hammer indication was detected by the transducers, as can be seen.

If a slug is formed it travels in the direction of the injection points, as already explained (see section 3.3 - item 1). As result, neither transducer would necessarily indicate this type of water hammer (Observe in figure - 3.9 the location of the injection points and of the transducers). However, during the filling period, no noise or pipe motion, which is normal in a water hammer event, was felt. Moreover, if a water hammer occurs in this configuration, two slugs would crash against each other at the injection points. This phenomenon would not bring any imbalance to the

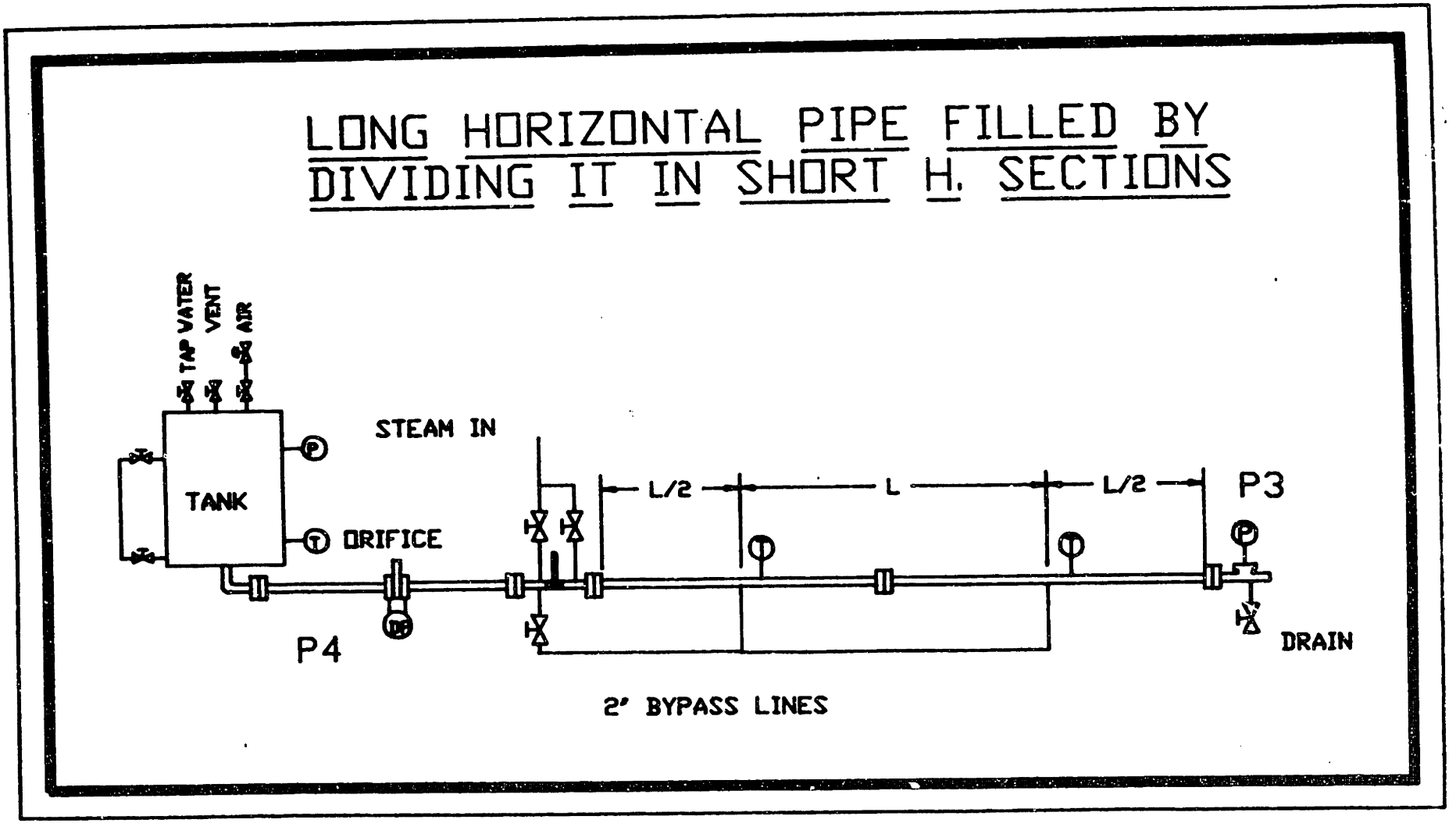

FIGURE - 3.9 Experimental apparatus used in the tests of the long horizontal pipe, filled by dividing it in short horizontal sections. The distance L is ≃ 48.D (short pipe limit), where D=2 in.

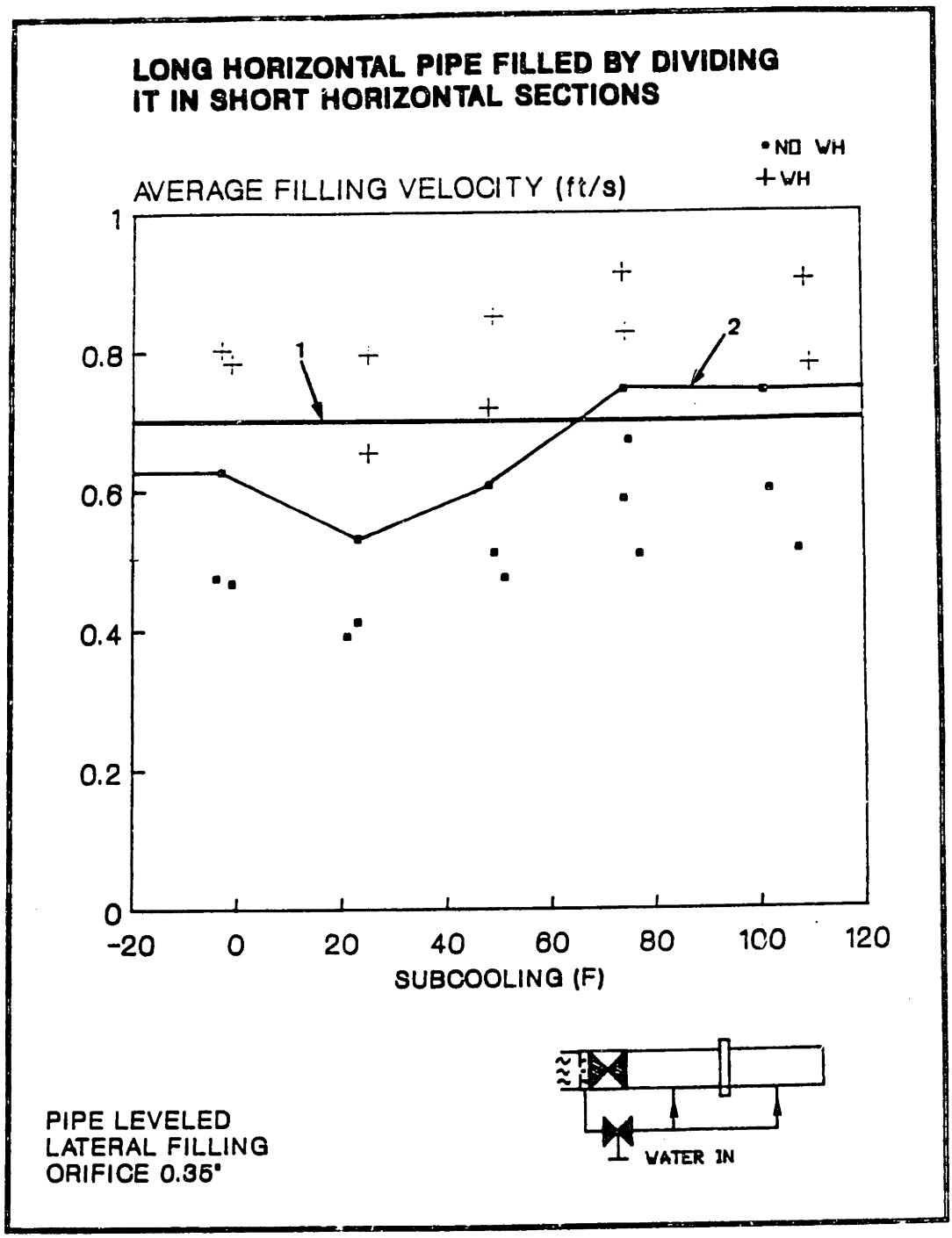

FIGURE - 3.10 Stability map for the long horizontal pipe, filled by dividing it in short horizontal sections.
Line-1 -> Experimental vertical up, single pipe stability boundary - 0.7 ft/s.
Line-2 -> Experimental stability boundary.

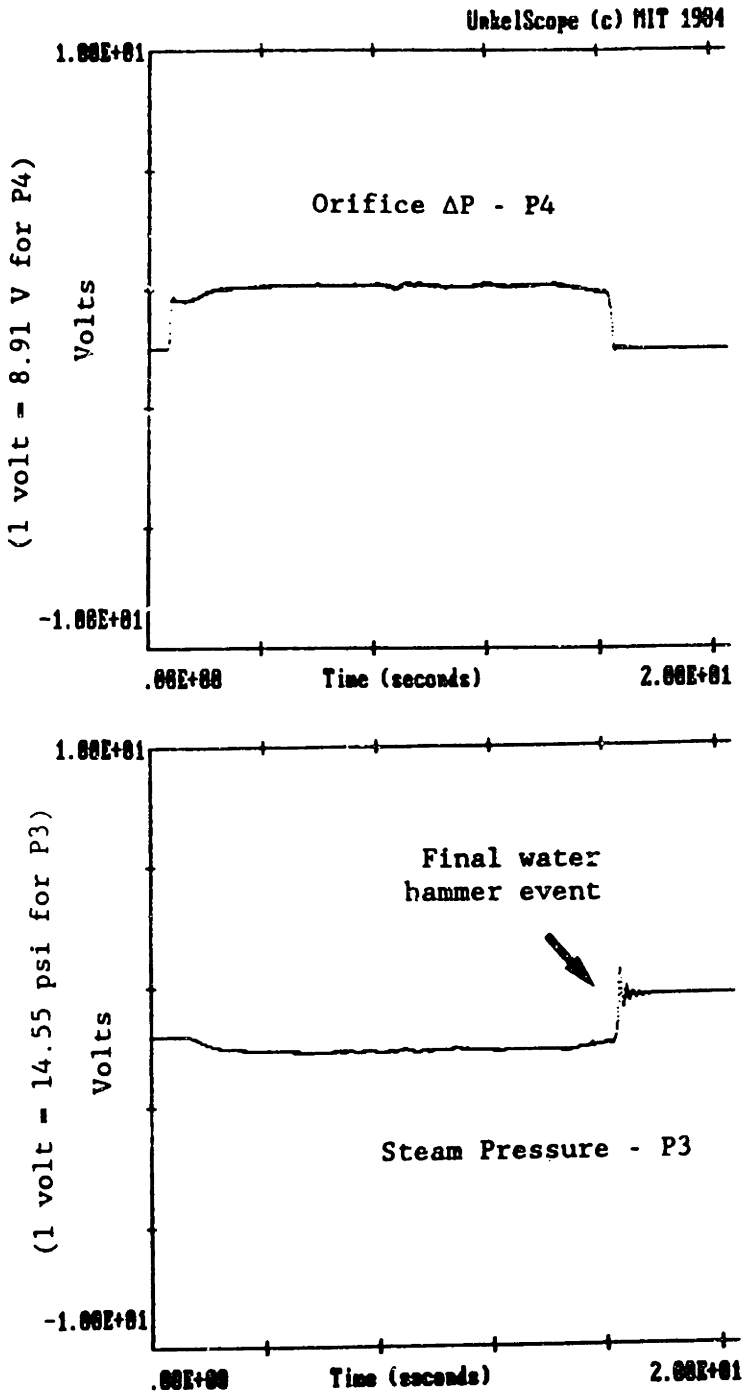

FIGURE - 3.11 Typical long horizontal pipe, filled by dividing it in short horizontal sections, pressure response curves. This procedure permits eliminate the intermediate water hammer.

Orifice 0.35 in - P_t=22 psia - T_w=150°F

T_{sub}=74°F - Av. Filling Veloc= 0.914 ft/s.

piping arrangement and nothing would happen to the pipe supports. A water hammer normally affects first these structures. The pipe would only suffer an increase in its hoop stress magnitude, because of the internal pressure spike. In order to damage the pipe a very high pressure would be necessary, which is very improbable with the distance selected between the injection nozzles.

The line 1 in figure - 3.10 is the vertical up single pipe experimental stability boundary. The reasons to use this data as reference are the same as in section 3.3 - item 1. The final conclusion is that, for this pipe configuration, we can use the vertical up single pipe theory to limit the filling rate. Doing so, no damage can be done to the pipe or its supports. It seems even possible to increase the distance between the injection points.

3.4 Theoretical Models for the Pressure and Force Signatures for Several Geometries

3.4.1 Bubble Collapse Tests

In section 3.2 two methods of filling long horizontal pipes were found. Both avoid the intermediate water hammer. The final water hammer can also be prevented if the filling rate is small enough. In this case, any trapped steam bubble will condense slowly enough, not causing any damage. However, the two methods require modifications to the already existent piping systems. Consequently, a calculation procedure that could establish a safe filling rate boundary would be extremely useful. As direct-contact condensation correlations of steam on water in the range of interest of the water hammer problem are still a research subject, conservative condensation independent models were tried in this section.

The first attempt was to find a simple method to predict the pressure spike and impulse due to the collapse of a steam bubble of known volume and shape. The driving pressure was used as parameter.

A scheme of the apparatus used during the bubble collapse tests is shown in figure - 3.12. It is basically the same equipment as that used in the long horizontal pipe tests. The modifications were that: 1) The length of the horizontal section was decreased to 7.75 ft ($\simeq$ 48.D); 2) The transducer was a Kistler model 701-A running with a Kistler model 566 charge amplifier and 3) A bend, a 2" ball valve and a vertical 2" pipe section were added. The test procedure was to:

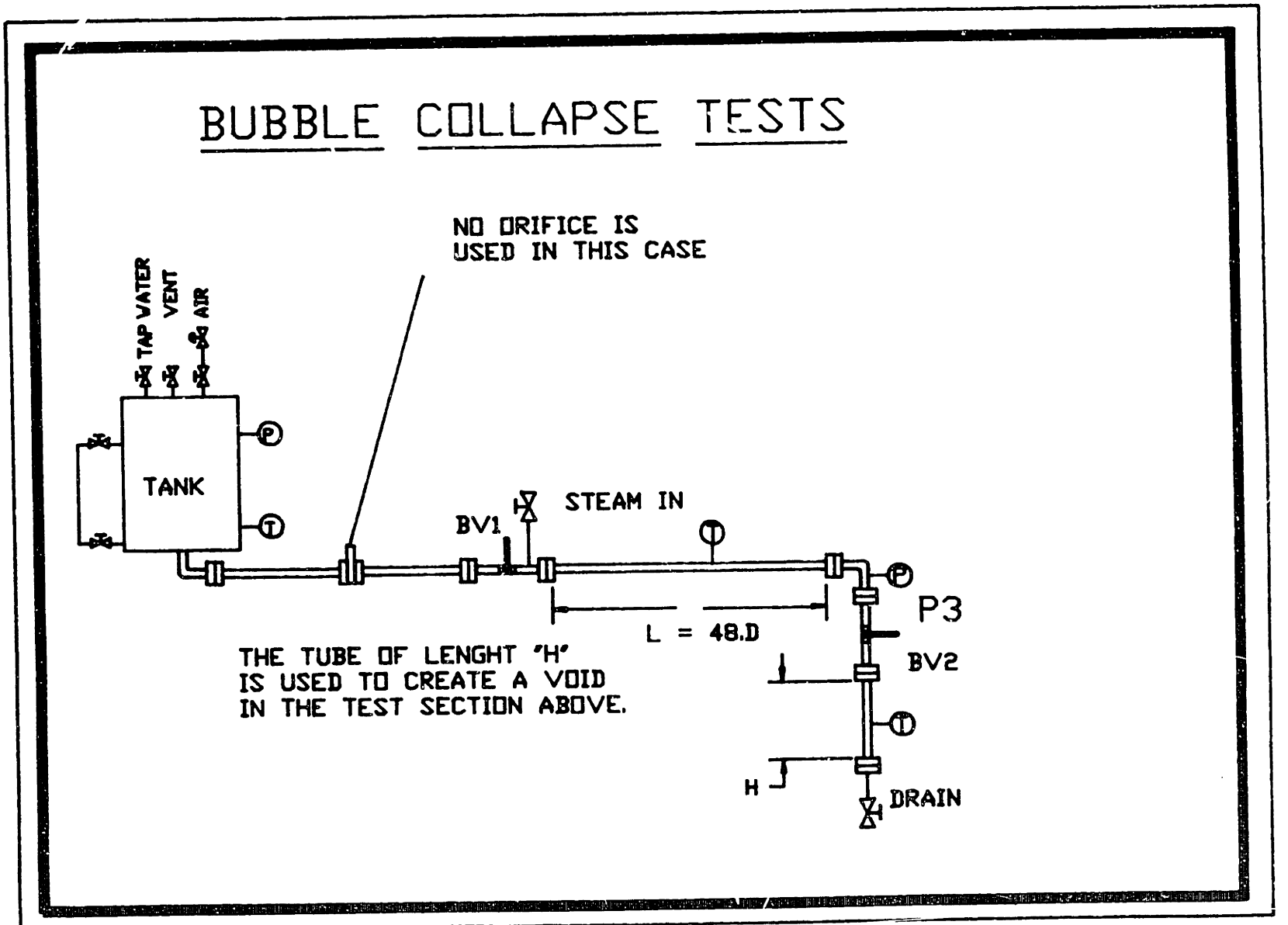

FIGURE - 3.12 Experimental apparatus used in the bubble collapse tests.

- Heat the water inside the tank, to 220^{o}F, by passing steam through valve BV1 to the tank vent valve. Valve BV2 remained closed at this time;

- The valve BV1 was closed and the test section was drained with the use of steam. Steam was allowed to flow for some time, in order to remove any remaining air. The drain valve was shut when the steam temperature was at $\simeq$ 220^{o}F ($P_o \simeq$ 17.2 psia). This made sure that no air would flow back into the pipes;

- Valve BV2 was then closed. The horizontal pipe section was filled with 220^{o}F hot water by opening valve BV1. After allowing some time to the system to settle down, valve BV1 was closed;

- A steam bubble of known volume was created in the horizontal section by opening valve BV2. Water would fill the vertical pipe section, whereas the steam that was originally in the vertical pipe would flow to the space that was voided in the horizontal pipe;

- Valve BV2 was closed and the driving pressure was set to the desired value by adjusting the air regulating valve. The bubble would then be forced to collapse by opening valve BV1. The resultant pressure spikes were then measured with the data acquisition system (sampling interval of 0.2 ms).

A typical pressure trace of these tests is shown in figure - 3.13. The range of the measured pressure spikes for 24.7 and 34.7 psia and three different values of vertical pipe length (H) are plotted in figures - 3.16 and 3.17.

In the next item a simple conservative calculation procedure to predict the pressure spike magnitude and final impulse is proposed.

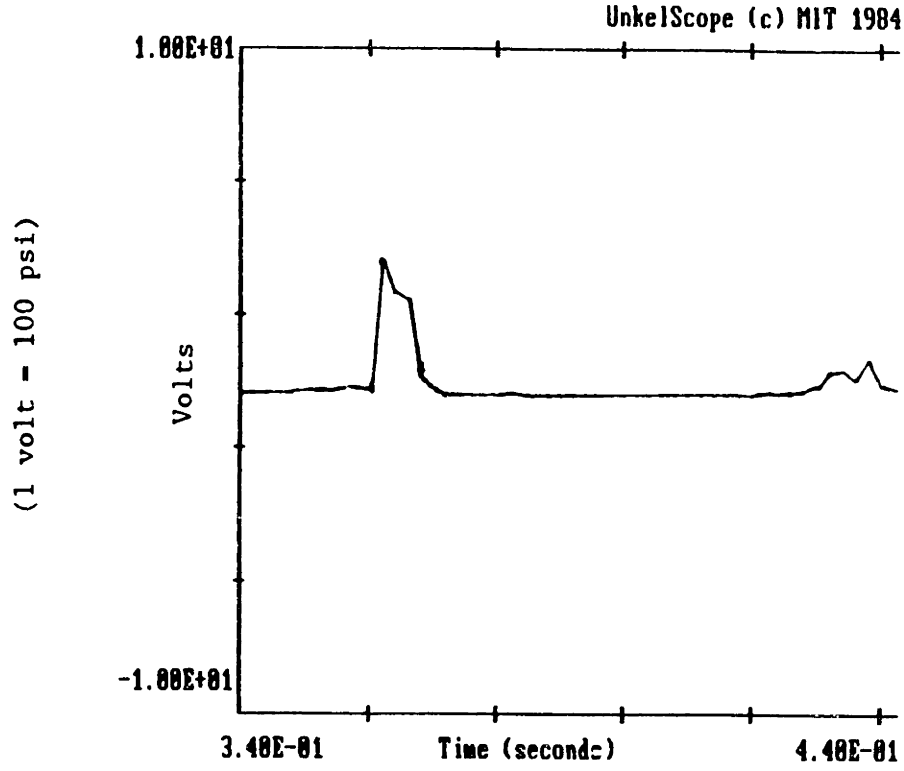

FIGURE - 3.13 Bubble collapse tests typical pressure response curve.

P_t=20 psia - T_w=213°F - T_{sub}=-10°F - L≃ 48.D.

3.4.2 Bubble Collapse Simple Conservative Model

The model which is proposed below simply solves the momentum equation and uses the final water velocity in the Joukowsky relation to calculate the pressure spike magnitude. The transmitted impulse is calculated assuming that the loading pulse is rectangular, and that the duration time is equal to the time for the pressure wave reach the tank and come back as a depressurization wave (As previously proposed by Block et al (12)). Figure - 3.14 illustrates the control volumes, assumptions, and terms used in the formulation below. See also detail "B" of figure - 3.14 on the top of figure - 3.15.

Definition of Terms

y -> length of the totally water filled pipe, starting from the tank interface;

y_o -> initial length of the totally water filled pipe, starting from the tank interface (before opening the ball valve). For this case y_o=6.8 ft;

x -> length of the totally water filled pipe, starting from the ball valve;

V_o -> velocity inside the water pool in front of the water plug;

V -> water plug velocity;

A -> pipe cross section area;

A_l -> liquid area = $(1-\alpha).A$;

A_g -> steam area above the water pool = $\alpha.A$; $(A_g = A_s)$

D -> pipe diameter;

α -> void fraction = A_g / A;

P_l -> tank pressure.

$-\dot{x}$ -> velocity of the water plug front;

$-H$ -> voided pipe length;

$-H_l$ -> water pool height;

$-H_g$ -> steam height; $(H_g = H_s)$

$-L$ -> length of the horizontal pipe - 7.75 ft;

$-P_o$ -> steam space pressure - initially = 17.2 psia;

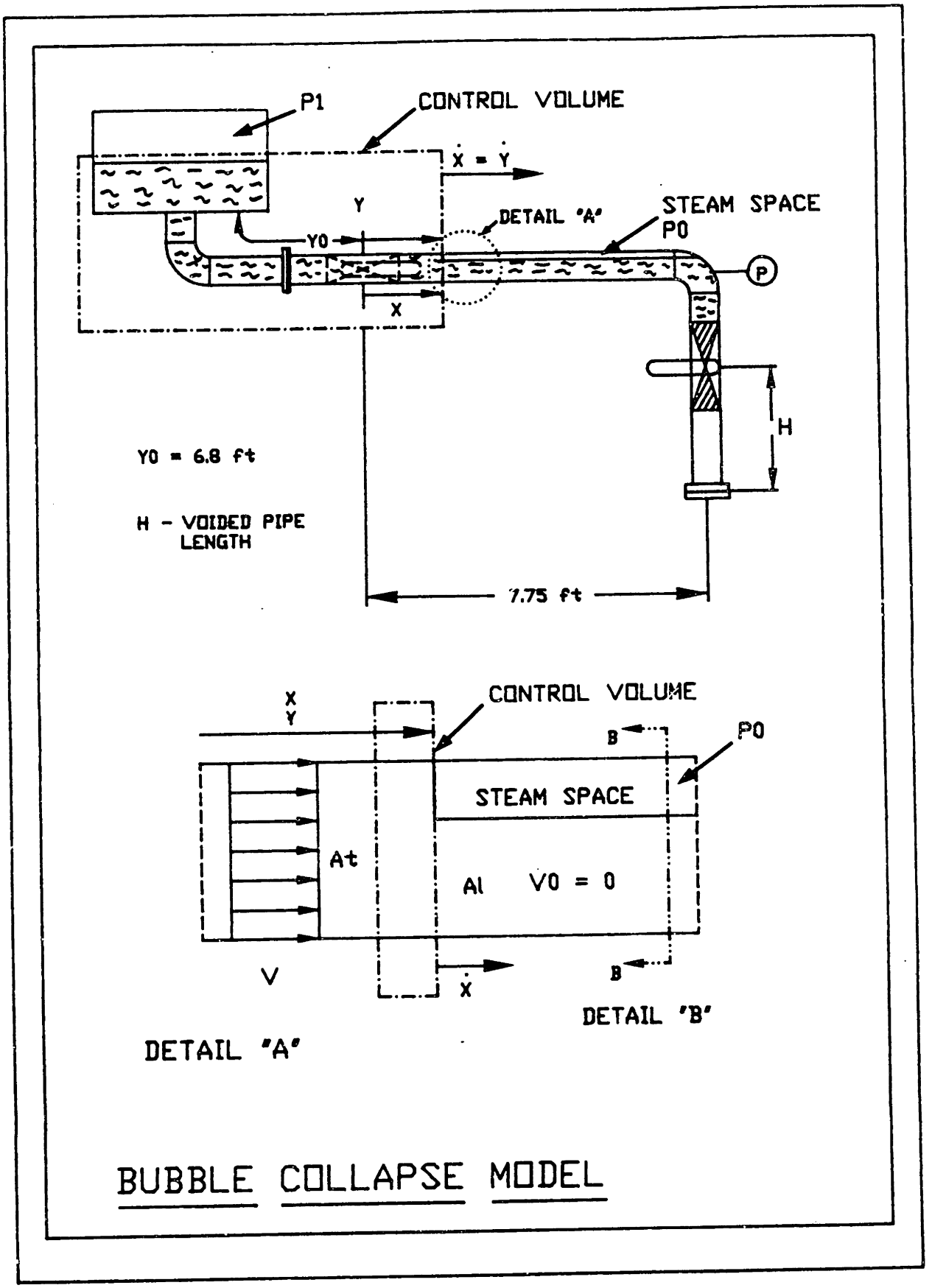

FIGURE - 3.14 Scheme of the bubble collapse model.

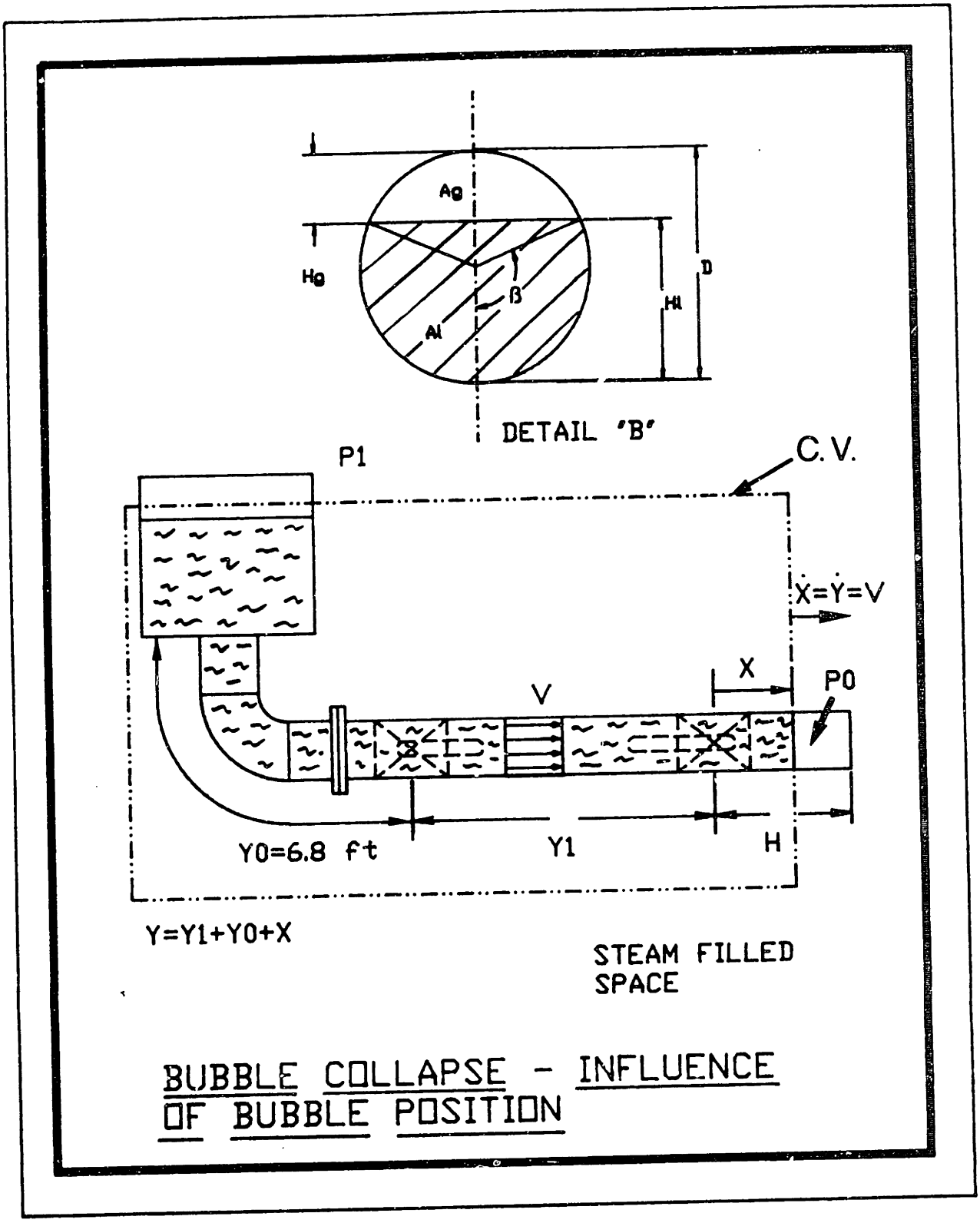

FIGURE - 3.15 Detail "B" of figure 3.14 and scheme to study the influence of the bubble position on the final pressure spike.

Model Assumptions

- The velocity inside the pipe, upstream of the plug front, is assumed constant and equal to V;

- The velocity inside the water pool (V_o), in front of the water plug, is assumed equal to zero;

- The condensation is assumed high enough so that P_o is equal to zero, as soon as the ball valve is opened.

Geometric Relations

From the definitions above:

$$\boxed{y = y_o + x} \qquad \text{where } y_o = 6.3 \text{ ft} \qquad \text{eq(3 - 1)}$$

The void fraction (α), the steam and water areas and the water pool height can be calculated by using the following geometric relations (see figure - 3.14 and the detail "B" in figure - 3.15):

$$\boxed{\alpha = \frac{H}{L}} \qquad \text{eq(3 - 2)}$$

$$\beta = \cos^{-1}\left(1 - \frac{2.H_1}{D}\right) \qquad \text{eq(3 - 3)}$$

and

$$A_1 = \frac{2.\beta - \sin(2.\beta)}{2.\Pi} \times \left(\frac{\Pi.D^2}{4}\right) \qquad \text{eq(3 - 4)}$$

Mass Conservation

Applying the mass conservation principle to the moving control volume defined in the detail "A" of figure - 3.14, it is possible to write:

$$(\dot{x} - V) \times \frac{\Pi.D^2}{4} = (\dot{x} - V_o) \times A_1 \qquad \text{eq(3 - 5)}$$

But as V_o is assumed equal to zero,

$$\boxed{V = \alpha.\dot{x}} \qquad \text{eq(3 - 6)}$$

or, $\overline{V = \alpha.\dot{y}}$ eq(3 - 7)

Momentum Equation

$$\frac{d}{dt}\int_{cv} \rho_l.V.dv + \int_{cs} \rho_l.V.(\vec{V}_{rel}.\vec{da}) = A.\Delta P.g_c - A.\Delta P_{fric.} - A.\Delta P_{loc.} \quad \text{eq(3 - 8)}$$

As can be seen in figure - 3.14, the defined control volume is assumed fixed inside the tank (air/water interface) and moves, at the right, with the plug front. As except at the plug front there is no mass flux in or out, it is possible to simplify the above equation to:

$$\frac{d}{dt}(\rho_l.y.V) - \rho_l.V_o.(\dot{x} - V_o).\frac{A_1}{A} = \Delta P.g_c - \Delta P_{fric.} - \Delta P_{loc.} \quad \text{eq(3 -9)}$$

Using equation (3 - 7), the fact that $V_o = 0$ and the sum of all $\Delta P_{loc.}$ (see appendix - A), the momentum equation can be written as:

$$\overline{\frac{d}{dt}(\rho_l.\alpha.\dot{y}.\dot{y}) = (P_1 - P_o).g_c - f.\frac{y}{D}.\rho_l.\frac{V^2}{2} - 0.94.\rho_l.\frac{V^2}{2}} \quad \text{eq(3 - 10)}$$

where:

$f = \frac{64}{Re}$ for the laminar regime and $\frac{0.164}{Re^{.25}}$ for the turbulent regime

When a water plug crashes against a water column, the coefficient k of the Joukowsky relation ($\Delta P = k.\rho.c.\Delta V$) should be equal to $\frac{1}{2}$ (see appendix - B). However, in this present case, the dead end reflected wave reaches the measuring spot before the depressurization wave (that comes from the tank) arrives. This reflected wave has twice of the magnitude of the one formed at

the crash moment. Consequently, the coefficient to be used here is k = 1. The water sound velocity can be calculated by using equation (3 - 11) (see Wylie and Streeter (27)).

$$c = \frac{\sqrt{\kappa_1/\rho_1}}{\sqrt{1 + [(\kappa_1/E)(D/e)]c_1}} \simeq 4500 \text{ ft/s} \qquad \text{eq(3 - 11)}$$

where:

κ_1 -> bulk modulus of elasticity of the water - 316,000 lbf/in^2

E -> steel Young's modulus of elasticity - 28.5×10^6 lbf/in^2

e -> pipe wall thickness

ρ_1 -> water density - 62 lbm/ft^3

c_1 -> constant that depends in how the pipe movements are restrained for this present case $c_1 = 1 - \mu/2$

μ -> steel Poisson's ratio - 0.265

Equation (3 - 10) was solved numerically. The initial conditions were $y_i = 6.8$ ft, $x_i = 0$ and $V_i = 0$. In figures - 3.16 and 3.17, the pressure spike values predicted by the model are plotted for driving pressures (P_1) of 34.7 and 24.7 psia, respectively. The steam pressure (P_o) is assumed equal to zero and equal to the steam saturation pressure (17.2 psia). Observing the two figures, it is clear that this simple model agrees better with the experimental results when the driving pressure has a higher value. Even for the same driving pressure, the model more closely predicts the real pressure spikes when P_o is equal to the steam saturation pressure. The explanation to this fact is that the assumption that the steam pressure goes to zero, as soon as the ball valve is opened, is too conservative. When higher driving pressures are used, the choice of P_o has a smaller impact on the final

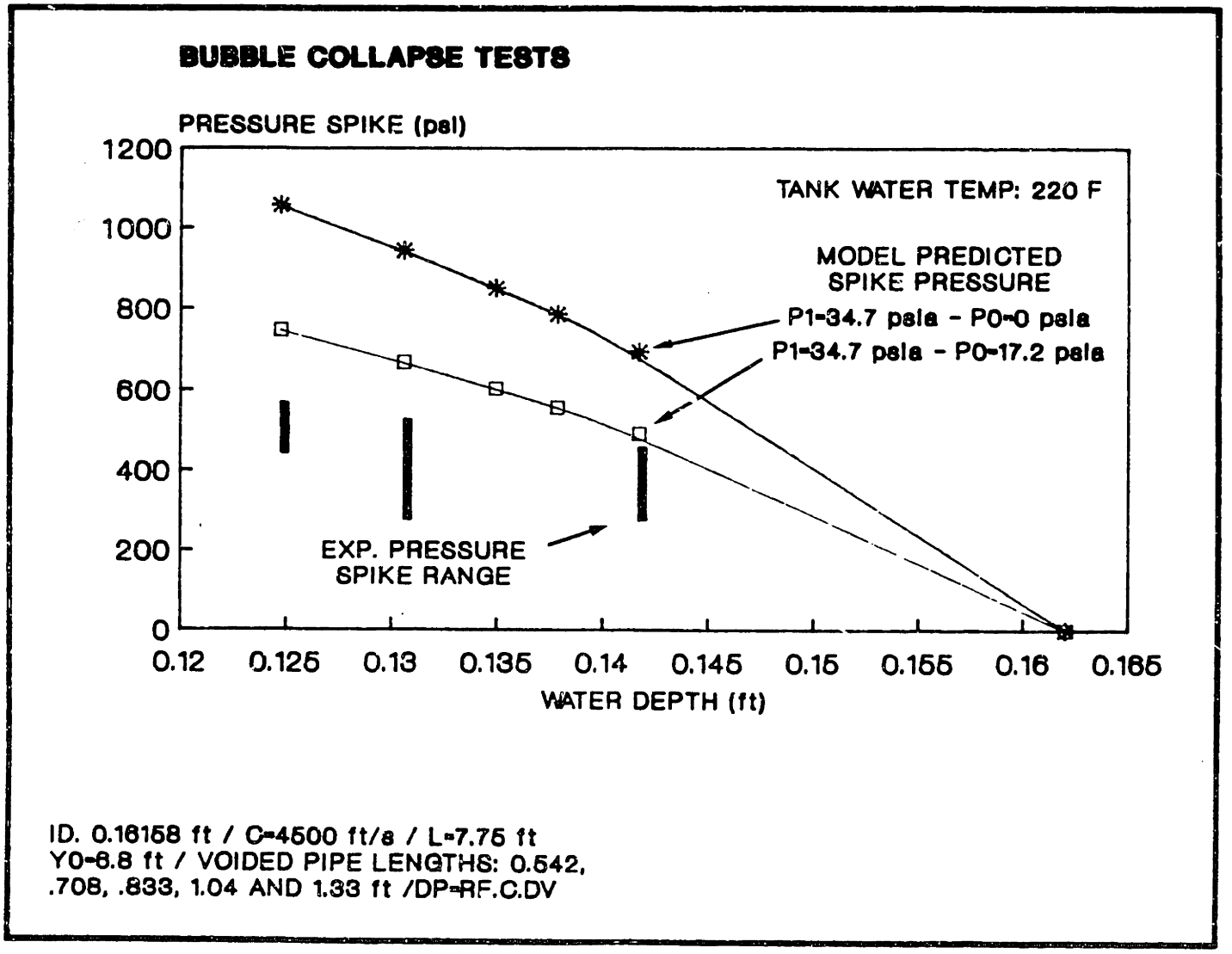

FIGURE - 3.16 Comparison of the model predicted spike pressures and the experimental pressure ranges. $P_t=P_1=34.7$ psia.

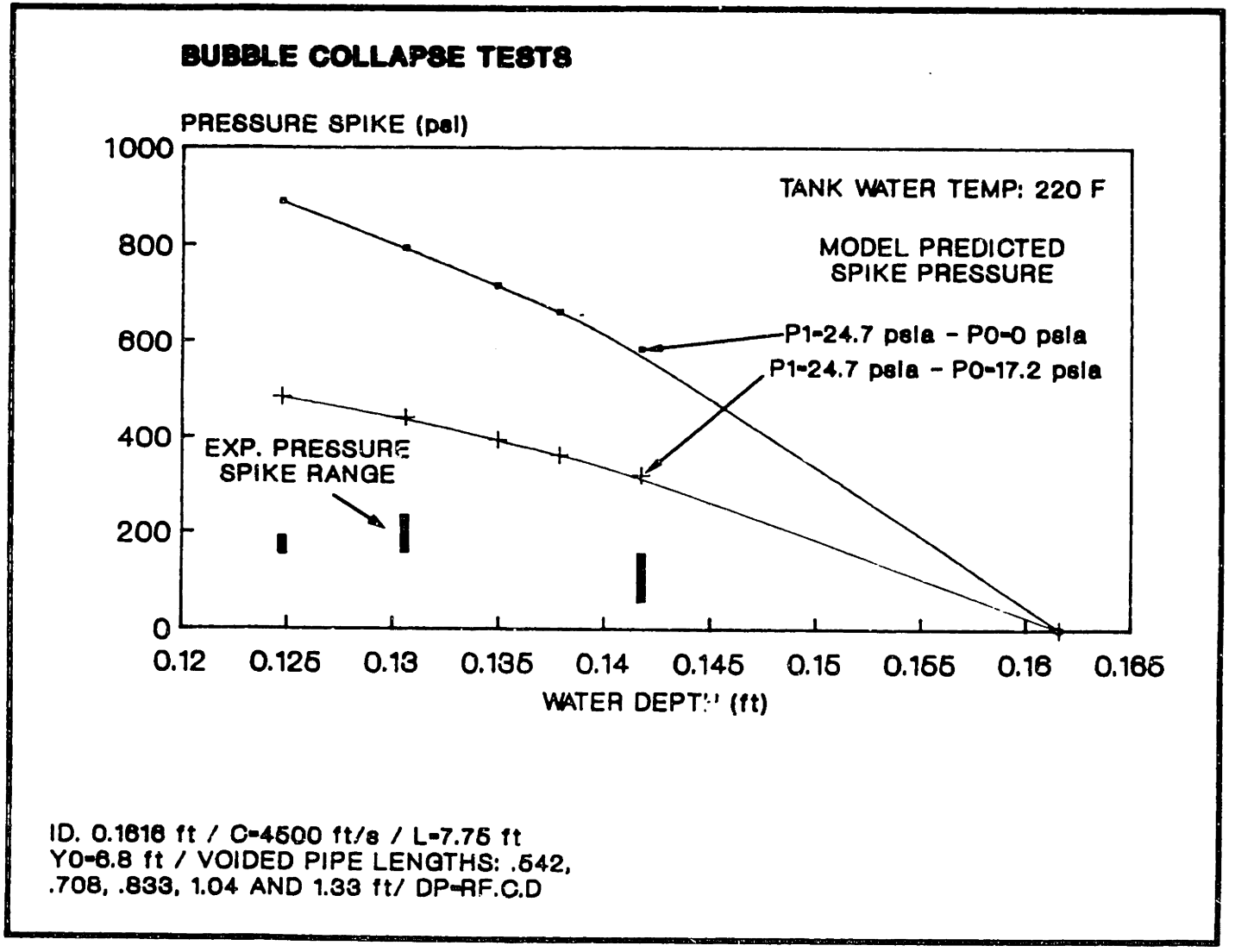

FIGURE - 3.17 Comparison of the model predicted spike pressures and the experimental pressure ranges. P_t-P_1-24.7 psia.

answer. However, the proposed simple analytical model is still an upper boundary of the possible pressure spike ranges. Moreover, when the driving pressure is reasonably greater than P_o, it gives a good agreement with the experimental results.

Figure - 3.18 shows a typical evolution of the plug velocity as function of the distance from the tank. From this drawing, it is possible to conclude that inertia forces are important to this type of problems. The plug velocity is still increasing when the plug reaches the dead end.

3.4.3 Influence of the Bubble Shape and Position on the Piping Response

The influence of the bubble shape and position was studied analytically by using figure - 3.15. Steam bubbles of different volumes (the value of H was changed) were positioned at different distances y_1, from the first ball valve. An experiment like this could eventually be done in practice by draining and filling with steam the space after a second ball valve, as is shown in figure - 3.15.

The following modifications were necessary, in order to adapt the previous calculation procedure to this present situation:

- The initial condition for the water filled pipe length was changed to $y_1 = y_o + y_1$;

- As for this case $V = \dot{x} = \dot{y}$, the void fraction (α) had to disappear from the inertia term in equation (3 - 10);

- The localized pressure drop ($\Delta P_{loc.}$) was increased, to take into account the second ball valve.

The results of these calculations are presented in figure - 3.19.

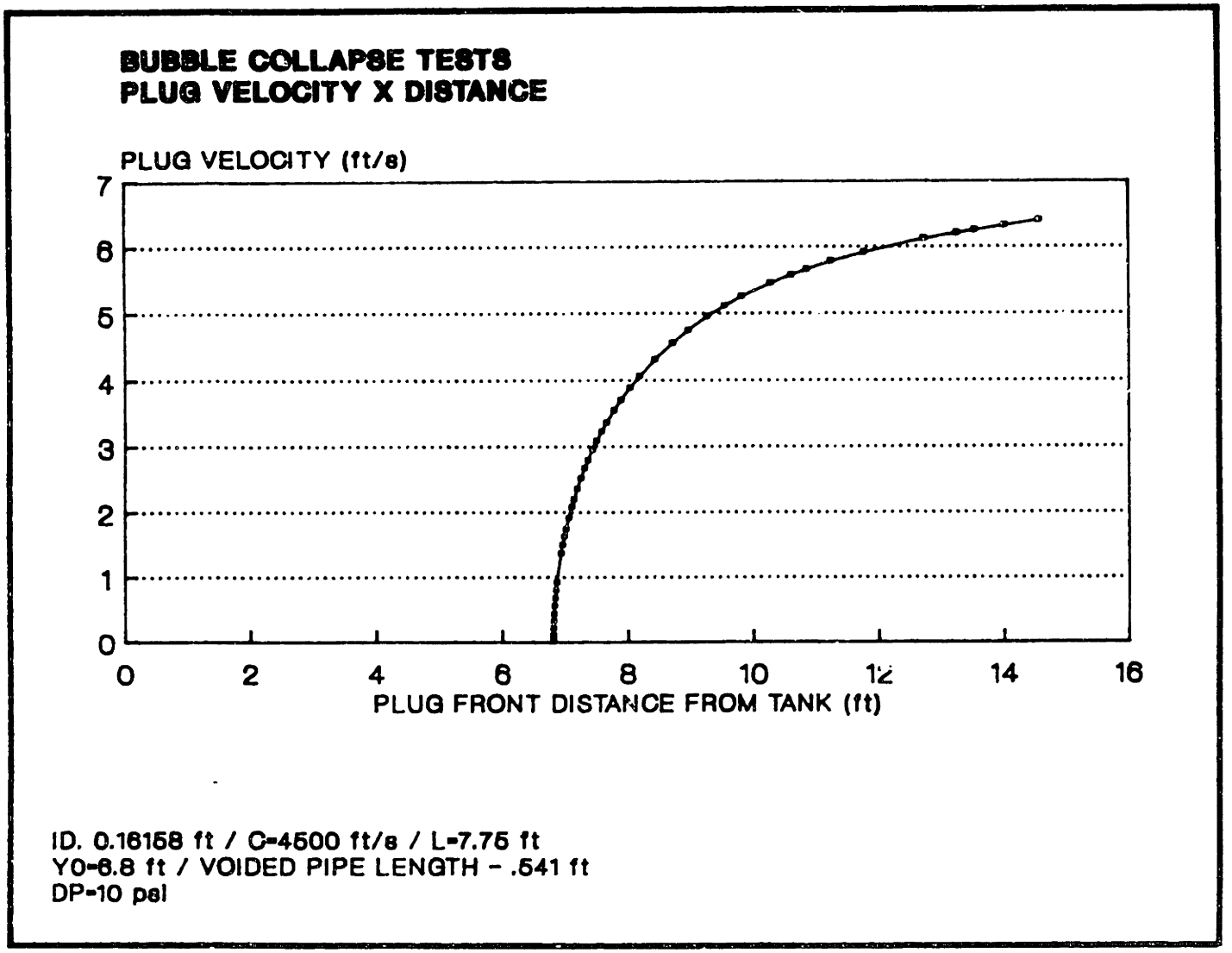

FIGURE - 3.18 Typical plug velocity as function of the distance from the valve.

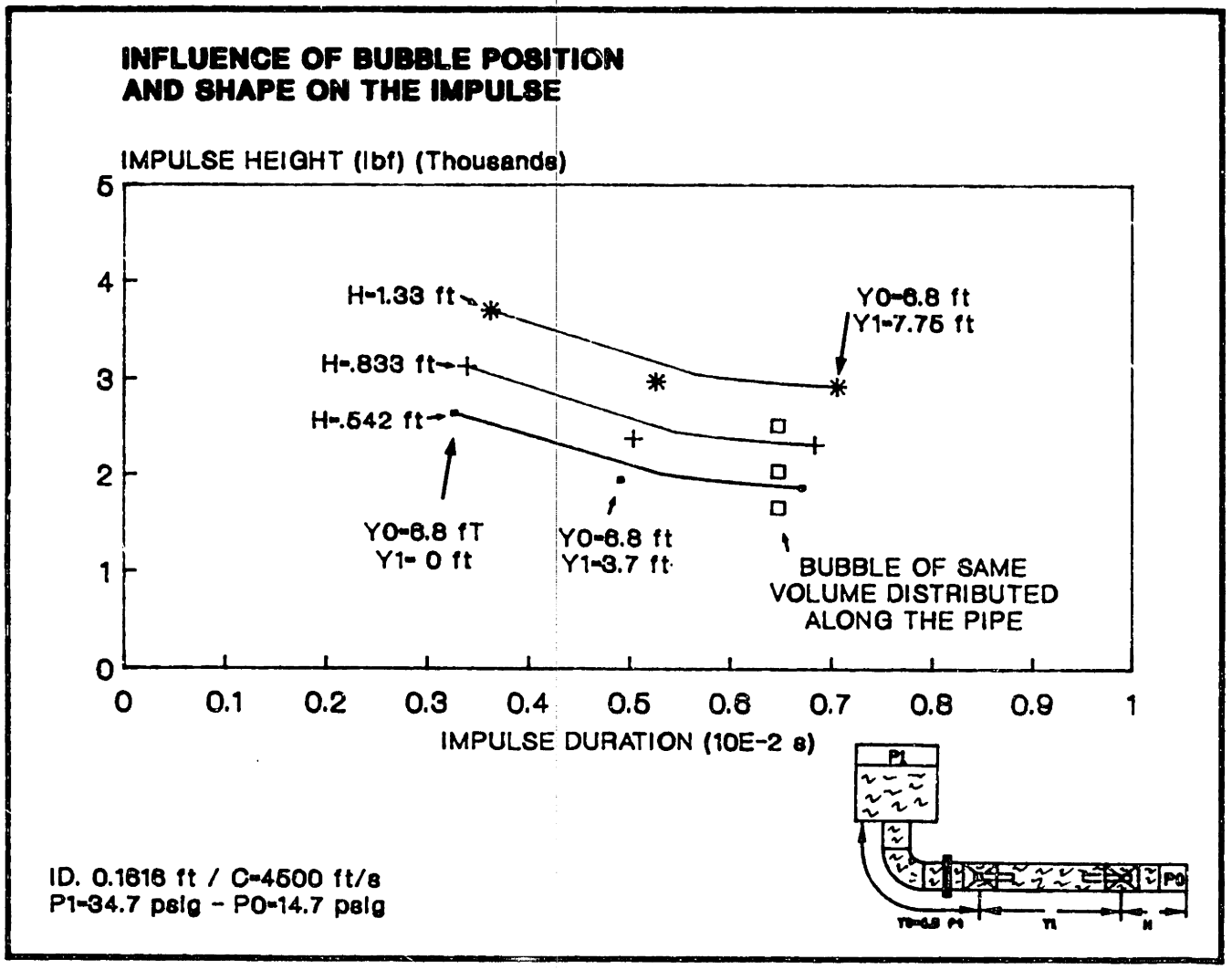

FIGURE - 3.19 Influence of the bubble position and shape on the final impulse. The square points are from a distributed bubble of equivalent volume as the ones from the curves. These square points do not belong to the plotted curves.

Although it is important to know the magnitude of the pressure spike due to a bubble collapse, that is not all the information required for a damage analysis. The structure interacts with the water hammer dynamic load and, depending on the structure characteristics and impulse shape, the initial load is amplified differently. A brief review of some selected results of structure dynamics (Based on Clough's book (28)) is given in appendix - C.

Figure - 3.20 is a displacement-response spectra for three different impulse shapes (28) (see also Wiggert (29)). Curves of this type are normally used to calculate the structure response to a dynamic load. The magnification factor, in these curves, is defined as:

$$D = \left| \frac{z_{max}}{p_{max}/K} \right| \qquad \text{eq(3 - 12)}$$

For short duration loads, the maximum displacement depends mainly on the impulse (the time integral of the load) (See equation (C - 3) - Appendix C). The load shape also influences the magnification factor values. However, this variation is more significant for $t_1 /T > 1$ (see figure - 3.20).

We are interested in knowing what is the influence of the bubble position and shape on the magnification factor (or in the structure response).

The only movement restriction of the horizontal test section, during the bubble collapse tests, was the bending stiffness of the vertical pipe section (of approximate length of 50 in) that connected the horizontal test section to the fixed tank. Consequently, a rough estimate of T can be calculated as follows:

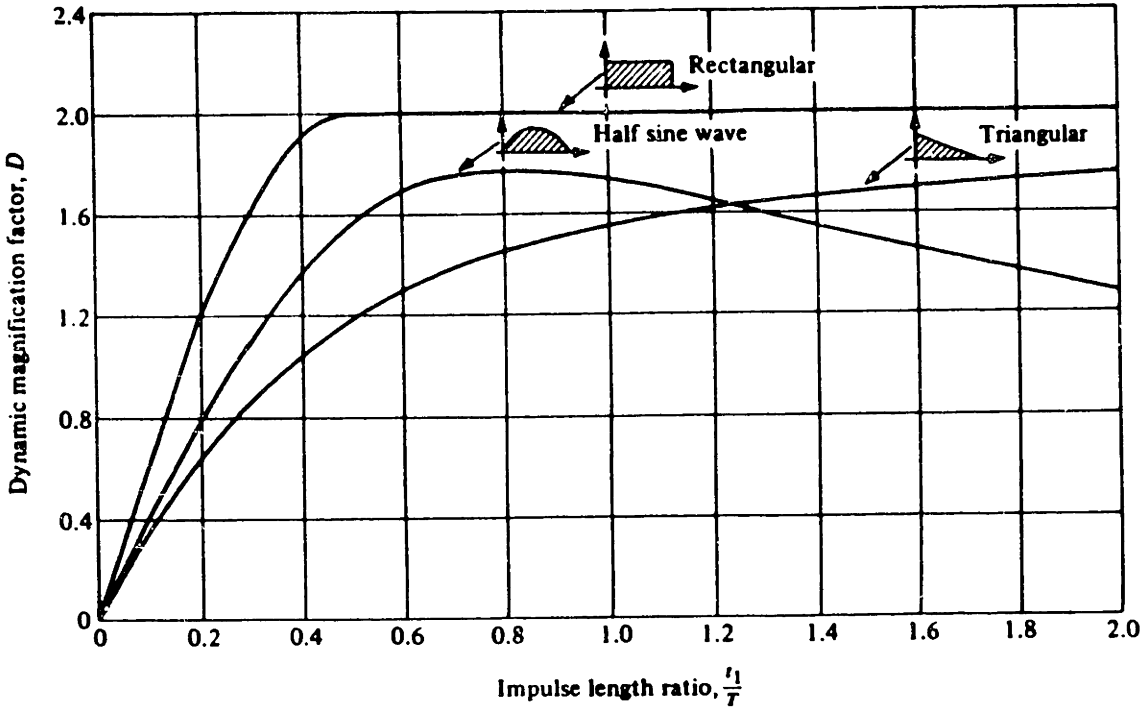

FIGURE - 3.20 Displacement-response spectra for three different impulse shapes. Reproduced from Clough. Source -> (28)

$$K = \frac{3.E.I}{l^3} = 594 \text{ lbf/in} \qquad \text{where:}$$

$l \simeq 50$ in $\qquad E_{(\text{cast steel})} = 28.5 \times 10^6$ lbf/in^2

$I = \frac{\Pi}{64}(OD^4 - ID^4) = 0.868$ in^4

$OD = 2.375$ in $\qquad ID = 1.939$ in

$M = M_{water} + M_{tube} = 108$ lbm $\qquad$ and,

$$T = \frac{2.\Pi}{\sqrt{K.g_c/M}} = 0.136 \text{ s}$$

From figure - 3.19, t_1/T is less than 7×10^{-2}. The recorded bubble impulse shapes were different from the simple shapes of figure - 3.20 (see figure - 3.13). However, observing figure - 3.20, it is possible to conclude that the impulse shape should not be important for such a low value of t_1/T. For the assumed values of mass and stiffness, the magnification factors D are very small. As the impulse height variation is also small, for this specific pipe arrangement there is no significant difference in the pipe deflection for the different bubble locations or bubble shapes.

3.4.4 Long Horizontal Pipe Simple Conservative Model

Comparing the experimental bubble collapse results with the simple conservative model (section 3.4 - items 2 and 3), the conclusion is that the proposed calculation procedure can establish an upper boundary for the water hammer pipe load. This served as the incentive to try to calculate a water filling rate to the long horizontal pipe, that was a conservative limit to the allowable pipe load.

For the long horizontal pipe, the most critical water hammer is caused

by a slug that is formed due to the counterflow of steam which, in turn, is induced by condensation.

The most simple and conservative analytical approach that we envisioned to model this phenomenon was to divide it into two independent problems: 1) Assuming that for every water height inside the horizontal pipe a slug is formed, calculate the minimum water height for which the resultant slug water hammer load will not exceed an established limit; and 2) Assuming the steam velocity equal to the one necessary to bring the incoming water to the saturation state, calculate the maximum water filling rate that will not cause the stratified-slug flow transition, for the previously calculated water height.

Problem 1

The long horizontal pipe initial condition is represented in figure - 3.21 (part a). Stratified flow of steam and water exists inside the pipe. Water is being injected into the pipe from the right.

Block et al (12) proposed a model for the dynamics of a slug of zero initial length and that is formed inside a pipe that is not connected to a reservoir (see figure - 3.21 - parts b and c). This represents well what was observed during several long horizontal pipe visualization experiments. Therefore, this calculation procedure was adopted here. A coefficient G was introduced to take into account the fact that, when the slug moves, some water is left behind (see figure - 3.21 - part c). In order to be again both simple and conservative and to avoid the use of a direct-contact condensation correlation (Block et al left the condensation rate as an

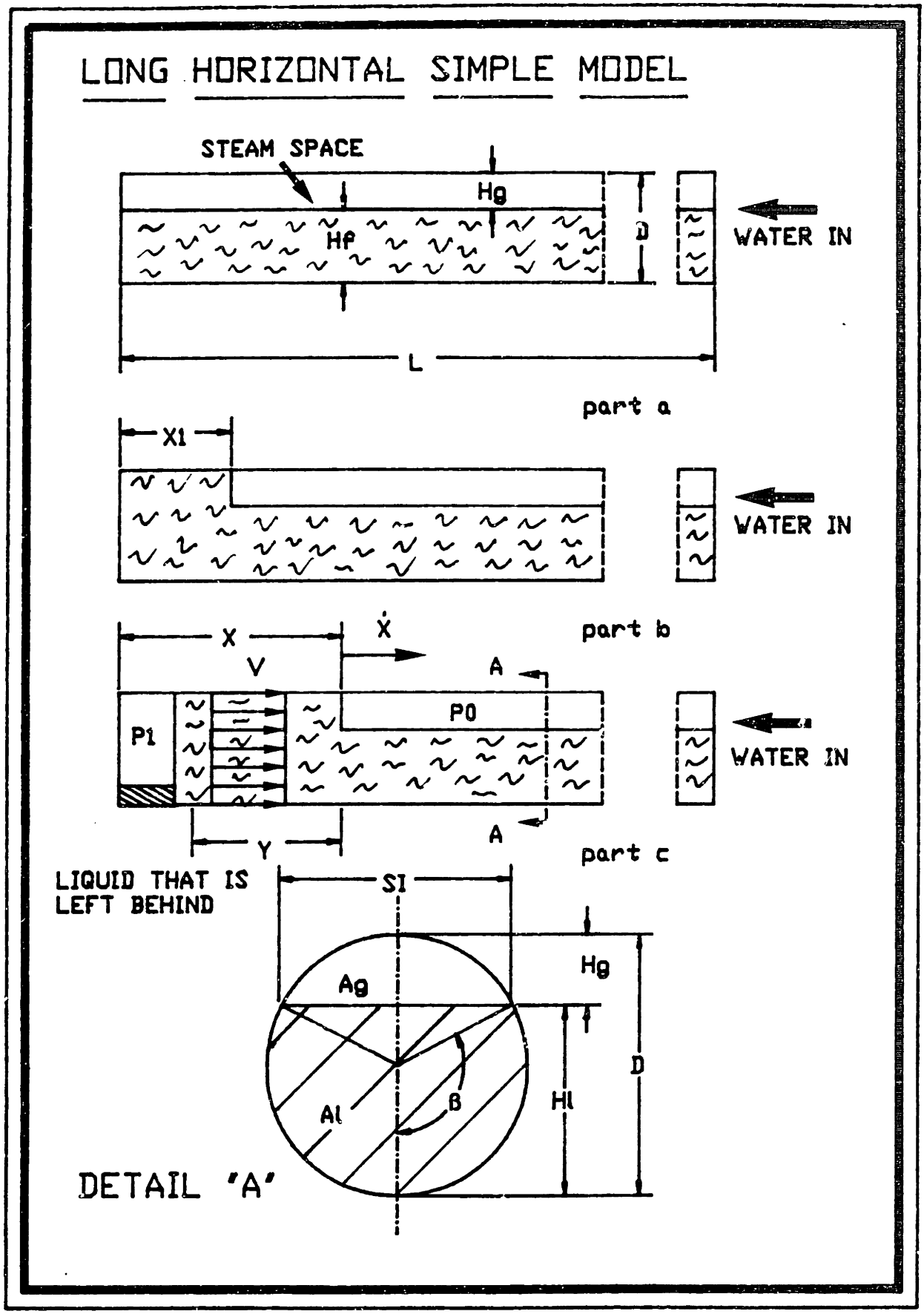

FIGURE - 3.21 Scheme used for the long horizontal simple model.

independent parameter), the slug downstream pressure (P_o) was assumed equal to zero and the slug upstream pressure was assumed equal to the system pressure (P_1).

The velocity in the pool ahead of the slug is assumed equal to zero. Although this assumption is not real, it should not modify significantly the final result because of the much higher slug velocity. The velocity inside the slug of length y is assumed uniform and equal to V.

Considering a moving control volume (velocity $\dot{x}$) at the slug edge and applying the mass conservation principle, it is possible to write:

$$V = \alpha.\dot{x} \qquad \text{eq(3 - 13)}$$

Applying mass conservation to a control volume defined by the slug front and the upstream pipe wall (Neglecting the void fraction variation due to the injected water, because the slug is very fast),

$$y = (1 - \alpha).x.G \qquad \text{eq(3 - 14)}$$

The one dimensional slug momentum equation is,

$$\frac{d}{dt}(\rho_1.y.V) = \Delta P.g_c - f.\frac{y}{D}.\frac{\rho_1.V^2}{2} \qquad \text{eq(3 - 15)}$$

Using equations (3 - 13 and 14) in equation (3 - 15) and assuming P_o = 0, we get:

$$\frac{d}{dt}(x.\dot{x}) = \frac{P_1.g_c}{\rho_1.(1 - \alpha).\alpha.G} - \frac{f}{2.D}.\alpha.x.\dot{x}^2 \qquad \text{eq(3 -16)}$$

where $f = \frac{64}{Re}$ and $\frac{0.3164}{Re^{.25}}$, for the laminar and turbulent regime, respectively.

Equation (3 - 16) was solved numerically with the following initial conditions:

$x_i = x_1 = 2.D \simeq y$ and $\dot{x}_i = V_i = 0$

In figure - 3.22, the slug final velocity is plotted versus the pipe water pool depth for different values of the coefficient G. From this plot, it is seen that the influence of the G factor in the final velocity is very small. In other words, the water fraction that is left behind is not important to the final answer.

Figure - 3.23 shows the evolution of the slug velocity with the pipe length, when the system pressure is equal to 14.7 psia. Observing this last figure, it is possible to conclude that what limits the slug velocity is mainly the pipe wall friction. This result is different from the one obtained in section 3.4 - item 2 (see figure - 3.18). The reason for this difference is that this slug starts with a small mass, whereas the water plug of section 3.4 - item 2 had a much longer initial length.

Figure - 3.24 illustrates the results of the above calculation for several different system pressures. The Joukowsky relation was used to calculate the pressure spike magnitudes.

Problem 2

For this calculation we need a criterion for the transition from stratified to slug flow regime. Wallis and Dobson (30), Mishima and Ishii (31) and Taitel and Dukler (17) have all proposed theories to predict this transition. The three give similar answers. We have chosen the last one because of its more common use. As already mentioned, in order to be

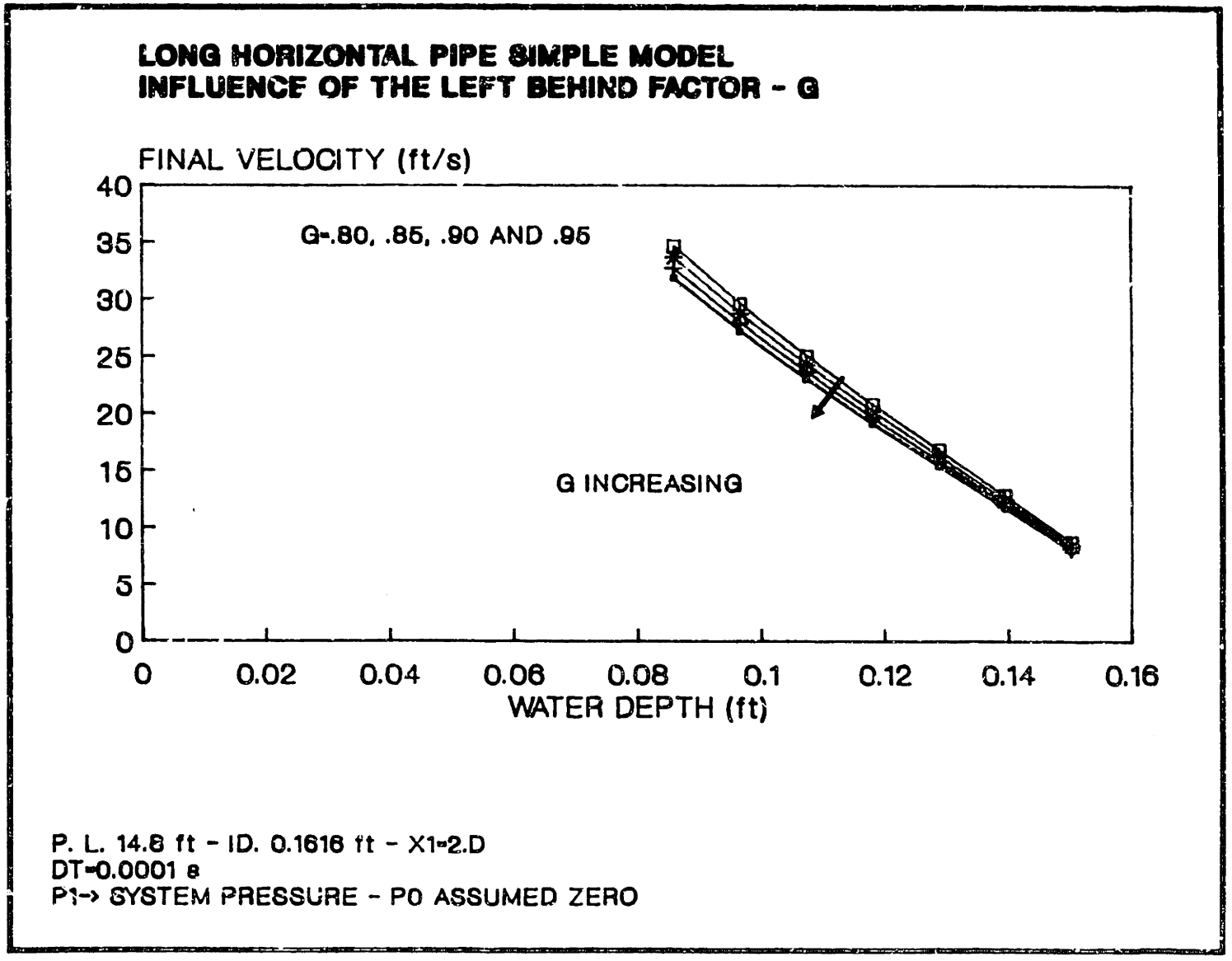

FIGURE - 3.22 Influence of the left over factor in the long horizontal pipe simple model.

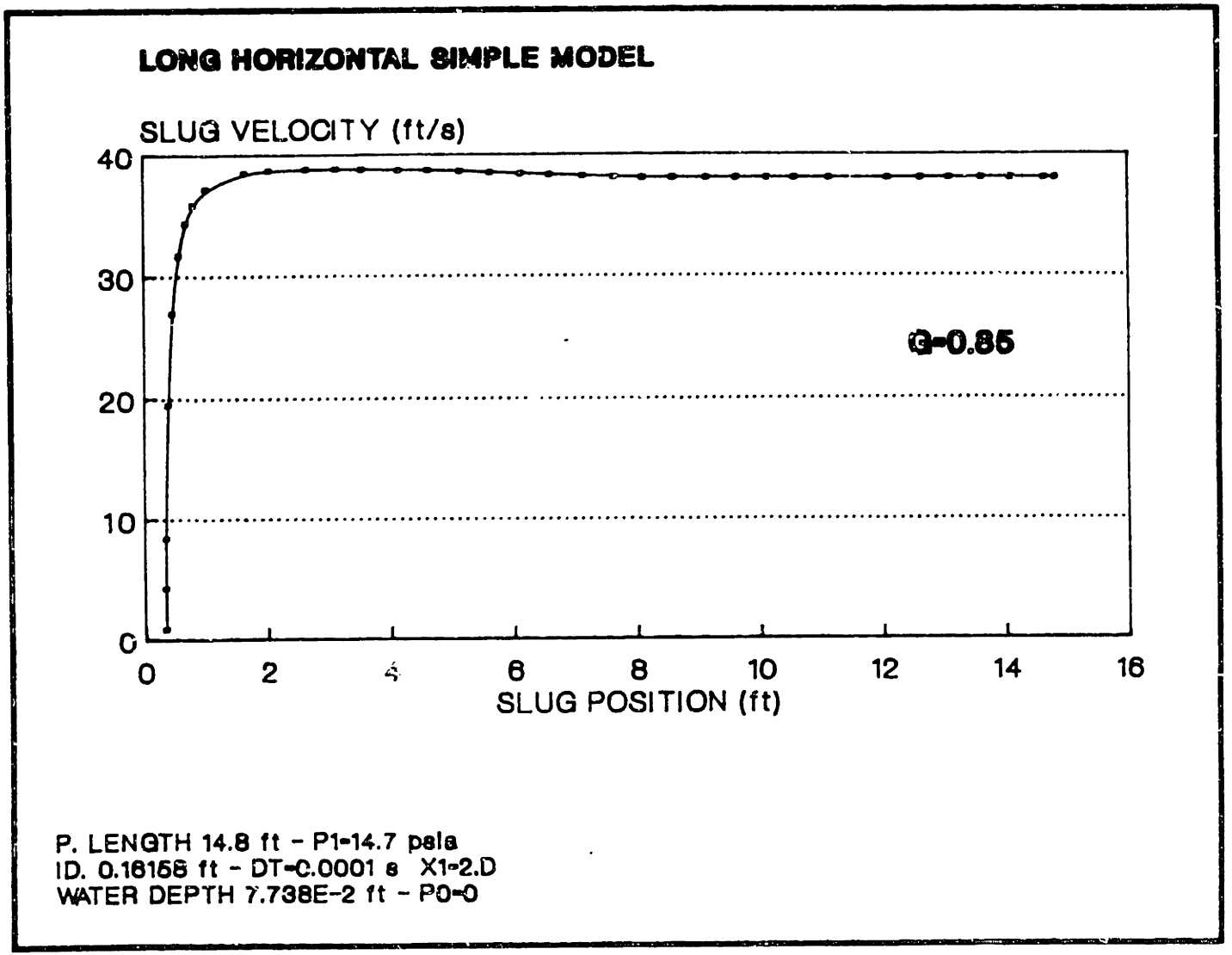

FIGURE - 3.23 Typical slug velocity as function of the distance from the slug formation point.

conservative and avoid using direct-contact condensation correlations, the steam velocity was assumed equal to the one necessary to bring the incoming water to the saturation state. Geometric relations plus the equations below were used to construct figure - 3.25:

Taitel and Dukler criterion,

$$V_s > C_2 \cdot \left[\frac{(\rho_1 - \rho_s) \cdot g \cdot \cos(\theta) \cdot A_s}{\rho_s \cdot (dA_1/dH_1)} \right]^{\frac{1}{2}} \qquad \text{eq(3 - 17)}$$

where,

$$C_2 = 1 - \frac{H_1}{D}, \quad \cos(\theta) = 1 \quad \text{and}$$

$$\frac{dA_1}{dH_1} = S_i = 2.\sqrt{H_1 \cdot (D - H_1)}$$

and the steam velocity necessary to bring the incoming water to saturation,

$$V_s = \frac{C_{pl} \cdot (T_s - T_w) \cdot \dot{m}_w}{A_s \cdot \rho_s \cdot h_{fg}} \qquad \text{eq(3 - 18)}$$

Discussion

The initial objective of the above calculation was to use figures - 3.24 and 3.25 to find a conservative allowable filling rate for the long horizontal pipe. Figure - 3.24 would give a minimum water height, if the maximum permitted pressure were known. Figure - 3.25 would give the maximum filling rate, if the minimum water height were known. However, unless very high pressures are permitted in the system, the resulting filling rate from these plots are too small for any practical use. In order to remove needless conservatism in this procedure, we need to use a direct-contact condensation

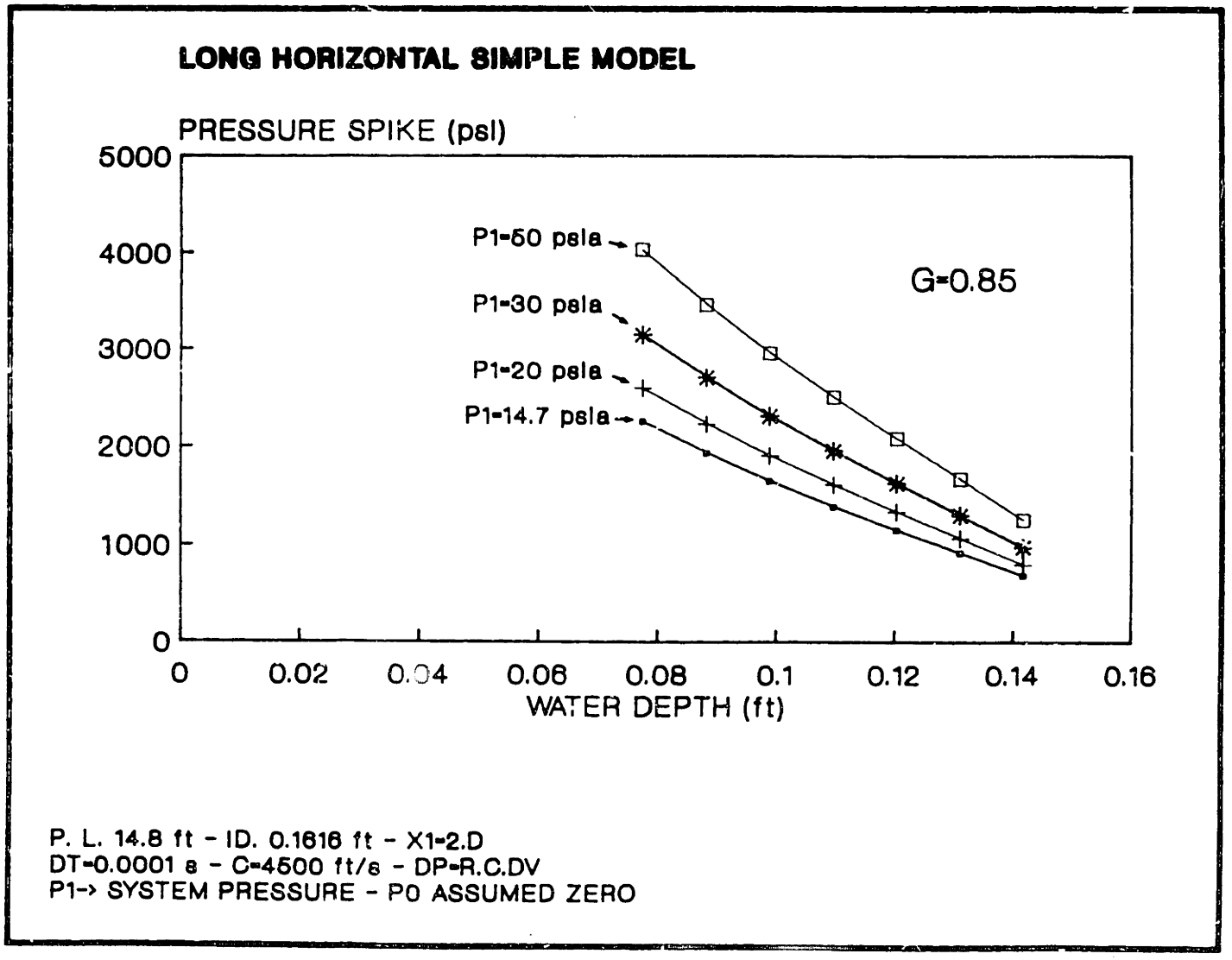

FIGURE - 3.24 Pressure spike X water depth - P. DIA. 2 in. Long horizontal pipe simple model.

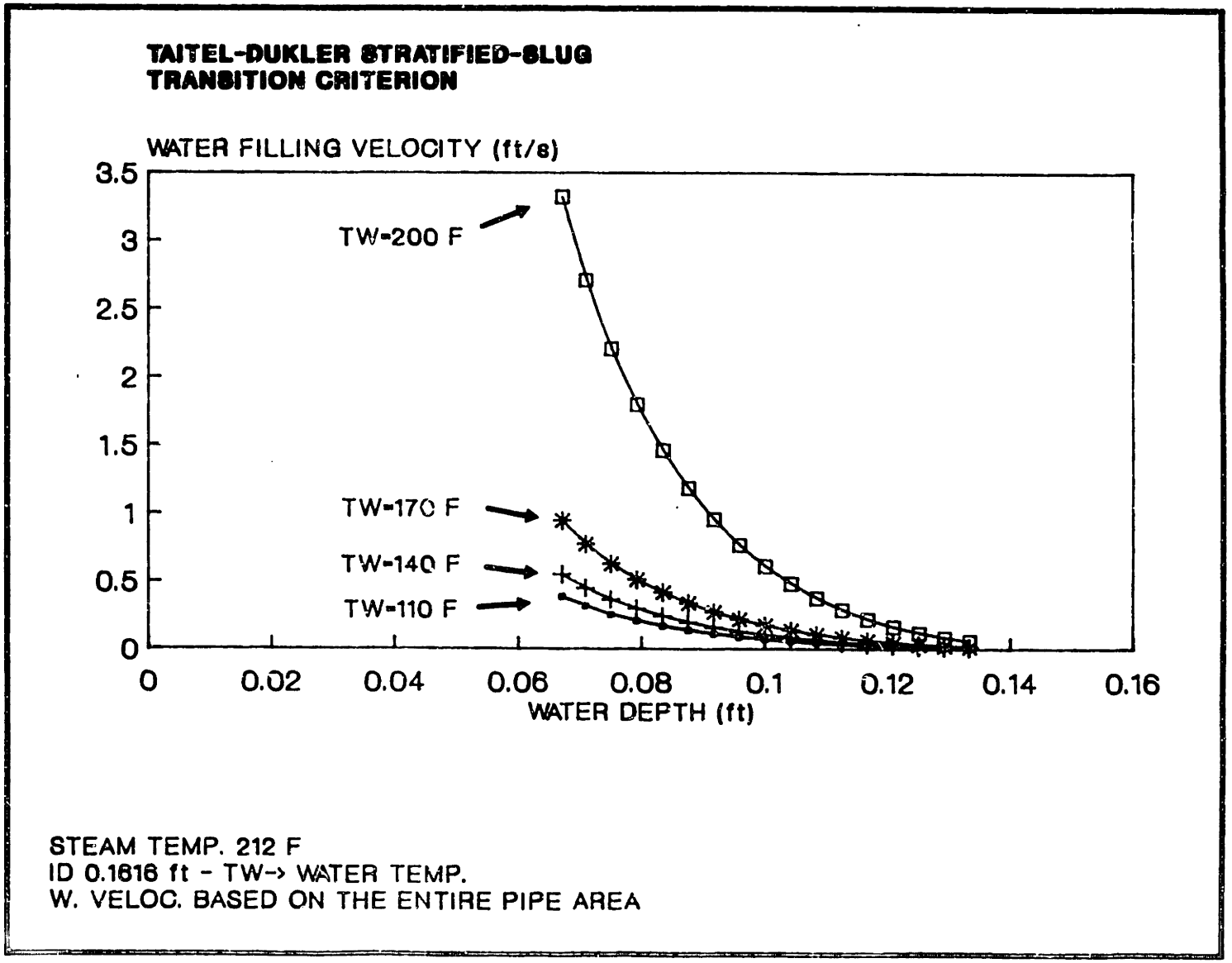

FIGURE - 3.25 Water filling velocity necessary to cause slug transition X water depth.

correlation. Unfortunately, it seems that still more research is necessary in this field, in the range of interest for water hammers.

3.5 Conclusion

Filling a long leveled horizontal pipe axially will always cause a slug flow transition induced water hammer, as it can be observed in figure - 3.5 (transducer P4 trace). However, for small filling rates, the resulting pressure spike from the slug water hammer is small. The reason why the conservative calculations for the long horizontal pipe gave such a high values of the final pressure spikes is because the assumptions of P_1 and P_o values were too conservative. In practice, condensation will decrease P_1 value and at the same time P_o is not zero. Indeed, for high pressure systems these two values can be quite different from the conservative assumptions used in section 3.4 - item 4.

Steam is condensed at the pipe wall and at the water interface, and this causes the pipe interior pressure to decrease. Because of this depressurization, boiling starts at the pipe wall, making the problem more complex.

Moreover, although Thomas (32), Segev et al (33), Theofanous et al (34) and Bankoff and Kim (18) have all proposed direct-contact condensation correlations of steam on water, none was based in experiments conducted over the range of parameters of interest for water hammers.

Surely, there is a limiting filling rate where no damage can be done to a piping system, as the resulting pressure spikes from slug water hammer events are too small. But, because of the limitations already cited, it seems to us that with the present knowledge no simple method will work in predicting, within a reasonable margin, the slug water hammer pressure

magnitude.

The simple conservative bubble collapse model (section 3.4 - items 2 and 3) can be used to predict the pipe load when there is a significant initial mass of water to be accelerated, and the steam bubble volume can be estimated. In this case, the bubble collapse model would give an upper boundary to the pressure spike range.

From this chapter's findings, the following filling procedures are recommended to an horizontal pipe that is partially or totally filled with steam:

Recommendations

- Incline the pipe (at least 0.5"/1') and fill it laterally from the bottom, or;

- Inject the subcooled water, perpendicularly to the pipe axis, through nozzles distributed along the pipe length, at distances smaller than 48.D;

- If the pipe is not connected to an open space, limit the filling rate by using Chou's vertical up pipe theory (see section 2.2 or (6)), in order to limit the final water hammer magnitude to the prescribed value.

CHAPTER - 4

FILLING "L" SHAPED PIPES

4.1 Apparatus Description and Test Procedure

In order to check if the water hammer safe filling theories for single pipes could be used in complex piping systems, five different "L" shaped pipes were tested.

These five piping schemes and their classifications are shown in figures - 4.1, 4.13, 4.22, 4.30 and 4.38. As can be seen, all possible ways of filling "L" shaped pipes were tried.

All this equipment was constructed with the same materials that were used for the long horizontal tests. The differences between these five "L" test sections and the description of section 3.2 are indicated in the various "L" pipe schemes. As can be observed in these figures the main differences were: 1) One or two more Validyne model-D 15 transducers were used; 2) More pipe sections and bends were necessary to construct the several configurations; and 3) For the vertical "L" filled through the vertical pipe an electrical probe was employed to measure the water level inside the horizontal pipe section. This probe is fully described in figure - 4.14, and was based on the design of one previously used by Griffith (35).

In a way similar to the long horizontal pipe tests, the horizontal sections of these "L" pipes could be slightly inclined up and down, and the water could be introduced laterally through a 2" copper bypass line. Each pipe section length was equal to approximately 48.D, where D is the pipe

diameter (2" pipes were used).

The test procedure for all "L" arrangements were all the same as the ones from section 3.2. The only exception occurred in the test series that investigated the influence, on the water hammer boundary, of the initial water pool height in the horizontal section of the vertical "L" filled through the vertical pipe. This will be described in section 4.3.

4.2 Horizontal "L"

For this configuration the apparatus of figure - 4.1 was used, as previously mentioned. The points marked P1, P3 and P4 in this figure show at what place the pressure signals were recorded.

The stability maps from the first test series are plotted on figures - 4.2 and 4.3. The cartoon and the text at the bottom of these maps describe the test conditions (As on all other stability maps presented in this work). Therefore, as can be seen in these two plots, the test conditions were: 1) Both pipes were leveled; 2) The water was injected through the pipe axis (center filling); 3) The plane of the equipment, represented by the cartoon, was the horizontal plane; and 4) Three different orifices were used (0.125", 0.21" and 0.413"). The holes of the orifices were positioned at the pipe axis (orifices centered). The classifications of the intermediate and final water hammer have already been given in section 3.3 - item 1. The key for the map indicating if there is a water hammer remains the same as before (no water hammer -> small black square / water hammer -> cross).

Except when the water is injected with subcooling less than $20^{\circ}F$, figure - 4.2 shows that for this case there is no lower intermediate water hammer boundary. The line 1 on figure - 4.2 is the short horizontal single pipe stability boundary (0.46 ft/s). This theory does not work here because this pipe configuration behaves like a long horizontal pipe (see figure - 3.2) rather than two short ones. The running full limit (Fr = 1 or V_{zv} = 2.3 ft/s) does not predict either the higher intermediate water hammer boundary. The reason for this is that although the first pipe of the "L" runs full for

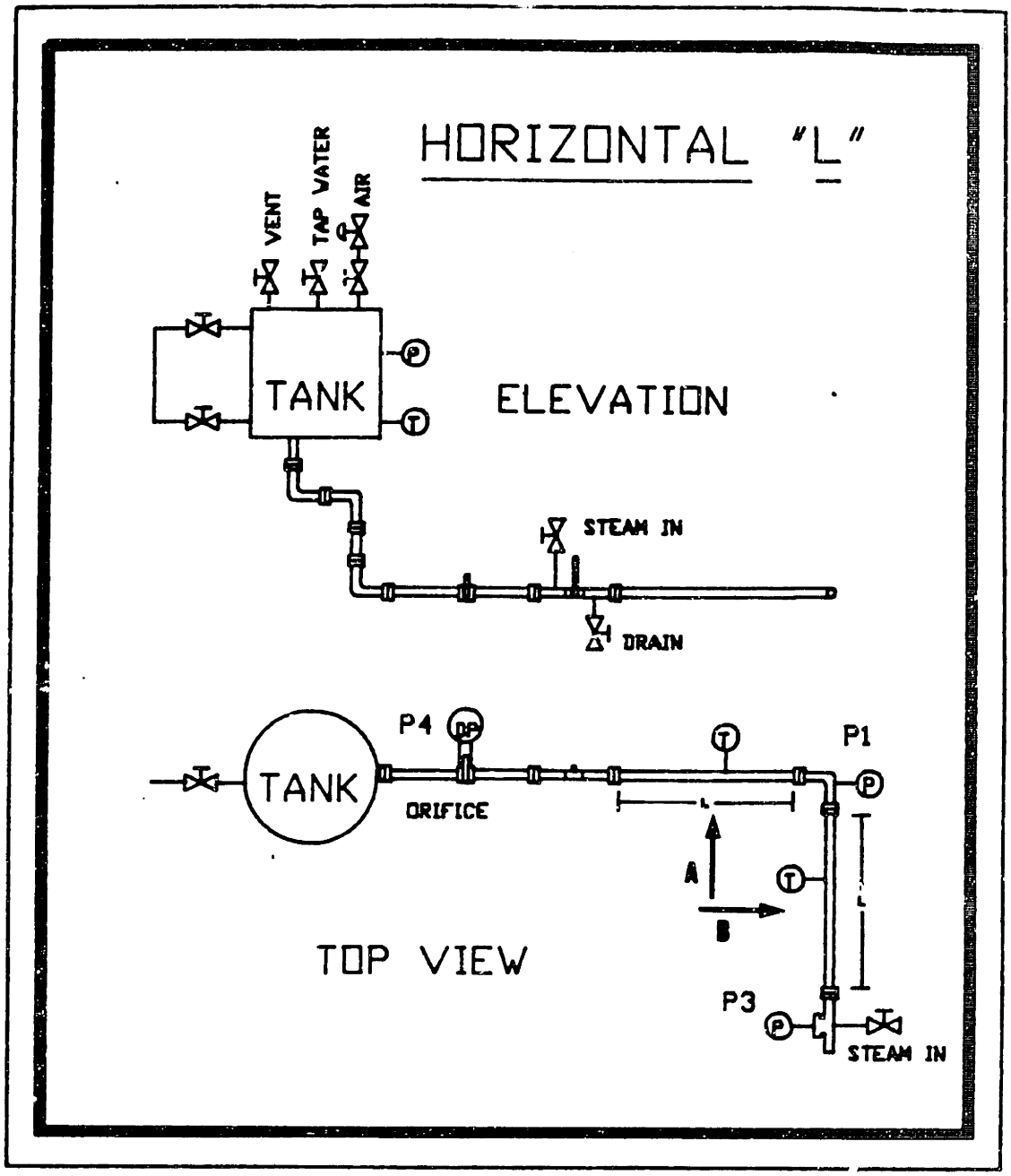

FIGURE - 4.1 Experimental apparatus used in the horizontal "L" tests. The distance L is ≈ 48.D (short pipe limit), where D=2 in.

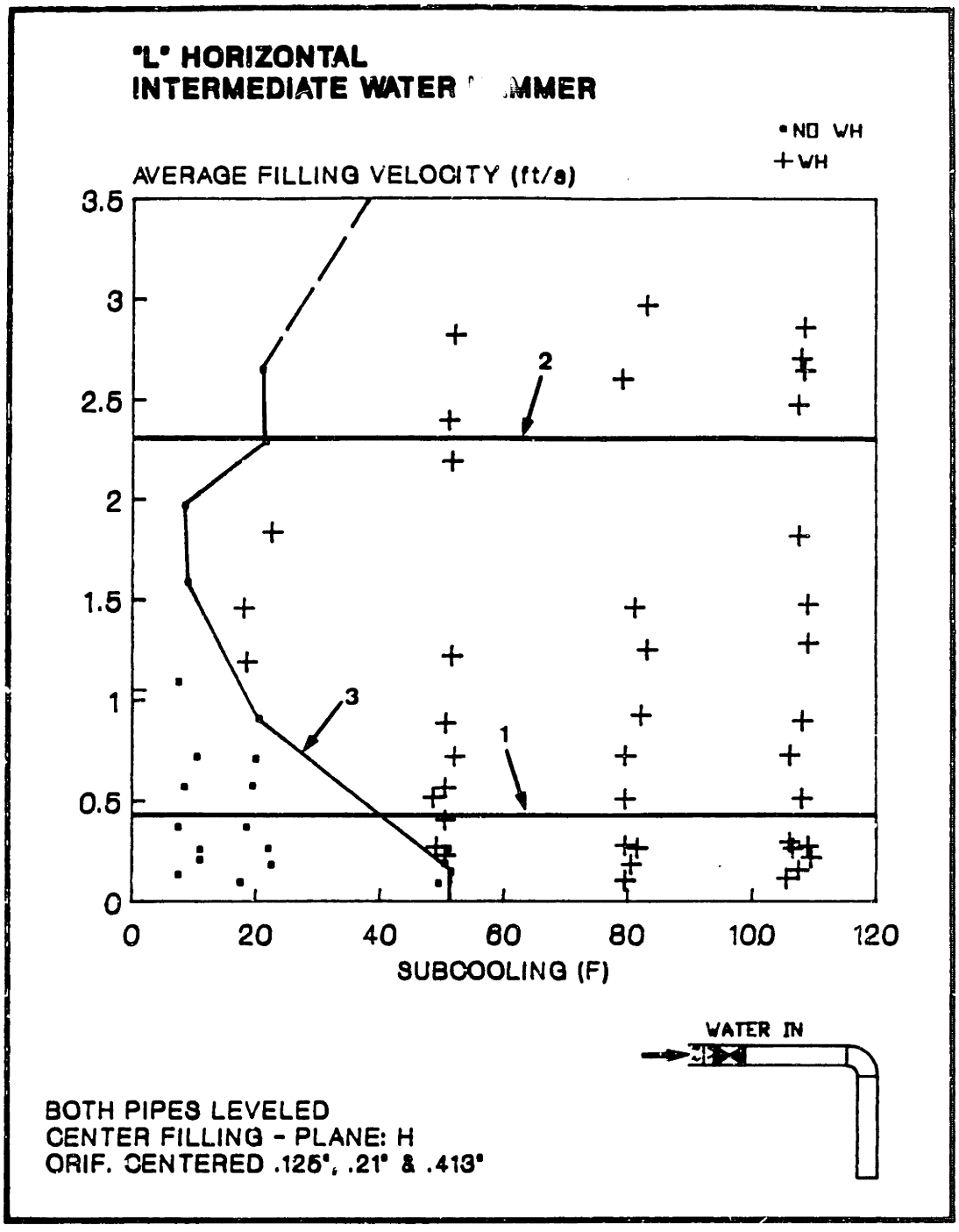

FIGURE - 4.2 Intermediate water hammer stability map for the horizontal "L" (both pipes leveled).
Line-1 -> Short horizontal, single pipe theoretical stability boundary - 0.46 ft/s.
Line-2 -> Running full pipe limit - Fr=1 or average filling rate of 2.3 ft/s.
Line-3 -> Experimental stability boundary.

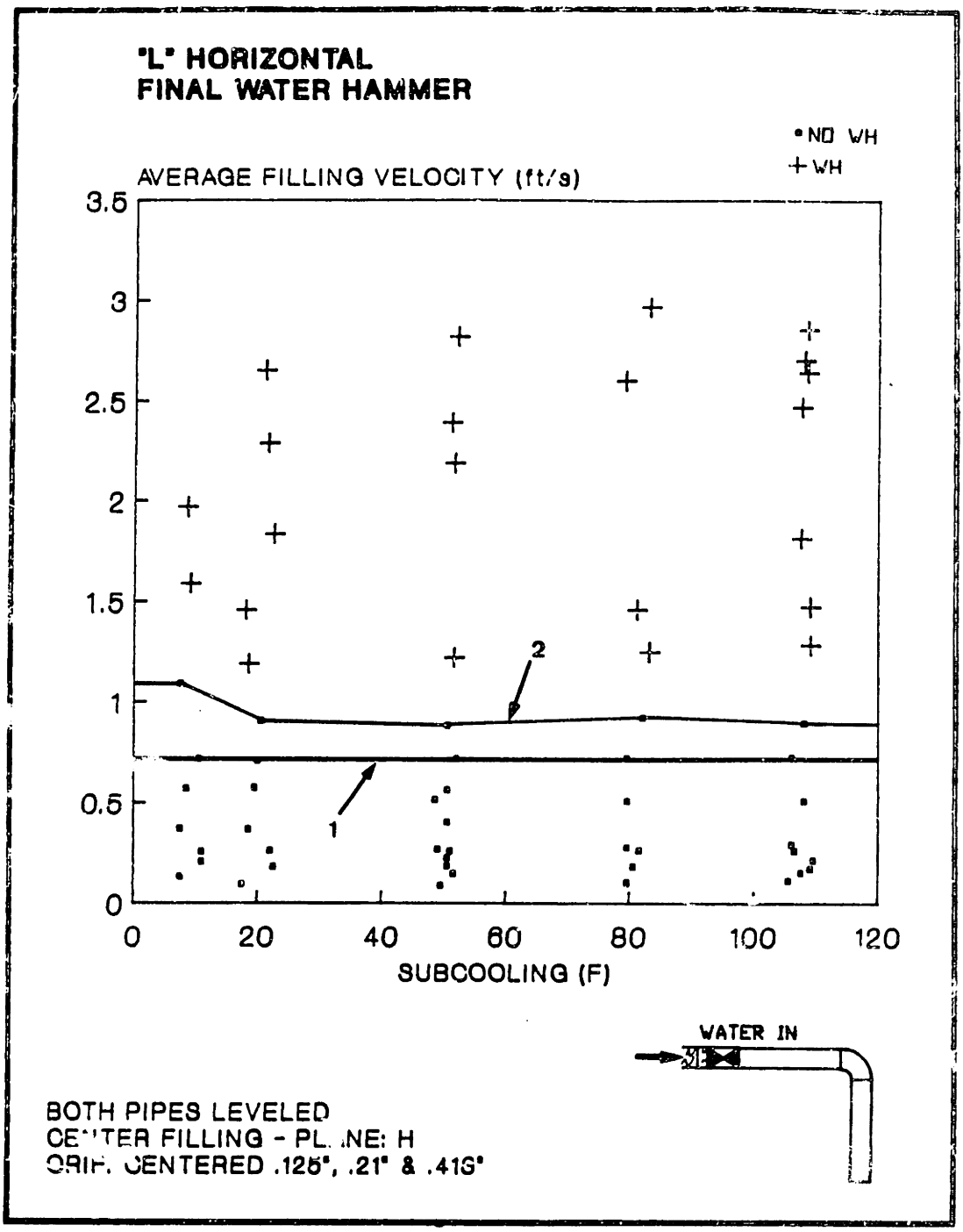

FIGURE - 4.3 Final water hammer stability map for the horizontal "L" (both pipes leveled).
Line-1 -> Experimental vertical up, single pipe stability boundary < 0.7 ft/s.
Line-2 -> Experimental stability boundary.

$V_{av} > 2.3$ ft/s, the second pipe does not because of flooding at the bend.

From figure - 4.3, the experimental vertical up single pipe stability boundary (0.7 ft/s), represented as line 1, is seen to be a conservative limit for the final water hammer for this pipe arrangement. The vertical up single pipe is used as reference for the final water hammer by the same reasons that were given in section 3.3 - item 1.

It is clear that the limiting water hammer is the intermediate one. In section 3.4 item 4 it was shown that conservative calculations result in very small values of water hammer safe filling rates. This approach is of no practical use. Therefore, we tried to find ways of filling the horizontal "L", avoiding the intermediate water hammer.

Several visualization tests, that will be described later, showed that a pool of saturated water always remained inside the pipes of a level test section. It was also observed that, as soon as subcooled water was injected into these pipes, evaporation started from the portion of the pipe wall that was wetted. This was the source of the counterflow of steam that caused the slug formation. It was then thought that filling from the higher point an inclined horizontal "L" (inclined down) would have the advantage of totally draining the pipes. Consequently, the source of steam would be eliminated and an improvement in the lower intermediate water hammer boundary could be expected. The results of a test series conducted with the horizontal "L" slightly inclined down (0.5"/1') are shown in figures - 4.4 and 4.5. The water was injected through an orifice with a hole in the center of the pipe. Observing these figures, the conclusion is that no improvement is obtained in this way. After changing the steel pipes to *LEXAN* ones, it was possible

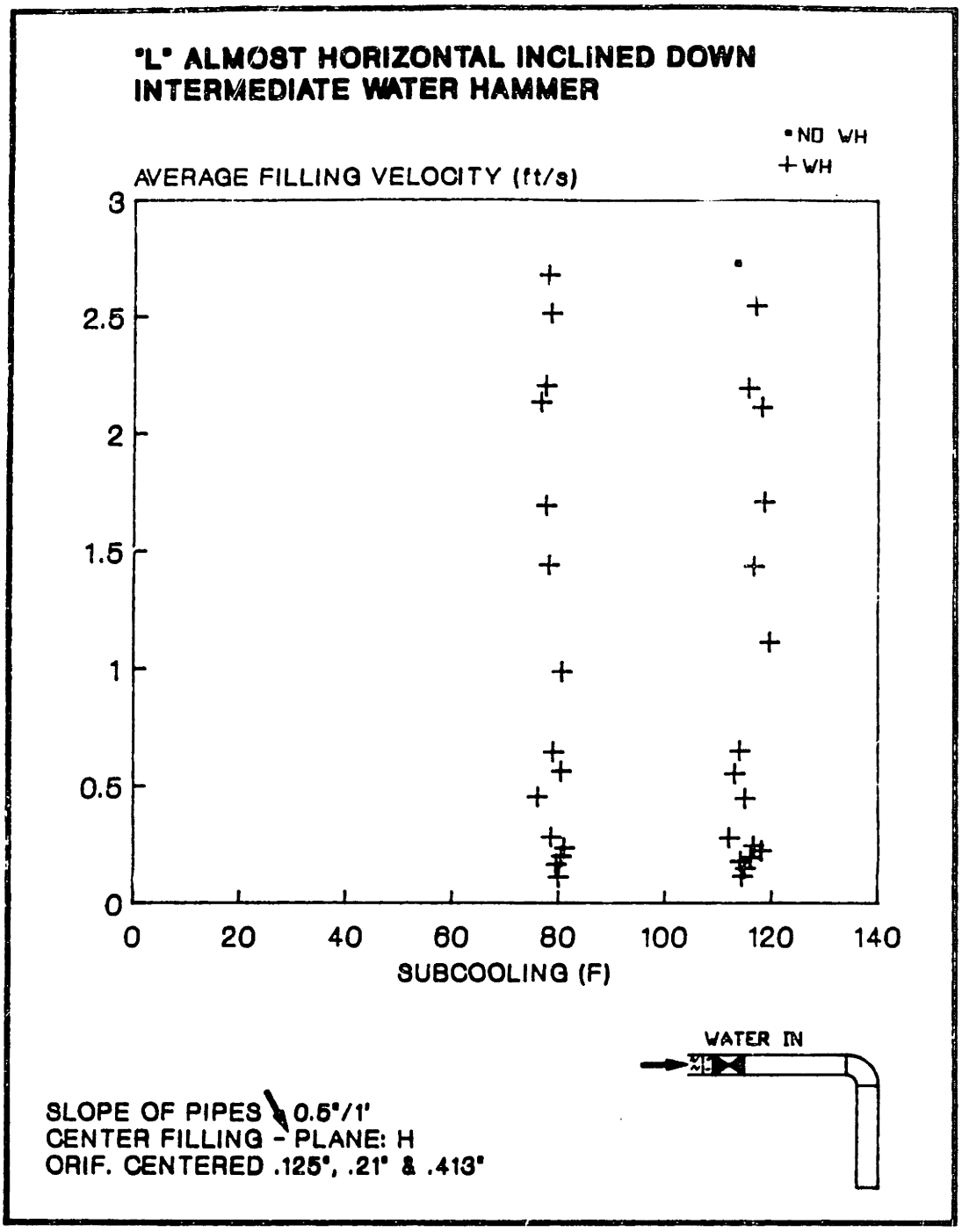

FIGURE - 4.4 Intermediate water hammer stability map for the horizontal "L" (both pipes inclined down and filled through the center).

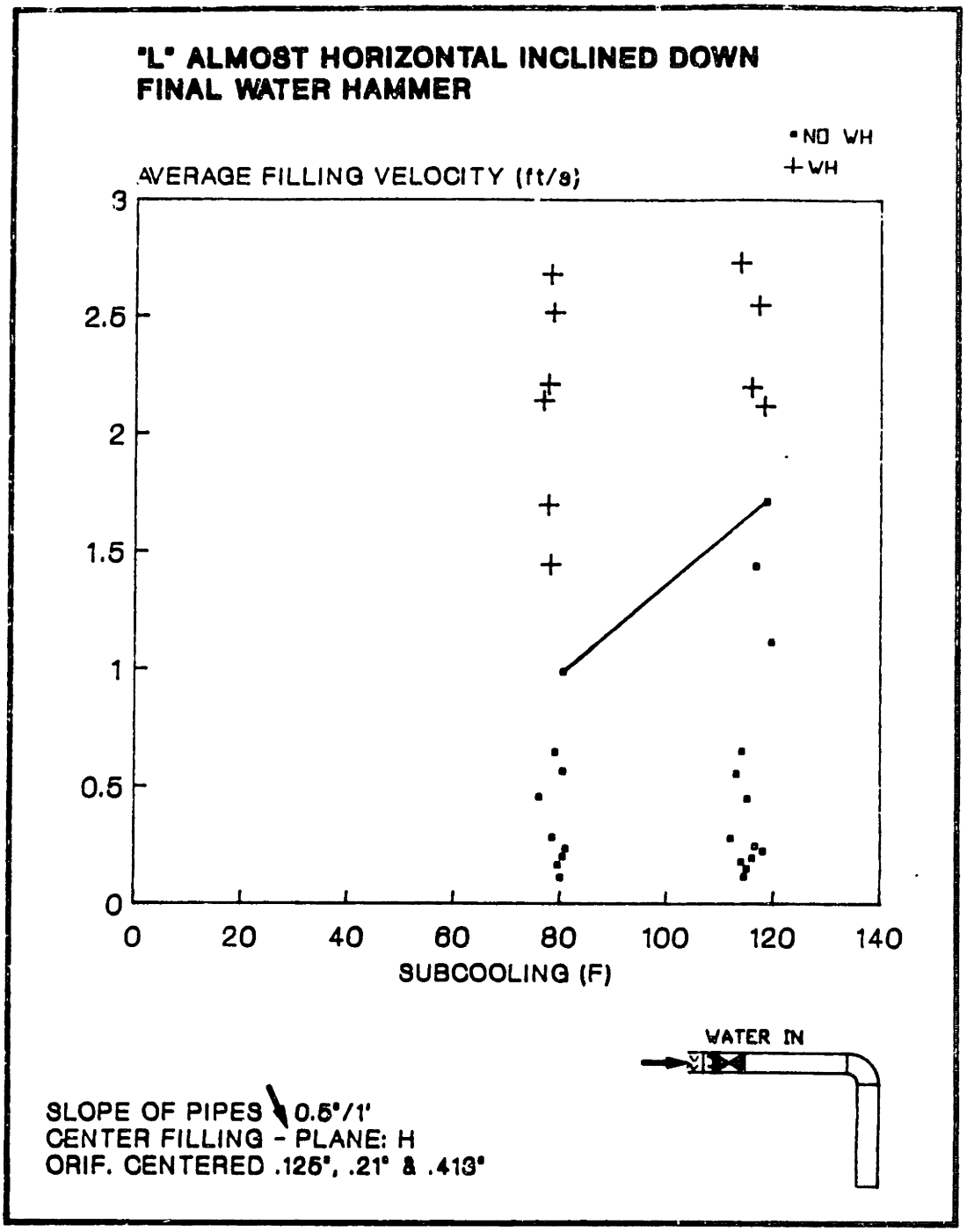

FIGURE - 4.5 Final water hammer stability map for the horizontal "L" (both pipes inclined down and filled through the center).

to see that the injected subcooled water, inside an inclined down pipe, advances first as a thin finger of water. This wets portions of the pipe wall and causes vapor generation by boiling. Therefore, the advantage of totally draining the pipes is lost, as previously explained in section 3.3 - item 2.

Inclining the horizontal pipes and filling them from the bottom (inclined up) also permits to totally drain the test section. Compared to the inclined down arrangement, in this configuration the subcooled injected water should wet a smaller portion of the pipe wall. Consequently, a test series, where the horizontal "L" was inclined up (0.5"/1') and filled through the pipe center, was tried next. Figures - 4.6 and 4.7 are the resulting stability maps. It can be seen that a significant improvement was obtained in relation to the two previous test series. However, the intermediate water hammer was not entirely eliminated.

Filling laterally an inclined up pipe has a similar effect to inclining the pipe further up, as already explained in section 3.3 - item 2. The propagating wave in this case is thicker and shorter, making the slug formation more difficult (see section 3.3 - item 2). Figure - 4.8 is the resulting stability map from tests conducted in an horizontal "L" inclined up (0.5"/1') and laterally filled (using a 2" copper bypass line). The intermediate water hammer disappeared in this configuration. From figure - 4.8, it can also be observed that the vertical up single pipe limit can be used as a boundary for the final water hammer.

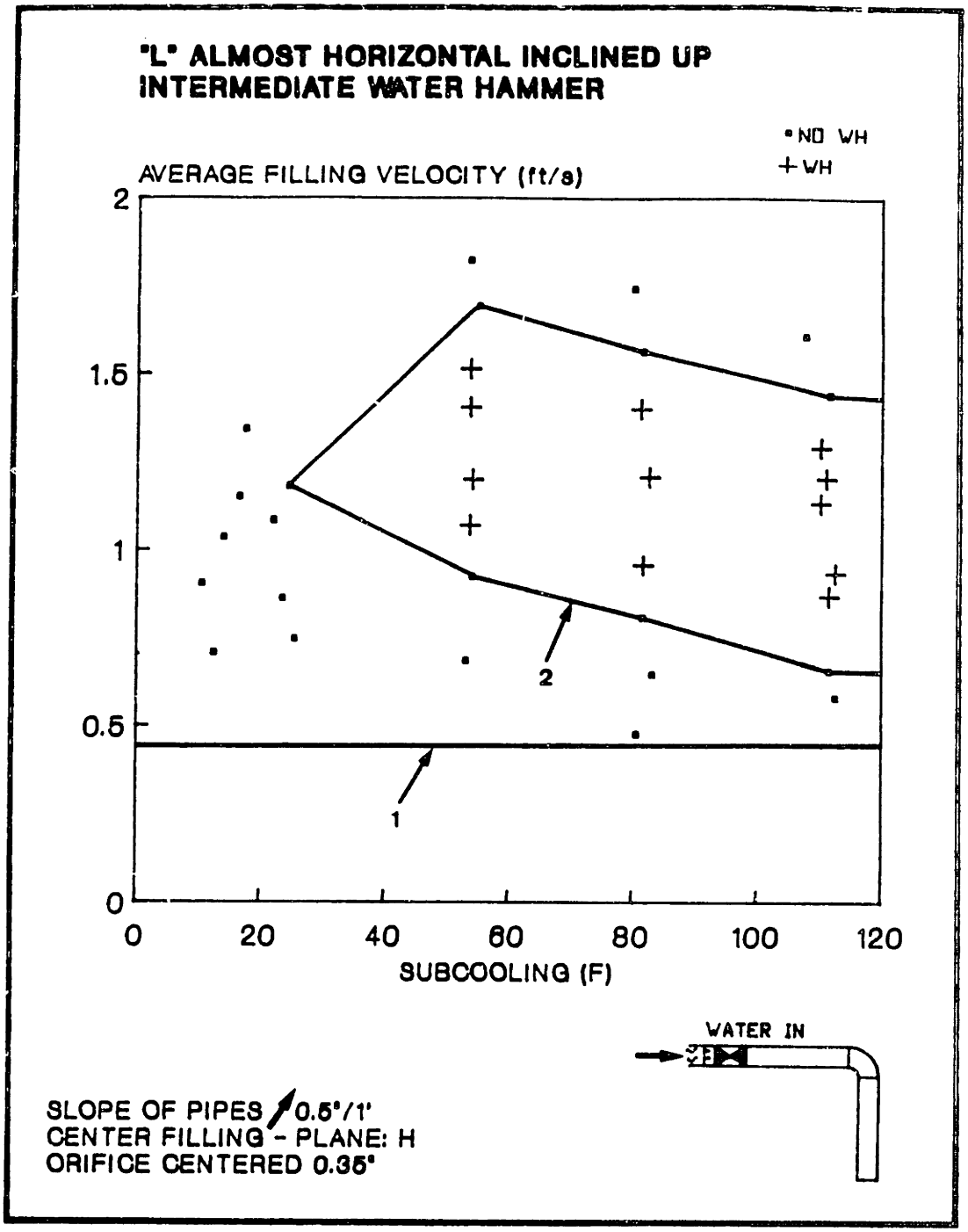

FIGURE - 4.6 Intermediate water hammer stability map for the horizontal "L" (both pipes inclined up and filled through the center).
Line-1 -> Short horizontal, single pipe theoretical stability boundary - 0.46 ft/s.
Line-2 -> Experimental stability boundary.

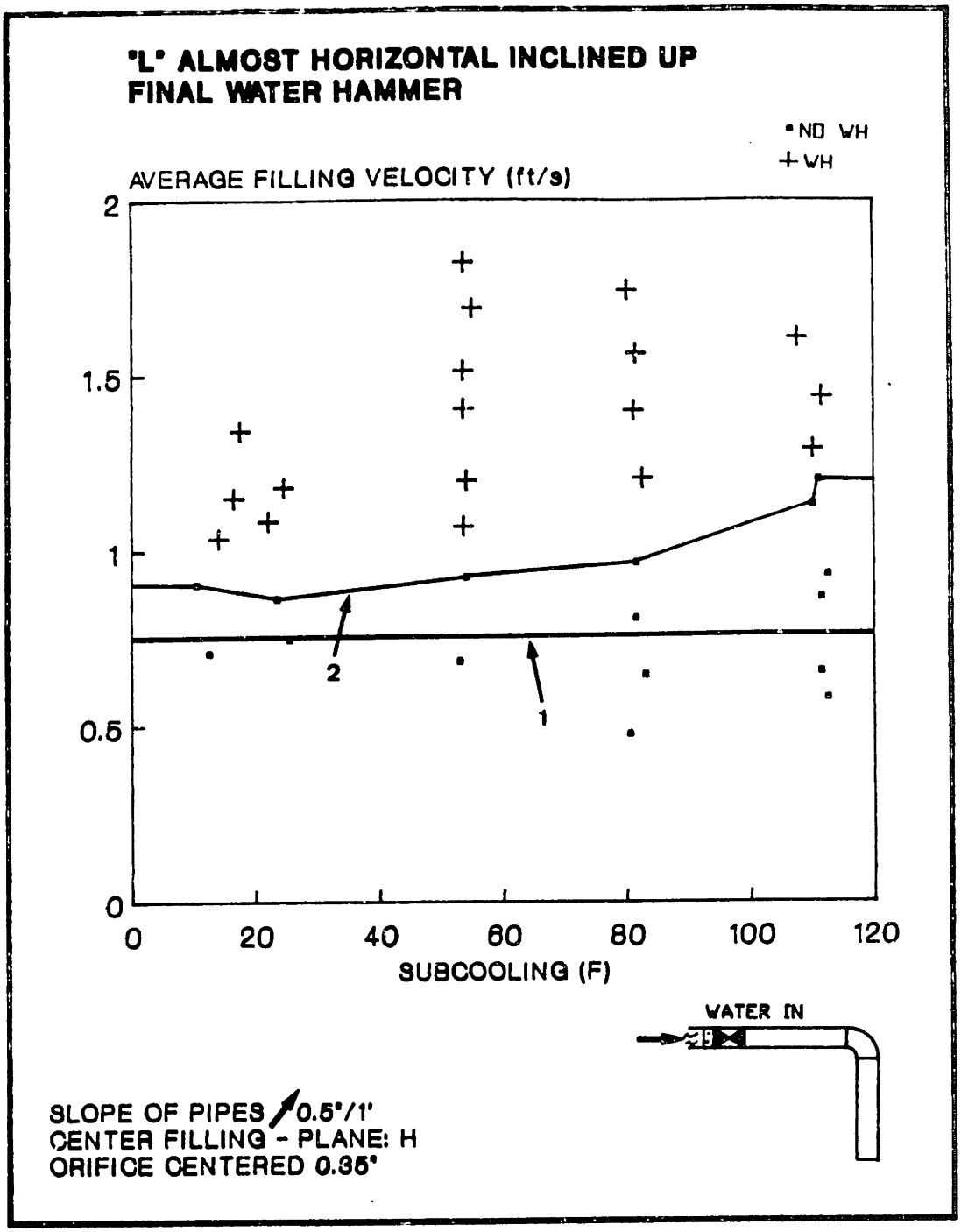

FIGURE - 4.7 Final water hammer stability map for the horizontal "L" (both pipes inclined up and filled through the center).
Line-1 -> Experimental vertical up, single pipe stability boundary - 0.7 ft/s.
Line-2 -> Experimental stability boundary.

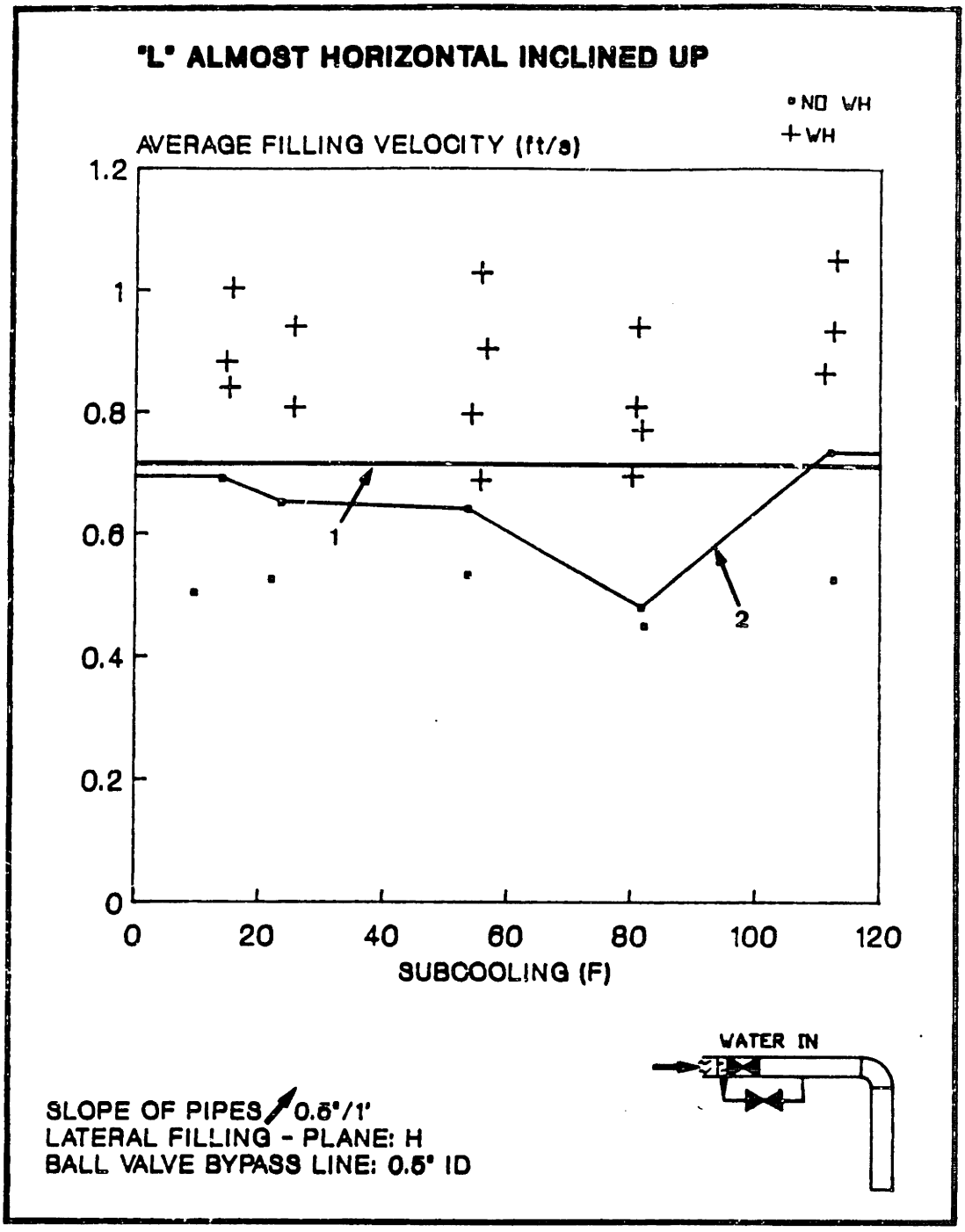

FIGURE - 4.8 Stability map for the horizontal "L", inclined up and laterally filled pipe.
Line-1 -> Experimental vertical up, single pipe stability boundary - 0.7 ft/s.
Line-2 -> Experimental stability boundary.

Visualization Tests

In figures - 4.9 and 4.10 the pressure traces of transducers P4, P3 and P1 are shown. The horizontal "L" pipes were leveled, the filling was through the pipe center and the average filling velocities were 1.28 ft/s and 0.293 ft/s, respectively. Pressure transducers can indicate a water hammer event if: 1) They are located at the position where the mass of water is forced to stop; or 2) There is a solid column of water between the impact point and the pressure transducer location, in order to the pressure wave be transmitted.

Figures 4.11 (part a) and 4.12 (part b) are a representation of what was observed in the horizontal sections of the "L" when the steel pipes were changed to LEXAN and both pipe sections were leveled. The views A and B of these figures are indicated in figure - 4.1.

Before the ball valve is opened, the test section is full of steam and a pool of saturated water remains inside the two horizontal pipes (figure - 4.11/1).

For small filling velocities (figures - 4.11/2a and figure - 4.12/2b and 2c), as soon as the ball valve is opened, water propagate as small waves inside the first pipe. Condensation at the water injection point creates a counterflow of steam. Boiling immediately starts at the wetted pipe wall due to the pipe depressurization. When the water pool height in the first pipe is high enough, the counterflow of steam causes a slug to be formed. The pressure difference between the two sides of the slug drives it to the condensation region. The slug crashes against the orifice plate causing a water hammer. This event is indicated only at the transducer P4 trace,

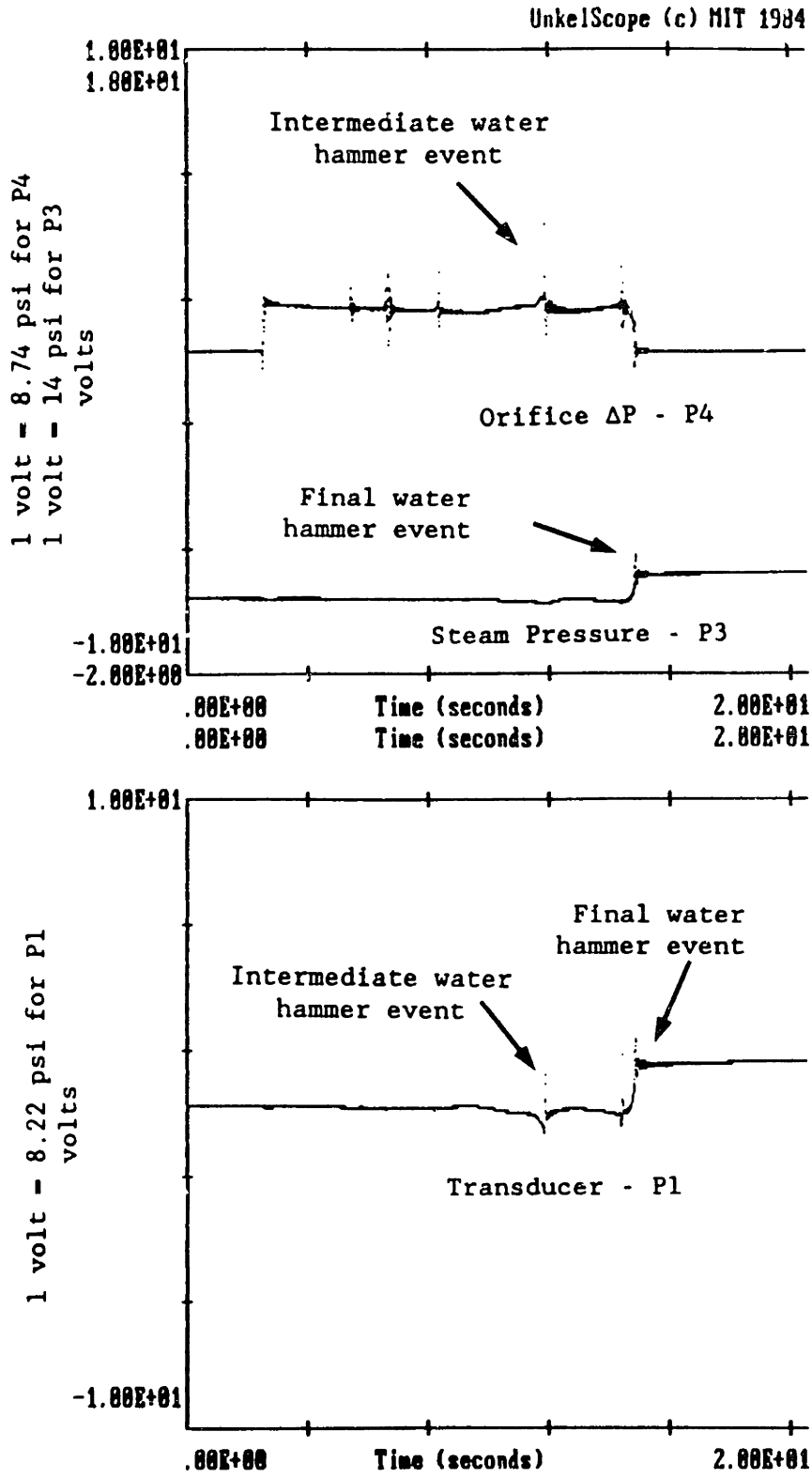

FIGURE - 4.9 Typical horizontal "L" pressure response curves for a case with intermediate and final water hammer events (pipes leveled).

Orifice 0.413 in - P_t=15 psig - T_w=110°F

T_{sub}=109°F - Av. Filling Veloc.= 1.28 ft/s.

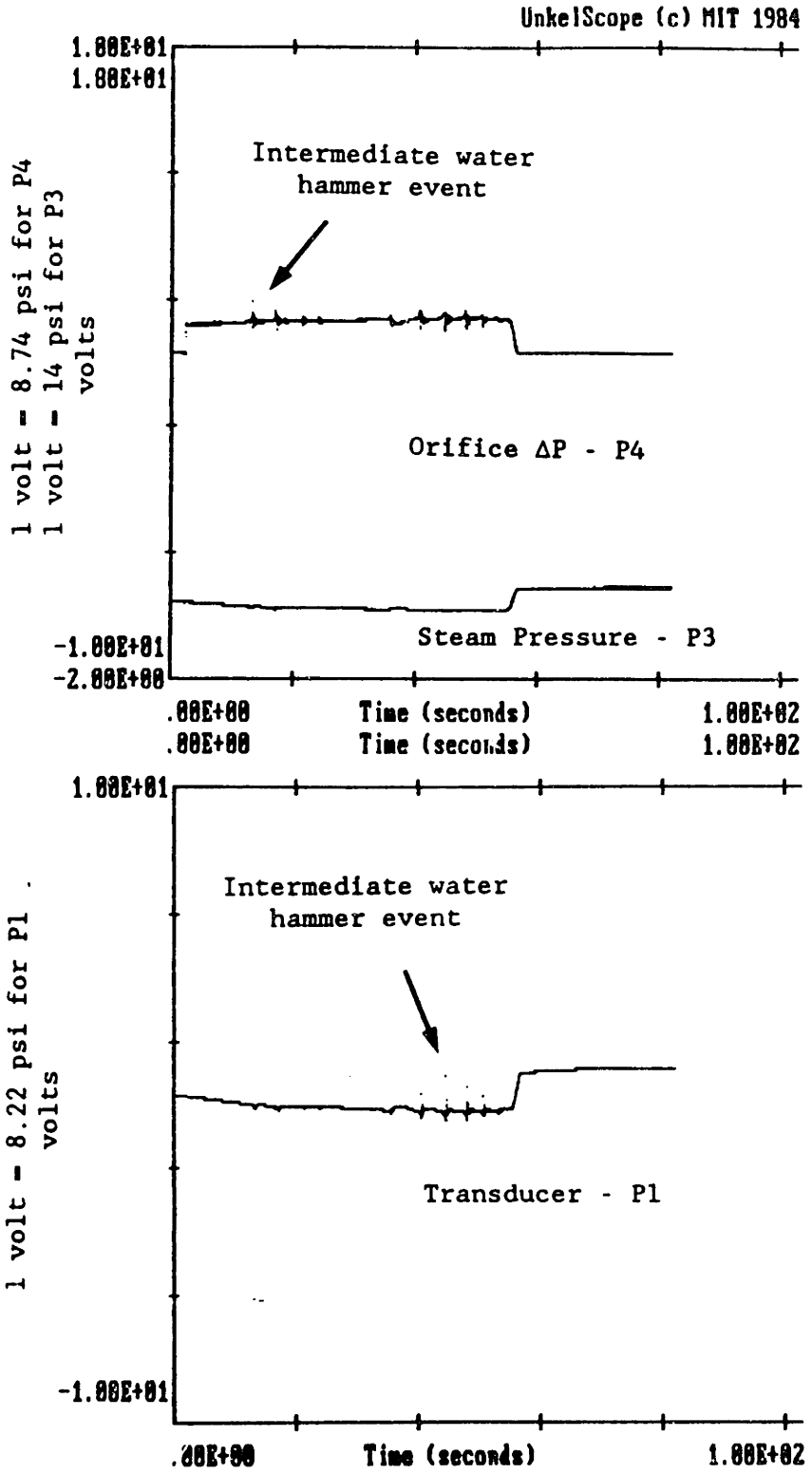

FIGURE - 4.10 Typical horizontal "L" pressure response curves. This plot shows that even for very low filling rates the intermediate water hammer does not disappear.

Orifice 0.210 in - P_t=10 psig - T_w=111°F

T_{sub}=106°F - Av. Filling Veloc.= 0.293 ft/s.

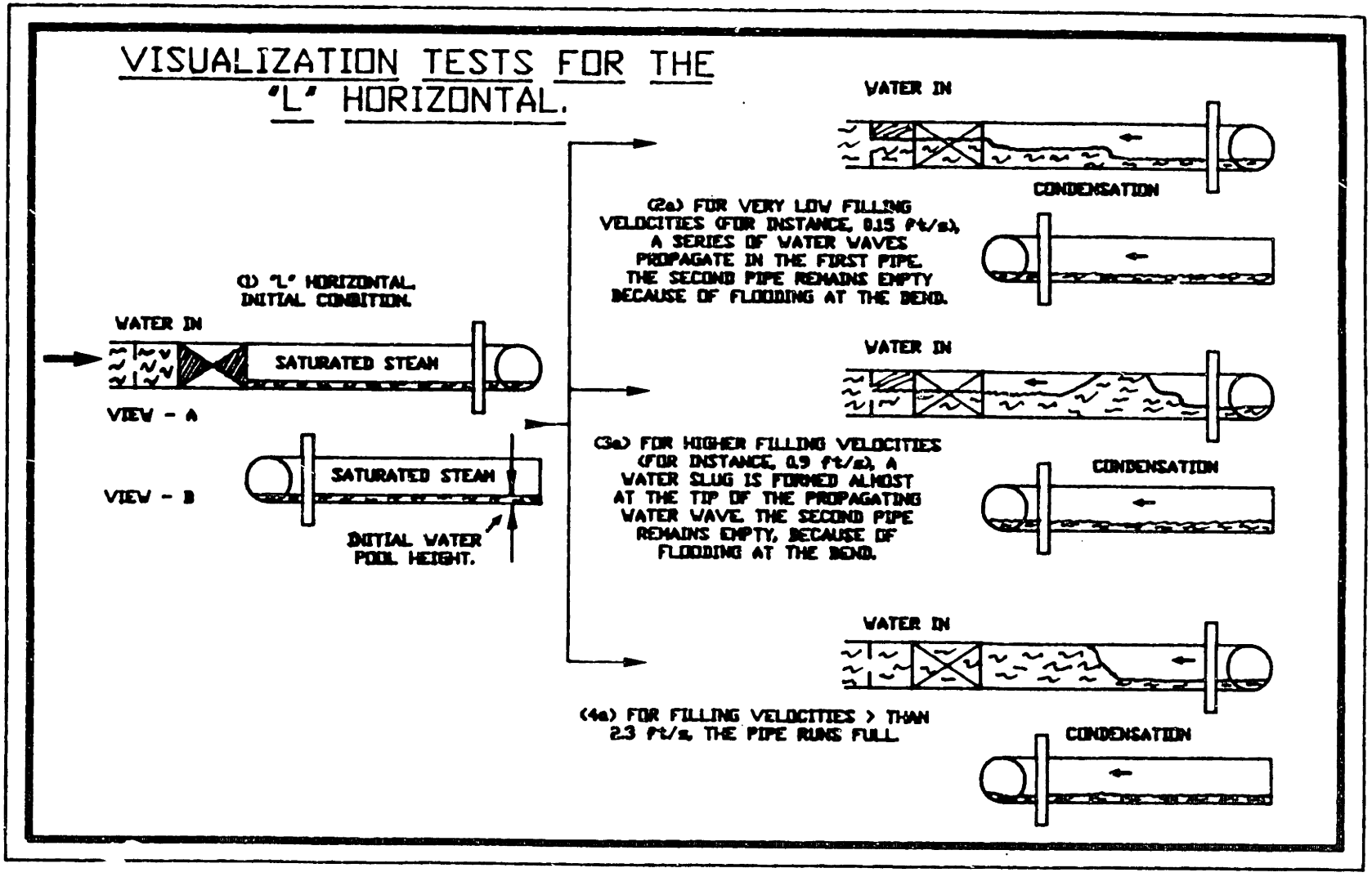

FIGURE - 4.11 (part - a) Visualization tests for the leveled horizontal "L".

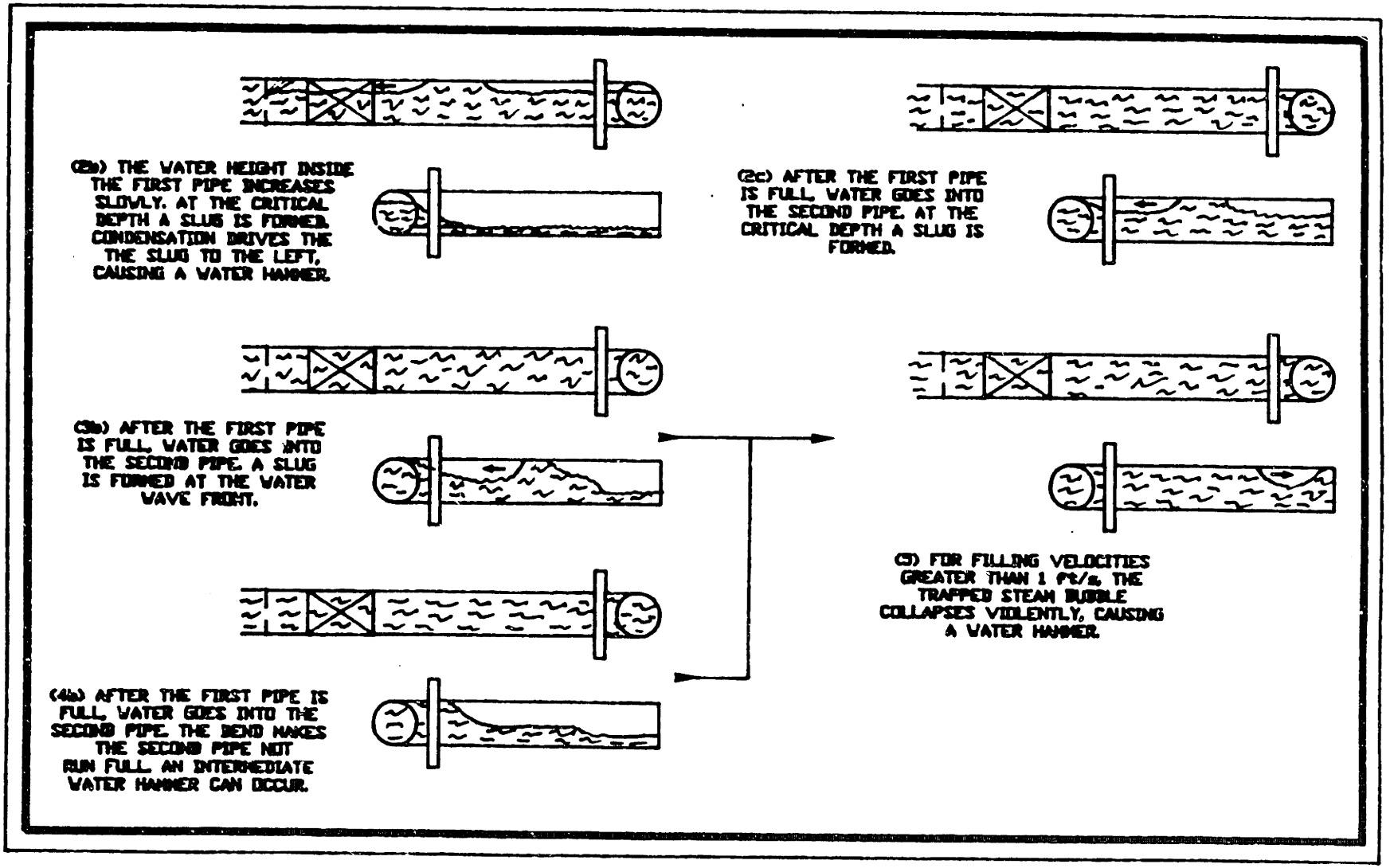

FIGURE - 4.12 (part - b) Visualization tests for the leveled horizontal "L".

because at the locations of P1 and P3 the pipes are partially filled with steam (see figure - 4.10). The disruption of the water surface facilitates the appearance of more slugs. During this period only a small amount of water goes into the second pipe, because of flooding at the bend. When the first pipe is totally full, water penetrates into the second pipe. What goes on then is a repetition of what happened in the first pipe. The slugs that are formed crash against the water column at the bend. These events are indicated at the traces of transducers P4 and P1 (see figure - 4.10).

For higher filling velocities the difference, from the visualization description above, is that the slug is formed almost at the wave front (see figure - 4.11/3a and figure - 4.12/3b). Water still fills the second pipe only after the first pipe is full, because of flooding at the bend.

For $V_{av} > 2.3$ ft./s the first pipe runs full. Flooding at the bend forces a water wave to propagate inside the second pipe (see figure - 4.11/4a and figure - 4.12/4b). A slug can then be formed. Consequently, Fr = 1 does not represent the higher intermediate water hammer boundary well.

The trapped steam bubble of figure - 4.12/5 will condense violently for filling velocities greater than 1 ft/s. See the water hammer event indication at transducers P3 and P1 traces, in figure - 4.9.

As the horizontal "L" inclined up and laterally filled behaves as a long horizontal pipe, figure - 3.7 can be used to illustrate this "L" configuration visualization tests.

4.3 Vertical "L" Filled Through the Vertical Pipe

4.3.1 Experimental Results

The apparatus used for these tests is shown in figure - 4.13. The 1" orifice, above the ball valve, was used to ensure that no steam would flow into the upper bend. The objective was to make sure that all recorded water hammer events occurred inside the "L" test section. The orifice flow area was calculated so that, for the filling rates used, the water velocity through it would be at least two times the bubble rise velocity. Consequently, no steam bubble could flow up through this orifice. The positions indicated as P1, P2, P3 and P4 in this drawing were from where the pressure signals were taken.

Figure - 4.14 is a detail of the electrical probe used during these tests. The probe could be slid intc the pipe until the copper wire would touch the water surface. At this occasion the resistance read by the multimeter would drop significantly. The water level inside the pipe could then be determined by using a caliper (The difference between touching the pipe bottom and touching the water surface).

Three test series were run in this pipe configuration.

In the first series the horizontal pipe was leveled and the test section was flushed with steam. No matter what we did, the electrical probe indicated that some water would always remain inside the horizontal pipe. For different tests, the measured water pool height varied between 0.2" to 0.5". The resultant stability map for this configuration is shown in figure - 4.15.

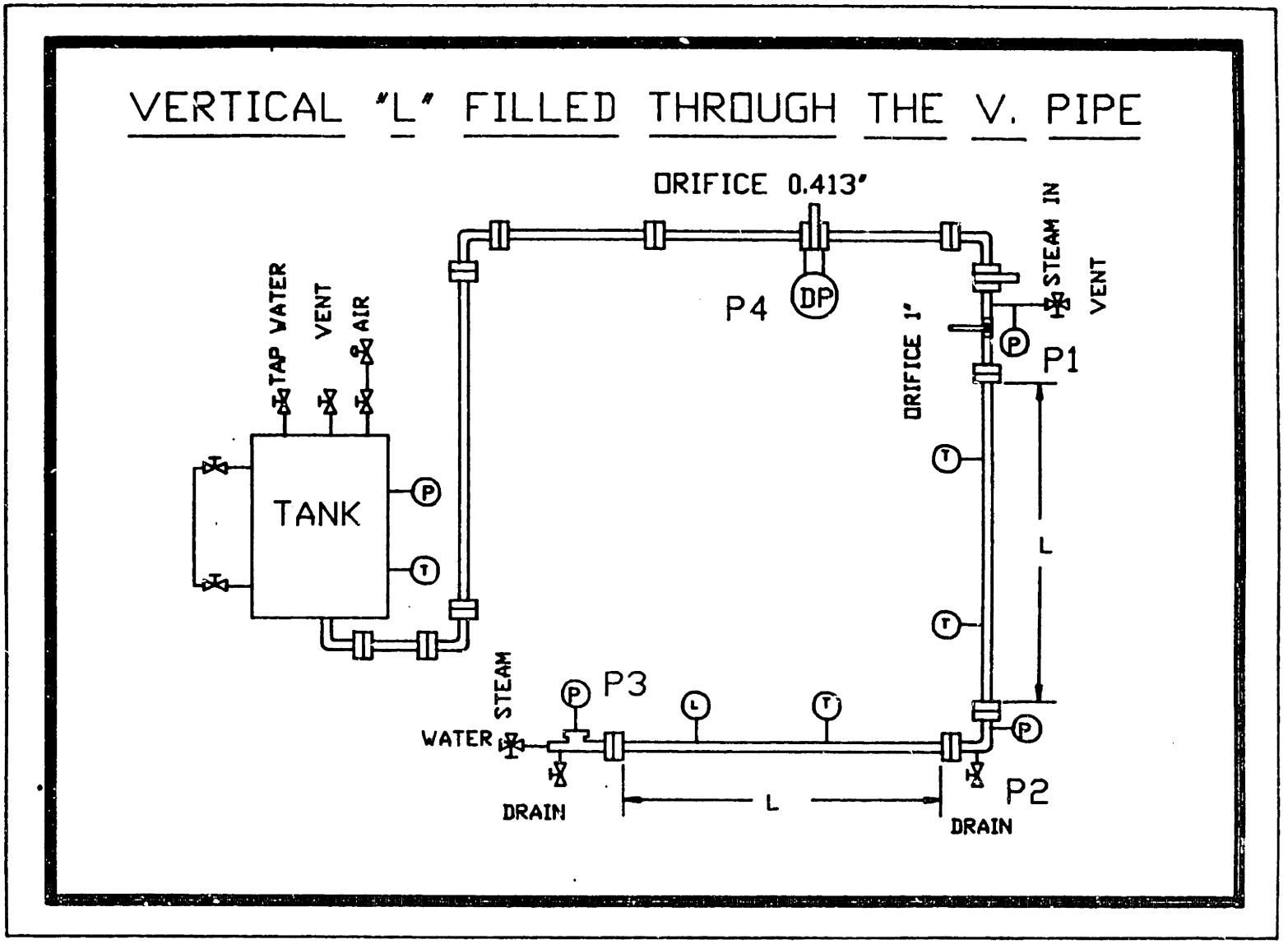

FIGURE - 4.13 Experimental apparatus used for the vertical "L" filled through the v. pipe. The distance L is ≃ 48.D (short pipe limit), where D=2 in.

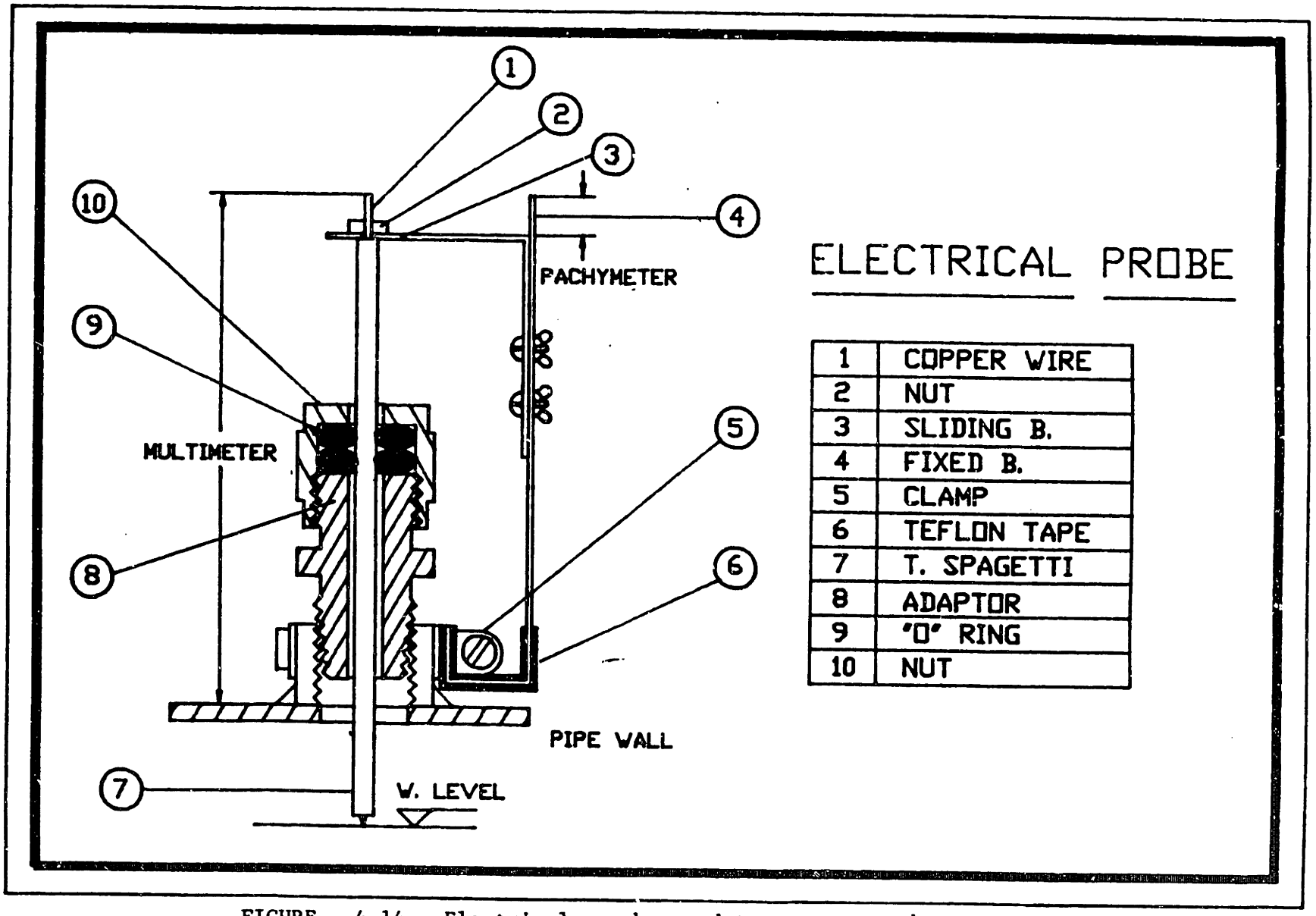

FIGURE - 4.14 Electrical probe used to measure the water level.

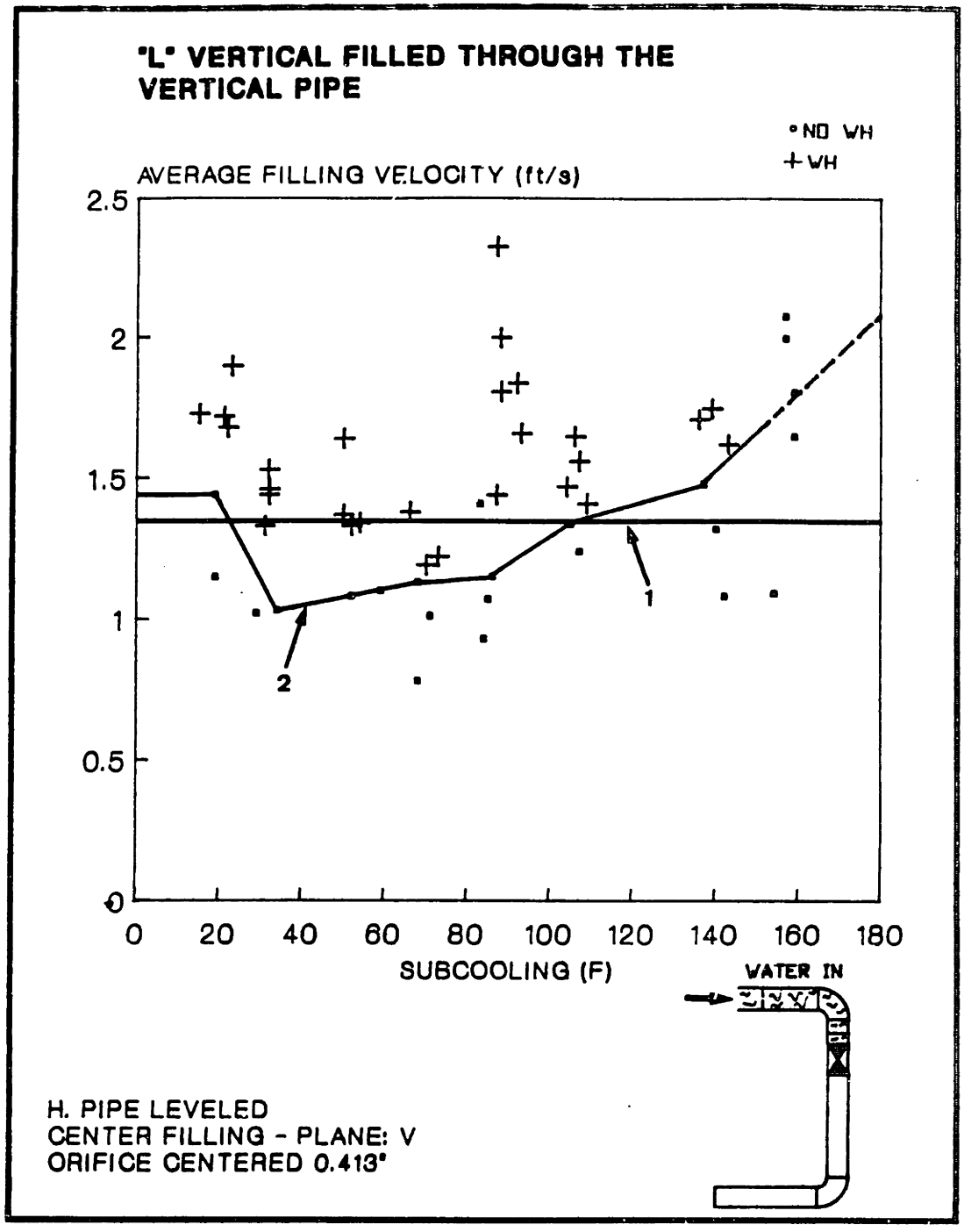

FIGURE - 4.15 Stability map for the vertical "L" filled through the v. pipe. Horizontal pipe leveled.
Line-1 -> Bend flooding limit.
Line-2 -> Experimental stability boundary.

In the second series the influence of the initial water pool height, inside the horizontal pipe, was studied. The water level was brought to a desired value by using the electrical probe and controlling the drain valve. The horizontal pipe was maintained leveled. The average subcooling of the injected water was 65^{o}F. Figure - 4.16 is the water hammer stability map obtained from these experiments.

Finally the horizontal pipe was inclined down of 0.5"/1' (The pipe end connected to the 90 degrees bend was at the higher point). Figure - 4.17 is the resultant stability map from this configuration tests.

Comparing figures - 4.16 and 4.17 to figure - 4.15, the conclusion is that the down inclination or the initial water pool height do not affect the position of the water hammer stability boundary. It is also noted that only the final water hammer appears. In order to explain this fact it is better to first describe the visualization tests.

Visualization Tests

In figures - 4.18 and 4.19 the recorded pressure transducers traces for the first test series are shown. The average filling velocities were 1.66 ft/s and 0.93 ft/s, respectively.

Figures - 4.20 (part a) and 4.21 (part b) are a representation of what was observed when the steel pipes were changed to *LEXAN* ones.

Before the ball valve is opened, the vertical "L" is full of steam and there is a pool of saturated water inside the horizontal pipe (see figure - 4.20/1). As soon as the ball valve is opened, a water jet of approximately 30" is formed. Intense condensation of steam at this water jet would then

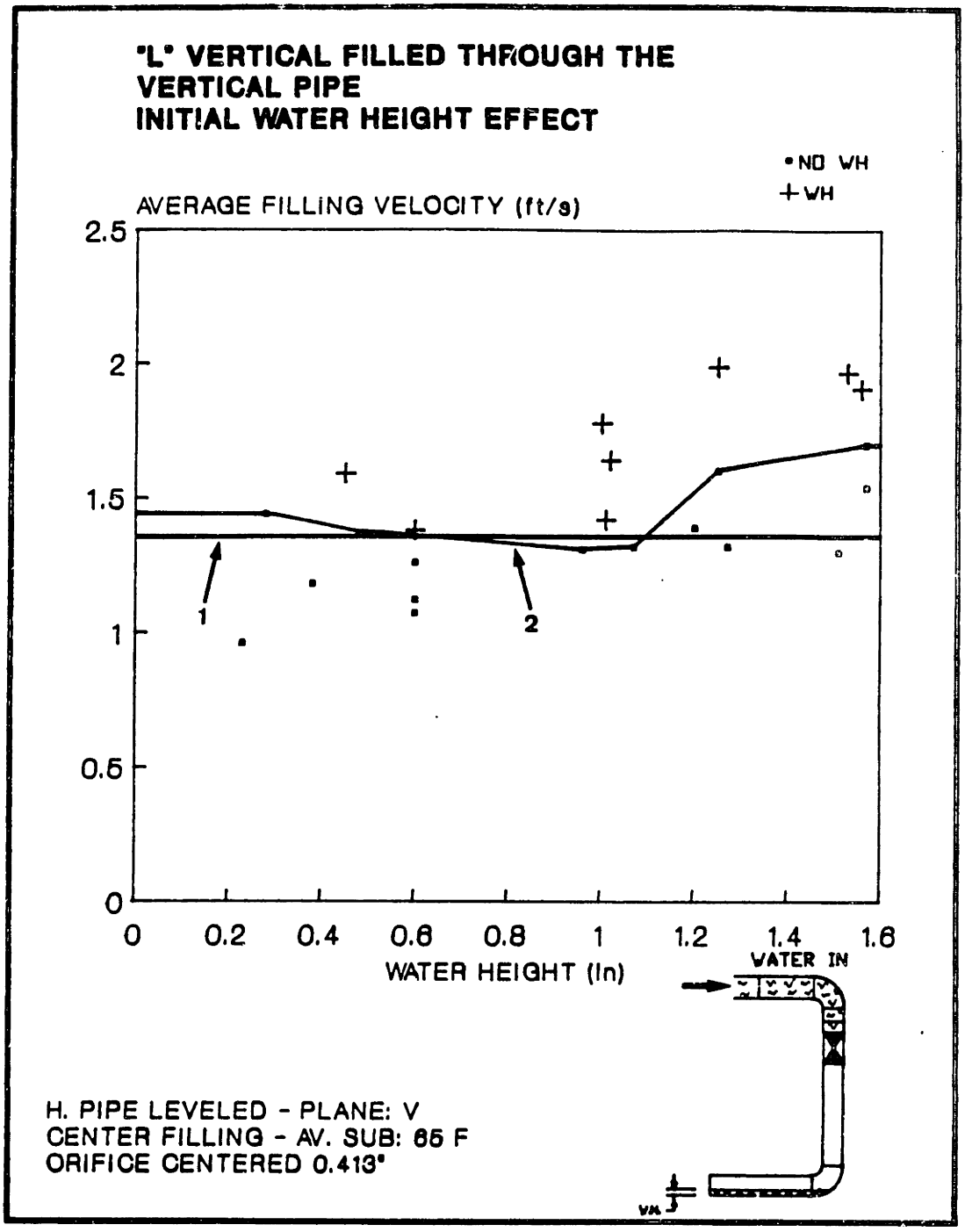

FIGURE - 4.16 Stability map for the vertical "L" filled through the v. pipe. Influence of the initial water height.
Line-1 -> Bend flooding limit.
Line-2 -> Experimental stability boundary.

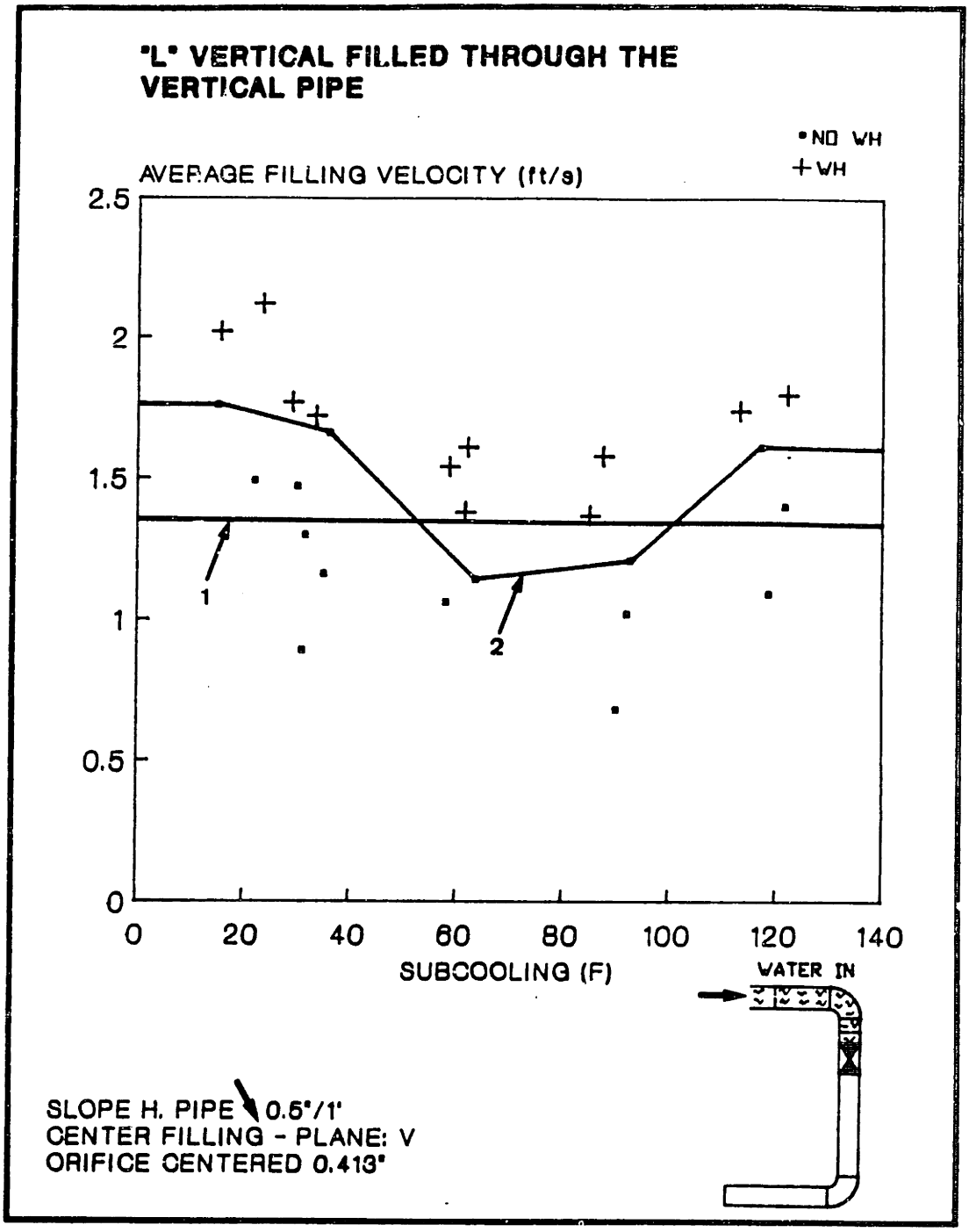

FIGURE - 4.17 Stability map for the vertical "L" filled through the v. pipe The almost horizontal pipe is inclined down.
Line-1 -> Bend flooding limit.
Line-2 -> Experimental stability boundary.

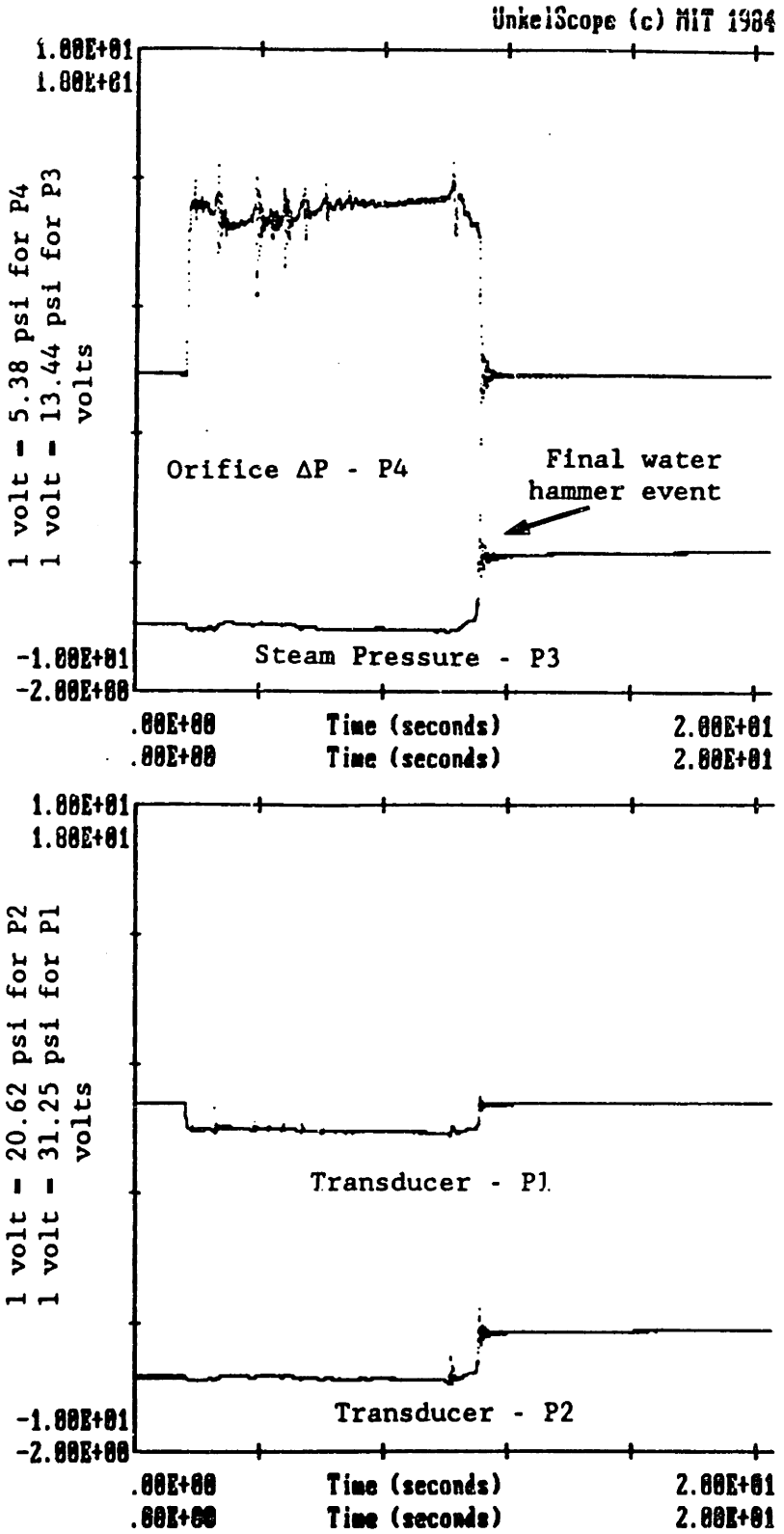

FIGURE - 4.18 Typical vertical "L" filled through the v. pipe pressure response curves for a case with a water hammer event (h. pipe leveled).

Orifice 0.413 in - P_t=32 psig - T_w=139°F

T_{sub}=93°F - Av. Filling Veloc.= 1.66 ft/s.

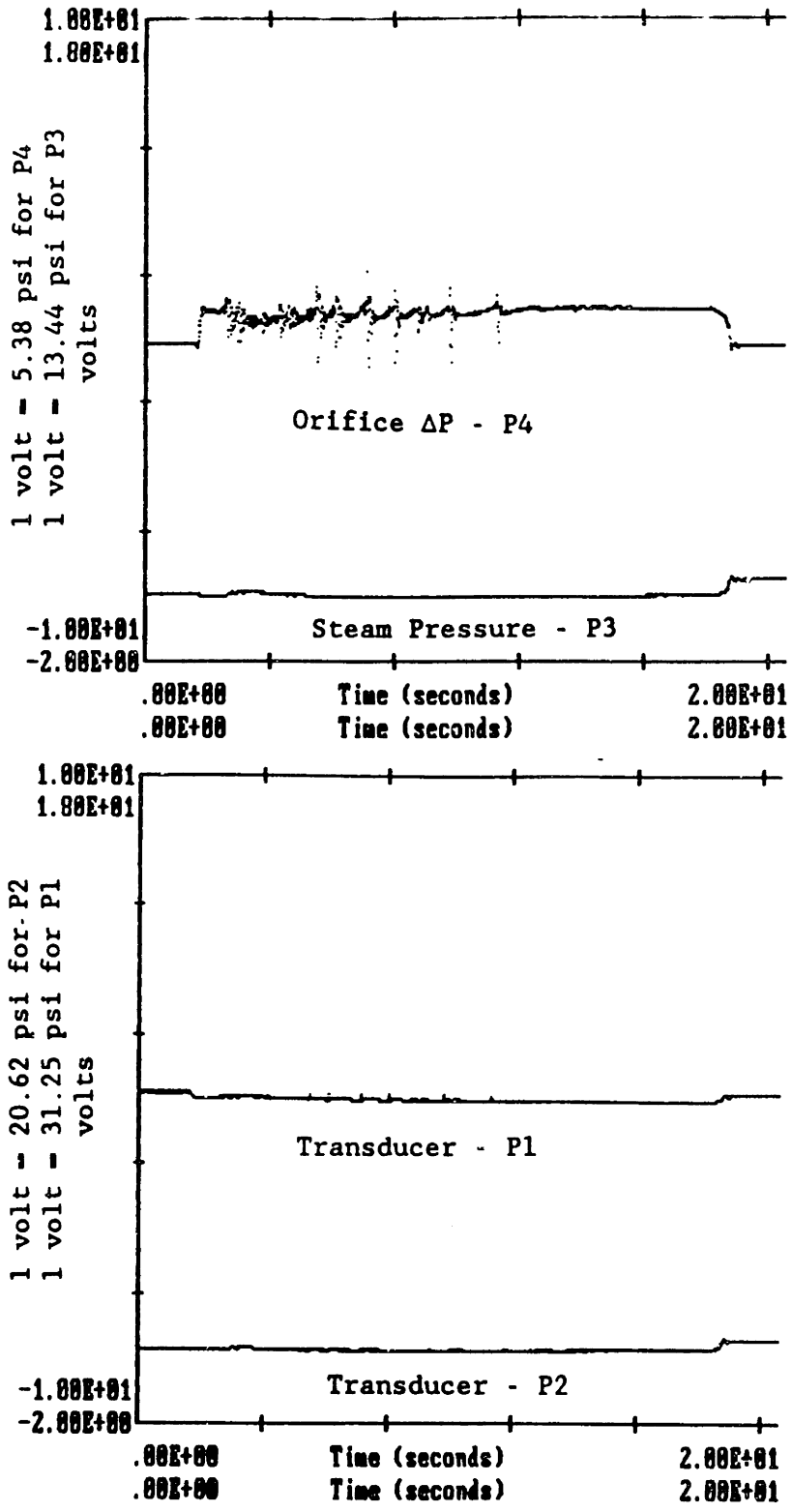

FIGURE - 4.19 Typical vertical "L" filled through the v. pipe pressure response curves for a case without a water hammer event (h. p. leveled).

Orifice 0.413 in - P_t=11 psig - T_w=144°F

T_{sub}=84°F - Av. Filling Veloc.= 0.93 ft/s.

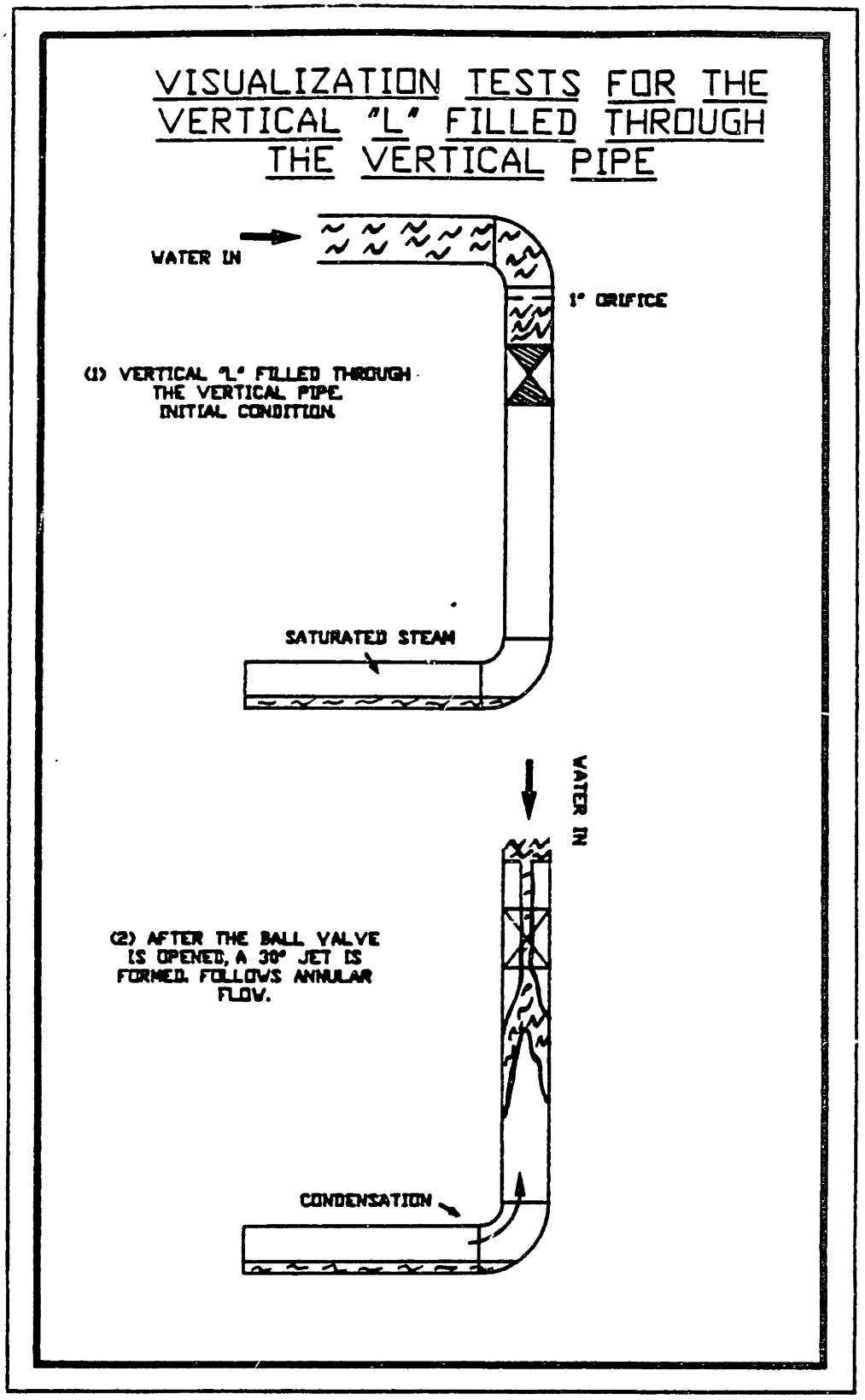

FIGURE - 4.20 (part - a) Visualization tests for the vertical "L" filled through the v. pipe (h. p. leveled).

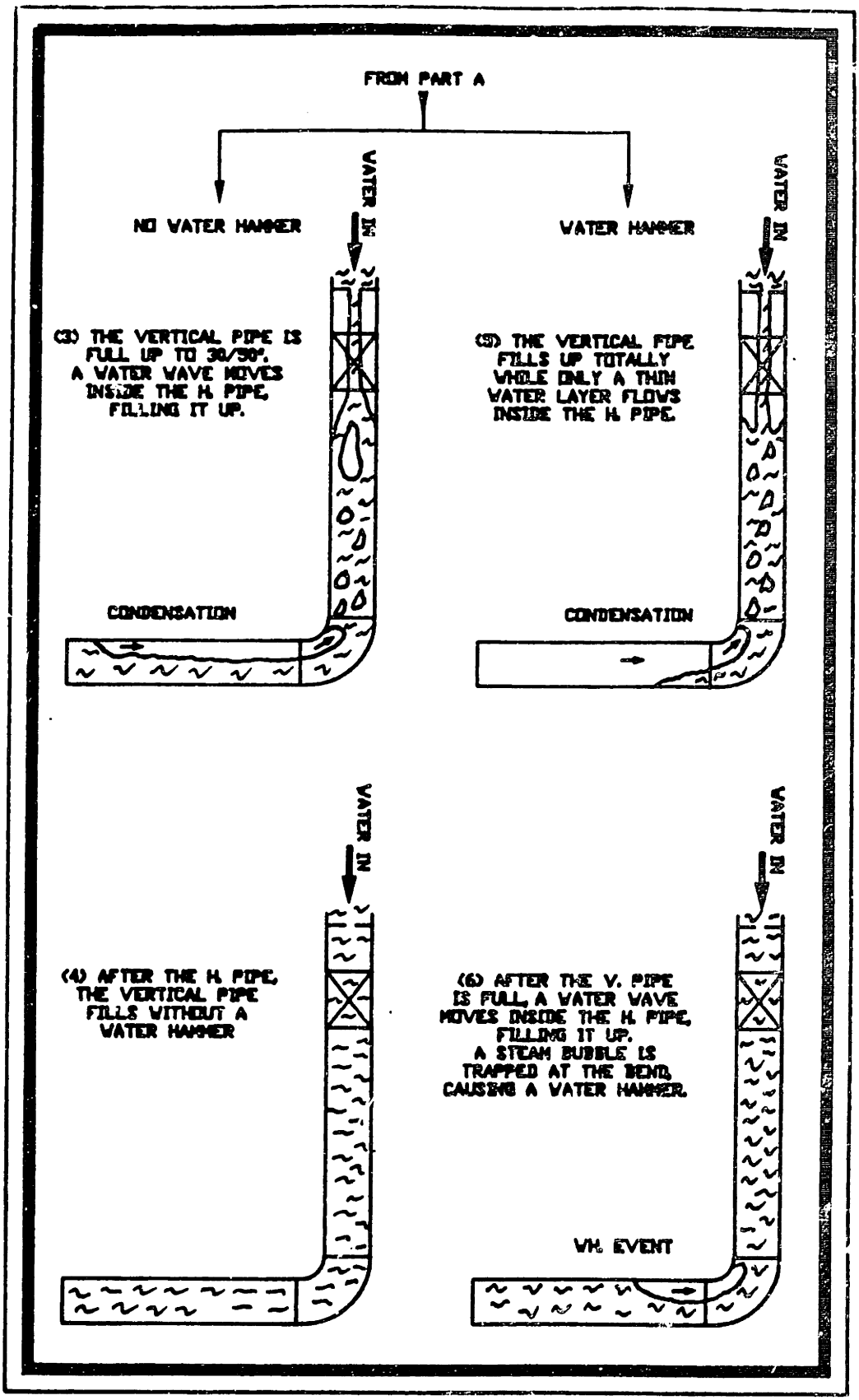

FIGURE - 4.21 (part - b) Visualization tests for the vertical "L" filled through the v. pipe (h. p. leveled).

occur.

For a test in which there was no water hammer event, the injected water would accumulate in the vertical pipe up to 30" to 50". At the same time the water would penetrate into the horizontal pipe, filling it up slowly. We understand that during this process most of the steam, that was inside the horizontal pipe, could escape. After the horizontal pipe was full the vertical pipe would fill up smoothly.

For a test with a water hammer event, the vertical pipe would fill up first. Flooding would slow the water penetration into the horizontal pipe. When the vertical pipe was almost full, the water would go into the horizontal pipe with a velocity that would not permit the steam to escape. Consequently, a steam bubble was trapped and a water hammer could occur. In section 4.3 - item 2 a way of predicting the water hammer stability boundary is proposed, using an already available bend flooding correlation.

As it seems that the bend flooding phenomenon is the governing factor, as far the appearance of a water hammer is concerned in this present pipe configuration, the downward inclination or the initial water pool height should not have much effect on the position of the water hammer stability boundary. Indeed, this was what was observed in figures - 4.15, 4.16 and 4.17.

For the pressure traces of the transducer P4, in figures - 4.18 and 4.19, there are several dips and spikes. These events were not considered as water hammers. The reason for this is that it was observed that they were caused by the collapse of steam bubbles inside the vertical pipe, while it was not full.

4.3.2 Proposed Model

In order to a water hammer occur, it is first necessary that a steam bubble be trapped inside a pipe. From the visualization tests description, given in section 4.3 - item 1, we understood that above a certain filling velocity the steam inside the horizontal pipe was not able to escape. This appeared to be related to the flooding phenomenon at the vertical "L" bend. Therefore, it is proposed here that a flooding correlation be used to establish the water hammer safe region.

When flooding is mentioned, the correlations by Wallis (20) or Pushkina and Sorokin (36) come to mind. However, Krolewski (37) showed that the gas velocity necessary to flood a bend is much smaller than the one predicted by Wallis' correlation (developed for a vertical pipe). In her study she was interested in determining flooding limits at nuclear reactor hot legs. Because nuclear reactors are not all the same, she determined flooding limits in five different vertical "L" shaped pipes. Siddiqui et al (38) ran more detailed experiments, which were designed to specifically study the flooding phenomenon at an elbow positioned between a vertical pipe and an horizontal or slightly inclined pipe. Their conclusion was that the flooding is related to the hydraulic jump that occurs when the water leaves the vertical pipe and goes into the horizontal pipe. Measuring the hydraulic jump height, at the onset of flooding, they were able to correlate the local void fraction to the nondimensional superficial gas velocity as:

$$j_s^* = 0.2 \times \alpha_s^{(3/2)} \qquad \text{eq(4 - 1)}$$

where: $$j_s^* = \frac{j_s}{\left[\frac{g.D.(\rho_1-\rho_s)}{\rho_s}\right]^{(1/2)}}$$

Ardron and Banerjee (39) used the above relation plus the mass and momentum conservation equations to develop bend flooding correlations. When the horizontal pipe is level their correlation takes the following form:

$$j_s^* = 1.444 - 0.004.\lambda - \cosh(\lambda^p.K^q.(j_1^{*\,1/2})^r) \qquad \text{eq(4 - 2)}$$

where:

$p = 0.057$, $q = -0.020$, $r = 0.70$, $n = 0.2$,

$$\lambda = \frac{L.(Re^{*\,-n})}{D},$$

$$Re^* = \frac{D}{\nu_s}.\left(\frac{g.D.(\rho_1-\rho_s)}{\rho_s}\right)^{1/2}$$

$$K = \frac{\nu_s}{\nu_1}.\left(\frac{\rho_s}{\rho_1}\right) \quad \text{and}$$

$$j_1^* = \frac{j_1}{\left[\frac{g.D.(\rho_1-\rho_s)}{\rho_1}\right]^{(1/2)}}.$$

Notice that all the terms in equation (4 - 2) are nondimensional. Any system of units can be used.

When no steam is escaping j_s^* is equal to zero. The corresponding limiting water filling velocity can be calculated using equation - 4.2, which results in 1.35 ft/s (At very low values of j_s^*, eq(4 - 2) predicts values of j_1^* similar to the ones that are predicted by Wallis flooding correlation (20)). This value is plotted as line 1 in figures - 4.15, 4.16 and 4.17. The agreement is seen to be good.

4.4 Vertical "L" Filled Through the Horizontal Pipe

The apparatus used for filling an "L" in the vertical plane through the horizontal leg is shown in figure - 4.22. The water was injected through an orifice with a hole positioned at the pipe axis.

Figures - 4.23 and 4.24 are the test series resultant stability maps with the horizontal pipe leveled and the water introduced through the pipe center. The line 1 in figure - 4.23 is the short horizontal single pipe theoretical boundary, whereas in figure - 4.24 is the experimental vertical up single pipe stability boundary. It can be seen in figure - 4.23 and 4.24 that: 1) The line 1 lies above the experimental boundary. Again, in this configuration, a short horizontal pipe behaves more like a long horizontal pipe; 2) The running full limit (Fr = 1 or V_{av} = 2.3 ft/s) predicts well the higher intermediate water hammer boundary; and 3) The vertical up single pipe theory can be used to establish the safe final water hammer region.

From the experience gained previously, inclining the horizontal pipe (0.5"/1') and filling it laterally from the bottom (inclined up) should eliminate the intermediate water hammer, in this configuration. This was confirmed by figure - 4.25. The vertical up single pipe theory can still be used to determine the final water hammer safe region.

Visualization Tests

The pressure traces for transducers P1, P3 and P4 are shown in figures - 4.26 and 4.27. They were recorded when the horizontal pipe was leveled, the water was injected axially and the end filling velocities were 1.45 ft/s

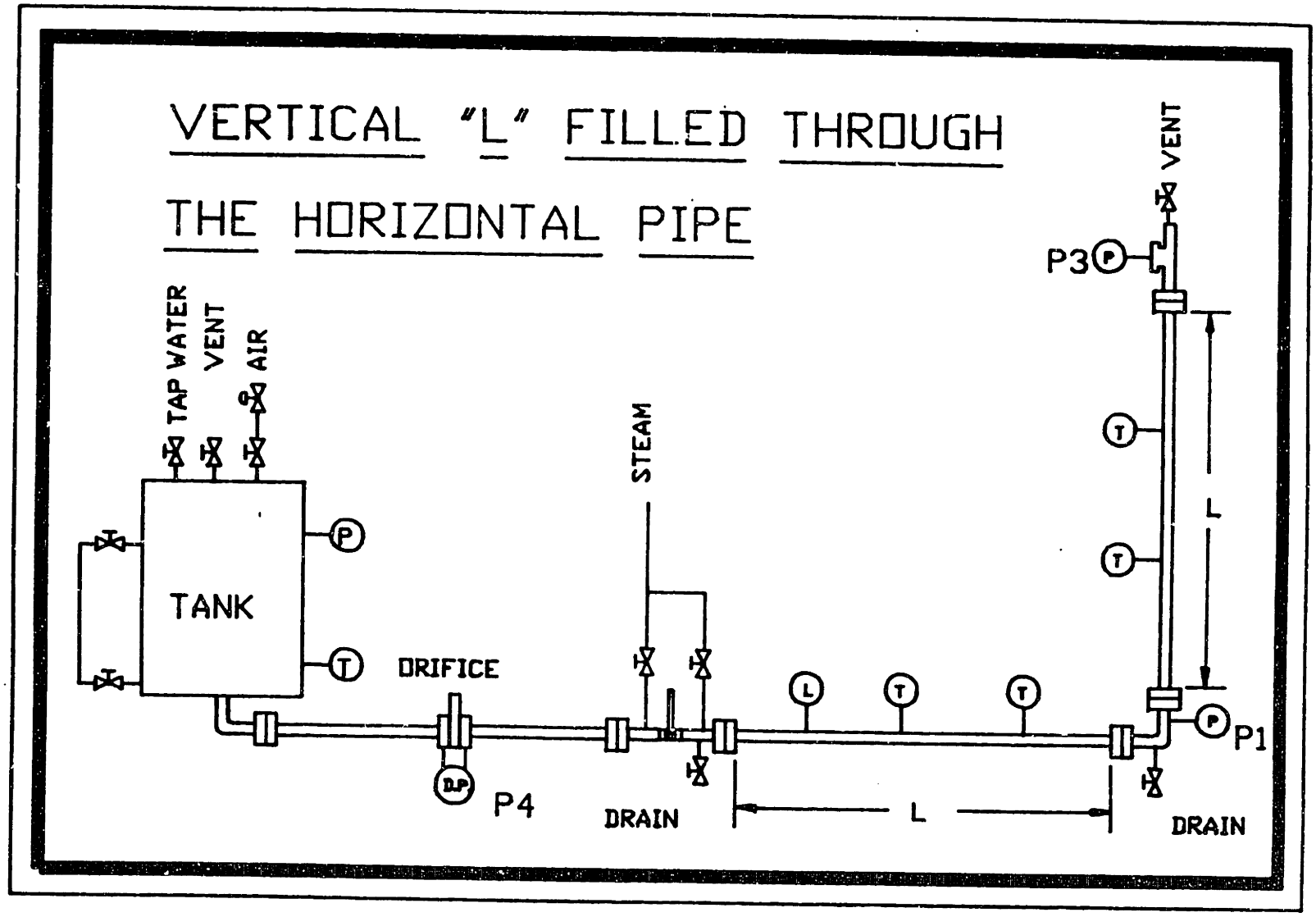

FIGURE - 4.22 Experimental apparatus used for the vertical "L" filled through the h. pipe. The distance L is ≃ 48.D (short pipe limit), where D=2 in.

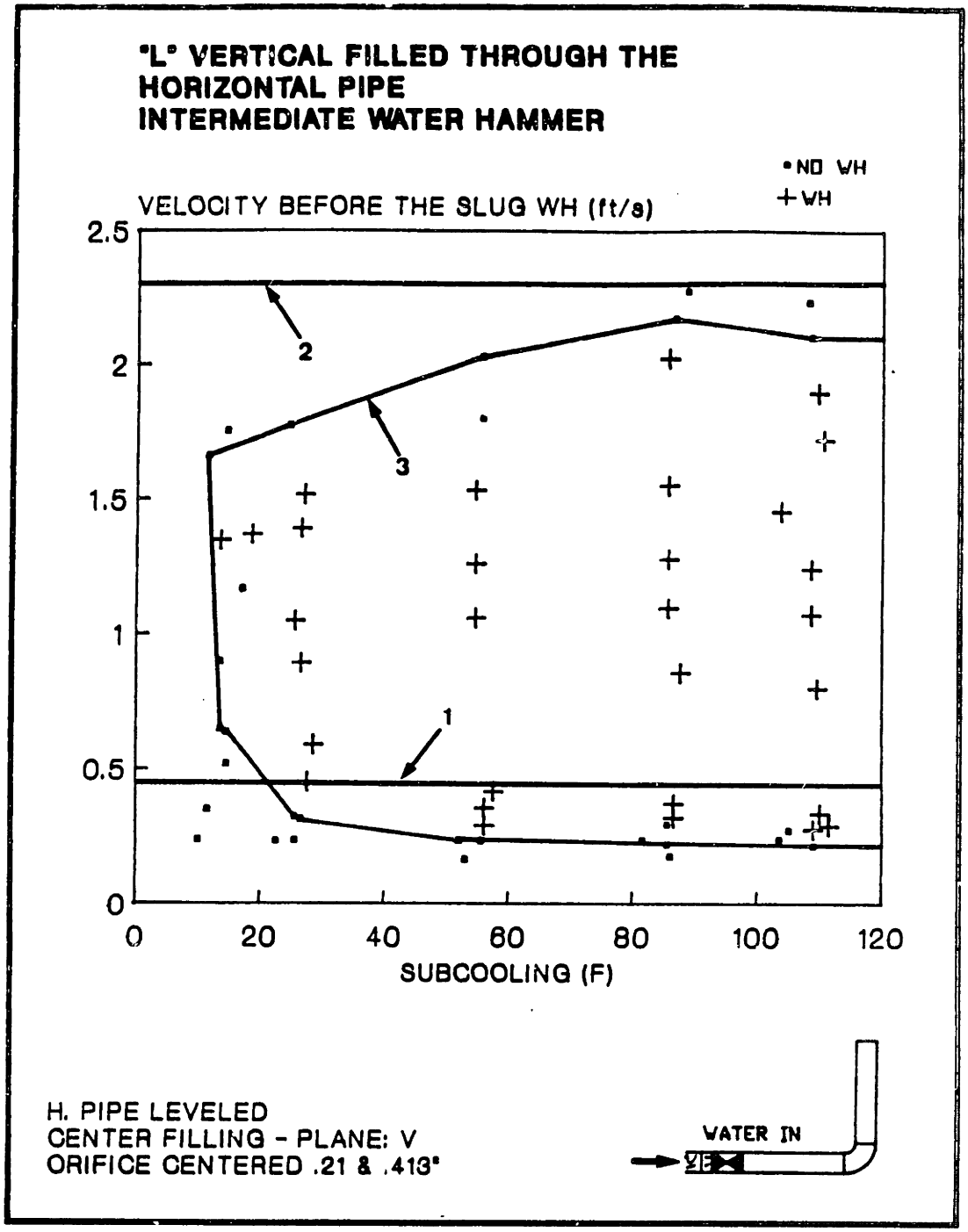

FIGURE - 4.23 Intermediate water hammer stability map for the vertical "L" filled through the h. pipe (horizontal pipe leveled).
Line-1 -> Short horizontal, single pipe theoretical stability boundary - 0.46 ft/s.
Line-2 -> Running full pipe limit - Fr=1 or average filling rate of 2.3 ft/s.
Line-3 -> Experimental stability boundary.

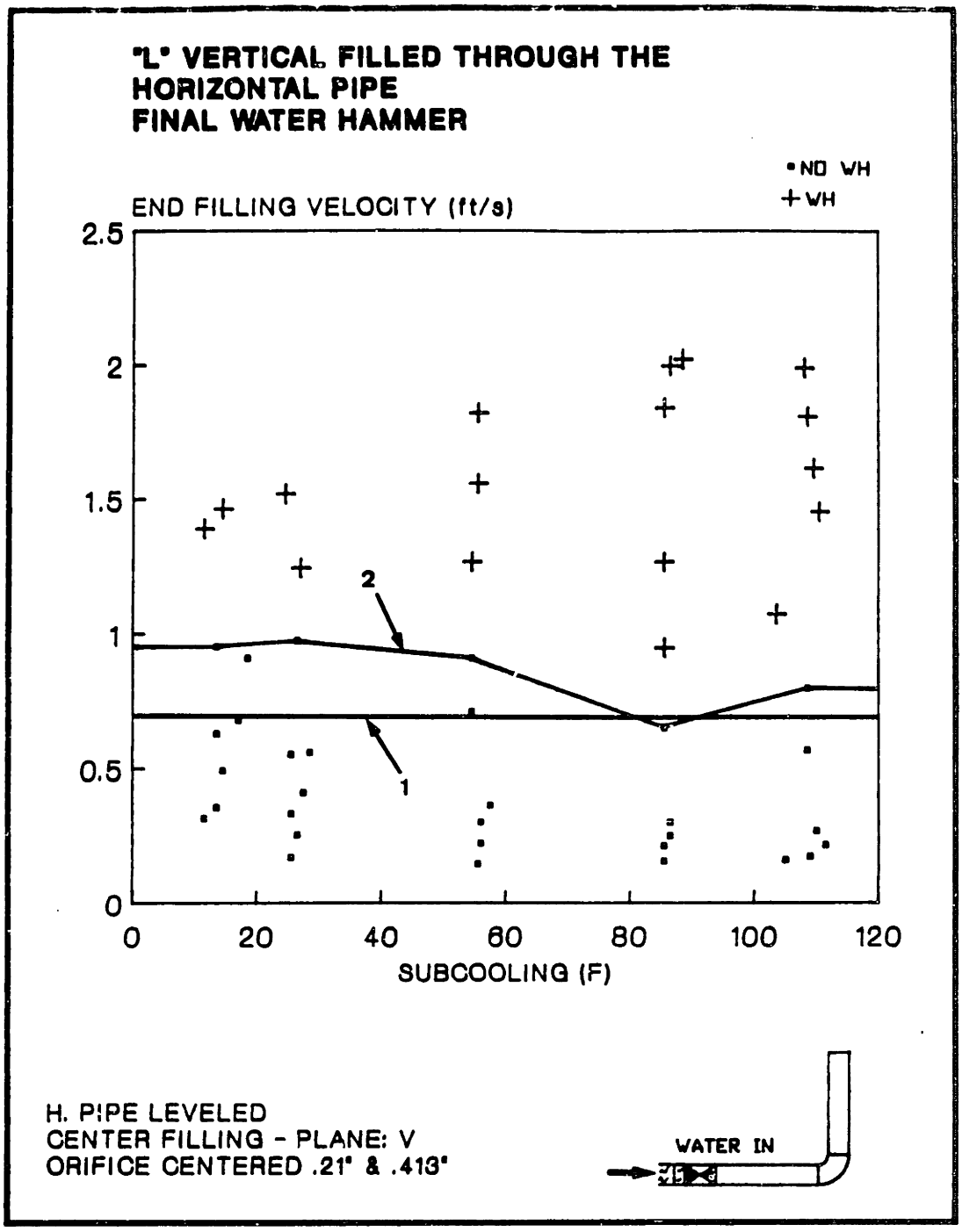

FIGURE - 4.24 Final water hammer stability map for the vertical "L" filled through h. pipe (horizontal pipe leveled).
Line-1 -> Experimental vertical up, single pipe stability boundary - 0.7 ft/s.
Line-2 -> Experimental stability boundary.

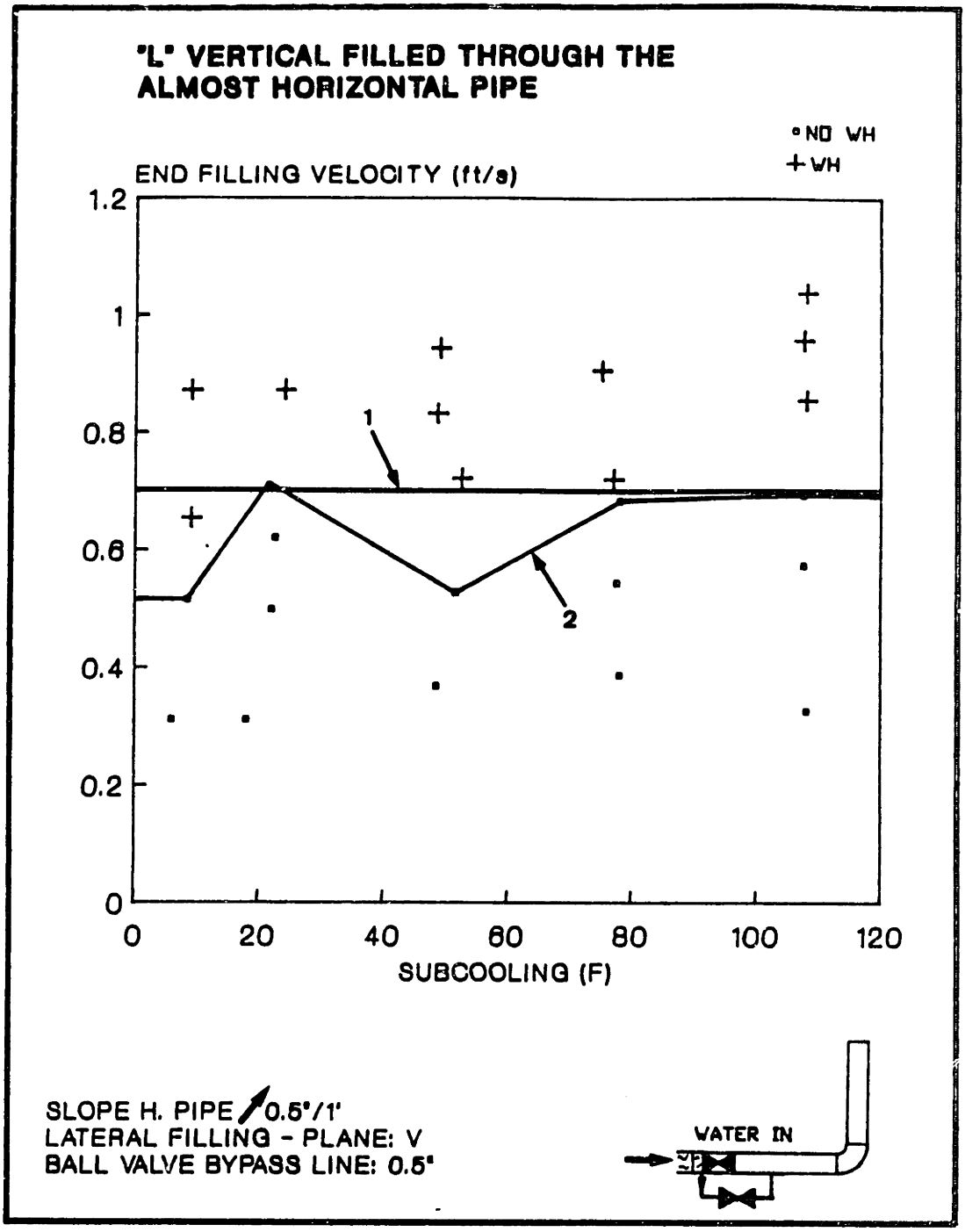

FIGURE - 4.25 Stability map for the vertical "L" filled through the h. pipe (h. p. inclined up and laterally filled).
Line-1 -> Experimental vertical up, single pipe stability boundary - 0.7 ft/s.
Line-2 -> Experimental stability boundary.

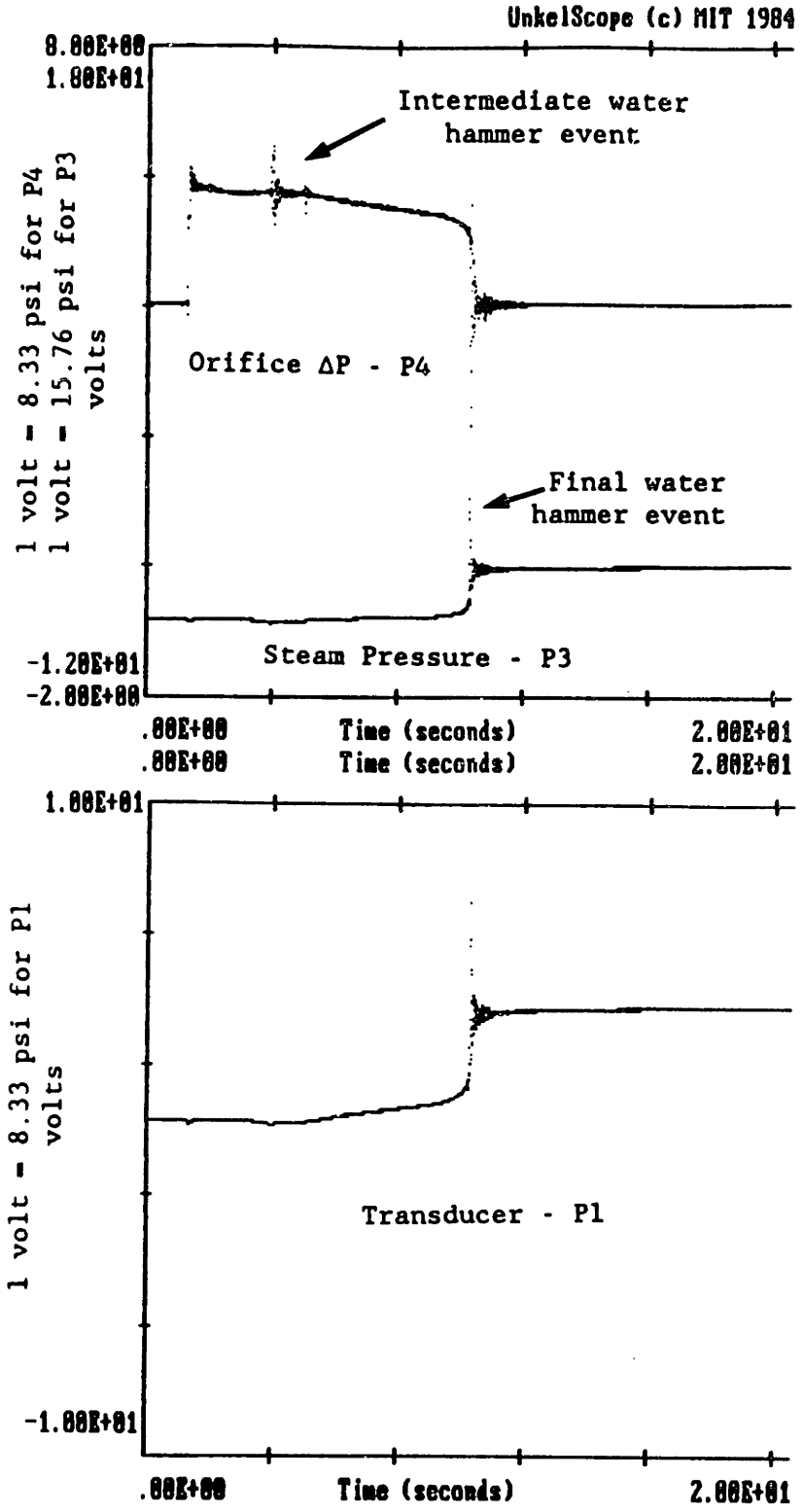

FIGURE - 4.26 Typical vertical "L" filled through the horizontal pipe pressure response curves for a case with intermediate and final water hammer events (pipes leveled).

Orifice 0.413 in - P_t=30 psig - T_w=112°F

T_{sub}=110°F - End Veloc.= 1.45 ft/s.

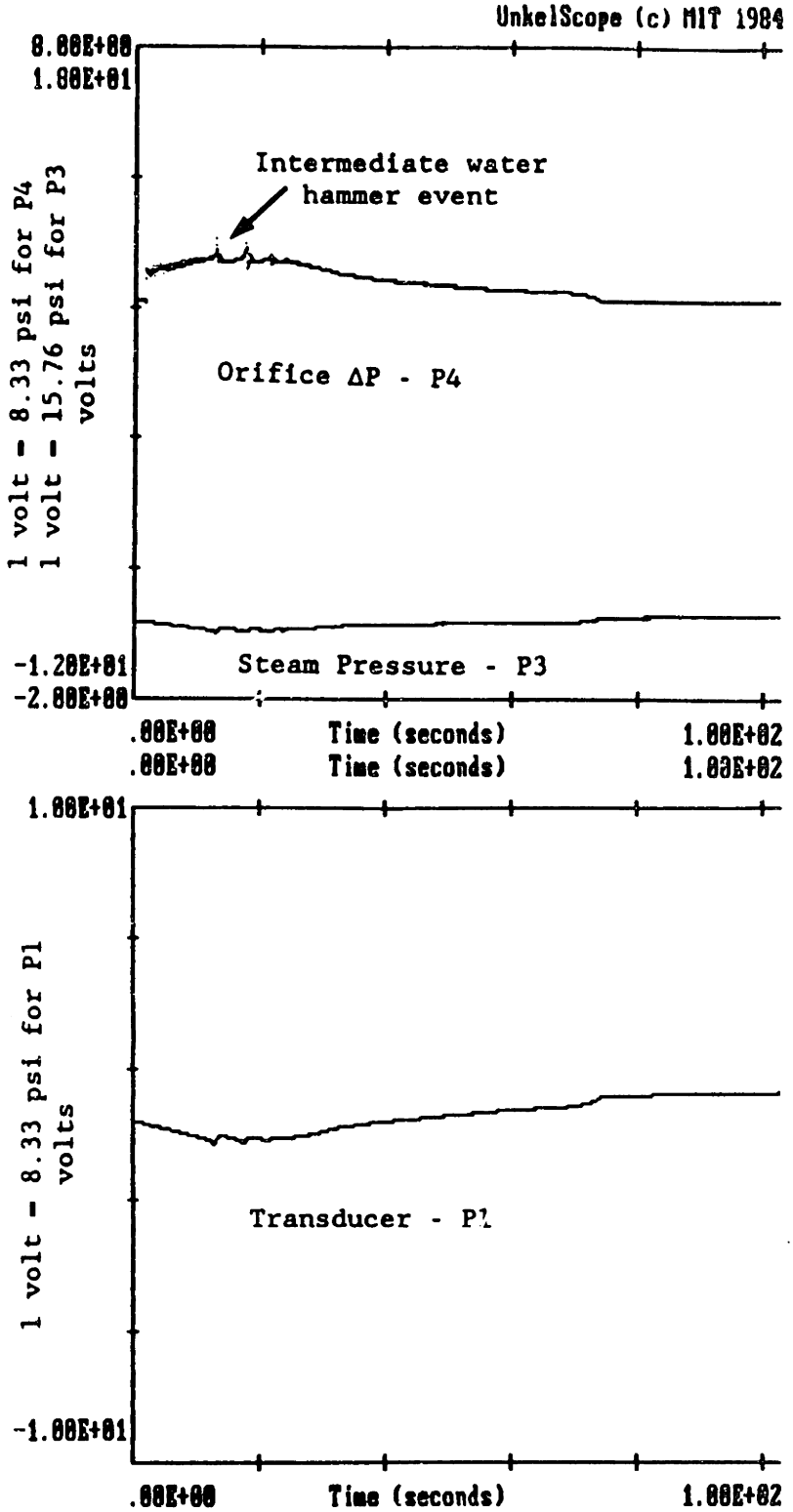

FIGURE - 4.27 Typical vertical "L" filled through the horizontal pipe pressure response curves. The plot shows that even for very low filling rates the intermediate water hammer does not disappear.

Orifice 0.210 in - P_t=11 psig - T_w=115°F

T_{sub}=105°F - End Veloc.= 0.160 ft/s.

and 0.160 ft/s, respectively. The positions of these transducers in the test apparatus are indicated in figure - 4.22.

When the steel pipes were changed to *LEXAN*, what was observed is represented in figures - 4.28 (part a) and 4.29 (part b). Comparing these drawings to figures - 4.11 and 4.12, it is seen that the horizontal pipe filling process, for all rates, is similar to what was described for the horizontal "L" pipes. After the horizontal pipe is full, the water advances into the vertical pipe. The water interface is smooth. At this point, the filling rate slows down, because the steam pressure increases (see transducer P3 traces in figures - 4.26 and 4.27). This is caused by the decrease of the steam condensation (the turbulence and the area of the interface is smaller). This fact forces the traces of the transducer P4 to dip (see figures - 4.26 and 4.27). When the final filling velocity is more then 1 ft/s, the trapped steam bubble collapses violently, causing a final water hammer.

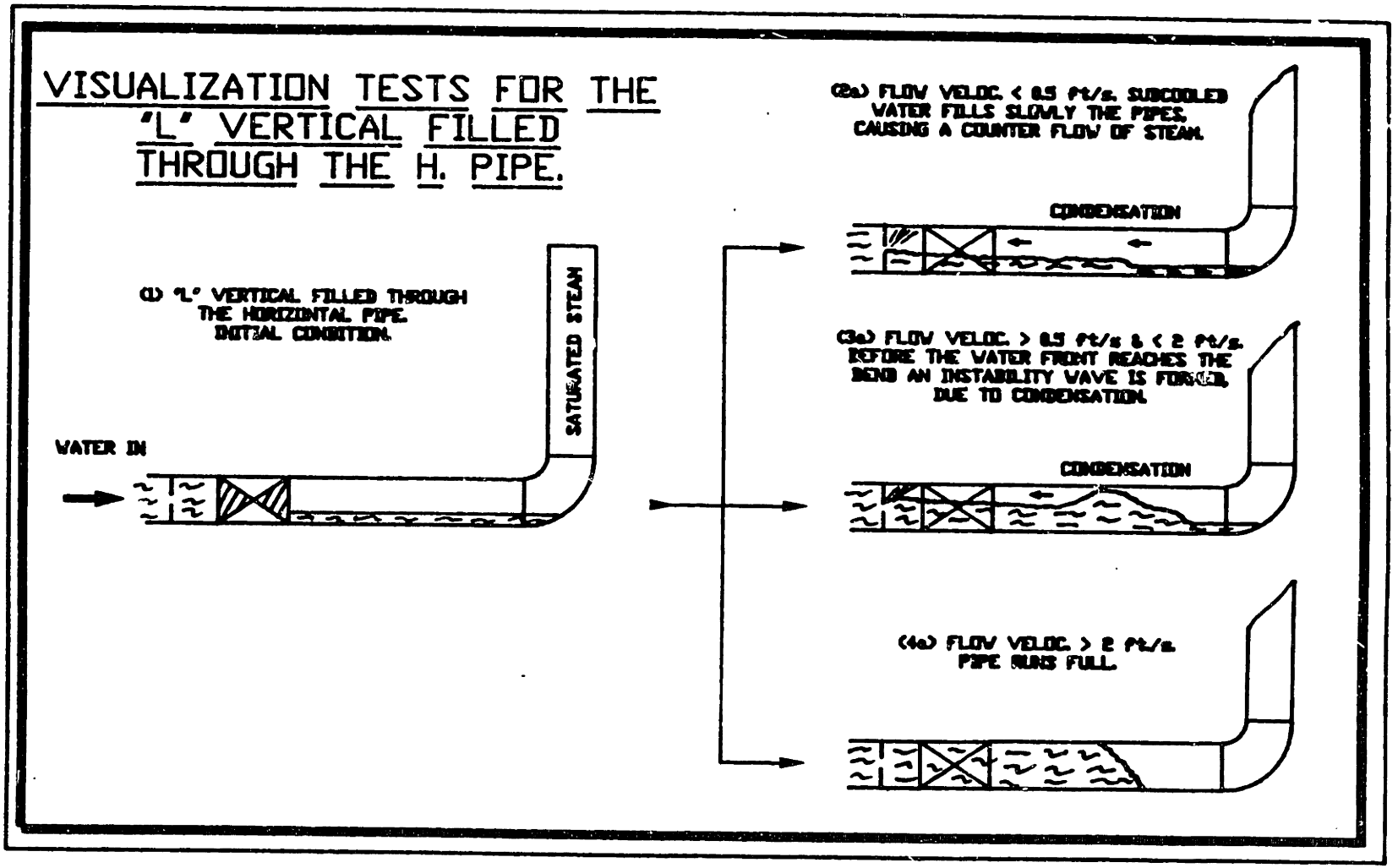

FIGURE - 4.28 (part - a) Visualization tests for the vertical "L" filled through the h. pipe (h. p. leveled).

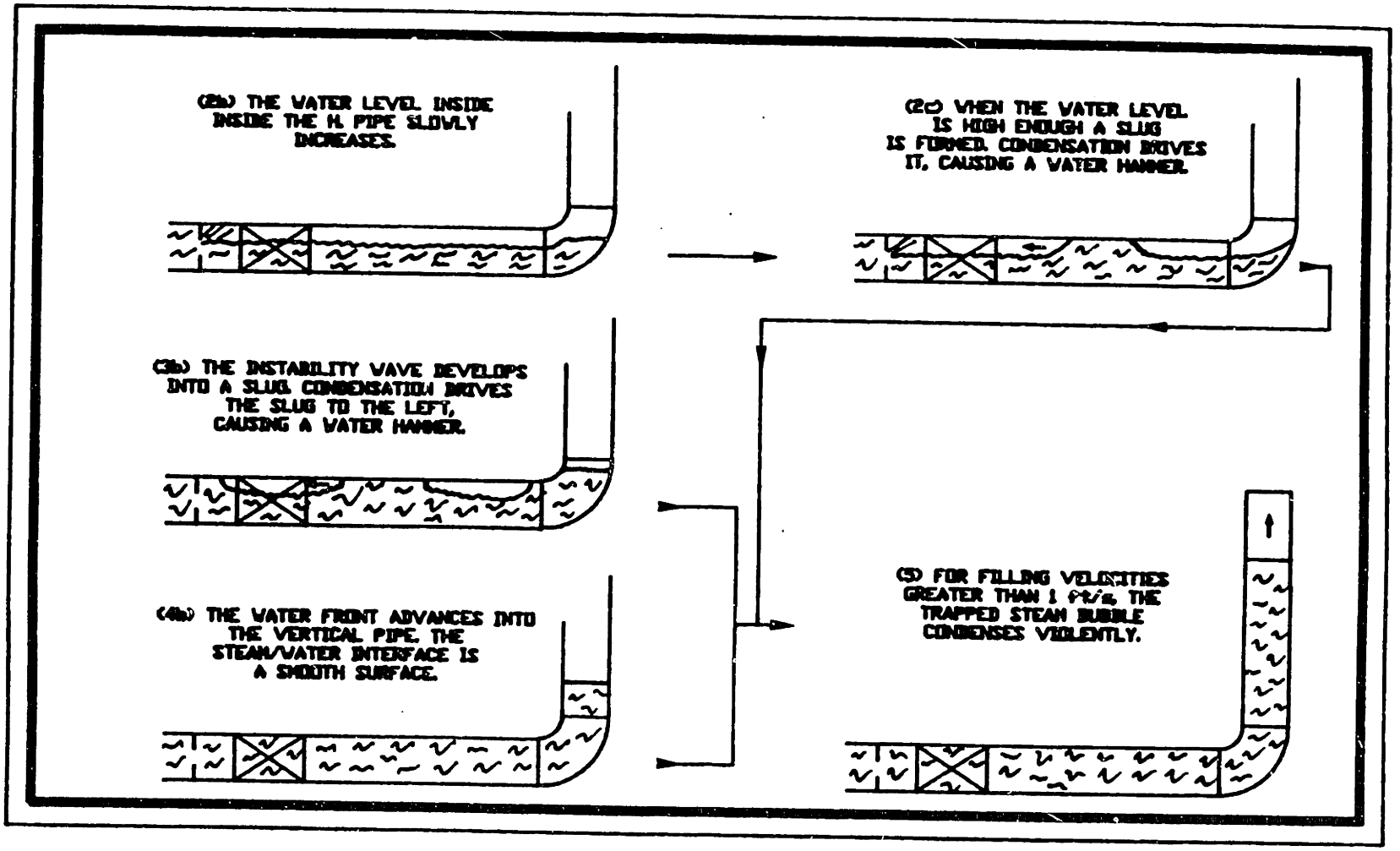

FIGURE - 4.29 (part - b) Visualization tests for the vertical "L" filled through the h. pipe (h. p. leveled).

4.5 Inverted "L" Filled Through the Horizontal Pipe

The scheme of the equipment used in the inverted "L" filled through the horizontal pipe is shown in figure - 4.30. The locations where the pressure signals were recorded from are indicated in this figure as P1, P3 and P4.

Figures - 4.31 and 4.32 are the resultant water hammer stability maps for a test series where the horizontal pipe was leveled and the filling was through the pipe center. As can be observed, when the injected water subcooling is more than 40^{o}F, there is no lower intermediate water hammer, whereas the running full limit (Fr =1) predicts the upper boundary well. Before the visualization tests, we expected that the vertical down single pipe theory would predict the final water hammer boundary, for this configuration. However, to predict this boundary position we should use the vertical up single pipe limit (see figure - 4.32). This will become clear when we discuss the visualization tests.

Figure - 4.33 proves that inclining the horizontal pipe and filling it laterally from the bottom (inclined up) also eliminates the intermediate water hammer, in this configuration. The vertical up single pipe theory should also be used to calculate final water hammer safe filling rates.

Visualization Tests

Typical measured transducer pressure traces are reproduced in figures - 4.34 and 4.35. They were recorded when the horizontal pipe was leveled, the filling was through the pipe center and the average filling velocities were 1.12 ft/s and 0.227 ft/s, respectively.

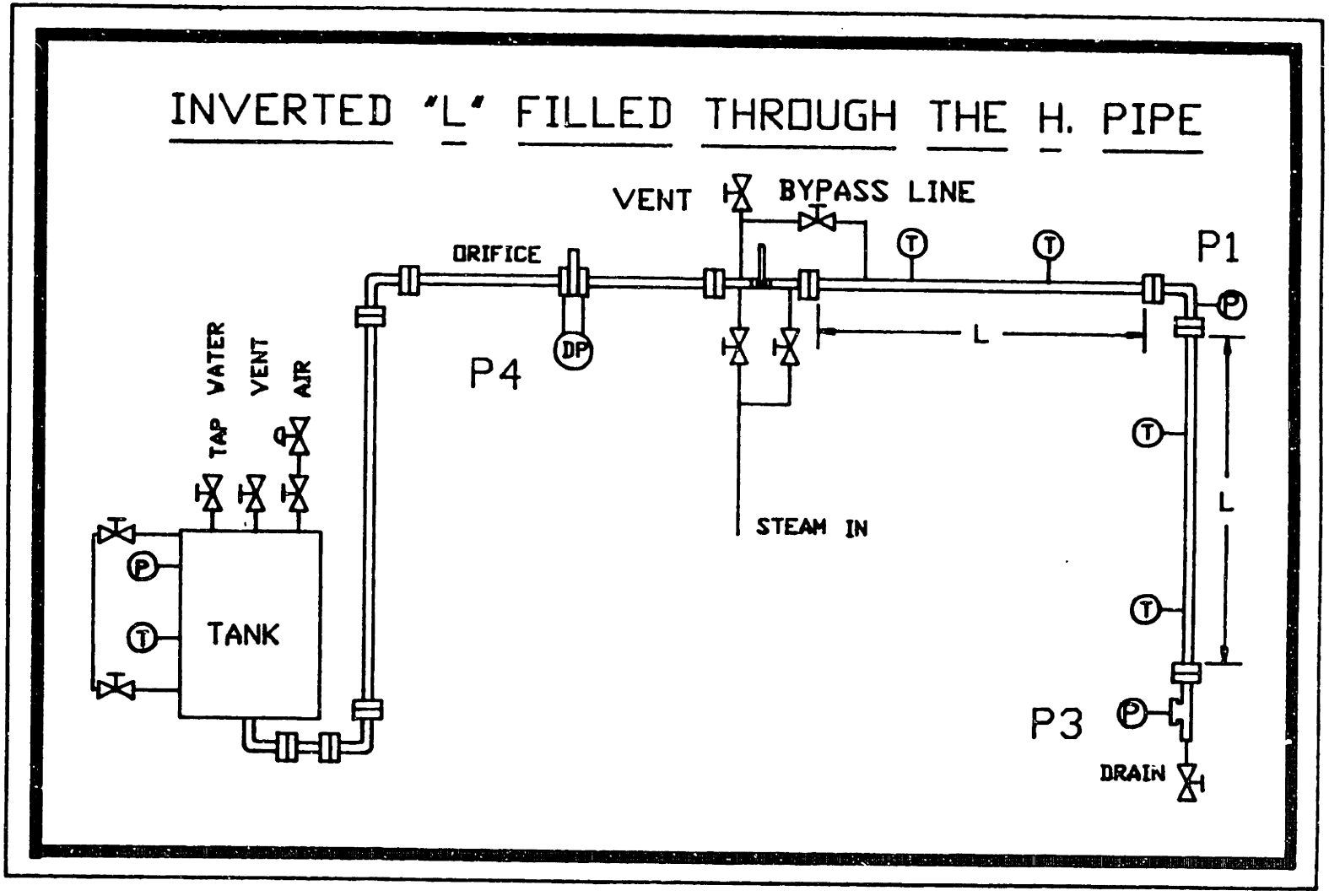

FIGURE - 4.30 Experimental apparatus used for the inverted vertical "L" filled through the h. pipe. The distance L is ≃ 48.D (short pipe limit), where D=2 in.

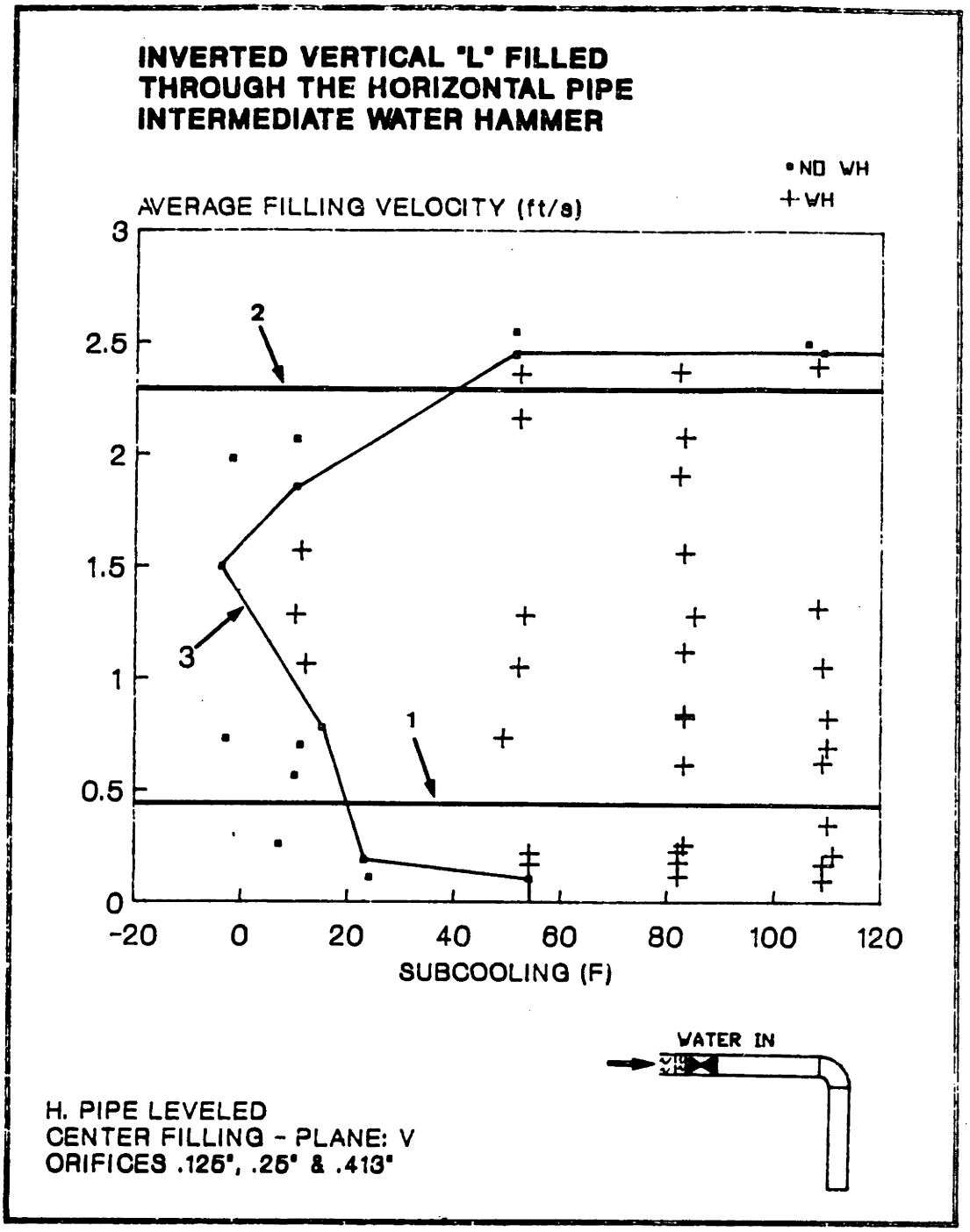

FIGURE - 4.31 Intermediate water hammer stability map for the inverted vertical "L" filled through the h. pipe (horizontal pipe leveled).
Line-1 -> Short horizontal, single pipe theoretical stability boundary - 0.46 ft/s.
Line-2 -> Running full pipe limit - Fr=1 or average filling rate of 2.3 ft/s.
Line-3 -> Experimental stability boundary.

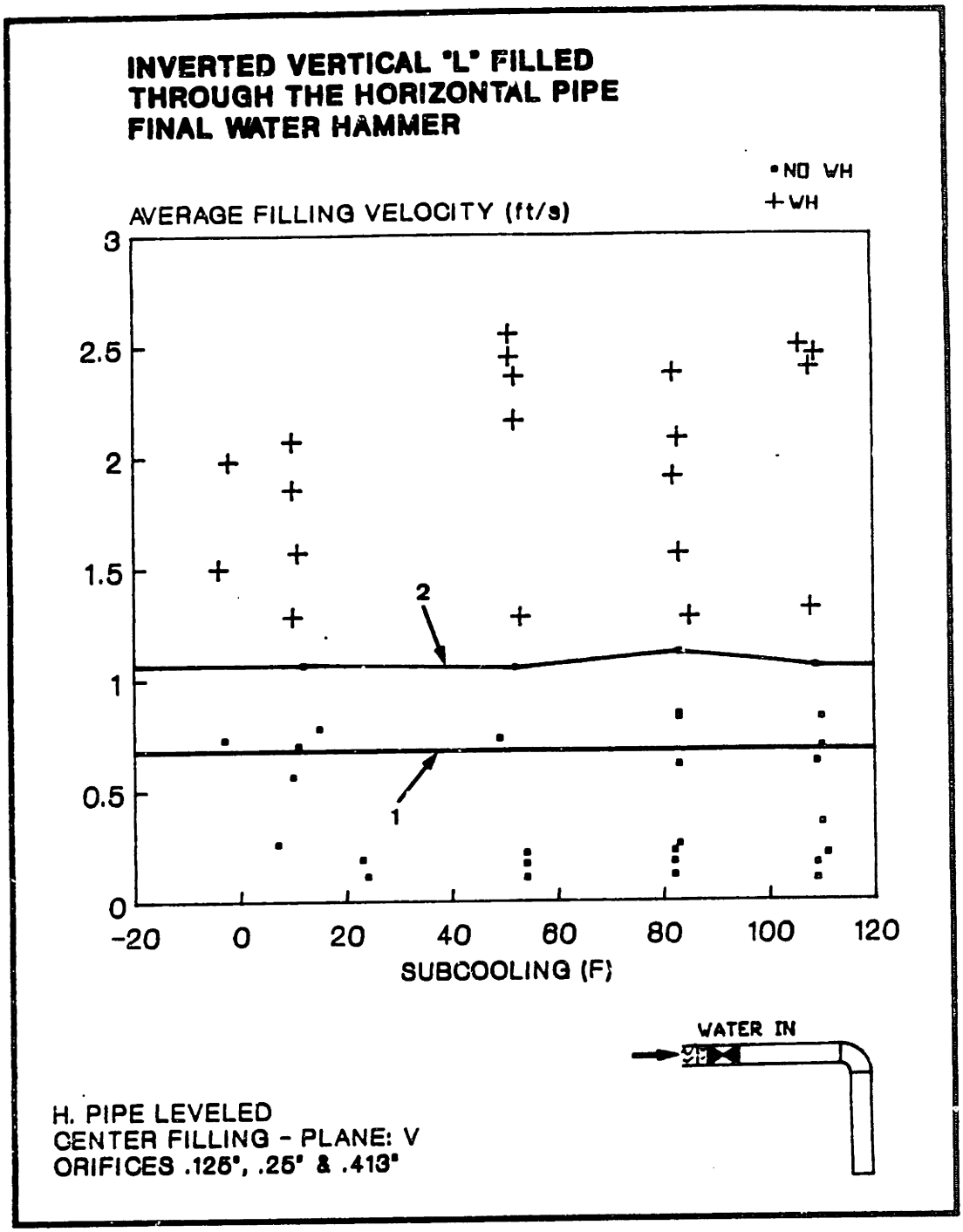

FIGURE - 4.32 Final water hammer stability map for the inverted vertical "L" filled through h. pipe (horizontal pipe leveled).
Line-1 -> Experimental vertical up, single pipe stability boundary - 0.7 ft/s.
Line-2 -> Experimental stability boundary.

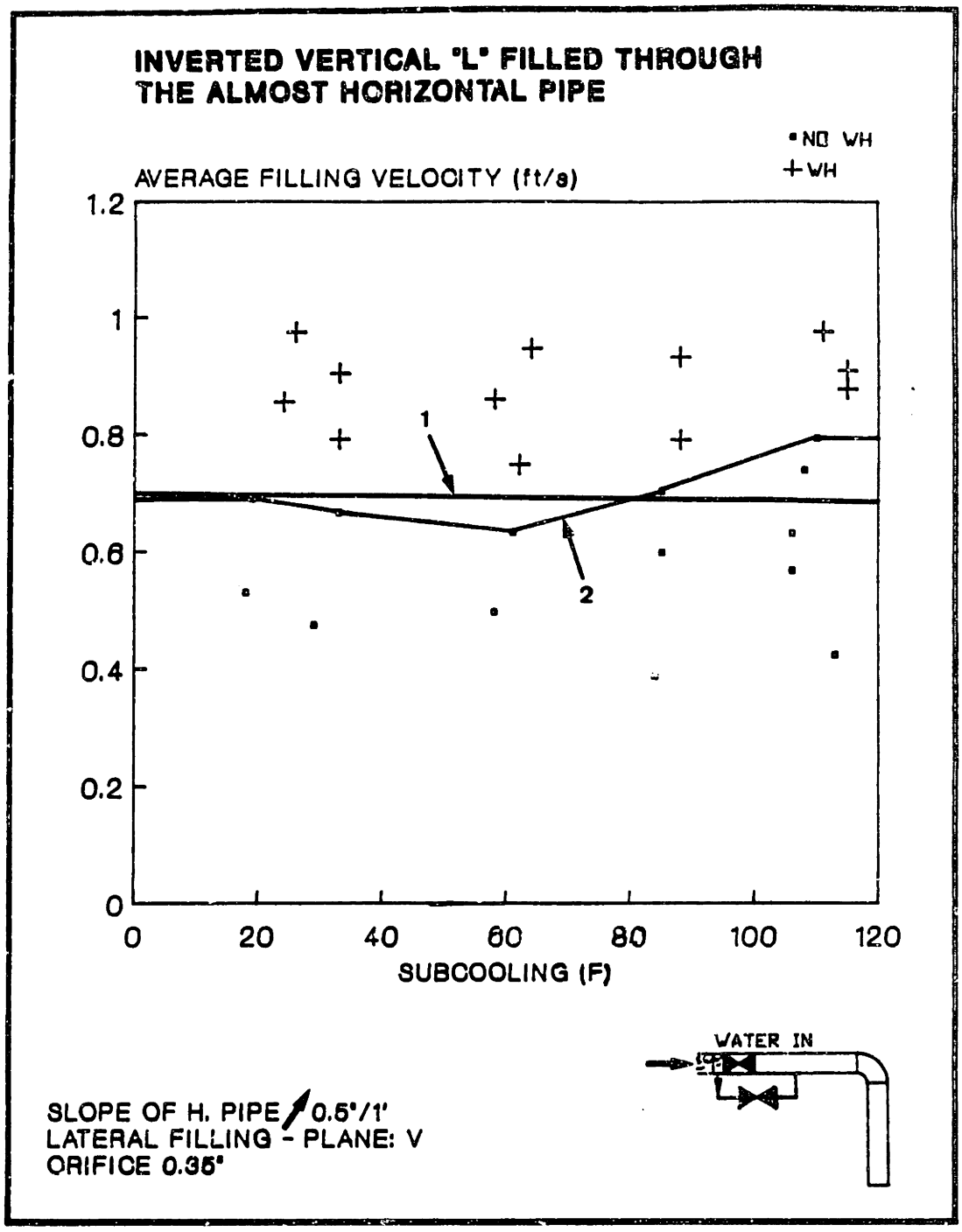

FIGURE - 4.33 Stability map for the inverted vertical "L" filled through the h. pipe (almost h. p. incline up and laterally filled).
Line-1 -> Experimental vertical up, single pipe stability boundary - 0.7 ft/s.
Line-2 -> Experimental stability boundary.

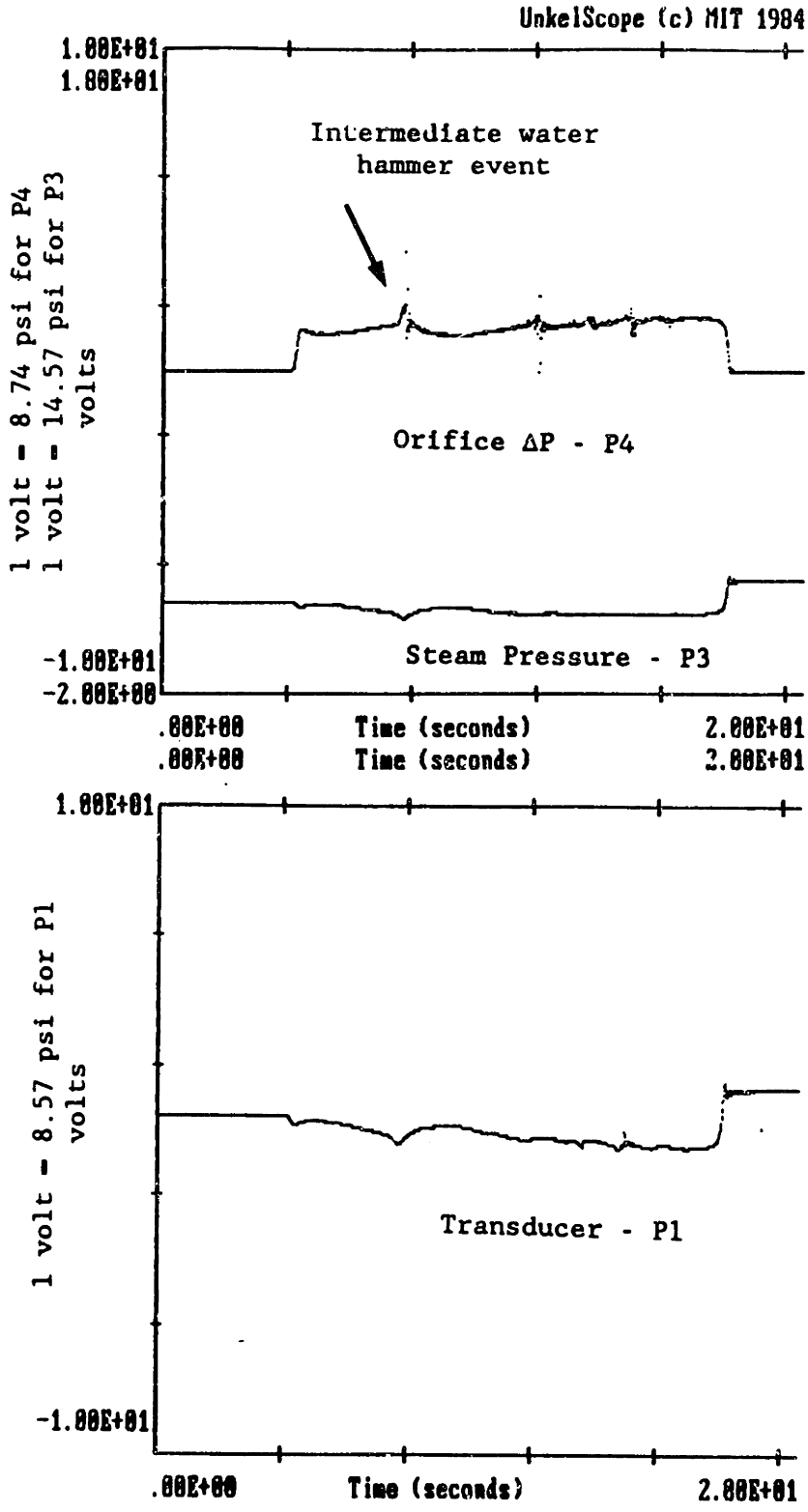

FIGURE - 4.34 Typical inverted vertical "L" filled through the horizontal pipe pressure response curves for a case with intermediate water hammer events (pipes leveled).

Orifice 0.413 in - P_t=15 psig - T_w=138°F

T_{sub}=83°F - Av. Filling Veloc.= 1.12 ft/s.

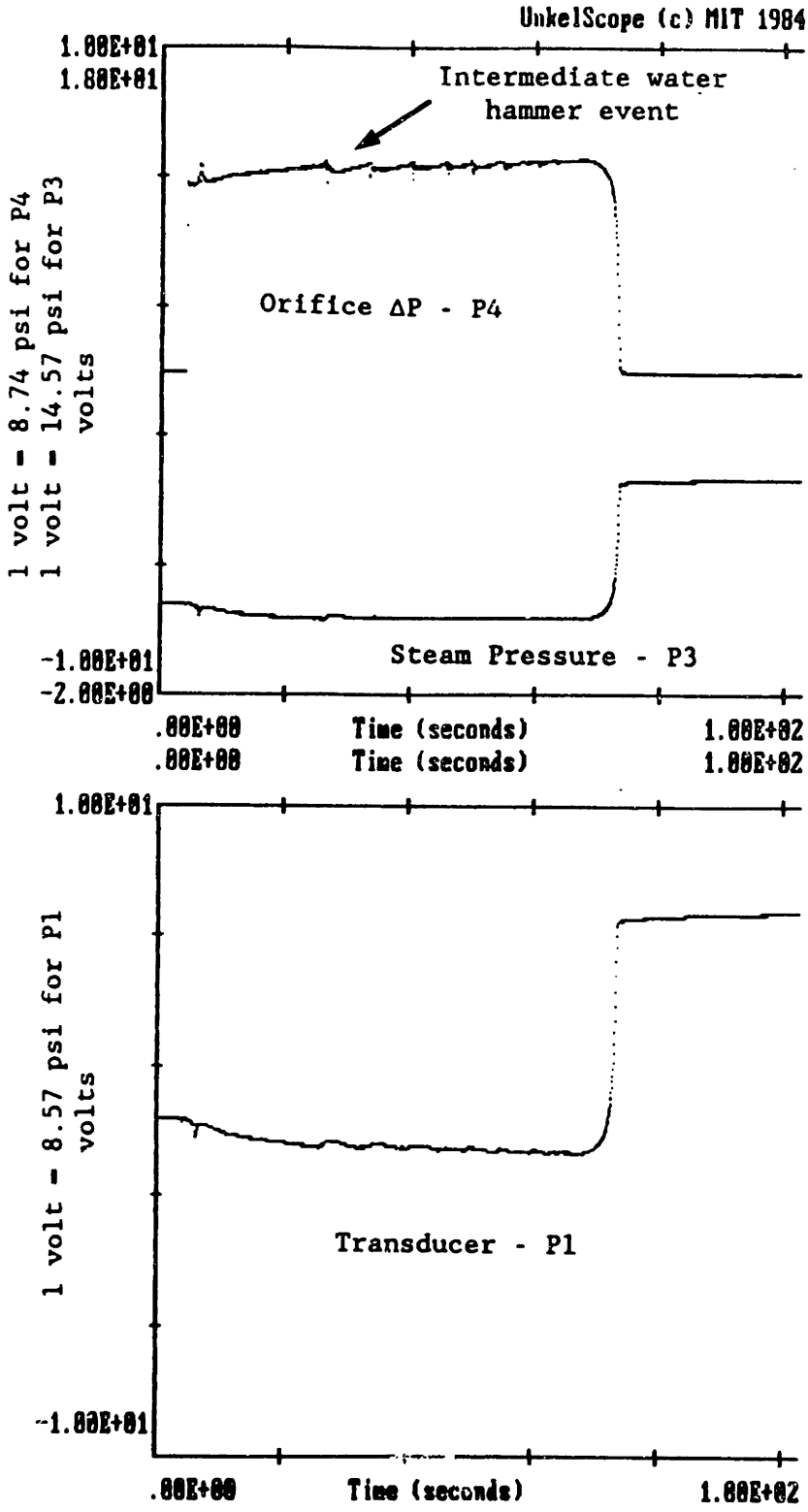

FIGURE - 4.35 Typical inverted vertical "L" filled through the horizontal pipe pressure response curves. The plot shows that even for very low filling rates the intermediate water hammer does not disappear.

Orifice 0.125 in - P_t=55 psig - T_w=139^{o}F

T_{sub}=82^{o}F - Av. Filling Veloc.= 0.227 ft/s.

For the visualization tests the steel pipes were changed to *LEXAN* ones. Figures 4.36 (part a) and 4.37 (part b) illustrate the way this inverted "L", with the horizontal pipe leveled, is filled for various water injection rates. Observing these drawings, it can be seen that what happens inside the horizontal pipe is only slightly different from the description already given for the "L" horizontal pipes. Although the bend floods, water can still flow into the vertical pipe. At the end there is a trapped steam bubble at the "L" elbow (see figure - 4.37/5). This is the reason why the final water hammer boundary should be predicted using the vertical up single pipe theory.

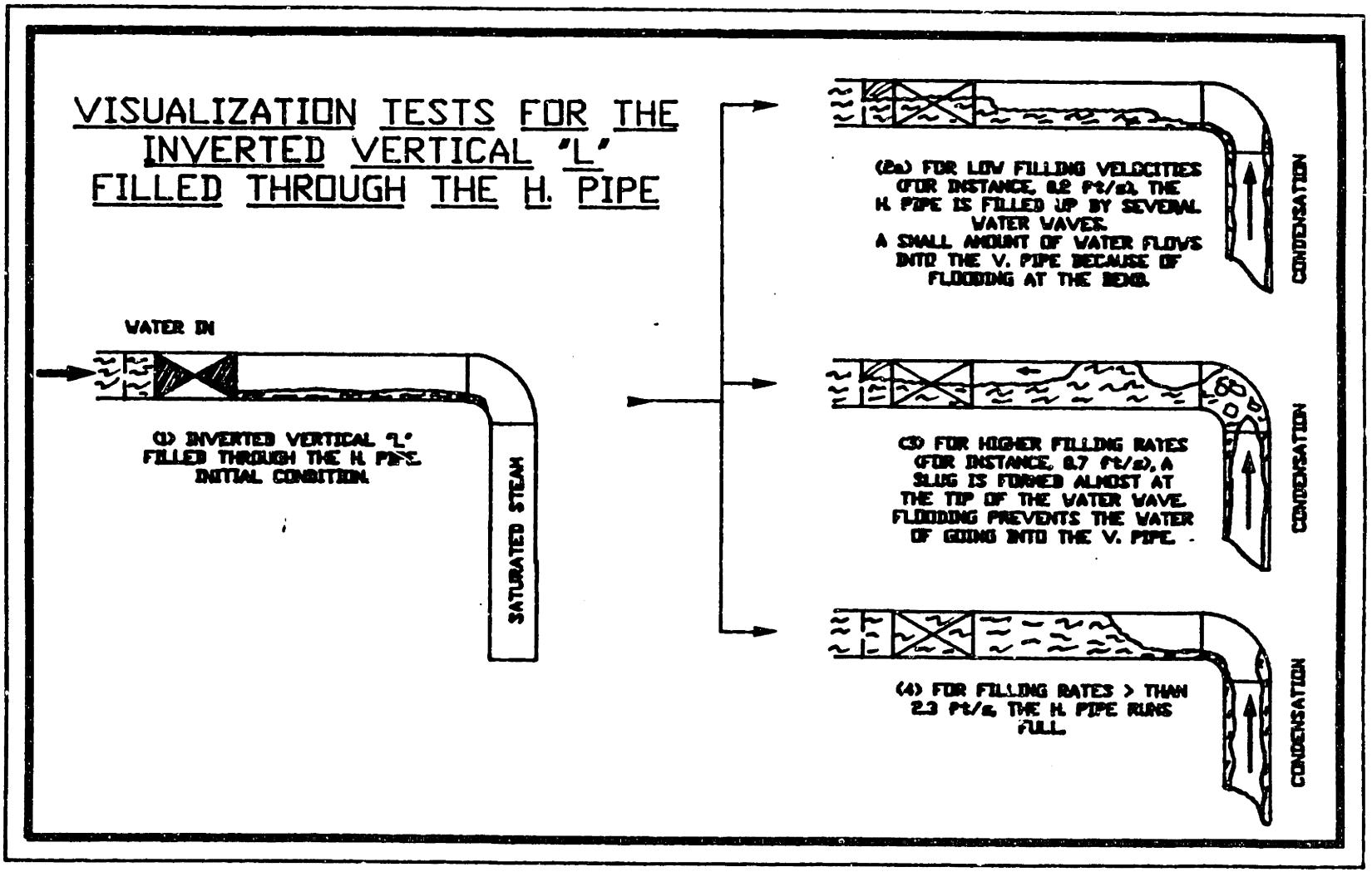

FIGURE - 4.36 (part - a) Visualization tests for the inverted vertical "L" filled through the h. pipe (h. p. leveled).

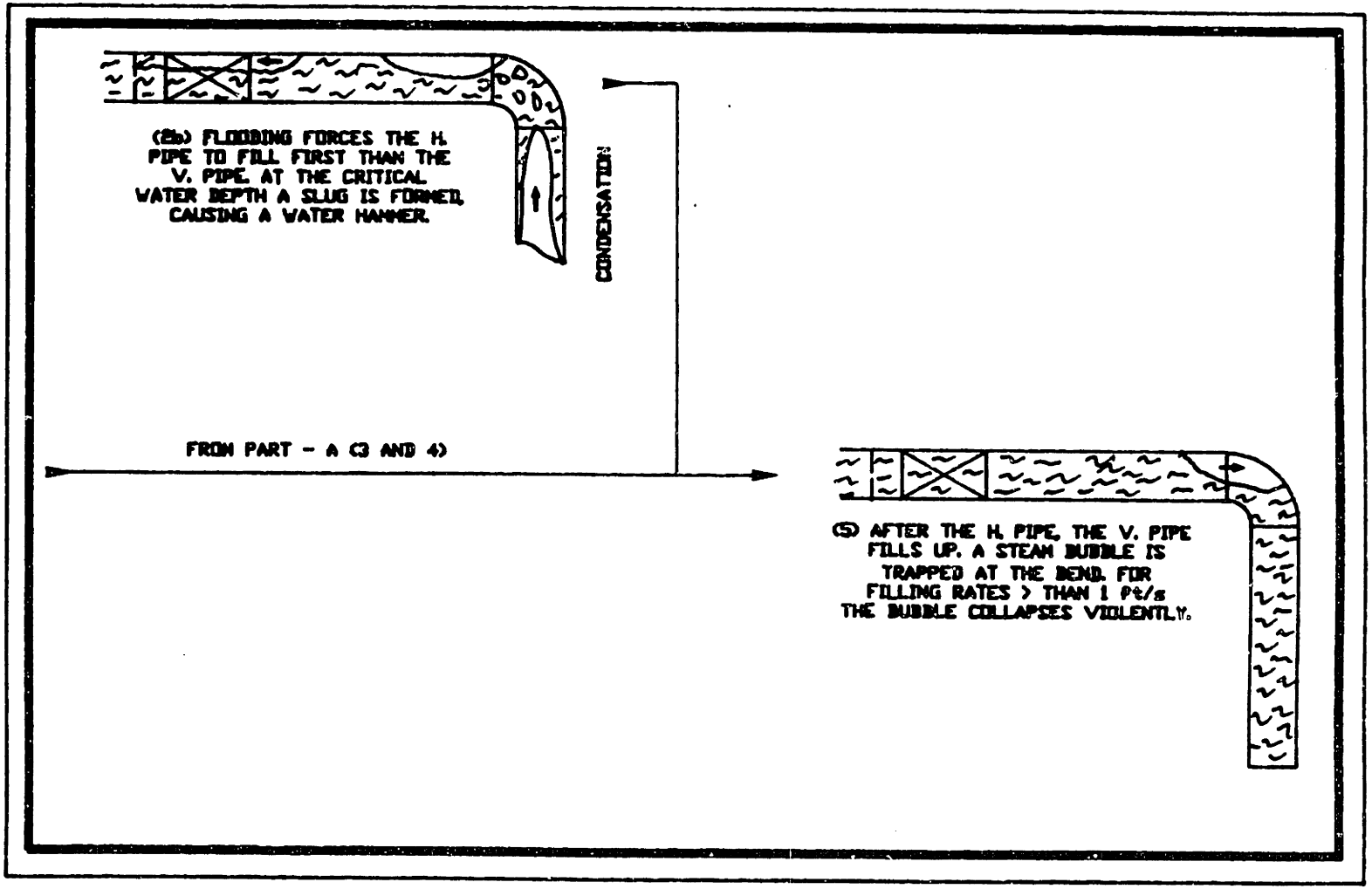

FIGURE - 4.37 (part - b) Visualization tests for the inverted vertical "L" filled through the h. pipe (h. p. leveled).

4.6 Inverted "L" Filled Through the Vertical Pipe

The last of the five "L" configurations that were tested was the inverted "L" filled through the vertical pipe (see figure - 4.38).

Figures 4.39 and 4.40 are the stability maps which result from a test series with the horizontal pipe leveled. From these plots it is possible to conclude that: 1) The short horizontal single pipe limit (line 1 -> figure - 4.39) (0.46 ft/s) lies above the lower intermediate water hammer boundary. This inverted "L" horizontal pipe behaves like a long horizontal pipe. We believe that this is because the water goes into the horizontal pipe without forward momentum; 2) The running full limit (line 2 -> figure - 4.39) (Fr =1 or V_{av}= 23 ft/s) is not a conservative limit for the upper intermediate water hammer boundary; and 3) The vertical up single pipe theory (line 1 -> figure - 4.40) (0.7 ft/s) can be used to determine the final water hammer safe region.

Inclining the horizontal pipe up (0.5"/1') or bypassing the water to the inverted "L" elbow eliminates the intermediate water hammer (see figures - 4.41 and 4.42). When the first procedure is used, the vertical up single pipe theory can be used to predict the final water hammer boundary. This is not a conservative approach to the second filling procedure.

Visualization Tests

Transducer pressure traces taken when the horizontal pipe was leveled are shown in figures - 4.43 and 4.44. The average filling velocities were of 0.99 ft/s and 0.302 ft/s, respectively. From these figures it can be seen

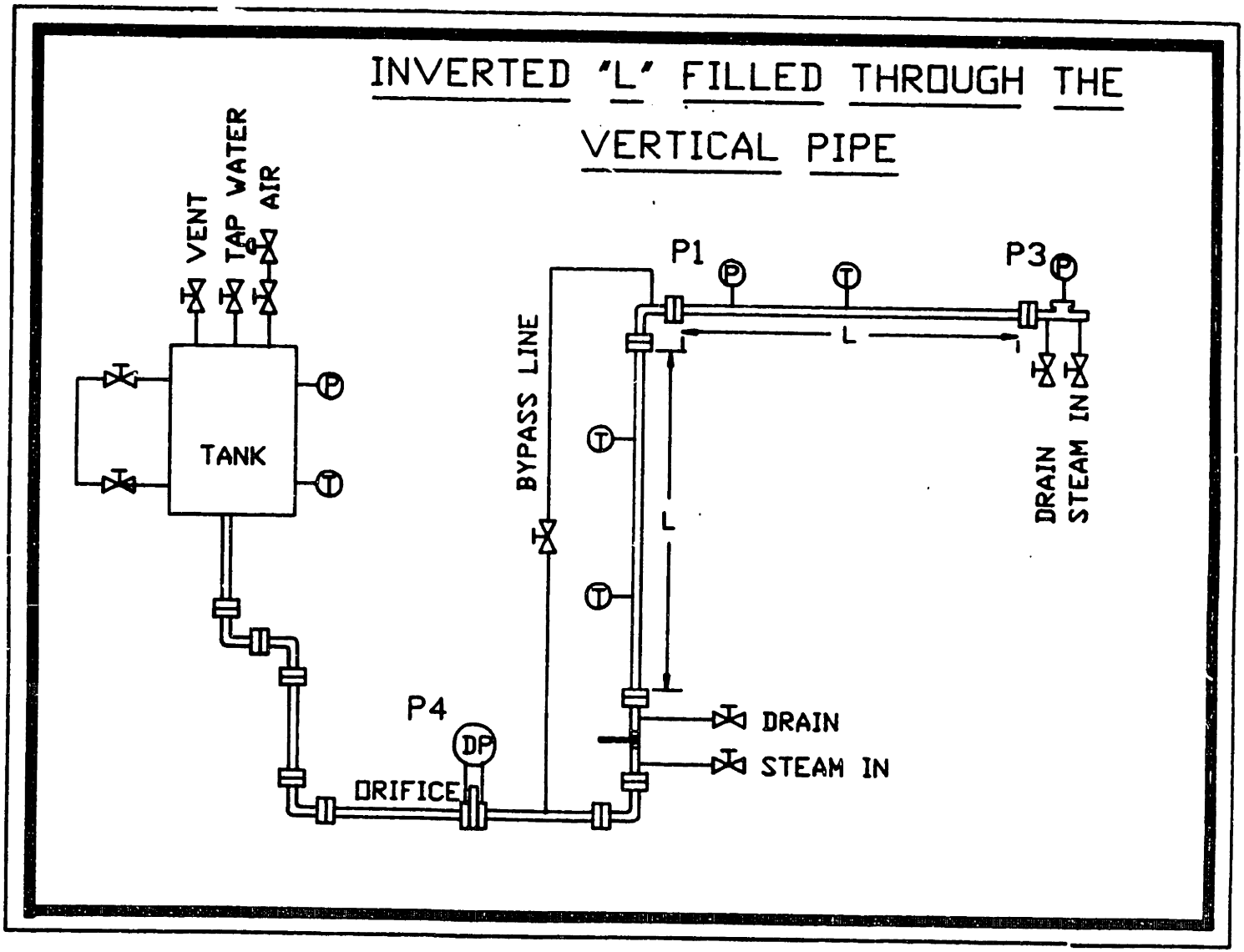

FIGURE - 4.38 . Experimental apparatus used for the inverted vertical "L" filled through the v. pipe. The distance L is ≃ 48.D (short pipe limit), where D=2 in.

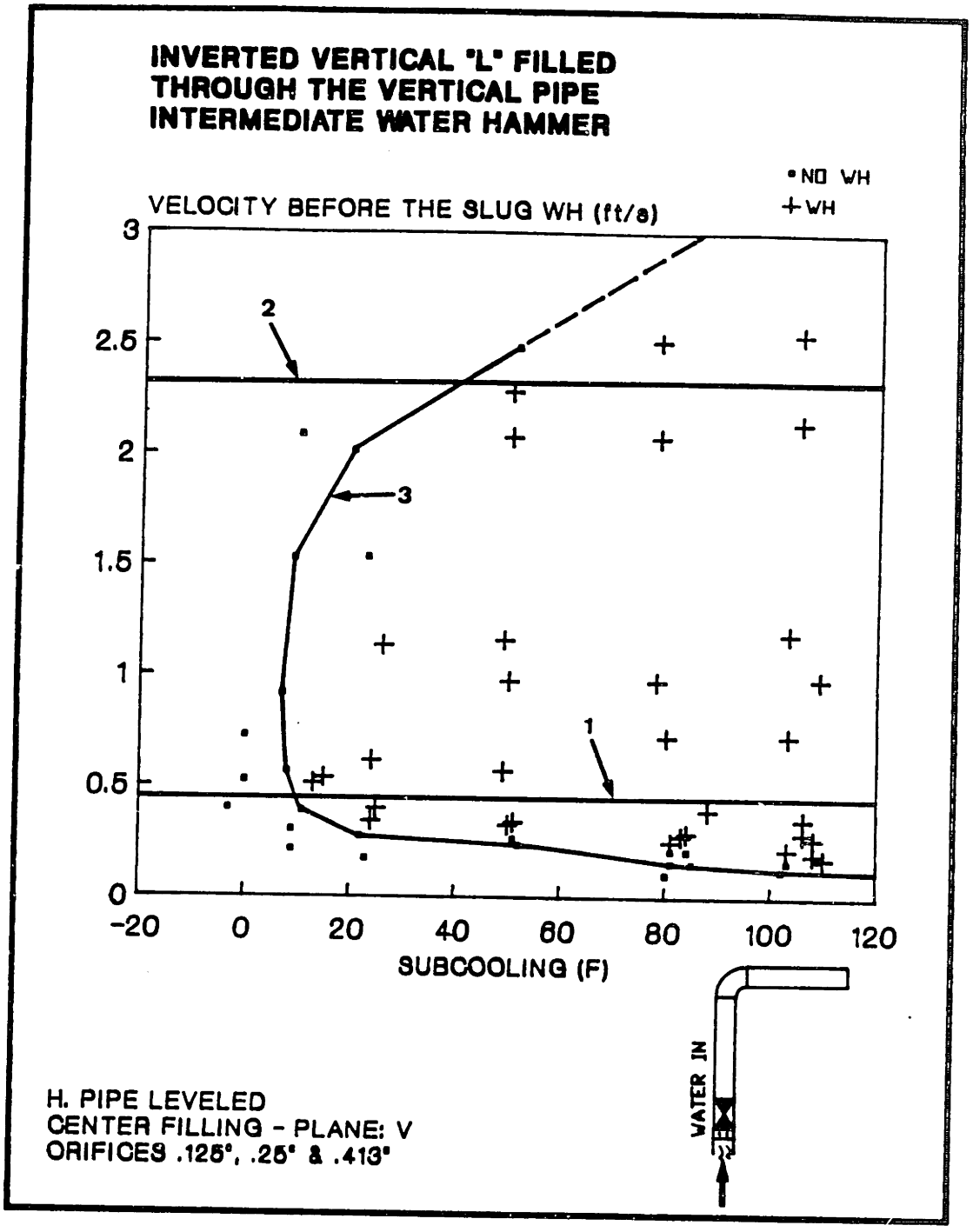

FIGURE - 4.39 Intermediate water hammer stability map for the inverted vertical "L" filled through the v. pipe (horizontal pipe leveled).
Line-1 -> Short horizontal, single pipe theoretical stability boundary - 0.46 ft/s.
Line-2 -> Running full pipe limit - Fr=1 or average filling rate of 2.3 ft/s.
Line-3 -> Experimental stability boundary.

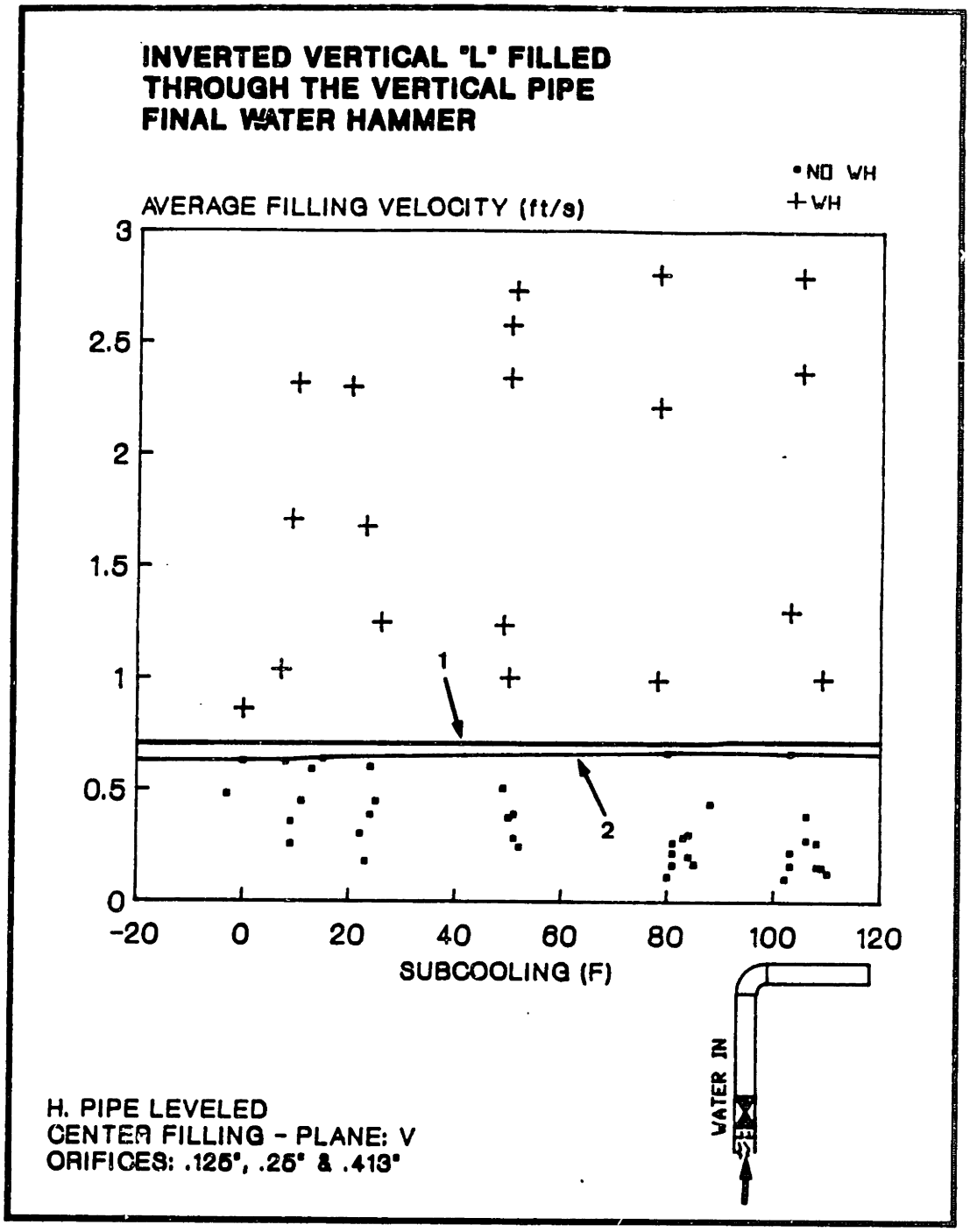

FIGURE - 4.40 Final water hammer stability map for the inverted vertical "L" filled through v. pipe (horizontal pipe leveled).
Line-1 -> Experimental vertical up, single pipe stability boundary - 0.7 ft/s.
Line-2 -> Experimental stability boundary.

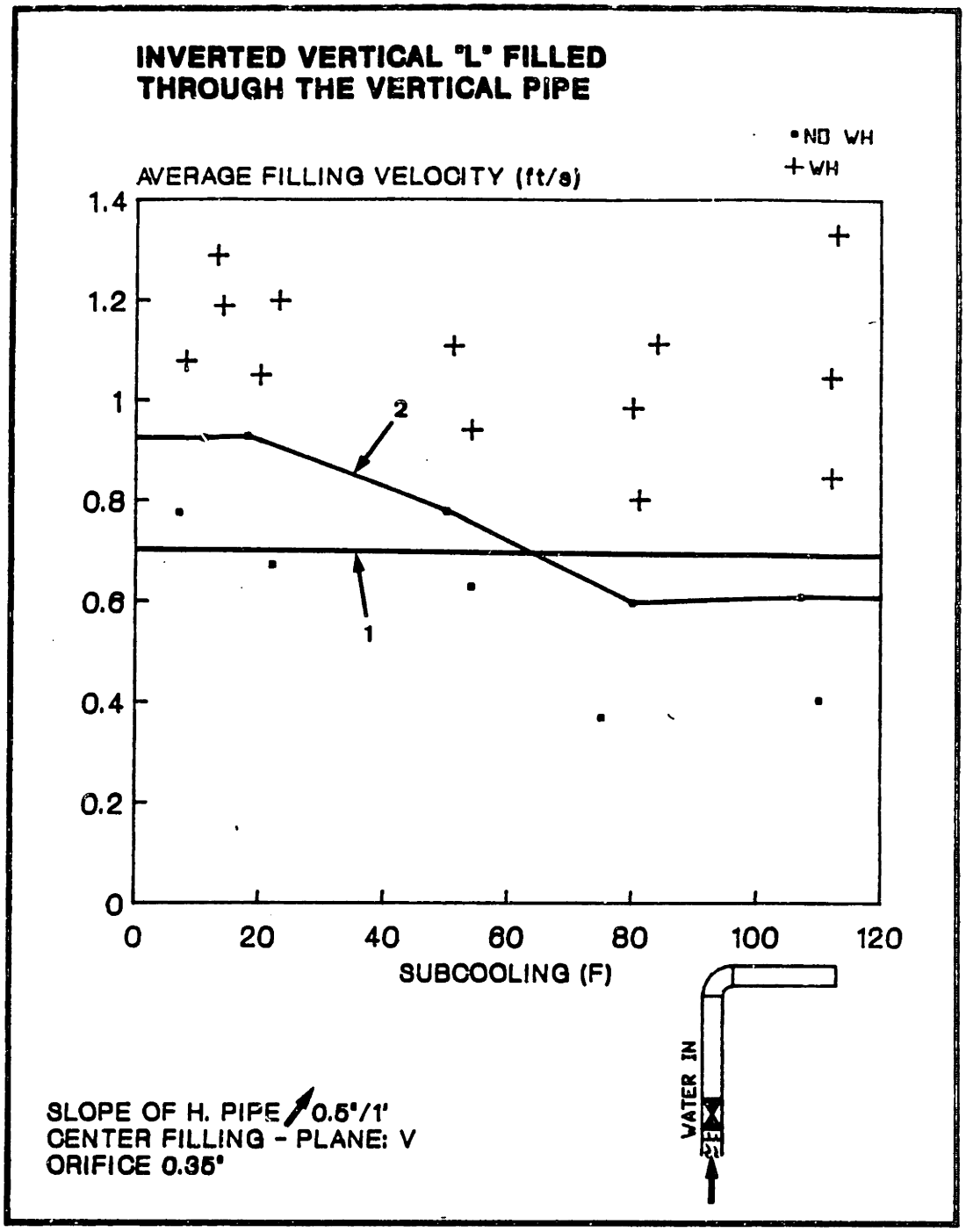

FIGURE - 4.41 Stability map for the inverted vertical "L" filled through the v. pipe (almost h. p. incline up - center filling).
Line-1 -> Experimental vertical up, single pipe stability boundary - 0.7 ft/s.
Line-2 -> Experimental stability boundary.

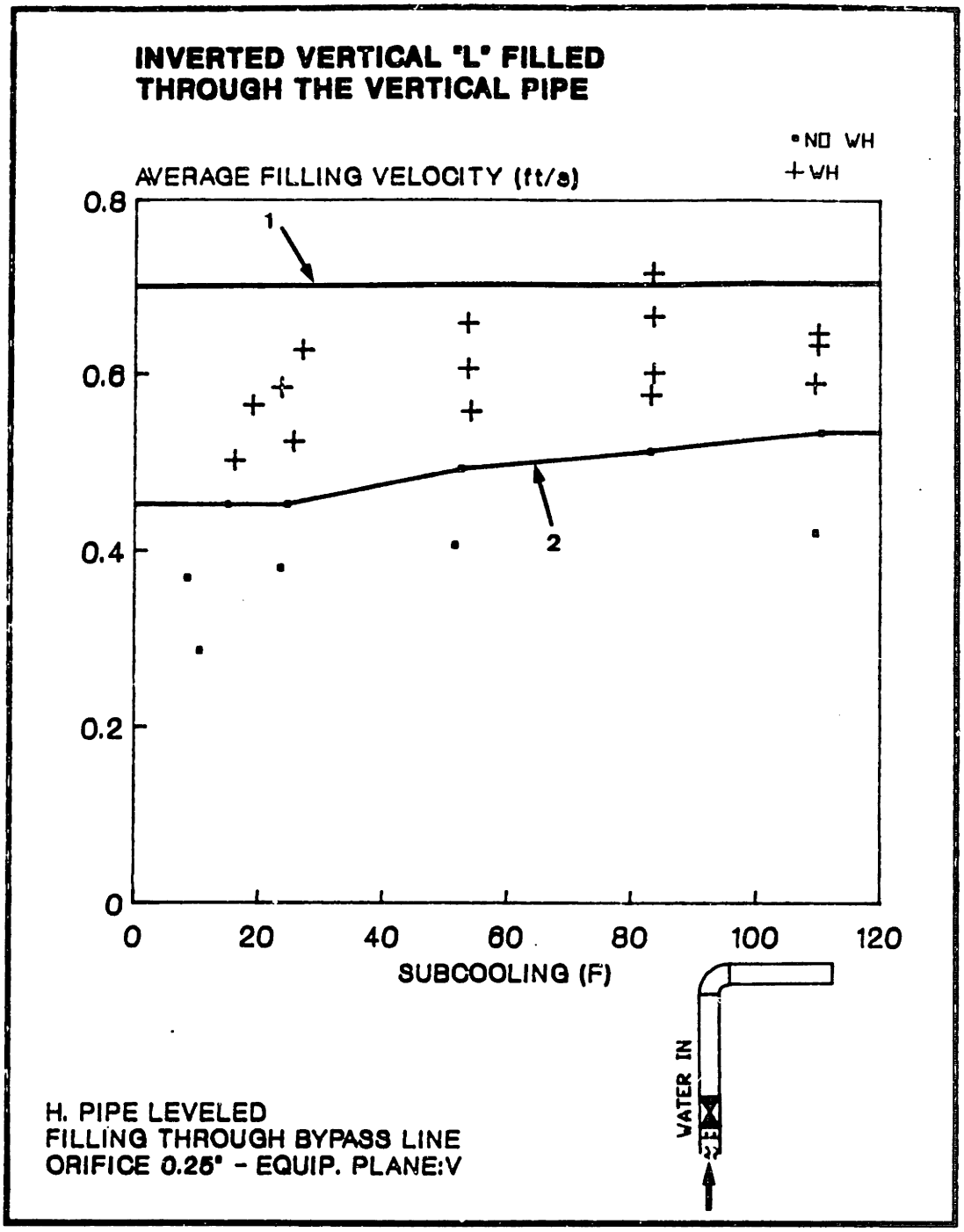

FIGURE - 4.42 Stability map for the inverted vertical "L" filled through the v. pipe (almost h. p. leveled and filled through the bypass line).
Line-1 -> Experimental vertical up, single pipe stability boundary - 0.7 ft/s.
Line-2 -> Experimental stability boundary.

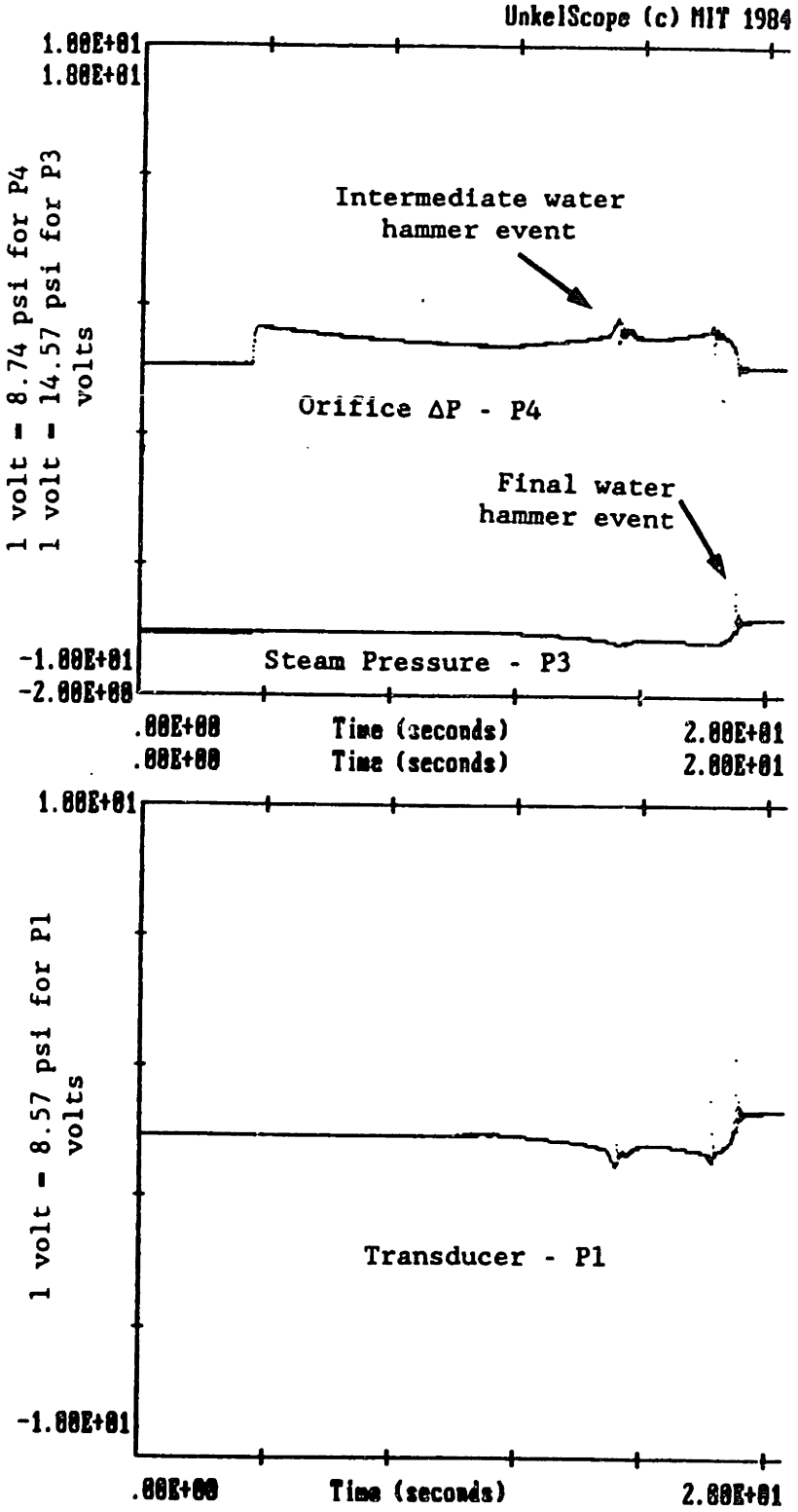

FIGURE - 4.43 Typical inverted vertical "L" filled through the v. pipe pressure response curves for a case with intermediate and final water hammer events (pipes leveled).

Orifice 0.413 in - P_t=15 psig - T_w=141°F

T_{sub}=141°F - Av. Filling Veloc.= 0.99 ft/s.

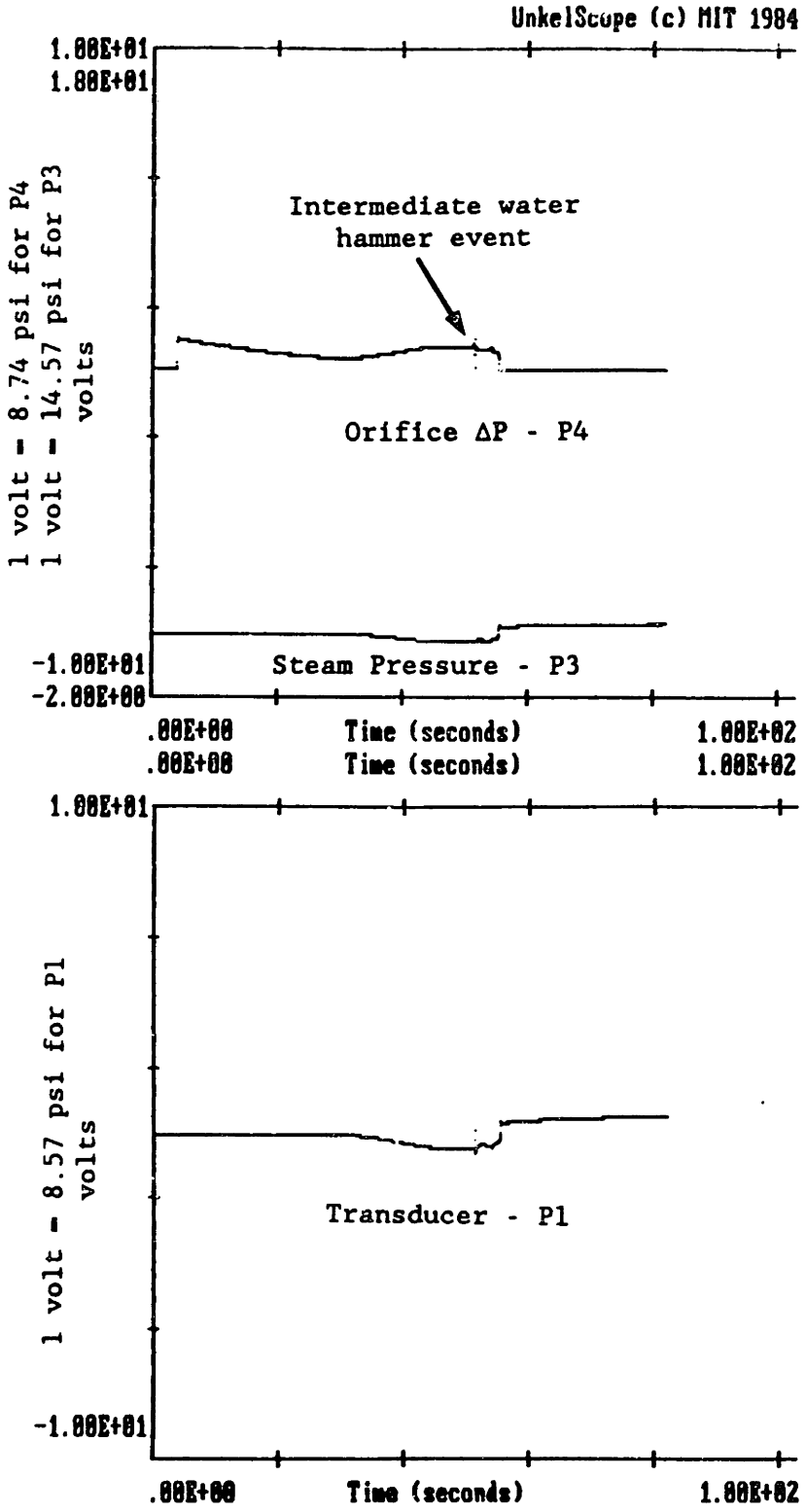

FIGURE - 4.44 Typical inverted vertical "L" filled through the vertical pipe pressure response curves. The plot shows that even for very low filling rates the intermediate water hammer does not disappear.

Orifice 0.250 in - P_t=14 psig - T_w=139°F

T_{sub}=84°F - Av. Filling Veloc.= 0.302 ft/s.

that the condensation rate increases when the water reaches the horizontal pipe, as the steam pressure decreases (P3) while the filling velocity (P4) increases.

What was observed during the visualization tests is represented in figure - 4.45. The horizontal pipe fills up in a similar way to the horizontal "L" pipes. No water surge was seen when the water reached the pipe end. The difference between these experiments and Chou's (6) leveled horizontal single pipe experiments may be caused by the smaller forward momentum of the water in these experiments.

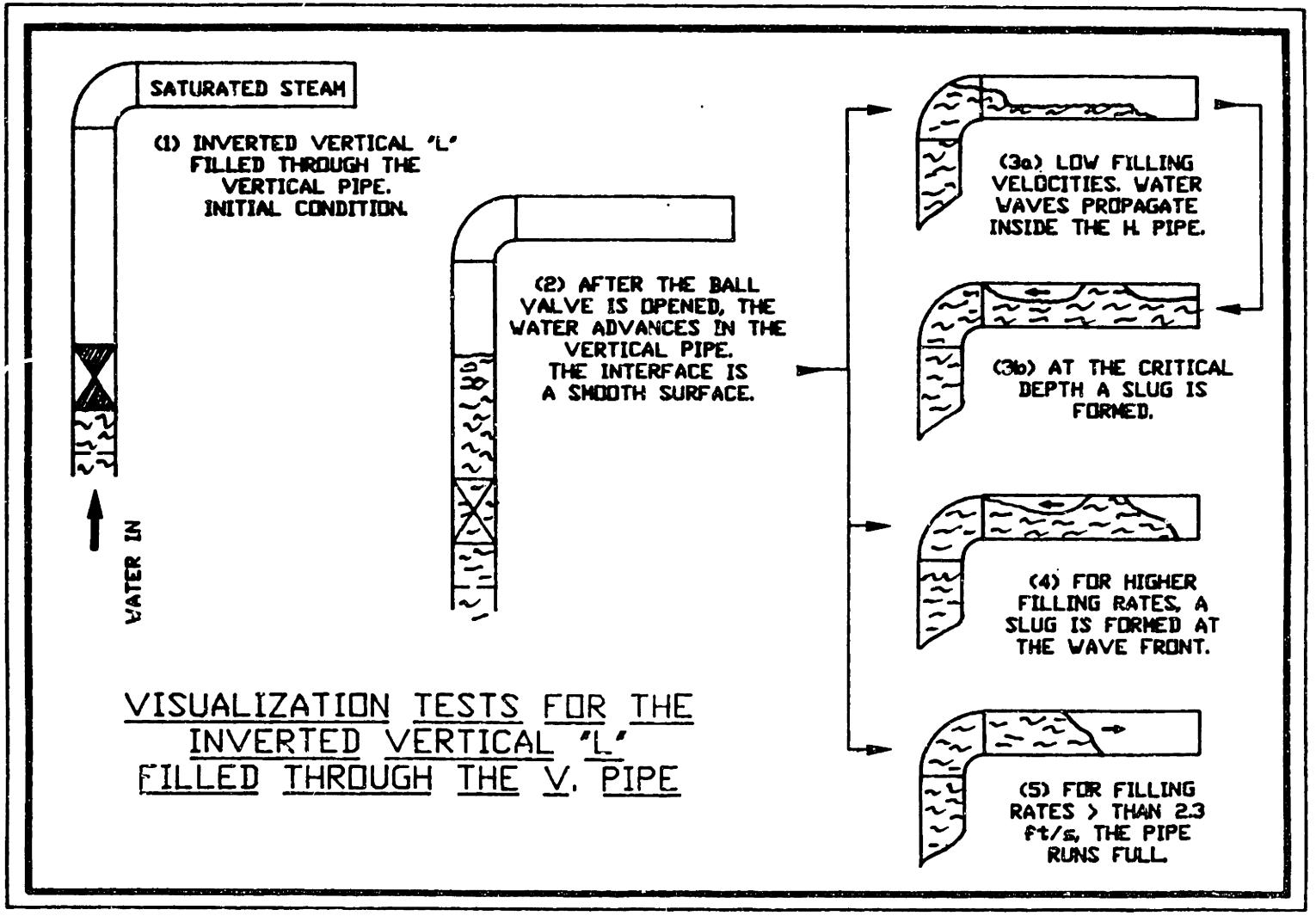

FIGURE - 4.45 Visualization tests for the inverted vertical "L" filled through the v. pipe (h. p. leveled).

4.7 Conclusion

After testing the five different "L" shaped pipes we concluded that:

1- The Horizontal "L"

This configuration behaves like a long horizontal pipe. The only difference is that the first pipe, where the water is being injected, fills up first. Only then does the water go into the second pipe.

As the long horizontal pipe, the pipe sections should be inclined (at least 0.5"/1') and the water should be injected laterally from the lower "L" point. If the pipe sections of the the "L" are long (> 48.D), another solution is to distribute water injecting nozzles along the pipes. The distance between the nozzles should be less than (48.D). Although this solution was not tested, it should work in the same way as in the long horizontal pipe (see Chapter 3).

After one of the above modifications is introduced, the filling velocity should be limited by using Chou's (6) vertical up single pipe theory. This will limit the load of the final water hammer to a desired value.

2- The Vertical "L" Filled Through the Horizontal Pipe and The Inverted Vertical "L" filed Through the Horizontal and the Vertical Pipe

The horizontal sections of these three configurations behave as long horizontal pipes. These horizontal legs should be inclined (at least 0.5"/1') and the water should be brought into them laterally from the low

end. This eliminates the intermediate water hammer.

After introducing this modification, the final water hammer load can be limited to a desired value, if Chou's (6) vertical up single pipe theory is used.

The inverted vertical "L" filled through the vertical pipe was also tested with the water being injected through the top 90 degrees bend. In this case a bypass line was used. This procedure also eliminates the intermediate water hammer.

3- Vertical "L" Filled Through the Vertical Pipe

No intermediate water hammer occurs in this configuration. The criterion that was used, based on a flooding correlation, to predict the water hammer boundary seems to work well. However, one should keep in mind that this result may be only valid for the particular configuration tested. If, for instance, the horizontal section of the vertical "L" is greater than 48.D, we cannot guarantee that no intermediate water hammer will occur.

Nevertheless, if the horizontal leg is inclined, with the 90 degrees bend being at the lower end, the intermediate water hammer is prevented. Then, the final water hammer load can be controlled by using Chou's (6) vertical up single pipe theory.

CHAPTER - 5

EXAMPLES OF IMPROVED FILLING PROCEDURES

5.1 Organization

The analyses of nuclear piping systems in this chapter are based on: 1) The introductory description of a Westinghouse's PWR nuclear power plant given by Masche (40); 2) The general description of GE's BWR/6 and Mark-III containment given by General Electric Company (41); 3) NUREG/CR-2781 (8) (which are the results of evaluations of reported water hammer events performed by Quadrex Corporation); 4) Tasks 2, 6 and 7 of the report "Water Hammer Prevention, Mitigation, and Accommodation" prepared by Stone & Webster to EPRI (draft version) (10) and (11); and 5) On typical PWR and BWR elevation diagrams (42) and (43).

First of all, it is necessary to stress that in the following sections there is no intention of exploring all possibilities of water hammer events in the piping systems which are used as examples. The objective here is rather to illustrate how the experience gained with the tests of the previous chapters can be used to improve the design of nuclear piping systems. The reader should bear in mind that it may be impossible to totally prevent water hammer events. However, we believe that substancial advances toward prevention can be made. It is clear that different engineers will have different point of views about how to improve their systems. For many piping systems a wide variety of options for preventing water hammer due to steam bubble collapse may exist. Consequently, economics, essential

operational procedures and perhaps personal preferences will decide whether or not to adopt the modifications proposed.

Before suggesting modifications, a brief description and purpose of the piping system will be given. After that, the system elevation diagram will be presented and previous water hammer events collected in NUREG/CR-2781 (8) and in Tasks 6 and 7 of Stone & Webster's report (11) will be explained. Only then, will the water hammer mitigation measures be suggested.

5.2 Core Spray System

5.2.1 System Description and Purpose

General Electric (41) cites two core spray systems:

-High Pressure Core Spray System, which has as its purpose decreasing the reactor pressure and providing makeup water in the event of a LOCA. The system consists of a sparger ring with spray nozzles, a motor driven pump, a diesel-generator (which makes the system self-sufficient), valves, piping and the necessary instrumentation. The main cooling water source is the CST (condensate storage tank). The possibility of using the suppression pool water is also provided.

-Low Pressure Core Spray System, which has as its purpose preventing fuel cladding damage (if the core uncovers) in the event of LOCA and the failure of other ECC systems to maintain the reactor vessel water level. It has the capacity for providing enough water to maintain the reactor water level for all postulated pipe breaks. The system consists of sparger ring with nozzles, a motor-driven pump, valves, piping and necessary instrumentation. Its main water source is the pressure suppression pool.

5.2.2 Elevation Diagram and Previous Reported Water Hammer Events

Figure - 5-1 (42) represents a typical low pressure core spray system.

As can be seen in the drawing, the main water source is the suppression pool.

The elevation difference between the suppression pool water level and

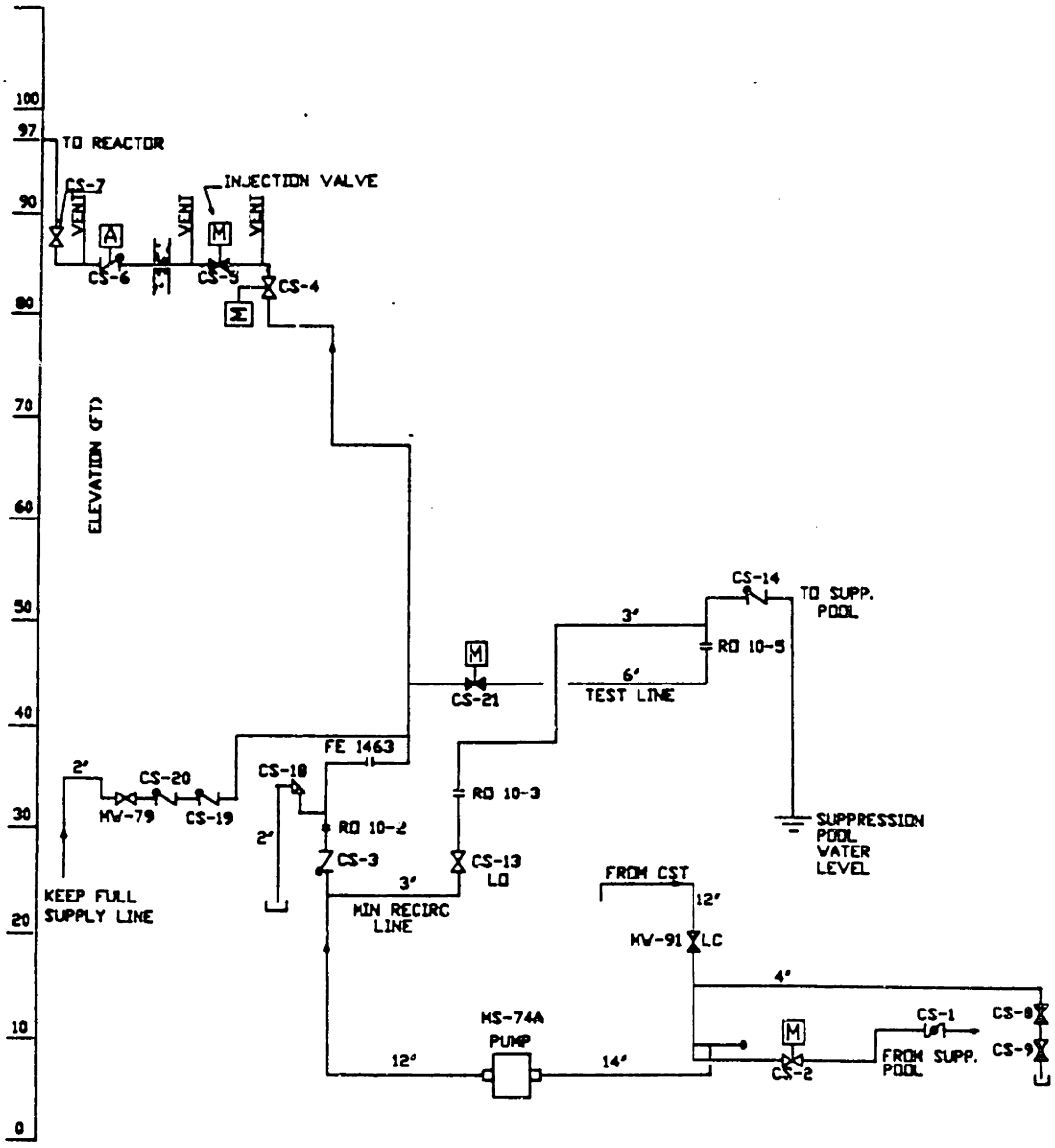

FIGURE - 5.1 Typical BWR Low Pressure Core Spray System Elevation Diagram. Source -> (42)

the spray injection point is approximately 60 ft. This elevation difference, if there is a leaky check valve CS-3 (atmospheric pressure can support only ≈ 30 ft), permits two paths which can cause voiding of the line downstream of the pump. The first is through the pump and suction valve (which remains open for safety reasons). The second is through the recirculation line (Which is necessary in order to avoid overheating the pump during the period of time between when it is switched on and when the differential pressure across the CS-5 injection valve permits this valve to open). Stone & Webster (10) concludes that, in some nuclear plants, the actuation time of valve CS-21 (in the test line) might be such that the valve would remain open after the pump had already stopped. If this is the case, this would provide another way of voiding the line downstream of the pump.

Indeed, in going through Stone & Webster's report (11) (Appendix A - BWR Utility Water Hammer Data Base), void in this line is one of the main causes of water hammer events. A total of 10 of the 11 cases reported were a result of void in the line downstream of the pump.

The second water hammer mechanism is subcooled water injected in a steam filled space (Millstone-1 /GE-3 suffered one event of this class in 2/20/80 - NUREG/CR-2781 (8)). This can be caused by a leaky air assisted check valve (CS-6). High pressure reactor water can then pass through this leaky valve and flash in the line downstream the injection valve (CS-5). A leaky CS-5 would also permit a steam bubble to migrate to the riser section.

5.2.3 Water Hammer Mitigation Measures

Nowadays, most nuclear power plants use a keep full system, as shown

in figure - 5.1, to avoid voiding the riser section.

There is no reason to modify systems that are working well. However, keep full systems are not perfect. They do not prevent steam bubble formation in the line downstream of the injection valve (CS-5), if the check valve CS-6 is leaking. Neither prevent the migration of the steam bubble to the riser section, in the case of a leaky CS-5 valve, as the pressure supplied by the keep full pump is less than the pressure in the reactor.

From the tests described in the previous chapters, it is possible to improve the system in the following way (a specific user may use any combination of the suggested modifications):

-A keep full system is clearly one solution for the riser section. It has, however, the limitations already cited;

-Incline all horizontal pipe branches and fill them laterally from the lower point. As there is still no experience on the effect of fittings on water hammer boundaries (as an air-assisted check valve, for instance), the initial water filling rate should be limited to that of the vertical up single pipe theory;

-The injection valve in some plants might be located outside the shield building. Therefore, the line marked A in figure - 5-2 could have a length of 40-50 ft. It would be then a long horizontal pipe. For pipes that are leveled, another solution (besides of inclining them up) is to distribute nozzles along the pipe with the spacing between the nozzles less than 48L/D;

-An alternative solution to the keep full system is to limit the initial water filling rate (using the vertical up single pipe theory - see

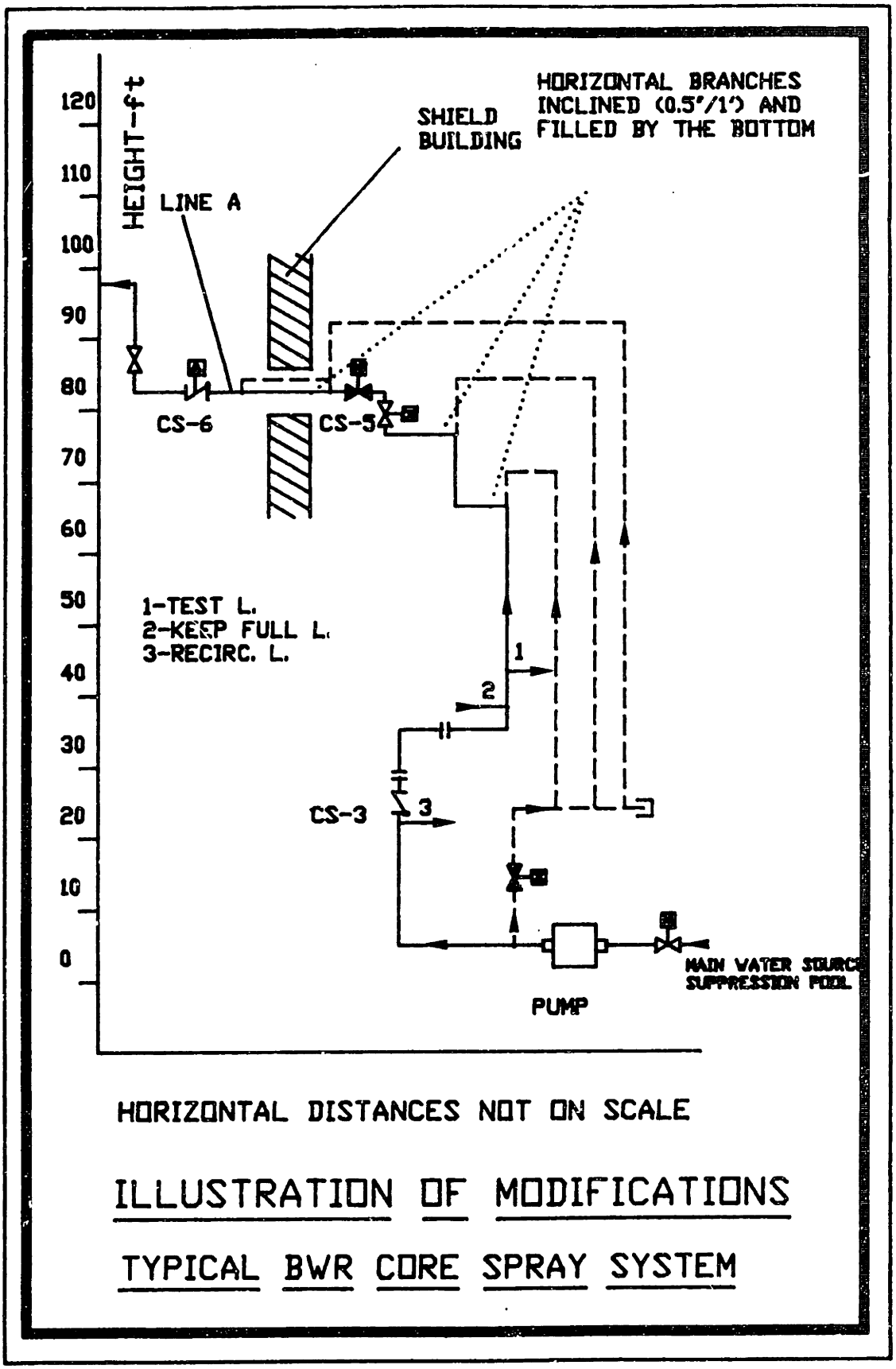

FIGURE - 5.2 Typical BWR Low Pressure Core Spray System Illustration of Proposed Modifications.

chapter 4) and use a series of bypass lines and injection nozzles (directing the water jet down through the vertical pipe), as shown in dashed lines in figure - 5-2. If any horizontal branch is longer than 48L/D, more nozzles should be distributed along the leveled horizontal pipes, as mentioned in the previous paragraph;

-As a subcooled water jet causes a significant depressurization, vacuum breakers could be located near the injection nozzles. This would help avoiding water hammer events. Admitting air, if allowable, is a very effective way to eliminate water hammer. The allowable primary water maximum air content can, however, impose a limit to this practice.

5.3 BWR Residual Heat Removal System (RHRS)

5.3.1 System Description and Purpose

Figure - 5.3 (43) is a typical functional diagram of a BWR RHR (Residual Heat Removal) system. In this drawing, only one loop is represented. Normally, there are two loops with a total of four RHR pumps (two pumps per loop). As can be observed in this figure, the RHRS consists of heat exchangers (cooled by service water), pumps, valves, and necessary instrumentation.

The RHR system performs several tasks depending on how its valves are aligned. Following GE's (41) classification it is possible to list the operation modes as:

-Low Pressure Coolant Injection (LPCI), which with the core spray systems and automatic depressurization has the task of maintaining the water level inside the reactor vessel in the case of a LOCA. As can be seen in figure -5.3, water from the suppression pool or condensate storage tank (CST) is pumped through the heat exchanger (or bypassed) to the line going to the recirculation pumps;

-Suppression Pool Cooling, is used to decrease the suppression pool temperature in the case of a blowdown (the suppression pool temperature should be always less than 170^{o}F). The water is pumped from the pool and returns to it by the test line, after passing through the heat exchanger;

-Reactor Steam Condensing, is used as an alternative steam path, when the main condenser is isolated. Steam from the HPCI turbine pump is diverted

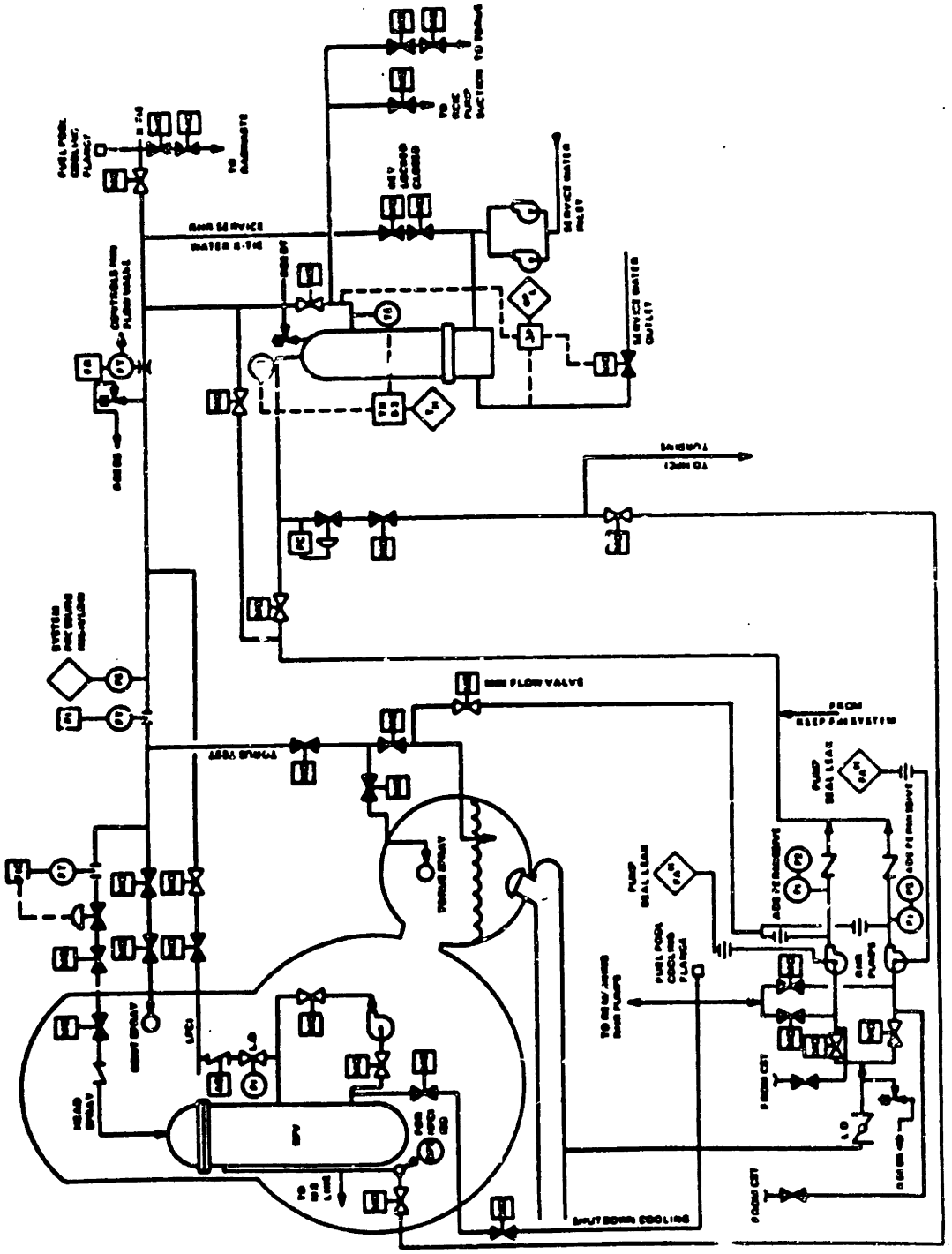

FIGURE - 5.3 BWR RHR Functional Diagram. Source -> (43)

through a restriction (to reduce its pressure to 200 psig) to the RHR heat exchanger;

-Nuclear Boiler Shutdown Cooling, is used to remove the residual heat after shutdown. As can be observed in figure -5.3, coolant water is taken from one recirculation loop, pumped through the heat exchanger and returned to the reactor core isolation cooling (RCIC) pump suction. Some water is also sent to the spray at the top of the reactor vessel. The system operates at pressures less than 135 psia and can lower the reactor temperature to 125°F in 20 hours;

-Containment Spray Cooling, is used to control the pressure inside the containment and torus (in old BWR versions). Steam is condensed using sprays (at the top of the containment and above the suppression pool) which are supplied with water from the suppression pool.

5.3.2 Elevation Diagram and Previous Reported Water Hammer Events

The BWR RHR system has two intrinsic features that make it especially prone to void and steam bubble collapse related water hammer events. First, there are significant elevation differences between the suppression pool water level and the water injection points and heat exchangers. Second, in this system, subcooled water and high pressure steam interface at isolation valves. These two characteristics, if the isolation valve is leaking, are responsible for the majority of the reported water hammer events in this system. In Stone & Webster's BWR Utility Water Hammer Data Base (appendix A - (11)) 41 reported water hammer events were collected, in this system.

Figure - 5.4 was made based on Lanik and Rubin's (43) simplified

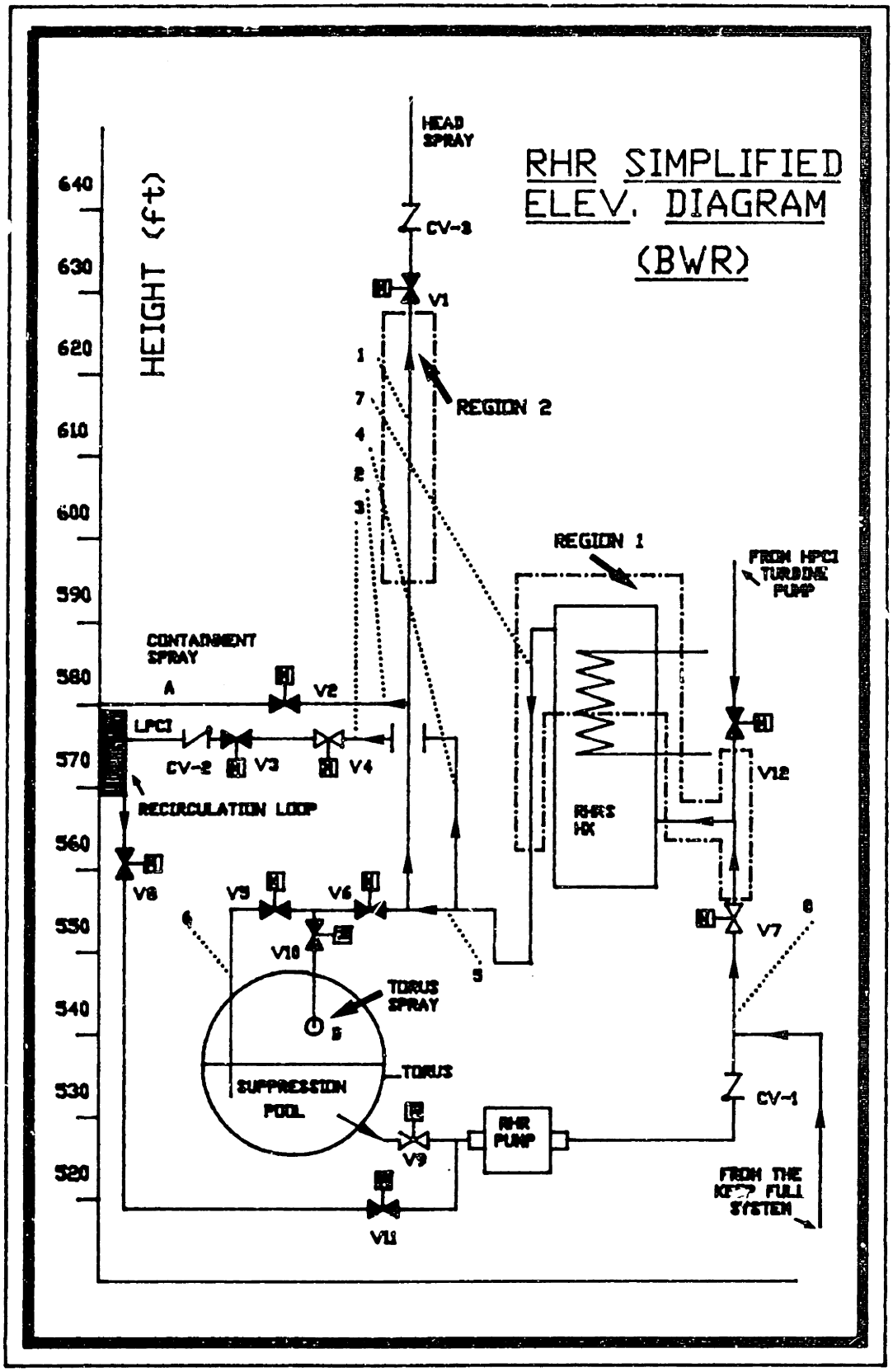

FIGURE - 5.4 BWR RHR Simplified Elevation Diagram.

elevation diagram of the Browns Ferry Unit 1 RHR system. Using the RHR functional diagram (figure - 5.3), the steam line from the HPCI turbine pump to RHR pump downstream line, the line connecting the reactor recirculation loop to the suction of the RHR pump and some valves were freely added to the original drawing. As can be observed in this figure, the RHR system is represented with its valves aligned to the LPCI mode. This is the normal alignment when the reactor is operating.

According to Stone and Webster (10), the majority of the reported BWR RHR water hammer events were identified in two regions (see figure - 5.4): 1) Fourteen events occurred in a region (region 1) that includes the heat exchanger and the lines connected to it (downstream of valve V12); and 2) Eighteen events occurred in the pipe region upstream of valve V1 (region 2). In these two regions the water hammer events can be attributed to the leakage of steam through the isolation valves V1 or V12.

In region 1, the steam that leaks through valve V12 will form steam pockets at (see figure - 5.4): 1) The top of the heat exchanger; 2) The top of line 7; and 3) The top of line 8, up to the valve V12. In region 2, the steam that leaks through valve V1 will form a steam pocket that will accumulate against valve V1. If the RHR pump is then started, the steam that is trapped in either region can collapse violently, causing a water hammer. The condensate that can eventually accumulate upstream of valve V12 can also be responsible for the water hammer events in region 1. However, this type of water hammer will not be covered here.

Besides water hammer events that have already been identified in other regions of this system, it is possible to postulate new scenarios where they

can occur. See, for instance, Huang (44) and Lanik and Rubin (43). However, the objective of this chapter is to only illustrate the use of the results of chapters 3 and 4. Consequently, the mitigation measures of the next item will cover only water hammer events due to the leakage of steam through valves V1 and V12. This kind of water hammer has been the most frequent kind in BWR RHR systems.

5.3.3 Water Hammer Mitigation Measures

As previously mentioned, the strategies that can be used to avoid water hammer events related to the leakage of high pressure steam through valves V1 and V12, and which are based on the results of chapters 3 and 4, will be discussed next.

As with most updated BWR nuclear power plants, Browns Ferry Unit 1 has a keep full pump installed in its RHR system, according to Lanik and Rubin (43) (see figure - 5.4). But for the type of problem being addressed in this item, a keep full system is not a solution.

If it is considered unlikely that the steam will reach any horizontal pipe, the problem of leakage for either of these two valves can be solved easily by using the vertical up single pipe theory, for choosing a filling velocity. Practically, this can be accomplished by adding the bypass line 9 and the valve V13 across the shut valve V7, as it is shown in figure - 5.5. Valve V7 would be changed to be normally closed, valve V13 would normally be open and the bypass line would limit the initial water filling rate into the system. When the filling was complete, valve V7 would be opened. A question may arise whether the vertical up single pipe theory is good for an heat

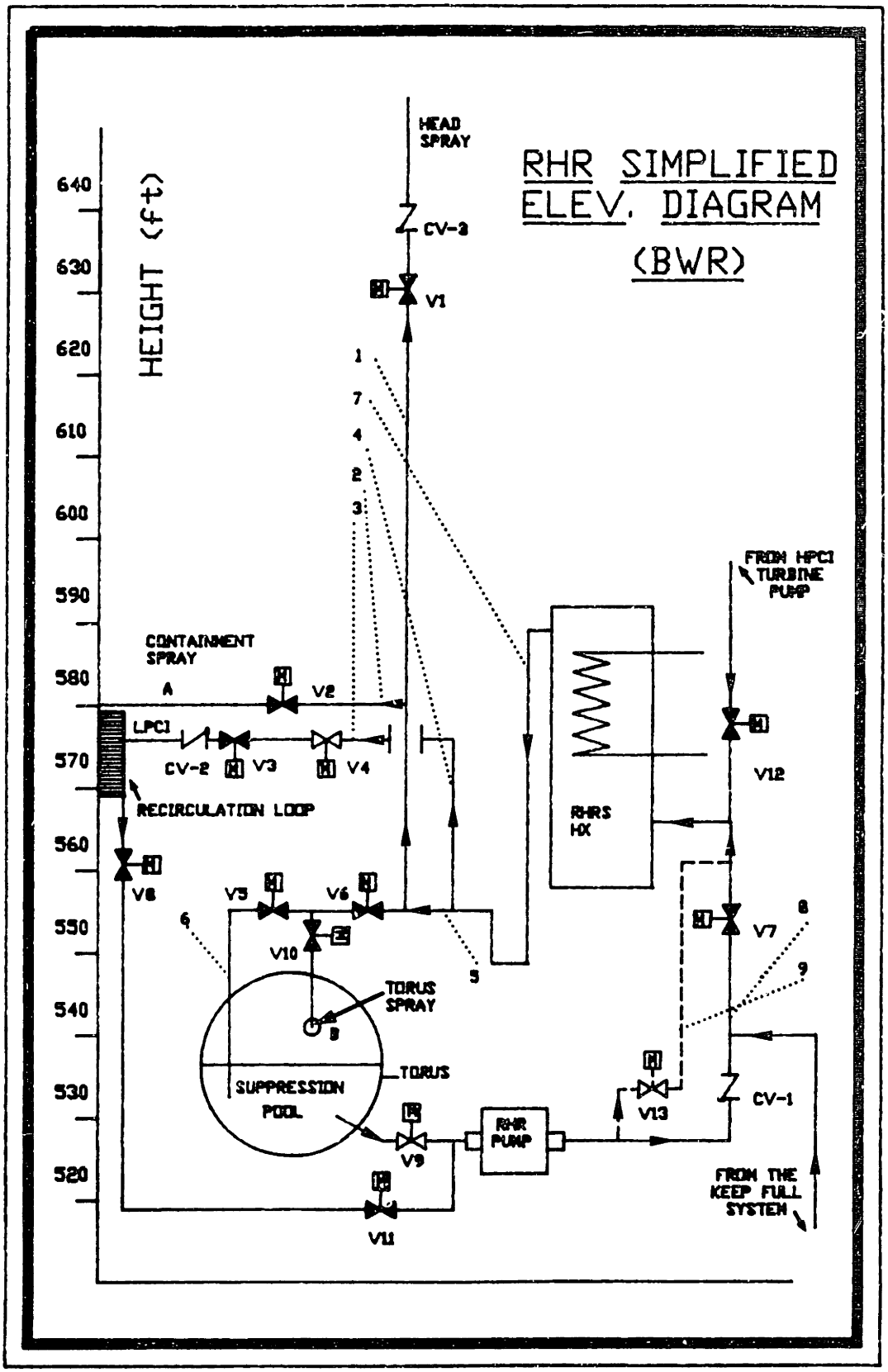

FIGURE - 5.5 BWR RHR Simplified Elevation Diagram with the Proposed Modification.

exchanger that is full of steam in its upper part, as this was not tested in chapter 3 or 4. However, as the water filling velocity will be limited by one of the vertical pipes, the water velocity inside the heat exchanger will so low that it is difficult to imagine the steam condensing in a violent way.

Assuming that it is possible for the steam to reach the horizontal pipe sections, these pipe branches should be inclined up (at least 0.5"/1') in the direction of the water flow. Filling any long leveled horizontal pipes by using bypass lines, that make them in effect short pipes, is another solution.

5.4 PWR Residual Heat Removal System (RHRS)

5.4.1 System Description and Purpose

The RHRS consists of two independent trains. Each train is made of a heat exchanger, a pump, valves, piping and necessary instrumentation (see figure - 5.6).

The primary function of the RHRS is to remove thermal energy from the Reactor Coolant System (RCS) and fuel during reactor shutdown and refueling operations (see figure - 5.7). The RHRS is only put into operation when the RCS water is at approximately 350^{o}F and 400 psig. When this occurs, the system is in the most critical condition. At the start of system operation, the throttle valve, located downstream of the RHR heat exchanger, is only slightly opened. This limits the flow through the RHR heat exchanger and minimizes the possibility of a thermal shock. The RHRS can also be used to transfer refueling water between the Refueling Cavity (RC) and the Refueling Water Storage Tank (RWST) (see figure - 5.7).

During normal operation of the RHRS some water is diverted to the Chemical and Volume Control System (CVCS) to adjust the RCS water boric acid concentration, to purify the RCS water and to adjust the RCS water volume (Thereby compensating for the RCS temperature variations). The CVCS operates at a low pressure.

The RHRS is also part of the Safety Injection System (SIS). During normal reactor operation the RHR pumps are aligned with the RWST. Thus, if a LOCA occurs, the low pressure, active, safety injection system can use the

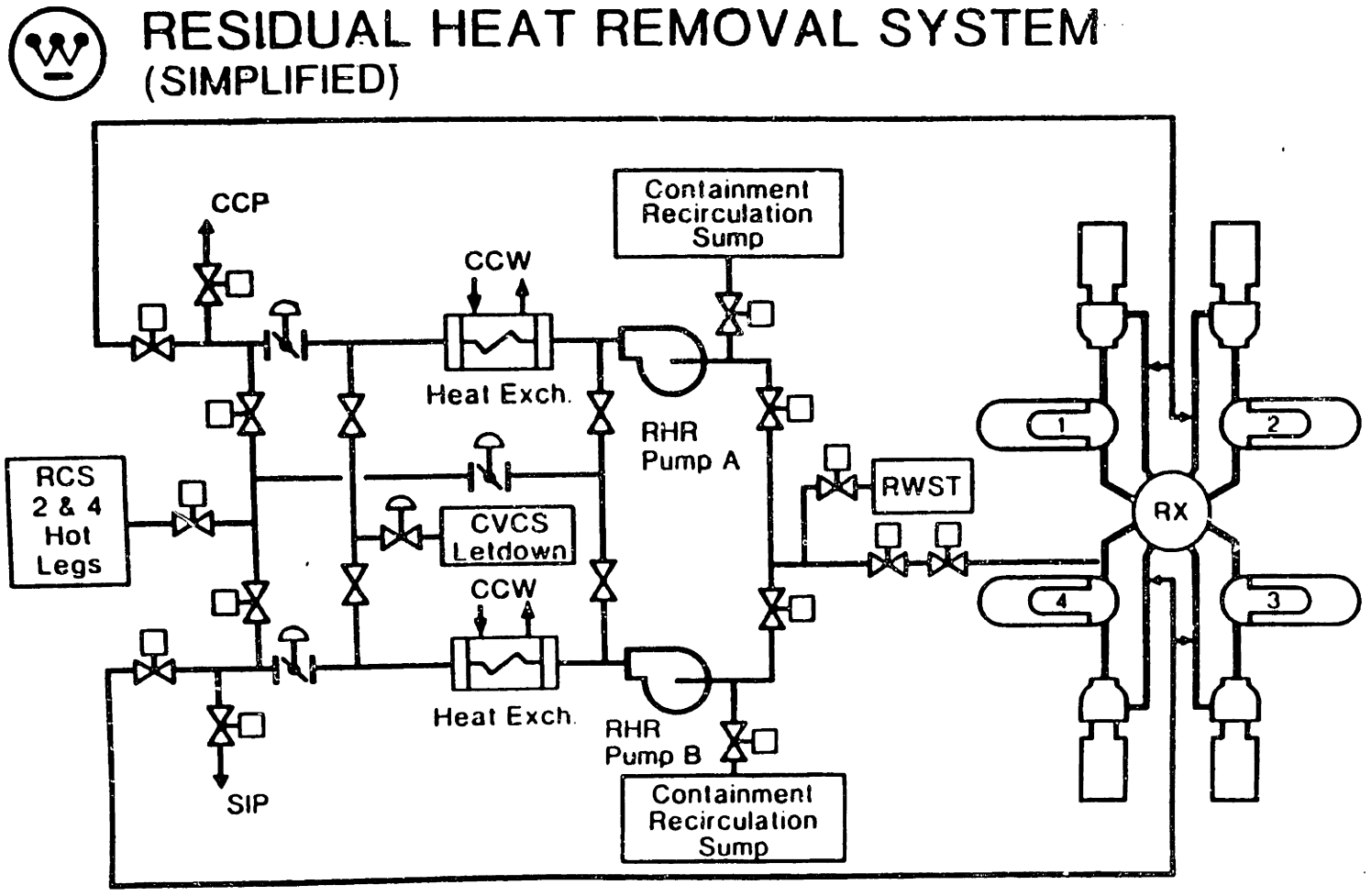

FIGURE - 5.6 PWR RHR Functional Diagram. Source -> (10)

two RHR pumps to bring borated water from the RWST into the RCS hot legs. During a LOCA, in order to provide long term core cooling capacity, the RHR pumps are able to bring water from the reactor sump into the RCS hot legs, in the course of which the water passes through the RHR heat exchangers.

5.4.2 Elevation Diagram and Previous Reported Water Hammer Events

The RHRS typical elevation diagram of figure - 5.7 was reproduced from (42). On this drawing, it can be seen that the RHRS is shown aligned to remove residual heat from the RCS. The reactor water is taken from the hot legs, is forced to pass through the heat exchanger and is injected back into the cold legs.

During normal reactor operation, the RHRS is connected to the RWST (valve 8812 remains open), as already explained. From figure - 5.7, the RWST water level is at a higher elevation than any pipe branch of the system. Therefore, the RHRS has an intrinsic feature that makes the void formation in it difficult. A second RHRS characteristic is that at the start of its operation the initial circulating water rate is small. Valve HVC-607 is only slightly opened. Consequently, any steam that might be found inside the RHR pipes can be condensed slowly. These two factors make the system unlikely to participate in any void or steam bubble collapse related water hammer events.

For the RHRS there are 6 reported water hammer events in the recently assembled Stone and Webster's PWR Utility Water Hammer Data Base (Appendix B from (41)). Two of these water hammer events can be attributed to the collapse of a steam bubble when subcooled water was injected into the RHR

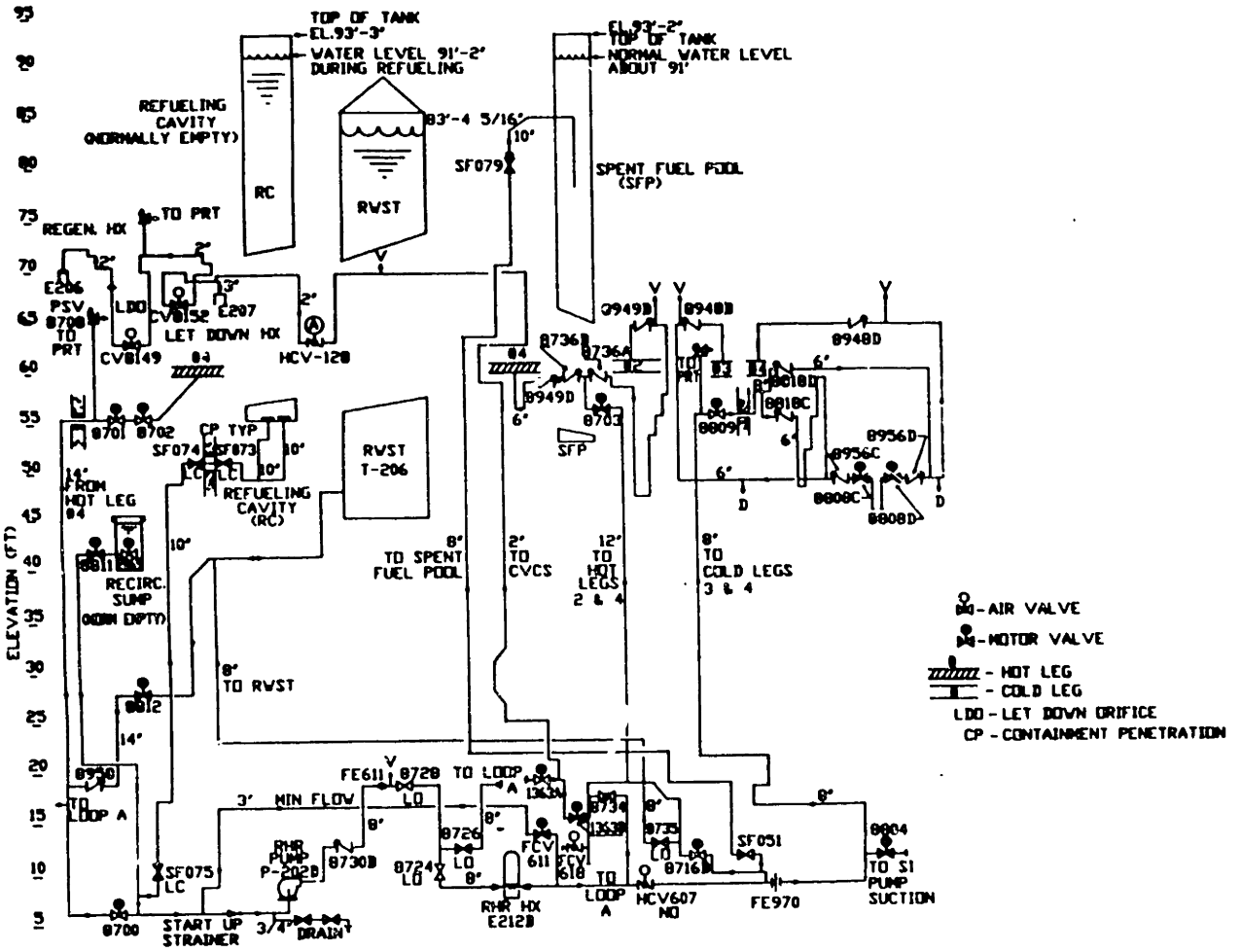

FIGURE - 5.7 Typical PWR RHR Elevation Diagram.
Source -> (42)

pipes. The other four events were initiated by other mechanisms, which are not discussed in this thesis.

In order to explain how steam bubble related water hammer events can occur in the RHRS, the elevation diagram of figure - 5.7 was simplified and redrawn. The result of this simplification is shown in figure - 5.8. As can be observed, the pipe train that connects the hot leg to the cold leg, during the residual heat removal, and the line that connects the RHRS to the CVCS were maintained in the new drawing.

Unless the RHRS is being used to remove residual heat, valves 1363b and HVC-128 (figure - 5.8) remain closed. If valve HVC-128 is leaking, water from line A (see figure - 5.8) will flow to the CVCS, as the RHRS pressure is greater. The pressure inside the line A will decrease and when it reaches the saturation value steam will be formed. Then, as soon as valve 1363B is opened a water hammer can occur.

A second place where steam bubbles can be formed is in region B of figure - 5.8. Leaky check valves (8948B and 8818C or 8948D and 8818D) would permit high pressure and high temperature RCS water to flow into the RHR pipes. The hot water would then flash into steam because of the lower pressure of the RHRS. A leaky valve 8809 would permit the steam to further migrate into the riser section (see figure - 5.8).

One reported steam bubble related water hammer event was at line A. The second was in region B.

5.4.3 Water Hammer Mitigation Measures

Considering first line A (figure - 5.8), the following suggestions,

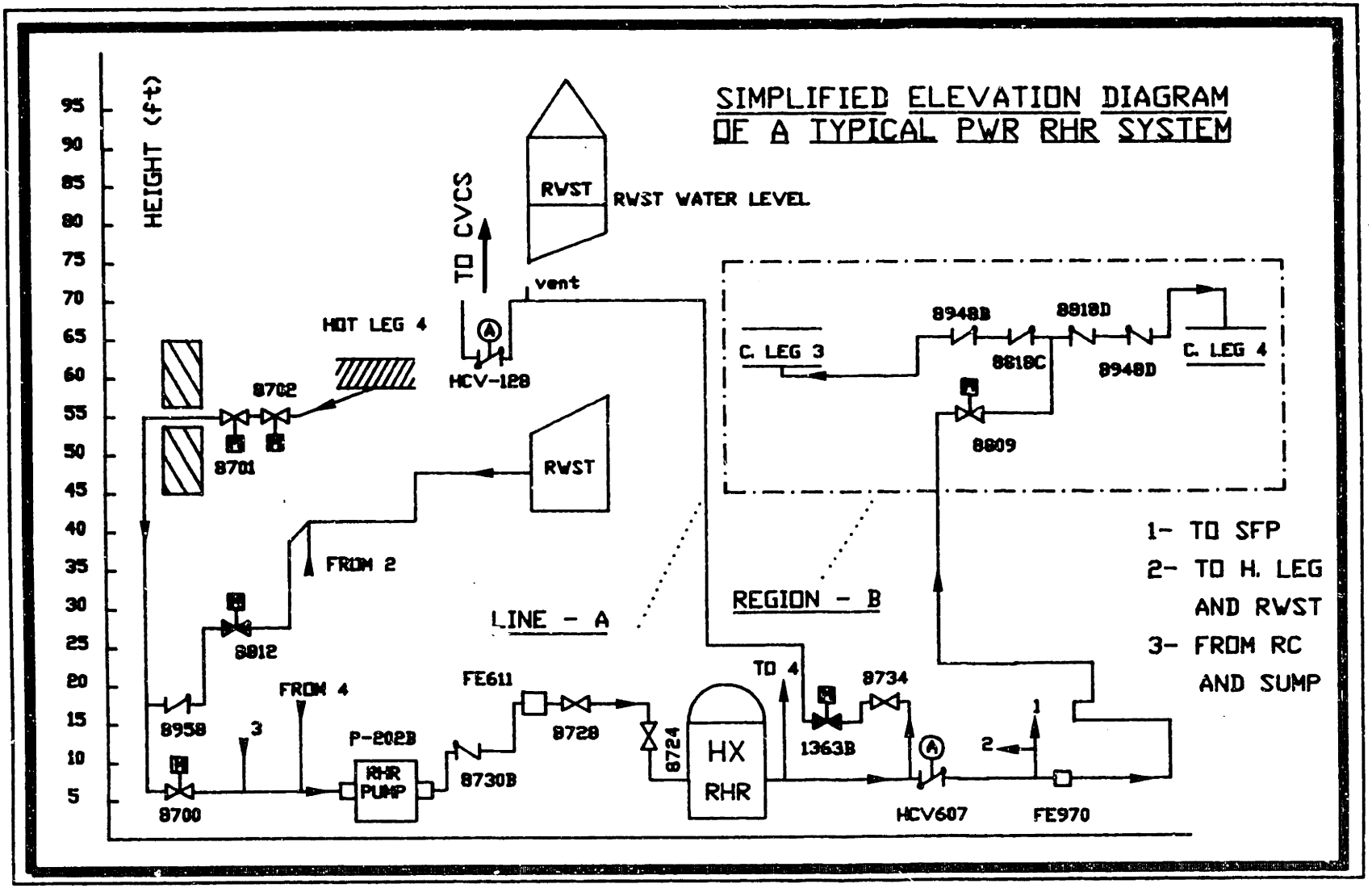

FIGURE - 5.8 Simplified PWR RHR Elevation Diagram.

based in the two previous chapters, can be given:

-Assuming that all horizontal sections of line A are smaller than 48.D, the initial filling rate into this line should be limited by the vertical up single pipe theory. For instance, a bypass line with an orifice could be added across valve 1363B; and

-A vacuum breaker or a manually operated vent valve positioned near control valve HCV-128 (see figure - 5.8) could also help avoiding a water hammer.

In region B the lines after the shut valve 8809 are only schematically represented in figure - 5.8. It can be expected that in some plants the lines contain horizontal pipe sections with lengths greater than 48.D. Taking this into account it is suggested that:

-Incline (at least 0.5"/1') all the horizontal pipe sections with the higher part in the direction of the cold legs;

-Limit the initial filling rate to the one from the vertical up single pipe theory. It might be able to do this by using the already existent control valve HCV-607;

Instead of inclining the horizontal pipe sections, bypass lines that would divide long horizontal pipes into short ones could be added to the system.

CHAPTER - 6

SUMMARY AND SUGGESTIONS FOR FUTURE RESEARCH

Summary

It has been experimentally demonstraced that it is possible to avoid condensation induced water hammer, in complex piping systems which contain steam, by controlling the initial filling process. This is done by limiting the initial filling rate and injecting the water in a suitable location and manner. The implementation of this idea should follow three basic steps.

Step 1 - The past water hammer experience of the piping system and various postulated failures of its components should be taken into account in order to establish possible water hammer scenarios. After that, it should be decided which of the possible scenarios are likely enough, so that eliminating water hammer events by design change be worthwhile.

Step 2 - If it is anticipated that steam will fill (totally or not) a truly horizontal pipe, one of the two following modifications has to be introduced into the piping system:

-The horizontal pipe should be inclined (at least 0.5"/1') and the water should be introduced from its bottom with no forward (axial) momentum; or

-Until the truly horizontal pipe is full, the water should be introduced by using injection nozzles distributed along the pipe length. The distance between these nozzles should be less than 48.D.

When the horizontal pipe contains a steam bubble, for which the maximum

volume can be estimated, the simple bubble collapse model of section 3.4 should be used.

used.

Step 3 - After using one of the above methods to eliminate the slug water hammer (intermediate) in the existing horizontal pipes, Chou's vertical up theory (6) should be used to determine the appropriate initial filling velocity. Hardware modifications will be eventually necessary to limit the initial filling rate (For instance, the use of bypass capillaries or bypass lines with orifices) to the desired value. This procedure will limit to a desired value the final water hammer load.

Suggestions of Future Research

As described, careful measures were taken during the tests to prevent air penetration into the pipes. Due to limitations of the MIT Heat Transfer Laboratory the test apparatuses were assembled by using threaded flanges on the pipes. When subcooled water was injected into the pipes it would cause the interior pressure to decrease. At this time, it is possible that air would penetrate into the pipes through the flanged or screwed connections. Although we expect that the test conditions did not differ much from those likely to be found in real systems, it was not possible to determine the air content in the steam.

Especially for mass fractions which are less than 1×10^{-2}, an increase in the content of noncondensibles in the steam sharply decreases the condensation rate (see Collier (46)). Therefore, further research is necessary to determine the effect of air on the water hammer boundaries that have been established.

Nevertheless, the procedures of steps 2 and 3 should have general validity because: 1) The solution for the slug water hammer in the horizontal pipe should be independent of the condensation rate; and 2) In Chou's (6) vertical up experiments, except at the beginning of the water injection, the pipe interior pressure would continuously increase. In other words, we should not expect that any air went into the pipes, and his theory should be a conservative boundary for systems with some air.

Among other still needed, related investigations, we can stress the following:

-Experimental verification of the influence of the pipe diameter and the system pressure in the water hammer boundary;

-Influence pipe components (For instance, check valves) on the water hammer boundary;

-Study of direct-contact condensation of steam on subcooled water, in the range of the water hammer interest; and

-Development of an analytical model to predict the pipe load due to a slug water hammer in a long horizontal pipe.

REFERENCES

1. D. A. Van Duyne. "Water Hammer Prevention, Mitigation, and Accommodation - Research Project 2856-3 - Progress Report." In The Second EPRI Workshop on Water Hammer in Nuclear Power Plants, 1988.

2. Water Hammer Prevention, Mitigation, and Accommodation - Task 1 - Plant Water Hammer Experience. Boston, MA: Stone & Webster Engineering Corporation, January 1988. RP 2856-3.

3. U. S. Nuclear Regulatory Commission. Compilation of Data Concerning Known and Suspected Water Hammer Events In Nuclear Power Plants, NUREG/CR-2059. Washington, D.C. 1982.

4. U. S. Nuclear Regulatory Commission. Loss of Power and Water Hammer Event at San Onofre, Unit 1, on November 21, 1985, NUREG-1190. Washington, D.C. 1986.

5. Andrew C. Kadak. "Water Hammer - A New Look at an Old Problem." In The Second EPRI Workshop on Water Hammer in Nuclear Power Plants, 1988.

6. Yuanching Chou. Avoiding Steam Bubble Collapse Induced Water Hammer in Piping Systems. Ph.D Thesis, Department of Nuclear Engineering, MIT, 1988.

7. U. S. Nuclear Regulatory Commission. Water Hammer in Nuclear Plants, NUREG-0582. Washington, D.C. 1979.

8. U. S. Nuclear Regulatory Commission. Evaluation of Water Hammer Events in Light Water Reactor Plants, NUREG/CR-2781. Washington, D.C. 1982.

9. U. S. Nuclear Regulatory Commission. Evaluation of Water Hammer Occurrence in Nuclear Power Plants, NUREG-0927. Washington, D.C. 1984.

10. Water Hammer Prevention, Mitigation, and Accommodation - Task 2 - Root Cause Analysis for Plant Water Hammer Experience. Boston, MA: Stone & Webster Engineering Corporation, August 1988. RP 2856-3.

11. Water Hammer Prevention, Mitigation, and Accommodation - Tasks 6 and 7 Collect and Review Water Hammer Data. Boston, MA: Stone & Webster Engineering Corporation, August 1988. RP 2856-3.

12. U. S. Nuclear Regulatory Commission. An Evaluation of PWR Steam Generator Water Hammer, NUREG-0291. Washington, D.C. 1976.

13. U. S. Nuclear Regulatory Commission. An Evaluation of Condensation Induced Water Hammer in Preheat Steam Generators, NUREG/CR-1606. Washington, D.C. 1980.

14. Robert L. Gruel. Steam Bubble Collapse and Water Hammer in Piping Systems: Experiment and Analysis. MS Thesis, Department of Mechanical Engineering, MIT, 1980.

15. Wayne M. Hurwitz. Piping Network Response to Steam Generated Water Hammer. MS Thesis, Department of Mechanical Engineering, MIT, 1980.

16. Robert W. Bjorge. Initiation of Water Hammer in Horizontal or Nearly-Horizontal Pipes Containing Steam and Subcooled Water. Ph.D Thesis, Department of Mechanical Engineering, MIT, 1982

17. Y. Taitel and A. E. Dukler. "A Model for Predicting Flow Regime Transition in Horizontal and Near Horizontal Gas-Liquid Flow." AIChE Journal, Vol. 22, No. 1, 1976, pp. 47-55.

18. U. S. Nuclear Regulatory Commission. Direct-Contact Condensation of Steam on Cold Water in Stratified Countercurrent Flow. NUREG/CR-4414. Washington, D.C. 1985.

19. Andrew B. Jackobek. Investigation of Cold Leg Water Hammer in a PWR Due to the Admission of ECC During a Small-Break LOCA. MS Thesis, Department of Mechanical Engineering, MIT, 1984.

20. Graham B. Wallis. One-Dimensional Two-Phase Flow. New York: McGraw-Hill, 1969.

21. C. S. Martin. "Vertically Downward Two-Phase Slug Flow." J. of Fluids Engineering, December, 1976, pp. 715-722.

22. Graham B. Wallis et al. "Conditions for a Pipe to Run Full When Discharging Liquid into a Space Filled with Gas." J. of Fluids Engineering, June, 1977, pp. 405-413.

23. Ven Te Chow. Open-Channel Hydraulics. New York: McGraw-Hill, 1959.

24. H. S. Bean. Fluid Meters. ASME United Engineering Center, 6th ed. - 1971, page 179.

25. W. Unkel. Unkelscope Level 1 Guide. Department of Mechanical Engineering - MIT, 1985.

26. T. Swierzawki - Stone & Webster Engineering Corporation. Personal Communication to Professor Peter Griffith. Department of Mechanical Engineering - MIT, February, 1988.

27. E. B. Wylie and V. L. Streeter. Fluid Transients. New York: McGraw-Hill, 1978.

28. R. W. Clough and J. Penzien. Dynamics of Structures. New York: McGraw-Hill, 1975.

29. Analysis of Three Water Hammer Mechanisms and the Resulting Piping Loads (Draft). David C. Wiggert. East Lansing, Mi: Michigan State University - Department of Civil and Environmental Engineering, August 1988. Prepared to Stone & Webster Engineering Corporation.

30. G. B. Wallis and J. E. Dobson. "The Onset of Slugging in Horizontal Stratified Air-Water Flow." Int. J. Multiphase Flow, Vol 1, 1973, pp. 173-193.

31. K. Mishima and M. Ishii. "Theoretical Prediction of Onset of Horizontal Slug Flow." J. of Fluids Engineering, Vol. 102, 1980, pp. 441-445.

32. R. M. Thomas. "Condensation of Steam on Water in Turbulent Motion." Int. J. Multiphase Flow, Vol. 5, 1979, pp. 1-15.

33. A. Segev et al. "Experimental Study of Countercurrent Steam Condensation." Journal of Heat Transfer, May - Vol. 103, 1981, pp. 307-311.

34. T. G. Theofanous et al. "Turbulent Mass Transfer at Free, Gas-Liquid Interfaces, with Applications to Open-Channel, Bubble and Jet Flows." Int. J. Heat Mass Transfer, Vol. 19, 1976, pp. 613-624.

35. Argonne National Laboratory. The Slug-Annular Flow Regime Transition at Elevated Pressure. ANL-6796. Washington, D.C.: Office of Technical Services, Department of Commerce, 1963.

36. O. L. Pushkina and Y. L. Sorokin. "Breakdown of Liquid Film Motion in Vertical Tubes." Heat Transfer - Soviet Research, Vol. 1, 1969, pp. 56-64.

37. Susan M. Krolewski. Flooding Limits in a Simulated Nuclear Reactor Hot Leg. BS Thesis, Department of Mechanical Engineering, MIT, 1980.

38. H. Siddiqui et al. "Flooding in an Elbow Between a Vertical and a Horizontal or Near-Horizontal Pipe - Part I." Int. J. Multiphase Flow, Vol. 12 - No. 4, 1986, pp. 531-541.

39. K. H. Ardron and S. Banerjee. "Flooding in an Elbow Between a Vertical and a Horizontal or Near-Horizontal Pipe - Part II." Int. J. Multiphase Flow, Vol. 12 - No. 4, 1986, pp. 543-558.

40. George Masche. Systems Summary of a Westinghouse Pressurized Water Reactor Nuclear Plant. Westinghouse Electric Corporation, 1971.

41. General Electric Company. BWR/6 General Description of a Boiling Water Reactor San Jose, California: General Electric Company, 1980.

42. Hemmat H. Safwat. "Progress Report of EPRI Water Hammer Project - Bechtel Power Corporation." In the Second EPRI Workshop on Water Hammer in Nuclear Power Plants, 1988.

43. U. S. Nuclear Regulatory Commission. Office for Analysis and Evaluation of Operational Data. The Potential for Water Hammer During The Restart of RHR Pumps at BWR Nuclear Power Plants. AEOD/E309 (8305040745). Washington D.C., 1983.

44. U. S. Nuclear Regulatory Commission. Office for Analysis and Evaluation of Operational Data. The Potential for Water Hammer During The Restart of RHR Pumps for BWR Nuclear Power Plants. (8210080165). Washington D.C., 1981.

45. I. E. Idelchik. Handbook of Hydraulic Resistance. Second Edition. Hemisphere Publishing Corporation, 1986.

46. John G. Collier. Convective Boiling and Condensation. Second Edition. New York: McGraw-Hill, 1981.

APPENDIX - A

CONCENTRATED PRESSURE LOSSES FOR THE BUBBLE COLLAPSE MODEL

The Handbook of Hydraulic Resistance, by Idelchik (45), was used as reference to this calculation. So:

$$\Delta P_{loc.} = \Delta P_{ball\ valve} + 2.\Delta P_{90^o\ bend} + \Delta P_{pipe\ entrance} \qquad \text{eq(A - 1)}$$

where,

$$\Delta P_{loc.} = (K_1 + K_2 + K_3).\frac{\rho_1.V^2}{2} = K_T.\frac{\rho_1.V^2}{2} \qquad \text{eq(A - 2)}$$

and,

Ball Valve Coefficient K_1

$K_1 = 0.02$ for $Re > 10^4$ -> Diagram 9.13 - page 447 (45)

Bend Coefficient K_2

$K_2 = 2.(K_{loc.} + 0.0175.\frac{R}{D}.\theta.f)$ -> Diagram 6.1 - page 289 (45)

Assuming that:

$R = D$, $\theta = \Pi/2$ and $f = 0.02$

$K_2 = 0.42$

Entrance Coefficient

$K_3 = 0.5$ -> page 113 (45)

Finally, $$\Delta P_{loc.} = 0.94.\frac{\rho_1.V^2}{2} \qquad \text{eq(A - 3)}$$

APPENDIX - B

JOUKOWSKY RELATION COEFFICIENT WHEN THE WATER CRASHES AGAINST A WATER COLUMN

The reason why the Joukowsky relation coefficient should be equal to $\frac{1}{2}$, when the water crashes against a water column, can be demonstrated by solving the momentum equation in the two fixed control volumes of figure - B.1.

Momentum Equation

$$\frac{d}{dt}\int_{cv} \rho_1 . V . dv + \int_{cs} \rho_1 . V . (\vec{V}_{rel} . \vec{da}) = A . \Delta P . g_c - A . \Delta P_{fric} - A . \Delta P_{loc}$$

eq(B - 1)

Neglecting losses and using figure - B.1, it is possible to write:

$$cv\ 1 \rightarrow -\rho_1 . g . \Delta H . A = \rho_1 . A . (c - V) . (V' - V) - \rho_1 . A . V^2 + \rho_1 . A . V'^2$$

eq(B - 2)

$$cv\ 2 \rightarrow \rho_1 . g . \Delta H . A = \rho_1 . A . c . V' - \rho_1 . A . V'^2 \qquad \text{eq(B - 3)}$$

Adding the two momentum equations we get:

$$V' = \frac{\rho_1 . A . c . V}{2 . \rho_1 . A . c - \rho_1 . A . V} \qquad \text{or}$$

$$V' = \frac{V}{2 - \frac{V}{c}} \qquad \text{eq(B - 4)}$$

For $c \gg V$, $V' \simeq \frac{V}{2}$. Using this value in equation (B - 2) we find:

$$g . \rho_1 . \Delta H = \rho_1 . c . \frac{V}{2} . (1 + \frac{V}{2 . c}) \qquad \text{eq(B - 5)}$$

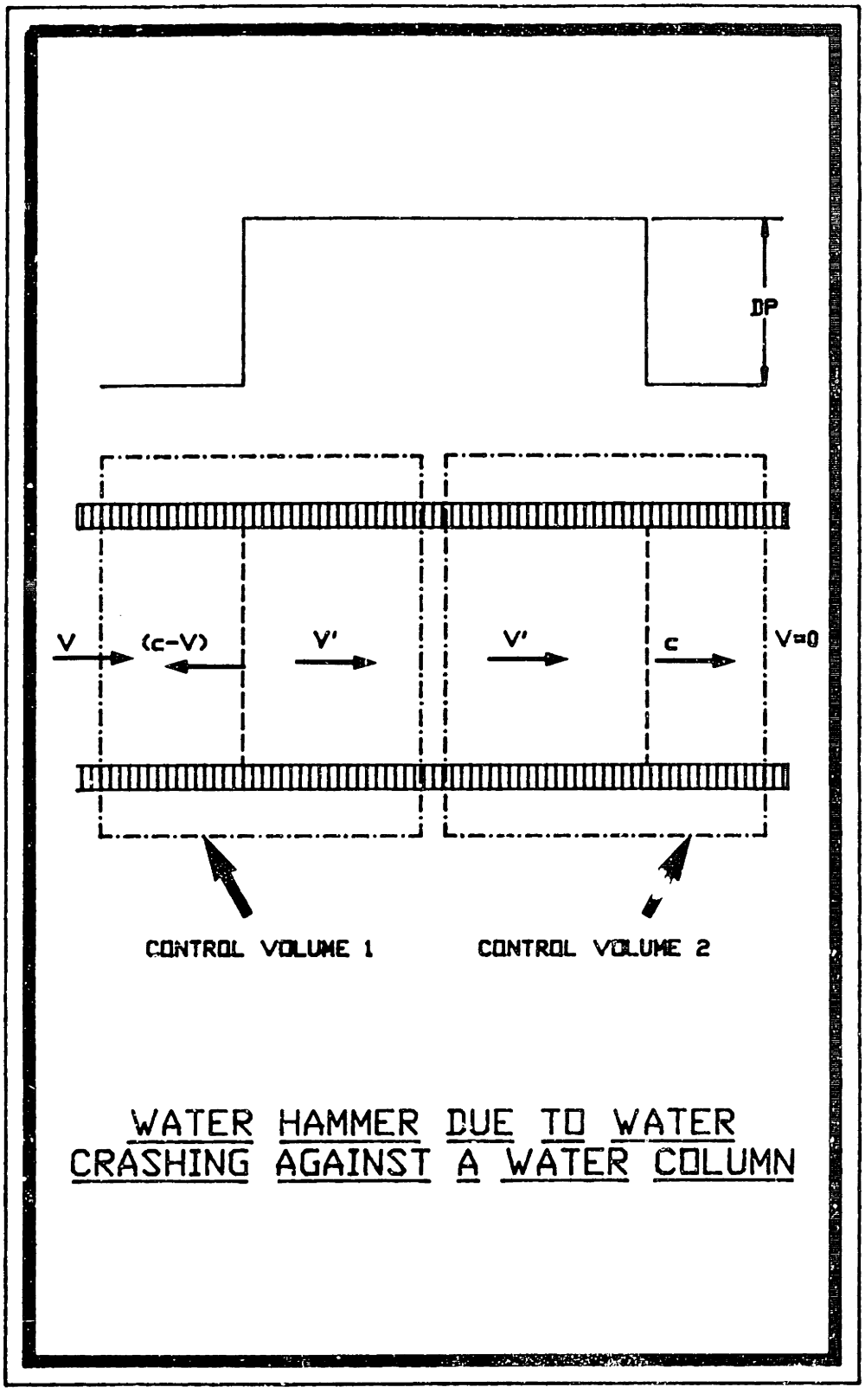

FIGURE - B.1 Appendix B scheme.

Neglecting $\frac{V}{2.c}$ again we get:

$$\Delta P = g.\rho_l.\Delta H = \frac{1}{2}.\rho_l.c.V \qquad \text{eq(B - 6)}$$

APPENDIX - C

SOME SELECTED RESULTS FROM

STRUCTURE DYNAMICS

For the following review we used some selected results from Clough's book (28).

A water hammer event subjects the pipe to an impulsive load of short duration. In this case, the structure response reaches its peak before the damping forces have time to absorb part of the water hammer energy. So, damping can be neglected. However, this is not the case of the inertia and elastic forces. Consequently, the equation of motion for a single degree of freedom system (SDOF) can be written as:

$$M.\frac{d^2z}{dt^2} + K.z(t) = p(t) \qquad \text{eq(C - 1)}$$

or

$$M.\dot{\Delta z} = \int_0^{t_1} \left[p(t) - K.z(t) \right].dt \qquad \text{eq(C - 2)}$$

for a small t_1, through an order of magnitude analysis, it can be shown that (see (28)):

$$z(\bar{t}) \simeq \frac{1}{M.w}.\left[.\int_0^{t_1} p(t).dt \right].\sin(w.\bar{t}) \qquad \text{eq(C - 3)}$$

where:

z(t) - single displacement (SDOF) p(t) - applied load

M - system mass w - circular frequency

K - system stiffness T - free vibration period

t_1 = impulse duration $\qquad \bar{t} = t - t_1$

and

$$w = \frac{2.\Pi}{T} = \sqrt{K / M} \qquad \text{eq(C - 4)}$$

$$K = \frac{P}{z} \qquad \text{eq(C - 5)}$$

Equation (C - 2) can be used to develop an exact formula for a general dynamic loading. This procedure, as described in chapter 7 of Clough's book (28), reaches to:

$$z(t) = \frac{1}{M.w} \int_0^t p(\tau).\sin w(t-\tau)d\tau \qquad \text{eq(C - 6)}$$

Using the above equation and knowing the variation of p (load) with time, it is possible to calculate z_{max}. Defining the magnification factor (D) as equation (C - 7), it is possible to construct curves of $\underline{D \text{ X } (t_1 / T)}$ (response spectra) for different loading shapes. Once p_{max}, t_1, M and the structure stiffness are known, z_{max} can be easily calculated using the response spectra curves. The structure stresses are calculated from z_{max}. Figure - 3.20 (Chapter - 3) is a reproduction of one of these plots from Clough's book (28) (see also Wiggert (29)).

$$D = \left| \frac{z_{max}}{p_{max/K}} \right| \qquad \text{eq(C - 7)}$$